DOCTOR OF PHILOSOPHY

The functional characterisation of leukaemia-associated protein TRAX

Almobadel, Nasser

Award date:
2013

Awarding institution:
Bangor University

The functional characterisation of leukaemia-associated protein TRAX

Nasser Saad Almobadel

Ph.D. thesis 2013

North West Cancer Research Fund Institute

School of Biological Science

University of Wales, Bangor

United Kingdom

Declaration and Consent

Details of the Work

I hereby agree to deposit the following item in the digital repository maintained by Bangor University and/or in any other repository authorized for use by Bangor University.

Author Name: ……...……...……..

Title: ……..……..…….

Supervisor/Department: .....

Funding body (if any): .....

Qualification/Degree obtained: …….

This item is a product of my own research endeavours and is covered by the agreement below in which the item is referred to as "the Work". It is identical in content to that deposited in the Library, subject to point 4 below.

Non-exclusive Rights

Rights granted to the digital repository through this agreement are entirely non-exclusive. I am free to publish the Work in its present version or future versions elsewhere.

I agree that Bangor University may electronically store, copy or translate the Work to any approved medium or format for the purpose of future preservation and accessibility. Bangor University is not under any obligation to reproduce or display the Work in the same formats or resolutions in which it was originally deposited.

Bangor University Digital Repository

I understand that work deposited in the digital repository will be accessible to a wide variety of people and institutions, including automated agents and search engines via the World Wide Web.

I understand that once the Work is deposited, the item and its metadata may be incorporated into public access catalogues or services, national databases of electronic theses and dissertations such as the British Library's EThOS or any service provided by the National Library of Wales.

I understand that the Work may be made available via the National Library of Wales Online Electronic Theses Service under the declared terms and conditions of use (http://www.llgc.org.uk/index.php?id=4676). I agree that as part of this service the National Library of Wales may electronically store, copy or convert the Work to any approved medium or format for the purpose of future preservation and accessibility. The National Library of Wales is not under any obligation to reproduce or display the Work in the same formats or resolutions in which it was originally deposited.

Statement 1:

This work has not previously been accepted in substance for any degree and is not being concurrently submitted in candidature for any degree unless as agreed by the University for approved dual awards.

Signed …….. (candidate)

Date ……..

Statement 2:

This thesis is the result of my own investigations, except where otherwise stated. Where correction services have been used, the extent and nature of the correction is clearly marked in a footnote(s).

All other sources are acknowledged by footnotes and/or a bibliography.

Signed ……. (candidate)

Date …….

Statement 3:

I hereby give consent for my thesis, if accepted, to be available for photocopying, for inter-library loan and for electronic storage (subject to any constraints as defined in statement 4), and for the title and summary to be made available to outside organisations.

Signed ……. (candidate)

Date …….

NB: Candidates on whose behalf a bar on access has been approved by the Academic Registry should use the following version of **Statement 3:**

Statement 3 (bar):

I hereby give consent for my thesis, if accepted, to be available for photocopying, for inter-library loans and for electronic storage (subject to any constraints as defined in statement 4), after expiry of a bar on access.

Signed …… (candidate)

Date ……

Statement 4:

Choose **one** of the following options

a) I agree to deposit an electronic copy of my thesis (the Work) in the Bangor University (BU) Institutional Digital Repository, the British Library ETHOS system, and/or in any other repository authorized for use by Bangor University and where necessary have gained the required permissions for the use of third party material.	
b) I agree to deposit an electronic copy of my thesis (the Work) in the Bangor University (BU) Institutional Digital Repository, the British Library ETHOS system, and/or in any other repository authorized for use by Bangor University when the approved **bar on access** has been lifted.	
c) I agree to submit my thesis (the Work) electronically via Bangor University's e-submission system, however I **opt-out** of the electronic deposit to the Bangor University (BU) Institutional Digital Repository, the British Library ETHOS system, and/or in any other repository authorized for use by Bangor University, due to lack of permissions for use of third party material.	

Options B should only be used if a bar on access has been approved by the University.

In addition to the above I also agree to the following:

1. That I am the author or have the authority of the author(s) to make this agreement and do hereby give Bangor University the right to make available the Work in the way described above.

2. That the electronic copy of the Work deposited in the digital repository and covered by this agreement, is identical in content to the paper copy of the Work deposited in the Bangor University Library, subject to point 4 below.

3. That I have exercised reasonable care to ensure that the Work is original and, to the best of my knowledge, does not breach any laws – including those relating to defamation, libel and copyright.

4. That I have, in instances where the intellectual property of other authors or copyright holders is included in the Work, and where appropriate, gained explicit permission for the inclusion of that material in the Work, and in the electronic form of the Work as accessed through the open access digital repository, *or* that I have identified and removed that material for which adequate and appropriate permission has not been obtained and which will be inaccessible via the digital repository.

5. That Bangor University does not hold any obligation to take legal action on behalf of the Depositor, or other rights holders, in the event of a breach of intellectual property rights, or any other right, in the material deposited.

6. That I will indemnify and keep indemnified Bangor University and the National Library of Wales from and against any loss, liability, claim or damage, including without limitation any related legal fees and court costs (on a full indemnity bases), related to any breach by myself of any term of this agreement.

Signature:……Date : …….

Abstract

Translin and its intimate binding partner TRAX are highly conserved proteins. Translin has been implicated in numerous biological functions ranging from cancer-associated chromosomal rearrangements in some types of leukaemia and other cancers to the control of mRNA transport in the brain. Translin is essential for TRAX stability whilst its own stability is unaffected by loss of TRAX. Two recent finding now give a more detailed insight into Translin and TRAX functions. First, these two proteins combine to form the C3PO complex, which functions in the removal of the passenger strand in RNAi mediated gene silencing. Second, Translin and TRAX are implicated in tRNA processing. However, in *S. pombe*, deletion of the two genes encoding these proteins causes no measurable phenotype change in mitotically proliferating cells. In this study, our aim was to investigate the biological role of TraX, in particular, in the regulation of the RNAi machinery used by cells to maintain the heterochromatin state of key functional genomic regions. We used different approaches to examine whether TraX (and Translin) play redundant roles with other RNAi regulators. Some intriguing observations led us to propose a novel Dicer-independent, Translin-dependent pathway for maintaining chromosomal stability. Additionally, whilst TraX does not seem to be essential for this novel pathway, its loss suppresses the genome instability phenotype of Argonaute-deficient cells and this suppression is Translin-dependent. This finding suggests that TraX functions to prevent Translin mediation of chromosome stability in the absence of Argonaute. Remarkably, microarray analysis to test this proposal indicates that TraX might link Ago1 (Argonaute) function to chromosome stability through the regulation of Rif1 levels or by the control of some replicative or recombinogenic process in which the Tlh2 RecQ-like helicase can serve as a substitute. This could indicate a major new role for Ago1, TraX and Translin in genome maintenance. Moreover, the functional relationship between Translin and TraX is cast into doubt as clear evidence emerges from this study for distinct roles for each of these fission yeast genes.

Acknowledgment

This work was funded by Saudi Arabian Armed Forces Medical Services Department. I extend my fondest thanks to my family, who supported me during my PhD journey. My deep gratitude also goes to my supervisor, Dr. Ramsay McFarlane, for all his guidance, support and encouragement. Many thanks are extended to all the people who supplied me with strains, especially Dr. David Pryce and Dr. Edgar Hartsuiker. I also thank Dr. Alessa Jaendling for her advice on molecular biology techniques. I am grateful to Dr. Jane Wakeman and Dr. Natalia Gomez Escobar for all their advice on tissue culture techniques. I also gratefully acknowledge the support from all my colleagues, past and present, and especially the members of the D7 Lab.

Abbreviations

ACT: activator of cremin testes

AML: acute myeloid leukaemia

BDNF: brain-derived neurotrophic factor

bp: base pair

CDGS: chromatin-dependent gene silencing

CDKs: cyclin-dependent kinases

Ch16: fission yeast minichromosome

CKIs: cyclin-dependent kinase inhibitors

CML: chronic myelogenous leukaemia

cnt: central core

CPT: camptothecin

CREM: cAMP-responsive-element modulator

C3PO: component 3 promoter of RISC

DAPI: 4'-6-diamidino-2-phenylindole

dHJ: double Holliday junction

DNA-PK: DNA-dependent protein kinase

DSBs: double-strand breaks

DSBR: double-strand break repair

dsDNA: double-stranded DNA

dsRNA: double-stranded RNA

ssDNA: single-stranded DNA

EM: electron microscopy

GADD: growth arrest and DNA damage

GRBP: glucose response element binding protein

hAgo2: human Ago2

HP1: heterochromatin protein 1

HR: homologous recombination

HRP: Horseradish Peroxidase (a secondary antibody)

HU: hydroxyurea

ICLs: DNA interstrand crosslinks

IP: immunoprecipitation

imr: inner most repeats

IR: ionizing radiation

kDa: kilodalton

LB: Luria-Bertani media

miRNAs: microRNAs

MMC: mitomycin C

MMS: methyl methanesulphonate

MRN: MRE11-RAD50-NBS1 complex

mRNA: messenger RNA

NB: nitrogen base

NBL: nitrogen base liquid

NES: nuclear export signal

NHEJ: non-homologous end joining

NLS: nuclear localization signal

ORF: open reading fame

otr: outer repeats

PCR: polymerase chain reaction

Ph^+: Philadelphia chromosome positive

piRNAs: piwi-interacting RNAs

pol II: polymerase II

pol III: polymerase III

PTGS: post-transcriptional gene silencing

rDNA: ribosomal DNA

RdRP: RNA-dependent RNA polymerase

RFs: replication forks

RISC: RNA-induced silencing complex

RITS: RNA-induced transcriptional silencing

RLC: RISC loading complex

RNAi: RNA interference

ROS: reactive oxygen species

rRNA: ribosomal RNA

RPA: Replication protein A (also known as human single-stranded DNA-binding protein)

r.p.m.: revolutions per minute

SCID: severe combined immunodeficiency

siRNA: small interfering RNA

SPA: synthetic sporulation media

SSA: single-strand annealing

ssDNA: single-stranded DNA

ssRNA: single-stranded RNA

T-ALL: T-acute lymphoblastic leukaemia

TB-RBP: testes brain RNA binding protein

TBZ: thiabendazole

TRAX: Translin-associated factor X

TraX: Translin-associated factor X (*S. pombe* nomenclature)

tRNA: transfer RNA

UTRs: untranslated regions

UV: ultra violet

V(D)J: variable (V), diversity (D) and Joining (J) coding segments

WCE: whole cell extract

YE: yeast extract

YEA: yeast extract agar

YEL: yeast extract liquid

CONTENTS

LIST OF FIGURES **Page**

LIST OF TABLES

CHAPTER 1

Introduction

1.1 Cancer

Cancer is one of the leading causes of death around the world, with approximately 7.6 million deaths every year attributed to cancer (Lai et al., 2012). More than 100 different types and subtypes of cancer are recognised and they are generated in many ways, resulting in distinct forms of cancer in every affected organ. Cancer can therefore be defined as a group of complex diseases characterised by uncontrolled cell proliferation and genome instability resulting in malignant cell growth. The genes involved in cancer formation/progression can exhibit alterations (mutations) in the normal DNA sequence or altered expression profiles (reviewed in Davis and Lin, 2011; reviewed in Jefford and Irminger-Finger, 2006). Mutational alterations can take the form of changes in large fragments of DNA, such as chromosomal translocations (see Section 1.3), with effects on chromosome structure, or they might be simple modifications of only one or few nucleotides (small scale mutations) (reviewed in Ruiz et al., 2012). Cancer development is generally thought of as a multistep process that usually arises from one abnormal somatic cell (clonal origin) that can, in some malignant tumours, penetrate the basal membrane barrier surrounding the injured part of the body and invade other tissues in a process called metastasis. Moreover, some inherited genetic changes can also result in a predisposition to cancer development (reviewed in McCarthy, 2012). Cancerous cells exhibit high levels of genome instability because some mutations affect genes that preserve genome integrity; these include mutations that occur in tumour suppressor genes, proto-oncogenes and DNA repair genes. Indeed, genome instability is a distinctive feature of cancerous cells (reviewed in Negrini et al., 2010). Interestingly, new evidence suggests the multiple genetic changes associated with cancers could also arise during a single, catastrophic event known as chromothripsis (reviewed in Jones and Jallepalli, 2012).

The genome undergoes a regular and continuous attack by external DNA-damaging agents such as ultraviolet radiation (UV) and by internal agents such as intracellular production of reactive oxygen species (ROS). Such agents can cause DNA lesions such as double-strand breaks (DSBs), which must be repaired as they can efficiently lead to

chromosomal translocation and genomic instability, thereby triggering oncogenic transformation (reviewed in Misteli and Soutoglou, 2009; Scott and Pandita, 2006). In addition to DNA sequence changes, epigenetic changes (e.g., changes in histones post-translational modifications and DNA methylation) can also occur and lead to carcinogenesis (reviewed in Katto and Mahlknecht, 2011)

Most cancerous cells acquire six biological features during their development, which are termed the Hallmarks of Cancer (reviewed in Hanahan and Weinberg, 2011). These are: resistance to programmed cell death (apoptosis), reduced response to growth inhibitory signals, sustained response to growth promotion signals, unlimited replicative capability, movement to other sites (metastasis) and sustained formation of blood vessels (angiogenesis). In addition, two emerging hallmarks in cancer cells development have also been suggested: first is the capability to avoid the immunological system, especially macrophages, T and B lymphocytes and natural killer cells; second is the ability to change cellular metabolism to influence cancerous cell proliferation (reviewed in Hanahan and Weinberg, 2011). Cancer has also been defined as representing the product of a failure in the regulation of the cell cycle (see Setion 1.2). In the normal cell cycle, defective or mutated cells undergo arrest or apoptosis. In contrast, cancer cells can circumvent cell cycle controls and continue to proliferate, thereby leading to an accumulation of additional genetic and epigenetic changes (reviewed in Blagosklonny, 2011; Foster, 2008; Jefford and Irminger-Finger, 2006).

Over half of cancer-specific chromosomal translocation breakpoints occur at chromosomal fragile sites; these are sites where the DNA sequence are prone to breaks or gaps during DNA synthesis, which makes them hotspots for chromosomal translocation (reviewed in Dillon et al., 2010).

1.2 Cell cycle and carcinogenesis

Cancer can be described as a cell cycle disease. The cell cycle process is a highly conserved and controlled system that includes checkpoints for appraisal of DNA integrity, cell size and extracellular growth signals. However, the cell cycle is deregulated during tumour development (reviewed in Eymin and Gazzeri, 2010).

The normal eukaryotic cell cycle consists of four distinct phases: the growth phase G_1, where the cells are prepared for S-phase; the S-phase, where the DNA is replicated; a growth phase G_2, where cells undergo continued growth and prepare for mitosis; and the M phase, where the chromosomes segregate and all cellular components are divided between two identical daughter cells. M phase is again followed by the G_1 phase. A fifth phase is a holding or quiescent phase named G_0, where the cell exits from the cell cycle upon terminal differentiation or under unfavourable growth conditions (reviewed in Budirahardja and Gönczy, 2009). The eukaryotic cell cycle is regulated by an enzyme family called the cyclin-dependent kinases (CDKs); these proteins are activated upon binding to regulatory proteins named cyclins to form a cyclin-CDK complex. This complex works as positive accelerator or regulator to influence the cell cycle process. The cyclin-CDK complex is deactivated when it binds to cyclin-dependent kinase inhibitors (CKIs), which work like brakes to stop the cell cycle in response to negative controlling signals (reviewed in Cross et al., 2011; Park and Lee, 2003). Unscheduled passage of cells through the cell cycle is prevented by the presence of checkpoints that exist at different points. These checkpoints react to internal signals (for instance, damaged DNA) or to external signals (for example, growth factors and stress), which causes either a cessation of the cell cycle, until DNA damage is repaired, or apoptosis, if repairs cannot be made. Three major checkpoints occur in the cell cycle: the G_1/S checkpoint, the intra-S checkpoint, and the G_2/M checkpoints (reviewed in Foster, 2008; Morgan, 2007) (Figure 1.1). Understanding the deregulation of the cell cycle process in cancer can give significant insights into how a normal cell becomes cancer cell. This new insight into cell cycle regulation can also provide clues for the design of new cancer therapies

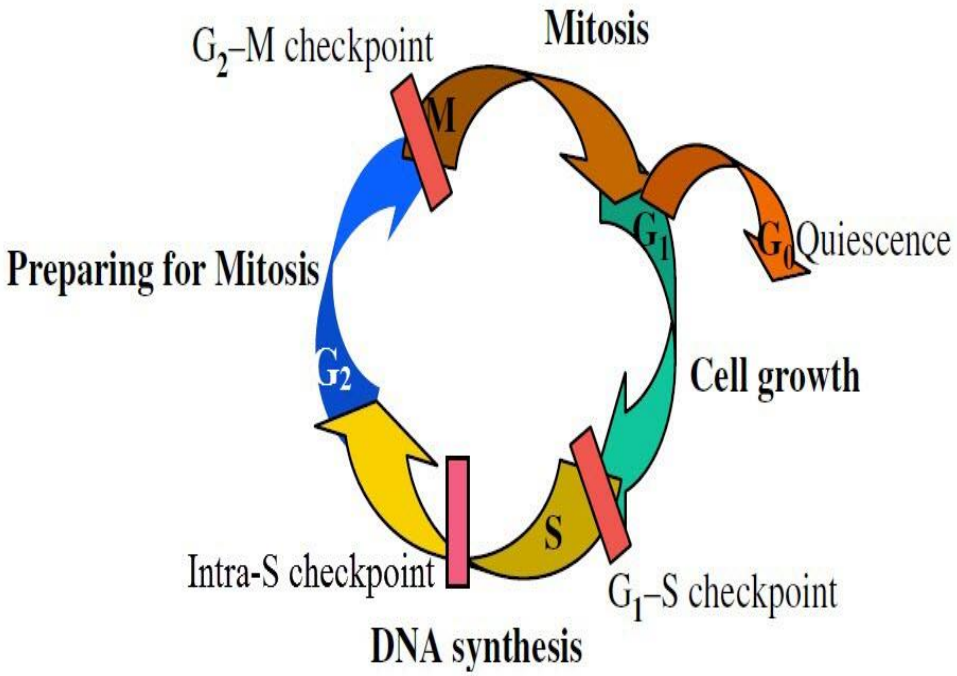

Figure 1.1 Cell cycle phases and checkpoints

The cell cycle consists of many sequenced events that are controlled by internal and external factors. The checkpoints work to prevent unscheduled passage of a cell through the cell division process. Checkpoints cause a cessation of the cell cycle until DNA damaged is repaired or cause apoptosis if repairs cannot be made (adapted from Foster, 2008).

1.3 Chromosomal translocation and cancer

Chromosomal translocations are abnormal genetic deviations. Translocation abnormalities occur when chromosomal breaks are repaired by inappropriate chromosome recombination. Translocations result in chromosomal rearrangement between heterologous chromosomes when a chromosome fragment is translocated from one chromosome to another, this may cause gene disruption, or can then lead to altered expression profiles of the genes located at the chromosomal breakpoint. Genes may be brought close to enhancer or promoter elements (juxtapositioning) or fusion of genes can be generated, all of which can cause oncogenic activation (reviewed in Agarwal et al., 2006; Nambiar et al., 2008; Nambiar and Raghavan, 2012). However, details of translocation mechanisms remain poorly understood (Chiarle et al., 2011). Translocation can lead to cancer when they occur in somatic cells (neoplastic translocations) and can result in inherited abnormalities when they occur during the first phases of embryogenesis (constitutional translocations), or at the meiotic steps of gamete formation (reviewed in Raghavan and Lieber, 2006). The most common chromosomal translocations have been reported in hematologic malignancies. However, chromosomal fusions have also been found in solid tumours and sarcomas (reviewed in Kumar-Sinha et al., 2008; Küppers, 2005; Nussenzweig and Nussenzweig, 2010).

One of the main initiators of chromosomal translocations is thought to be the formation of DSBs. These can be generated by exogenous DNA damaging agents or by normal physiological events, such as DNA replication failures during the cell cycle. However, DSBs can occur in normal processes controlled manner such as V(D)J recombination during B and T lymphocyte development (reviewed in Schatz and Swanson, 2011).

The first specific translocation recognised in human cancer was t(9;22) (q34;q11), discovered by Nowell and Hungerford in patients with chronic myelogenous leukaemia (CML) as an abnormal mini chromosome, and which has since become known as the Philadelphia Chromosome (Nowell and Hungerford, 1960). The reciprocal translocation between chromosome 9 and 22 is represented by t(9;22) and the breakpoint bands are represented by 9q34 and 22q11, respectively. This translocation causes gene fusion by juxtapositioning a part of the *BCR* gene onto chromosome 22 region q11 with a part of the *ABL1*gene on chromosome 9 region q34, thereby truncating chromosome 22 to form

the Philadelphia chromosome and elongating chromosome 9 (designated as der 9) (Figure 1.2). These two gene fusions create a *BCR-ABL* hybrid gene located on the Philadelphia chromosome. This *BCR-ABL* hybrid gene produces a hybrid mRNA that codes for an abnormal tyrosine kinase. This abnormal protein encourages myeloid cells to produce CML cells that are resistant to apoptosis (reviewed in Mitelman et al., 2007; Nowell, 2007; Nussenzweig and Nussenzweig, 2010).

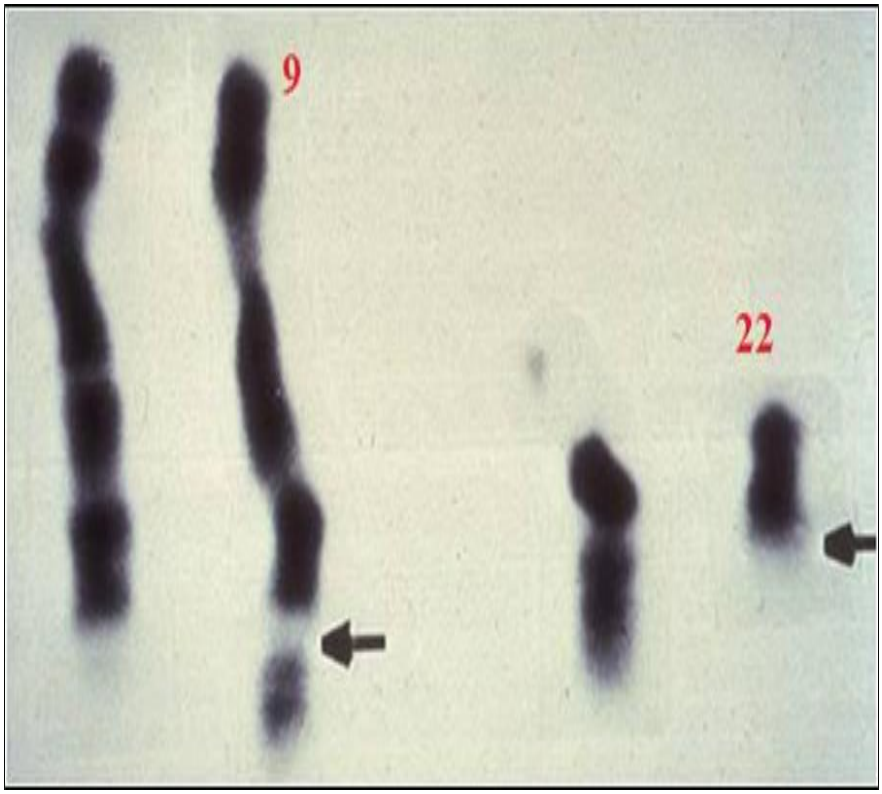

Figure 1.2 Karyotype of a CML patient.

The small truncated chromosome 22 (the Philadelphia chromosome) is indicated by the right hand arrow and results from a reciprocal translocation between chromosomes 9 and 22. The portion of chromosome 22 is transplaced to chromosome 9 and indicated by the left hand arrow. Chromosomes were prepared at metaphase and stained with Giemsa. (Nowell, 2007).

Chromosomal translocations are divided into two types: reciprocal and non-reciprocal translocations. Reciprocal translocations occur when two chromosomes exchange segments of their arms, resulting in two translocated portions. Reciprocal translocations often lead to an exchange of genetic material between non-homologous chromosomes. Reciprocal translocations can be balanced (where no fundamental net gain or loss of nuclear DNA occurs and the chromosomes potentially remain completely functional) or unbalanced (where chromosome segments are deleted or duplicated). Reciprocal translocations are usually balanced. Reciprocal translocations have been seen in a variety of cancers, such as leukaemia, lymphoma and sarcomas (reviewed in Gollin, 2007).

The second type of translocation is the nonreciprocal type (Robertsonian translocation), which is described as a one-way translocation where only a single chromosomal fragment is translocated to another nonhomologous chromosome (Figure 1.3). Nonreciprocal translocations frequently involve two acrocentric chromosomes, which fuse close to the centromere region, with loss of the short arms (Bandyopadhyay et al., 2002; Ferguson and Alt, 2001; reviewed in Nussenzweig and Nussenzweig, 2010).

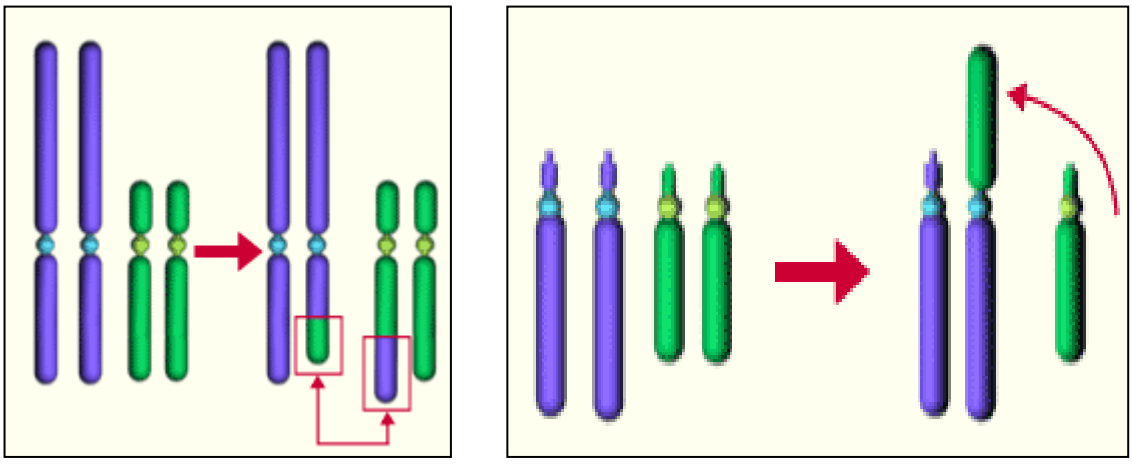

A **B**

Figure 1.3 Reciprocal and nonreciprocal translocations.

A. Reciprocal translocations occur between two non-homologous chromosomes, where the two broken ends re-join to form a new hybrid chromosome.
B. Nonreciprocal translocations occur when two non-homologous chromosomes lose their short arms and the q-arms fuse to each other, causing centric fusion.

1.4 DNA double-strand breaks repair pathways

Every day, many tens of thousands of DNA lesions occur in a single human cell (reviewed in Jackson and Bartek, 2009). There are many factors that can cause DNA lesions in eukaryotic cells, ranging from exogenous factors such as certain chemotherapeutic drugs, UV and ionizing radiation (IR) to endogenous factors such as reactive oxygen species (ROS; e.g., hydrogen peroxide, superoxide anions and hydroxyl radicals) which can arise as by-products of intracellular metabolism. Regardless of their source, these lesions need to be repaired correctly to avoid mutations. DSBs are considered the most dangerous lesions that exist within the genome of eukaryotic cells, as both strands in the double helix are broken. If not repaired correctly, DSBs may lead to large-scale rearrangement of chromosomes, which can cause carcinogenesis. Specific proteins in the nucleus recognise the damage at the site of a lesion and bind to other protein complexes. Eventually, by signal transductions, the cell cycle is arrested by the checkpoints or apoptosis may be induced. The cell cycle arrest continues until the lesions go through DSBs repair pathways. However, DSBs also occur normally in a controlled manner in V(D)J recombination during B and T lymphocyte development and during meiosis to initiate recombination between homologous chromosomes. DSBs must therefore be repaired quickly and accurately otherwise, illegitimate repair of these DNA lesions may cause chromosomal translocations and carcinogenesis (reviewed in Houtgraaf et al., 2006; Symington and Gautier, 2011).

Mammalian cells have two main pathways for the repair of DSBs: homologous recombination (HR) and non-homologous end joining (NHEJ). The HR pathway occurs if the DNA homologous sequence is available and sufficient. HR is initiated at the site of DNA lesions and includes a search for homologous sequences, and it is guided by specific proteins such as Rad51, followed by the use of the homologous sequence as a repair template (reviewed in Lieber et al., 2010; Mazin et al., 2010). On the other hand, NHEJ is a crucial pathway when the intact DNA template is not available to initiate the HR process. In this case, the DNA broken ends can ligate together without a requirement for the homologous sequence. The cell cycle phase is yet another important factor that dictates which repair pathway will be used either HR or NHEJ. HR is limited to the S and G_2 phases, when the replicated sister chromatid is available for use as a repair template.

In contrast, the NHEJ pathway is used predominantly during the G_1 phase (reviewed in Symington and Gautier, 2011).

1.4.1 Homologous recombination repair pathway

Homologous recombination is a high-fidelity, template-dependent repair mechanism which usually described as an error-free processes. The HR repair of DSBs requires an undamaged template, usually a sister chromatid. The HR repair process has been found in all forms of living cells (reviewed in Li and Heyer, 2008) and HR plays fundamental roles in mitosis and meiosis. In meiosis, HR is crucial for recombination between maternal and paternal chromosomes to allow exchange of genetic information and to increase genetic diversity by making new chromosomal variants. In meiosis, the HR process also establishes a physical linkage between homologous chromosomes, to guarantee their proper alignment at meiosis I. In mitosis, the primary role of HR is to repair single-strand gaps and DSBs that can arise due to the collapse of replication forks (RFs), which can be caused by endogenous processing of spontaneous damage or by exogenous DNA-damaging agents (Kasparek and Humphrey, 2011; reviewed in McFarlane et al., 2011). Furthermore, HR is essential for telomere maintenance and the repair of DNA interstrand cross-links (ICLs) (reviewed in Symington and Gautier, 2011).

The HR process begins by resection of the broken DNA ends at the DSB region to generate overhangs of single-stranded DNA (ssDNA) with 3ˈ OH ends; these are capable of invading the homologous sequence and work as primers for copy synthesis (Figure 1.4). In mammals, the MRE11-RAD50-NBS1 protein complex (MRN) (in *Schizosaccharomyces pombe*, Rad32-Rad50-Nbs1) plays two main functions; first, MRN has an enzymatic function that promotes DNA end resection and generates ssDNA. Second, MRN helps the DNA broken ends to recognise and align with the homologous sequence (Ueno et al., 2003; Yuan and Chen, 2010). In *S. pombe*, the exonuclease Exo1 is thought to be involved in the resection process as well (Szankasi and Smith, 1995). Afterward, the single stranded binding protein RPA (in *S. pombe*, Rad11) coats the overhangs of the ssDNA (Ono et al., 2003; Parker et al., 1997). The role of RPA is to help in the removal of the secondary structure before binding to RAD51 (Rhp51 in *S. pombe* and RecA in *Escherichia coli*) (reviewed in Grabarz et al., 2012; Krogh and Symington, 2004). After that, the BRCA2/PALB2 protein complex removes RPA from the ssDNA and binds to RAD51 (reviewed in Grabarz et al., 2012). RAD51 is a DNA-dependent

ATPase that forms nucleoprotein filaments. In addition, RAD51 in mammalian cells binds to BRCA2 which eventually activates it to form a nucleoprotein filament on the ssDNA (reviewed in McFarlane et al., 2011). Subsequently, ssDNA invades the homologous duplex DNA to form a displacement loop (D-loop) by the physical dissociation of a homologous duplex DNA strand by the invading ssDNA, in a process called strand invasion. Then, RAD52 mediates formation of a double Holliday Junction (dHJ) from the D-loop (reviewed in Krejci et al., 2012). Then, Rad54 promote the HJ branch migration, subsequently HJ resolution is facilitated by resolvase such as GEN1, SLX1/4 and Mus81-Eme1. The D-loop structure could be processed in different pathways, which can result in crossover or non-crossover events (Suwaki et al., 2011) (Figure 1.4). Several proteins (such as BLM) can disturb the D-loop or dissolve Holliday junctions, which stops mitotic crossovers and eventually reduce the risk of genome instability (reviewed in Chu and Hickson, 2009; Holthausen et al., 2011; McFarlane et al., 2011).

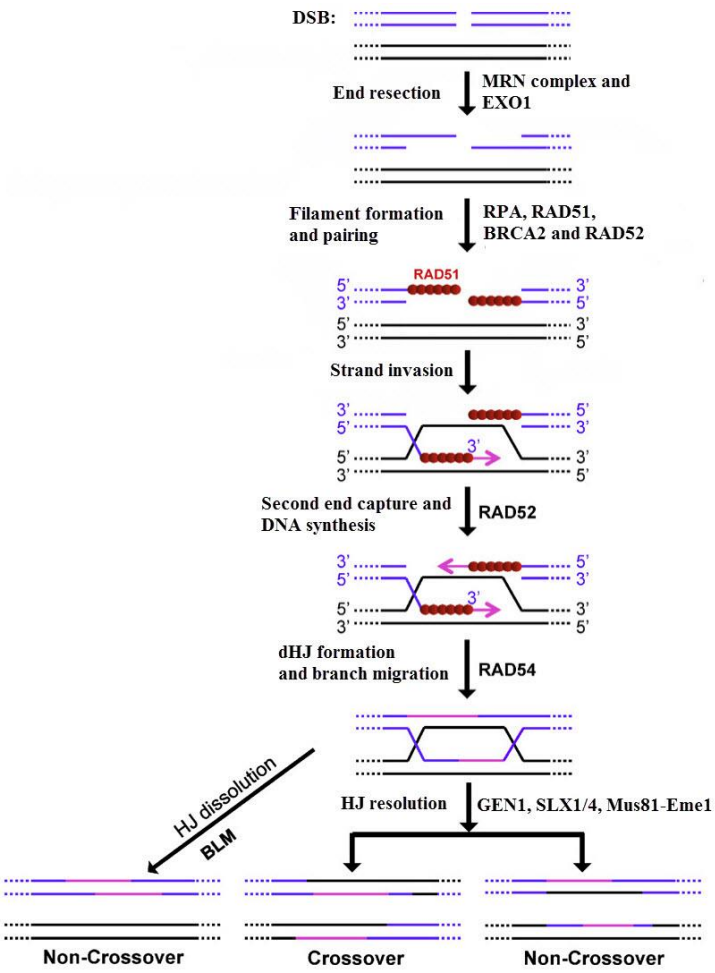

Figure 1.4 Sequential steps model for homologous recombination (HR) repair of a two sided double strand break.

HR requires sequential steps, as illustrated here: MRN recognises the DSBs. Then, ssDNA is generated by resection. After that, ssDNA binds to RPA. Then BRCA2 eliminates RPA before binding to RAD51. RAD52 mediates formation of dHJ. Subsequently, the ssDNA invades the homologous template, creating a D-loop and a Holliday junction, to prime DNA synthesis and to copy and ultimately restore genetic information that was disrupted by the DSB. Rad54 promote the HJ branch migration, subsequently HJ resolution is facilitated by resolvase such as GEN1, SLX1/4 Mus81-Eme1 which can result in crossover or non-crossover events. However, HJ dissolution can occur by specific protein such as BLM leading to non-crossover event (adapted from Suwaki et al., 2011).

1.4.2 Non-homologous end joining repair pathway

Non-homologous end joining is the simplest mechanism for DSB repair and it does not require an homologous chromosome. In this pathway, a short sequence homology region (1-6 bp) close to the DNA ends facilitates re-joining. The two severed DNA ends are rejoined directly in a sequential and independent fashion (reviewed in Weterings and van Gent, 2004). The first step in NHEJ is binding of the Ku protein to the two broken DNA ends. Ku is a heterodimer complex that contains Ku70 (69 kDa) and Ku80 (83 kDa) and forms a ring-shape structure. The loss of Ku leads to an increase in the rates of chromosome end fusions and telomeric shortening (Doherty and Jackson, 2001). The second step of NHEJ requires nuclease activity. In vertebrates, the nuclease contains a complex of two proteins, which are DNA protein kinase catalytic subunit (DNA-PKcs) and Artemis. Artemis has a weak nuclease activity of its own. However, once Artemis is bound to DNA-PKcs to form a complex at the DNA end, the complex becomes phosphorylated and forms a highly active endonuclease that can cleave both 5´ and 3´ overhangs of any length (Ma et al., 2002). The use of the MRN complex (MRE11-RAD50-NBS1), along with other nucleases, has also been suggested for processing of the DNA ends before ligation (Doherty and Jackson, 2001; Helleday et al., 2007). However, MRN complex orthologues are not essential for NHEJ in *S. pombe* (Manolis et al., 2001). In the third step, the two DNA ends are juxtaposed and then XLF-XRCC4 ligase IV complex rejoins the two DNA ends. Both the XLF and XRCC4 cofactors are required for ligase IV to target the DNA ends (Grawunder et al., 1997; Helleday et al., 2007) (Figure 1.5). In *S. pombe*, ligase IV (Lig4), Ku70 (Pku70) and Ku80 (Pku80) orthologues have been identified (Manolis et al., 2001; Miyoshi et al., 2003); however, no orthologues of DNA-PKcs and XRCC4 have been found (Callebaut et al., 2006).

The NHEJ mechanism is crucial for V(D)J recombination. In fact, defects in some NHEJ components can lead to several diseases; for instance, defects in DNA-PKcs and Artemis proteins in humans lead to severe combined immunodeficiency (SCID) (reviewed in Hefferin and Tomkinson, 2005; Moshous et al., 2001; Moshous et al., 2000) .

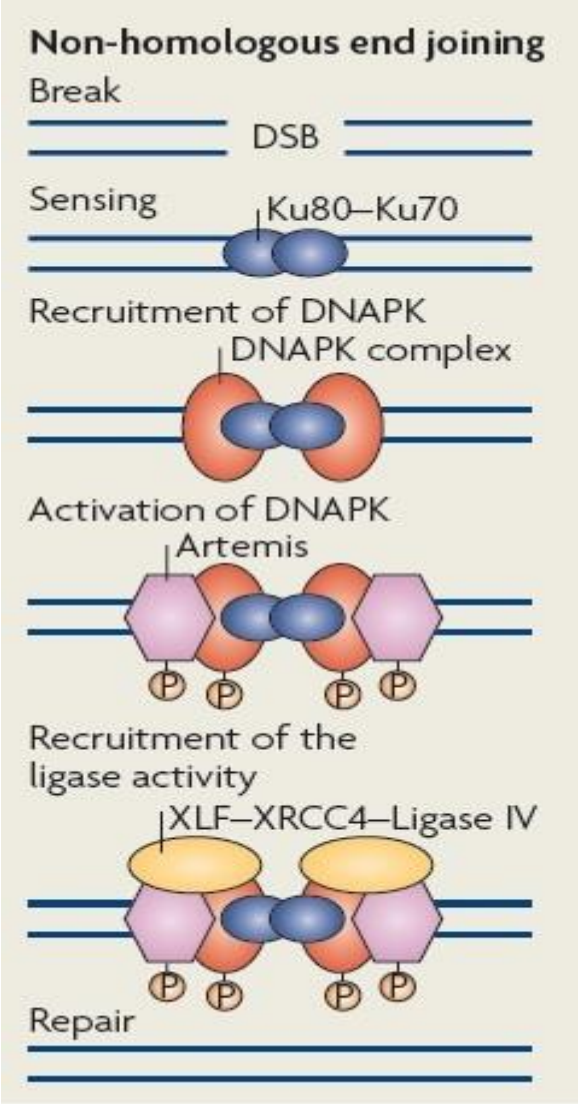

Figure 1.5 Non-homologous end joining repair pathway.

A DSB is recognised by the Ku80–Ku70 complex. This complex recruits the DNAPKcs, which cause activation of its kinase activity and the assembly of the DNAPK complex. DNAPK regulates and facilitates the processing of DNA ends and enhances the recruitment of DNA ligase IV, XLF, Artemis and XRCC4, which then accomplish the end joining repair (adapted from Misteli and Soutoglou, 2009).

1.5 Translin and TRAX

The *Translin* gene was identified in human cells as a novel gene that encoded a protein that binds specifically to chromosomal translocation breakpoint junctions. Its identification in a specific type of leukaemia and in many other different types of human lymphoid neoplasms (Aoki et al., 1995) has led to the suggestion that Translin is involved in chromosomal translocations and cancer formation. The mouse Translin orthologue was identified independently and has been linked to mRNA metabolism, particularly in the testes and neurons, and has been termed TB-RBP (Testes-Brain RNA-Binding-Protein) (Wu et al., 1997). A second protein, discovered by yeast two hybrid studies, was identified as binding partner of Translin and designated TRAX (Translin-associated factor X) (Aoki et al., 1997b). TRAX was also confirmed to interact with Translin by immunoprecipitation (IP) in mouse cytosolic extracts (Wu et al., 1999).

Translin and TRAX are highly conserved proteins with orthologues found in a broad range of eukaryotic species, including *S. pombe* and humans, which has suggested that they play an important biological function (Gupta et al., 2012; reviewed in Jaendling and McFarlane, 2010). However, the budding yeast, *Saccharomyces cerevisiae,* does not have a Translin orthologue (Laufman et al., 2005). Translin and TRAX have been implicated in many biological activities, such as carcinogenesis, genome stability regulation, neuronal function and development, spermatogenesis, mRNA processing, cell growth regulation and, recently, RNA interference (RNAi) and tRNA processing (Aharoni et al., 1993; Chennathukuzhi et al., 2003b; Cho et al., 2004; Han et al., 1995a; reviewed in Jaendling and McFarlane, 2010; Kasai et al., 1994; Kobayashi et al., 1998; Li et al., 2012; Li et al., 2008; Liu et al., 2009). However, the precise function of TRAX and Translin in some of these processes remains unclear. In addition, investigations using null mouse , *Drosophila* and *S. pombe* mutants showed that Translin and TRAX are not essential proteins (Chennathukuzhi et al., 2003b; Claussen et al., 2006; Jaendling et al., 2008).

Both TRAX and Translin expression patterns are similar in various human tissues (Meng et al., 2000). In mice, *TRAX* mRNA is found in various tissues such as brain, testes, spleen, heart, liver , kidney, and at a lower level in lung and skeletal muscle (Devon et al., 2000). Translin and TRAX have been found as components of the GRBP (Glucose Response element Binding Protein) in liver (Wu et al., 2003). In the mouse brain neurons, TRAX and TB-RBP form a complex, and are proposed to have a role in dendrite RNA

processing (Finkenstadt et al., 2000). The *TRAX* and *Translin* genes also seem to be expressed in more tissues than originally thought, as demonstrated by localisation in haematopoietic cells (Fukuda et al., 2008), suggesting they have some functional role in most cell types.

1.5.1 Role in chromosomal translocation and tumorigenesis

At the chromosomal level, *in vitro* gel mobility shift assays revealed that Translin protein bound to the chromosomal translocation breakpoint hotspots in patients diagnosed with T-acute lymphoblastic leukaemia (T-ALL) who carried the t(1;14)(p32;q11), t(8;14)(q24;q11) mutation and in patients who were diagnosed with many other different types of human lymphoid neoplasms (Aoki et al., 1995). In addition, Translin showed particularly strong binding to the consensus sequence motifs ATGCAG and GCCC(A/T)(G/C)(G/C)(A/T) at the breakpoint junctions of chromosomal translocations in different cases of lymphoid malignancies. Indeed, the name Translin was derived from Translocation (Aoki et al., 1995; reviewed in Jaendling and McFarlane, 2010; Kasai et al., 1994). Translin also showed specific binding to the chromosomal breakpoint junction in a patient diagnosed with Acute myeloid leukaemia (AML) carrying t(9;11)(p22;q23) (Atlas et al., 1998) and in a patient diagnosed with Chronic Myeloid Leukaemia (CML) carrying t(9;22)(q34;q11) (Martinelli et al., 2000). Translin binding specificity was also recognised in other types of cancer-associated translocation breakpoints (Abeysinghe et al., 2003; Chalk et al., 1997; Hosaka et al., 2000; Kanoe et al., 1999; Wei et al., 2003).

Translin can form an octameric ring (Figure 1.6) and it has been suggested this can recognise the DNA ends at recombination hotspots in the human genome (Kasai et al., 1997). Different studies have demonstrated Translin can bind to ssDNA or RNA (Aharoni et al., 1993; Jacob et al., 2004; Li et al., 2008). Thus, Translin has been proposed to mediate chromosomal translocations and tumour formation via a direct nucleic acid binding mechanism (Gajecka et al., 2006a; Gajecka et al., 2006b).

In contrast, TRAX shows no capability to bind either to DNA or RNA on its own (Li et al., 2008). However, the TRAX-Translin heteromeric complex has the capability and preference to bind to G-rich DNA sequences, whereas Translin on its own shows a preference for binding to G-rich RNA sequences (Lluis et al., 2010). In addition, a recent study has identified that TRAX protein, in the form of the heteromeric Translin-TRAX complex, directly binds to ssDNA (Gupta and Kumar, 2012). Human Translin has

binding affinities for single-stranded microsatellite repeats ($d(GT)_n$) and G-strand telomeric repeats ($d(TTAGGG)_n$) (Jacob et al., 2004), suggesting a possible role in telomere function. Additionally, Translin binding sequences have been found in human meiotic recombination hot spots, suggesting a possible role in meiotic chromosome dynamics (Badge et al., 2000).

Chromosomal translocations are associated with cancer formation (see earlier). Thus, all of the findings that indicate Translin and TRAX to have binding characteristics associated with the breakpoint hotspots in many cancer chromosomal translocations have led to the proposal that these two proteins are perhaps implicated somehow in tumorigenesis. However, the significance of these binding sites at breakpoint junctions is still unclear.

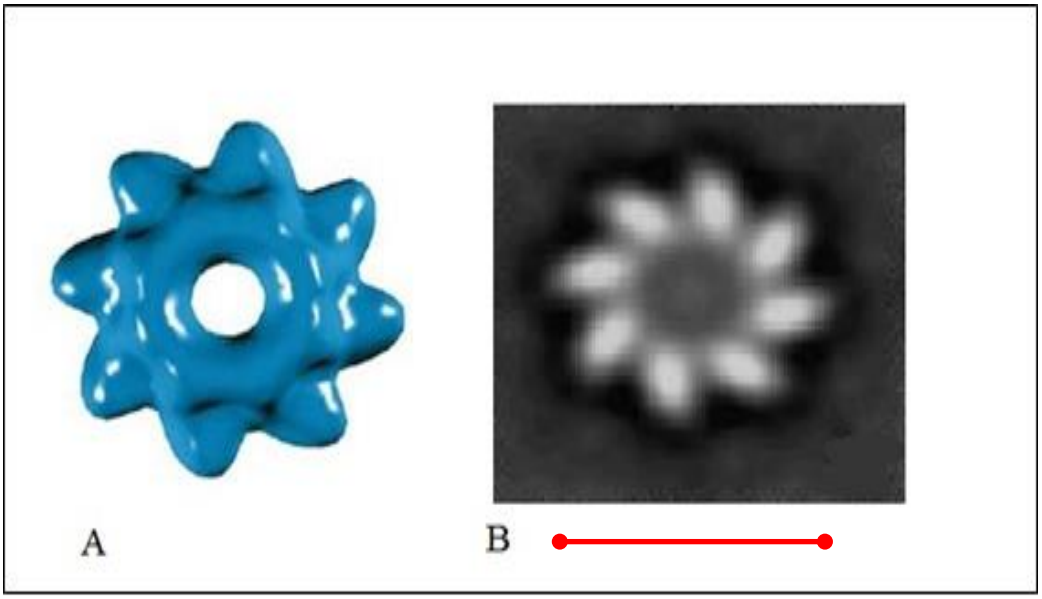

Figure 1.6 The Translin octameric ring-shaped structure

A. 3-D electron microscopy (EM) reconstruction of Translin.
B. Native Translin octameric ring as seen by electron microscopy. Scale bar in red is 100 A˚ (adapted from VanLoock et al., 2001).

1.5.2 Biochemical characteristics of Translin and TRAX

Both human and mouse Translins consist of 228 amino acids and have just three amino acid differences from each other. In contrast, *S. pombe* Translin consists of 236 amino acids and shares 54% similarity and 36% identity with the human Translin (Laufman et al., 2005). Gel chromatography analysis estimated the human Translin monomeric molecular mass at 26 kDa, whilst the native Translin molecular mass was estimated at approximately 220 kDa, which suggested that Translin forms an octameric ring (Aoki et al., 1995). The ability of Translin to form octomeric toroids was subsequently confirmed by electronic microscopy studies (Figure 1.6) (VanLoock et al., 2001). Translin was proposed to have a leucine zipper motif, which is essential for formation of the octameric ring (Aoki et al., 1995). However, crystallographic study indicates that the predicted leucine zipper motif is unlikely to form a functional leucine zipper (Sugiura et al., 2004). TRAX also contains a predicted leucine zipper at the N-terminal segment (residues 73-108) of human TRAX; however, the functionality of this leucine zipper is also unclear (Meng et al., 2000; Tian et al., 2011).

The TRAX molecular mass is 33 kDa and the protein has a significant similarity in homology to Translin (see Figure 1.7). A role for TRAX in nuclear transport of Translin has been suggested (Aoki et al., 1997b). TRAX possesses a NLS (nuclear localization signal) whilst Translin possesses a NES (nuclear export signal) (Laufman et al., 2005) (Figure 1.8). A conserved biochemical function of Translin is that TRAX stability is dependent on the presence of Translin, which indicates a close functional relationship between them (Chennathukuzhi et al., 2003b; Claussen et al., 2006; Jaendling et al., 2008; Yang and Hecht, 2004). TRAX levels are post-transcriptionally regulated by Translin; this fact was demonstrated by comparing the *TRAX* mRNA and protein levels in wild-type cells and *Translin* null cells, which indicated no alteration in *TRAX* mRNA levels and yet a big reduction in protein levels was observed (Jaendling et al., 2008; Yang et al., 2004). Whilst TRAX stability requires Translin, the stability of Translin is not affected by loss of TRAX (Claussen et al., 2006). Translin RNA binding activity is also not inhibited by TRAX level (Finkenstadt et al., 2000). Where *TRAX* gene homologues are identified in a species, *Translin* gene orthologues are found, which further indicates a functional relationship between them (Laufman et al., 2005).

Translin has RNAse activity but no identified DNAse activity (Wang et al., 2004), which led to the proposal that Translin plays a role in the regulation of RNA. Furthermore, Translin has the capability to bind to ssDNA, single-stranded RNA (ssRNA) and double-stranded-RNA (dsRNA), but has no ability to bind to dsDNA (double-stranded DNA), whilst TRAX, on its own, has no capability to bind to either DNA or RNA (Laufman et al., 2005; Wang et al., 2004). Only when complexed with Translin does TRAX show direct binding to ssDNA (Gupta and Kumar, 2012).

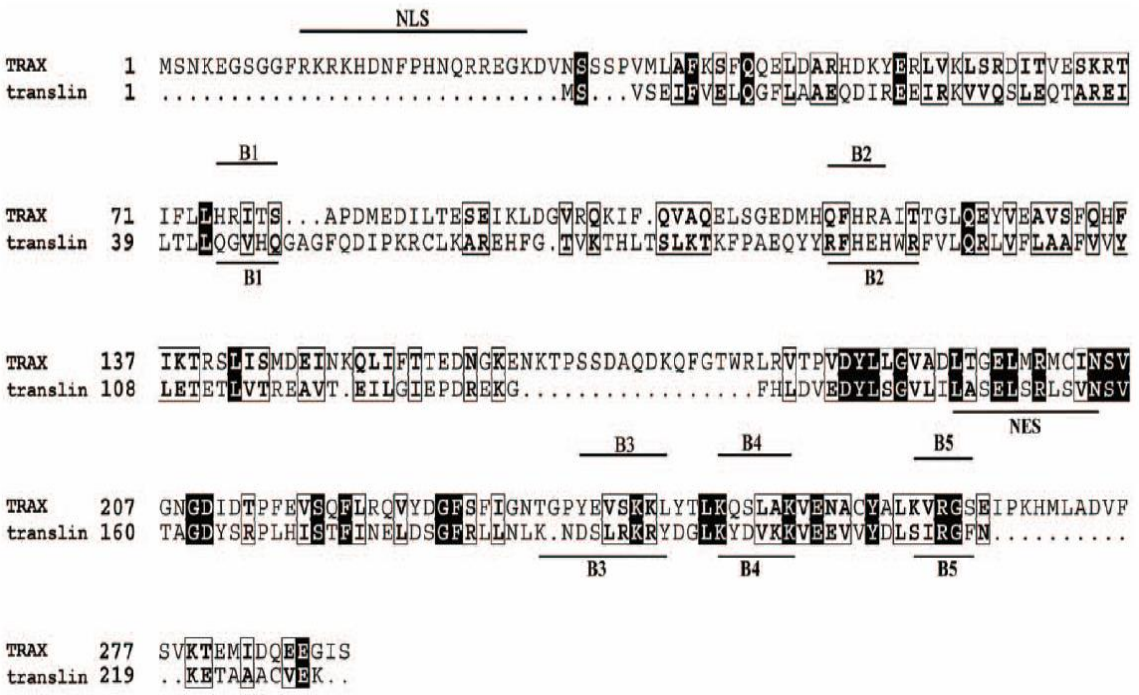

Figure 1.7 Alignment of amino acid sequences of human TRAX and Translin.

Similar sequences in Translin and TRAX are boxed and the identical sequences are highlighted in black. The NES sequence of Translin and the NLS sequence of TRAX are marked as well. The DNA binding sites on Translin and TRAX are shown (Gupta and Kumar, 2012).

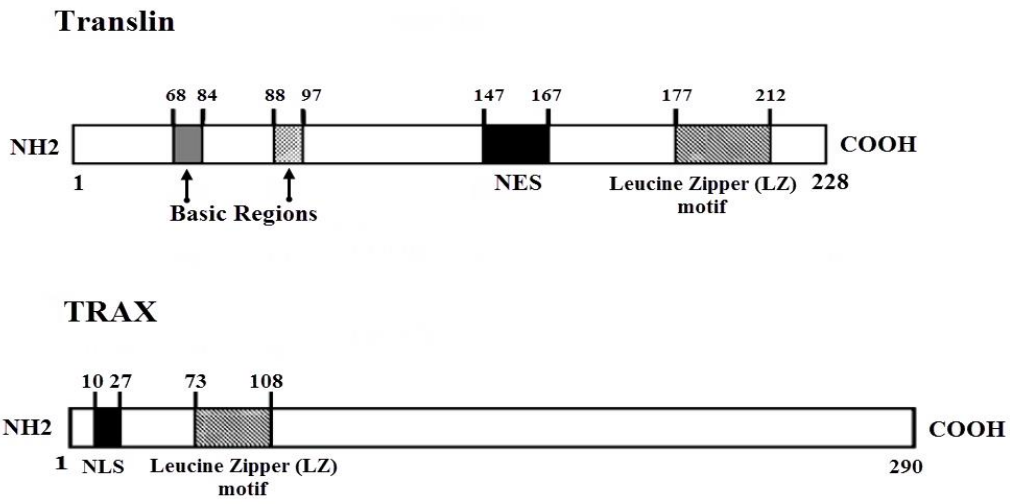

Figure 1.8 Schematic illustrations of Translin and TRAX proteins

Translin is characterised by having two nucleic acid binding domains (basic region). A Translin leucine zipper was identified near its C-terminal, whilst a TRAX leucine zipper was identified near its N-terminal. The regions of a nuclear export signal (NES) on Translin and nuclear localization signal (NLS) on TRAX are highlighted in black (adapted from Li et al., 2008). A recent study has found that TRAX in the form of a TRAX-Translin complex shows direct binding to ssDNA (Gupta and Kumar, 2012). However, the TRAX binding region is not shown here.

1.5.3 Possible role in DNA repair

Different studies have implicated Translin and TRAX proteins in maintaining genome stability, especially in response to DNA damage. Translin was localised mainly in the cytoplasm in many different cell lines; however, in lymphoid cell lines, it was localised in the nucleus (Aoki et al., 1995). Moreover, in mouse cell lines, Translin was localised in the nucleus six hours after treatment with the DNA damaging agents mitomycin C and ionising irradiation, whereas incubation for longer times led to a decrease in nuclear Translin levels (Fukuda et al., 2008; Kasai et al., 1997). Furthermore, the formation of hematopoietic colonies was severely delayed in Translin knockout mice compared to wild-type mice after exposure to ionising irradiation, which indicated a role for Translin in protection from radiation-induced damage (Fukuda et al., 2008). Because Translin does not have a NLS, therefore, its transport to the nucleus was suggested to occur in conjunction with another protein that had a NLS, possibly TRAX (Aoki et al., 1997a; Aoki et al., 1997b). Mouse Translin also interacted with GADD34 (DNA damage inducible and growth arrest protein) (Hasegawa and Isobe, 1999), a factor that stopped terminally differentiated myeloid leukaemia cells from undergoing apoptosis (Chou and Roizman, 1994). Involvement of GADD34 was also suggested in the translocation of Translin from the cytoplasm to the nucleus in response to DNA damage (Hasegawa et al., 2000).

TRAX interacts with a DNA binding protein C1D (gamma-irradiation inducible nuclear matrix protein that induce apoptosis) after exposure of mammalian cells to γ irradiation; this prevented binding of TRAX to Translin which stops formation of the Translin/TRAX complex and prevents this complex from binding to DNA. Thus, the C1D protein may play essential role in the formation of TRAX/Translin complex, thereby regulating its function (Erdemir et al., 2002). *In vitro* competition experiments showed that when TRAX bound to Translin, it prevented TRAX binding to C1D, and *vice versa*, suggesting the possibility that TRAX could be implicated in DSB repair (Erdemir et al., 2002). Moreover, when DNA is damaged by γ-irradiation, C1D is induced and targets DNA-PK which is essential for NHEJ repair pathway (see Section 1.4.2) and V(D)J recombination (Yavuzer et al., 1998).

Despite the evidence for a role in DNA damage recovery , *TRAX* and *Translin* mutants of *S. pombe* exhibit no negative responses to a range of DNA damaging agents, including

MMS (methyl methanesulphonate), HU (hydroxyurea), Phleomycin, mitomycin C and UV ultraviolet irradiation (Jaendling et al., 2008). Thus, any role in DNA damage recovery might be species or tissue specific.

1.5.4 Role in mRNA transport

Translin has been linked to mRNA transport in conjunction with other proteins. For example, in a male mouse germ line, Translin was identified as a component of a mRNP (mRNA ribonucleoprotein) complex responsible for intercellular and intracellular transport of specific mRNAs (Morales et al., 2002). Moreover, during meiosis, Translin is primarily found in the nucleus; however, during the subsequent developmental stages, Translin is localised in cytoplasm. Therefore, Translin may regulate mRNA processing through the ratio of TRAX and Translin levels (Morales et al., 1998).

Many studies have linked TRAX and Translin proteins to mRNA translational regulation and mRNA translocation in distinct types of tissue. For example, Translin was suggested to bind to mRNAs at the H and Y elements of 3ˈend of untranslated regions (3ˈ-UTRs) in mouse brain and testis cells (Han et al., 1995b; Han et al., 1995c; Thompson and Towle, 1991; Wu et al., 1997; Wu and Hecht, 2000). However, the importance of these binding specificities is still unknown because H and Y elements are G-rich loci and Translin binds to most G-rich ssRNAs. However, Translin binding to the 3ˈ-UTRs of mRNA in germ cells and neurons was suggested to lead to cessation of translation (Finkenstadt et al., 2000; Kobayashi et al., 1998; Kwon and Hecht, 1991).

Neurons and male germ cells undergo important polarization and differentiation steps. These steps require the translocation of specific mRNAs, proteins, organelles and vesicles. The translocation is conducted by motor proteins, which are needed for the trafficking of macromolecules, including mRNAs, along the microtubules. Examples of these motor proteins are the dynein and kinesin protein family members (Zou et al., 2002). In fact, early studies on Translin lead to the suggestion that it aids translocation of mRNAs along microtubules by an interaction with kinesin molecules (Wu et al., 1997). Coimmunoprecipitation studies on mouse testis cells showed that KIF17b (a member of the kinesin family) was coimmunoprecipitated with TRAX and Translin, which linked these two proteins to mRNA trafficking. KIF17b has been proposed to control mRNA translation and transcription in specific male germ cells (Chennathukuzhi et al., 2003a)

and it plays an important role in transcription and translocation of the activator of the cAMP-responsive-element modulator (CREM) in testes (ACT). In male germ cells, ACT is responsible for the activation CREM (Macho et al., 2002), which is a crucial protein for the spermatogenesis (Weinbauer et al., 1998). Transcription of mRNAs that bind to Translin is dependent on CREM, which has linked KIF17b and Translin to post-meiotic mRNA regulation of translation and transcription (reviewed in Jaendling and McFarlane, 2010).

A model was suggested for the export of the mRNP complex containing Translin/TRAX and mRNA from the nucleus to the cytoplasm via the nuclear pores. This complex is bound to KIF17b, and Translin is bound to the CRM1 exportin by its NES region (Cho et al., 2004). CRM1 is important for the nuclear export of many proteins that have NES regions. The mRNP complex is subsequently moved via the nuclear pores and then mRNP is attached firmly to the microtubules by KIF17b or Translin. The mRNA translation is suppressed temporarily by the attachment to KIF17b and activated by the detachment of KIF17b and Translin. On the other hand, in the cytoplasm, when mRNA translation is suppressed, KIF17b dissociates from the complex and the Translin/TRAX complex returns to the nucleus, probably facilitated by the NLS located on TRAX (Cho et al., 2004) (Figure 1.9). In mouse testes, TRAX interacted with the KIF2Aβ protein (a member of the kinesin family), as shown in yeast two hybrid studies, which indicated that TRAX could be implicated in mRNA movement in germ cell lines (Bray et al., 2002; Bray et al., 2004). However, Translin does not interact with KIF2Aβ; therefore, a Translin-independent role for TRAX in this pathway remains a possibility (Bray et al., 2004).

An involvement of TRAX and Translin was also apparent in the intracellular targeting of mammalian mRNAs of brain-derived neurotrophic factor gene (*BDNF*) (Chiaruttini et al., 2009). BDNF is a growth factor protein that is implicated in neuron survival and differentiation (Bath and Lee, 2006; Chiaruttini et al., 2009). Defect in BDNF result in an array of complex behavioural disorders such as obesity, autism, schizophrenia, depression and dementia (Chaldakov et al., 2009). The open reading frame of *BDNF* contains an exon that includes a Translin binding site and a mutation (G196A) in this region prevents dendritic targeting of BNDF mRNA and causes many psychological disorders (Bath and Lee, 2006; Krishnan et al., 2007; Pezawas et al., 2004). Moreover, *Translin* knockdown

by siRNA led to an inability of *BDNF* mRNA to achieve dendritic localisation (Chiaruttini et al., 2009). At present, many studies have linked distinct human neurological disorders with the *TRAX* gene, which supports the suggestion of a relationship between TRAX/Translin and mRNA processing in the human brain (Cannon et al., 2005; Hennah et al., 2005; Okuda et al., 2010; Palo et al., 2007; Schosser et al., 2009; Thomson et al., 2005). Supporting evidence comes from studies that show mice with *Translin* knockout display neurological and behavioural disorders (Chennathukuzhi et al., 2003c; Stein et al., 2006).

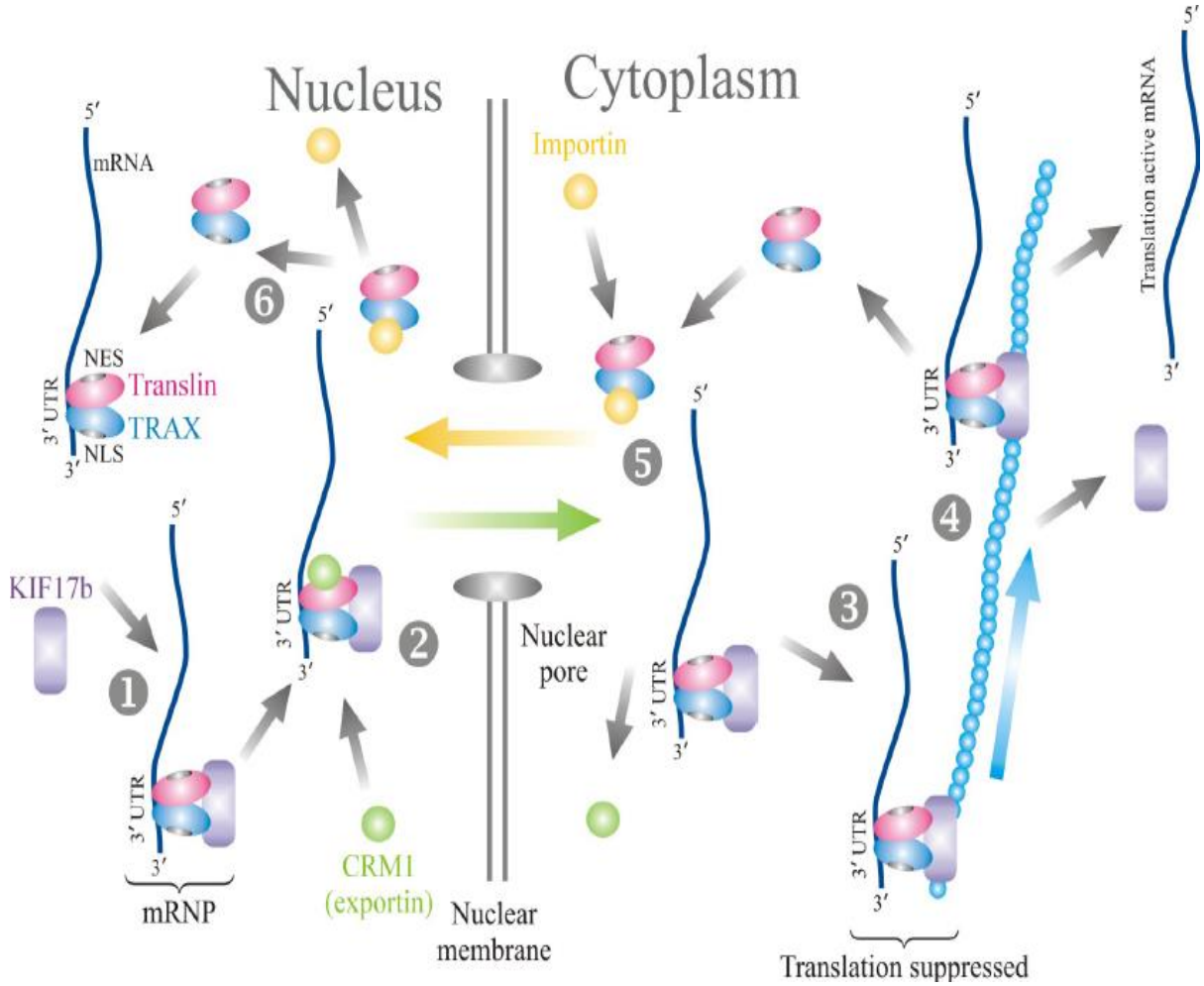

Figure 1.9 Diagram showing the steps of the suggested function of the TRAX-Translin complex in suppression of mRNA transfer and translation.

Step 1: TRAX and Translin bind to mRNA on the 3'-UTR and a kinesin (KIF17b) is recruited to form the mature mRNP complex. Step 2: The exportin (CRM1) is bound to NES on Translin to mediate export of mRNP from the nucleus to the cytoplasm via the nuclear pores. Step 3: CRM1 is dissociated from the complex, and then mRNP is attached to the microtubules (blue joined circles).Translin then mediates the microtubule transport to the site of mRNA translation. Step 4: The mRNA separates from the microtubules and translation is activated by the dissociation of TRAX and Translin. Step 5: Importin is attached to NLS on TRAX and then the TRAX-Translin complex is returned to the nucleus. Step 6: Importin is dissociated from TRAX, and then the cycle of the TRAX-Translin complex is initiated again to form a new mRNP (reviewed in Jaendling and McFarlane, 2010).

1.5.5 Role in tRNA processing

Heitz, in 1928, reported that chromosomes can be distinguished as having euchromatin and heterochromatin regions depending on condensed state at interphase (Heitz, 1928). The less condensed regions are called the euchromatin regions and contain active genes that are usually transcribed, whereas the highly condensed regions are called the heterochromatin regions and contain silenced genes that are not transcribed (Huisinga et al., 2006). Heterochromatin regions such as the centromere and the telomeres are characterised by repetitive DNA elements, such as transposable elements, or groups of satellite sequences and they retain their inaccessible and highly condensed structure during all phases of the cell cycle (Birchler et al., 2000; Grewal and Jia, 2007). Heterochromatin protects the genome stability by repressing illegitimate recombination between the repetitive DNA elements (Hannon, 2003). Heterochromatin formation in *S. pombe* and many other eukaryotes is enhanced by hypermethylation and hypoacetylation of histone H3 at lysine K9 (Grewal and Elgin, 2002).

Heterochromatin does not spread on chromosome to lead to silencing of adjacent euchromatin loci (Talbert and Henikoff, 2006). Heterochromatin spreading is restricted by chromatin barriers that create boundaries to this spreading (Sun and Elgin, 1999). The absence of these barriers leads to malfunctions in chromosome segregation, which indicates the important role of these barriers in the centromere (Scott et al., 2007).

In yeast, transfer-RNA (*tRNA*) genes, along with transcription factors TFIIIB and TFIIIC and RNA polymerase III (Pol III), work to stop heterochromatin spreading and create boundary barriers in the centromere and in the mating type loci (McFarlane and Whitehall, 2009; Scott et al., 2007). Similar observations of this role for *tRNA* genes in creating heterochromatin barriers were also seen in mice (Ebersole et al., 2011). The *tRNA* genes are highly distributed, either as tiny clusters or individually, in the centromere of *S. pombe* and are allocated between euchromatin and heterochromatin loci to prevent spreading of heterochromatin (Haldar and Kamakaka, 2006; Iwasaki et al., 2010; White, 2011). Mutations in *tRNA* gene promoter loci or even in the factors that bind to the promoter cause tremendous decreases in the barrier activity, which illustrates the importance of *tRNA* gene transcription (Oki and Kamakaka, 2005; Scott et al., 2007).

The barrier activity at centromere 1 (*cen1*) in *S. pombe* is dependent on an intact *tRNA*^{Ala} gene (Scott et al., 2007). In fact, *tRNA*^{Ala} gene knockout caused heterochromatin spreading (West et al., 2004). In addition, transcription of the *tRNA* gene repressed transcription of its neighbouring genes that were transcribed by RNA pol II (Kinsey and Sandmeyer, 1991). This phenomenon was called *tRNA* gene-mediated silencing (Kendall et al., 2000).

tRNAs are small RNA chains (73-93 nucleotides) that also have a fundamental function in protein synthesis. Maturation of pre-tRNAs to tRNAs requires a precise mechanism to process both 5′ and 3′ ends of the pre-tRNAs with RNase P (Hartmann et al., 2009; Phizicky and Hopper, 2010; Walker and Engelke, 2006). Recently, the *Neurospora* TRAX-Translin protein complex was shown to work as an RNase that, along with RNase P, digests the 5′ pre-tRNA fragments (Li et al., 2012). Knockout of *Neurospora TRAX* and *Translin* genes led to dramatic accumulation of pre-tRNA fragments (Galagan et al., 2003). Deletion of *Translin* in mice led to elevation of six tRNAs, which indicated that the mammalian TRAX-Translin complex is also implicated in tRNA processing. Cell growth, protein translation activity and tRNA levels were also elevated in *TRAX* and *Translin* knockout cells (Li et al., 2012). This finding was similar to the previous observation in *TRAX* and *Translin* knockout of *S. pombe* cells, where the rate of cell proliferation was increased slightly (Laufman et al., 2005). TRAX and Translin were also implicated in normal cell proliferation in mouse embryonic stem cells (Yang et al., 2004).

Recently, the Translin-TRAX complex was shown to interact with RNAi machinery and to play an important role as a promoter for the RISC complex (RNA-induced silencing complex) (see below). In fact, the TRAX-Translin complex was designated as C3PO (component 3 promoter of RISC) because the TRAX-Translin complex was implicated in RISC activation (Liu et al., 2009). The function of C3PO in the RNAi machinery was established in *Drosophila* (Liu et al., 2009). However, RNAi is not found in *Neurospora*, which suggests that the role of TRAX and Translin in tRNA processing is more ancient than their function in the RNAi machinery (Li et al., 2012). On the other hand, the function of TRAX and Translin in tRNA processing could give us a clue to their roles in many other different biological activities.

1.6 RNA interference (RNAi)

In eukaryotes, RNAi is a highly conserved mechanism for controlling gene silencing. The term originally referred to the capability of exogenously inserted dsRNA (double-stranded RNA) molecules to silence the gene expression of homologous sequences in *Caenorhabditis elegans* (Fire et al., 1998). Subsequently, small RNA molecules (approximately 20-30 nucleotides) have been identified to have a fundamental role in controlling which genes are silenced and which genes are active, and how active they are.

Small RNA molecules (sRNAs) have been implicated in gene silencing by two mechanisms. First, sRNAs target chromatin directly to generate heterochromatin, which leads to suppression of transcription; this mechanism is termed chromatin-dependent gene silencing (CDGS). Second, sRNAs targets the mRNAs to destroy it or to inhibit its translation; this mechanism is termed post-transcriptional gene silencing (PTGS) (reviewed in Valencia-Sanchez et al., 2006). In addition, sRNAs are involved in genome defence against viral infection and retrotransposition, a function also conserved in plants (reviewed in Castel and Martienssen, 2013; Moazed, 2009; Tomari and Zamore, 2005). Three types of sRNAs have been identified: siRNAs (small interfering RNAs), miRNAs (microRNAs) and piRNAs (piwi-interacting RNAs) (Ohnishi et al., 2010).

The siRNAs contain between 21 to 25 nucleotides that are produced from dsRNA by a cleaving RNase III enzyme called Dicer, which cleaves dsRNA into siRNAs. These siRNAs have a fundamental role in controlling which polyribonucleotide molecules will be degraded or translated. These siRNAs then load onto the Argonaute protein and work as guides for Argonaute to target selected nucleic acids though base-pairing, thereby inactivating targeted sequences by different pathways (reviewed in Moazed, 2009). siRNAs also perform positive feedback in some organisms and promote the resynthesis of the dsRNAs using the target complementary RNAs as template, through the activity of an enzyme called RdRP (RNA-dependent RNA polymerase). This creates more substrates for Dicer (Volpe and Martienssen, 2011). The small RNAs are guided to their RNA targets by RISC (RNA-induced silencing complex) or its nuclear form, RITS (RNA-induced transcriptional silencing complex). In *S. pombe*, siRNAs play an important function in heterochromatin assembly (see below); for example, siRNAs can guide RITS to recruit the H3K9 histone methyltransferase to sites of heterochromatin forming (reviewed in Moazed, 2009).

miRNAs contain between 21 to 25 nucleotides and are found in plants and metazoans. They are produced from hairpin precursors by cleavage by two enzymes; Drosha (nuclear RNase III) and Dicer (cytoplasmic RNase III but nuclear in plants). The miRNAs work mainly in the regulation of PTGS. Furthermore, when miRNAs base-pair to mRNAs, they cause translational inhibition or even mRNA destruction (reviewed in He and Hannon, 2004). However, in plants, miRNAs are implicated in destruction of mRNAs but not in inhibition of mRNA translation (Hake, 2003).

piRNAs contain between 24 to 31 nucleotides and are produced from RNA transcribed heterochromatic clusters, as seen in *Drosophila.* The piRNAs are implicated in the defence mechanism against mobile DNA sequences named transposable elements (transposons) in animal germlines. Transposons can excise themselves and move, thereby causing potential genomic instability, and they form half of the human genome and one third of the *Drosophila* genome (Halic and Moazed, 2009). piRNA mechanism protects the genome against these parasitic elements by packing them into heterochromatin through an RNAi mechanism (Obbard et al., 2009).

In *S. pombe*, the RNAi mechanism plays an essential role in heterochromatin formation. The RNAi machinery is necessary for maintaining the heterochromatin state at the pericentromeric DNA region by maintaining Swi6 (heterochromatin protein 1) localisation and maintaining H3K9 methylation (Verdel et al., 2004; Volpe et al., 2002). However, RNAi is a redundant pathway for maintaining the heterochromatin state at the telomeres and the *mat* loci, because RNAi genes are dispensable once heterochromatin loci have been established (Hall et al., 2002; Kanoh et al., 2005). *S. pombe* contains just one copy of each of the key RNAi gene, such as RNA-dependent RNA polymerase (*rdp1*), Argonaute (*ago1*), Dicer (*dcr1*). *S. pombe* has a RITS complex (in fact, the RITS complex was firstly identified in *S. pombe*) and deletion of any RITS complex component genes causes a loss of Swi6 recruitment at the pericentromeric chromatin and loss of H3K9 methylation (Verdel et al., 2004). All these findings, along with the conservation of RNAi components, make *S. pombe* a good model to study RNAi mechanisms.

Recently, Halic and Moazed (2010) were suggested a possible Dcr1-independent, Ago1-dependent pathway that involve RNAs to trigger heterochromatin formation. They reported that H3K9me of the heterochromatin region was not reduced in a *dcr1*Δ mutant to the same degree of *ago1*Δ mutant. Therefore, a model was suggested for Dcr1-

independent, Ago1-dependent pathway in fission yeast for formation of H3K9me in the centromeric repeats (*dh* and *dg*) (Figure 1.10)

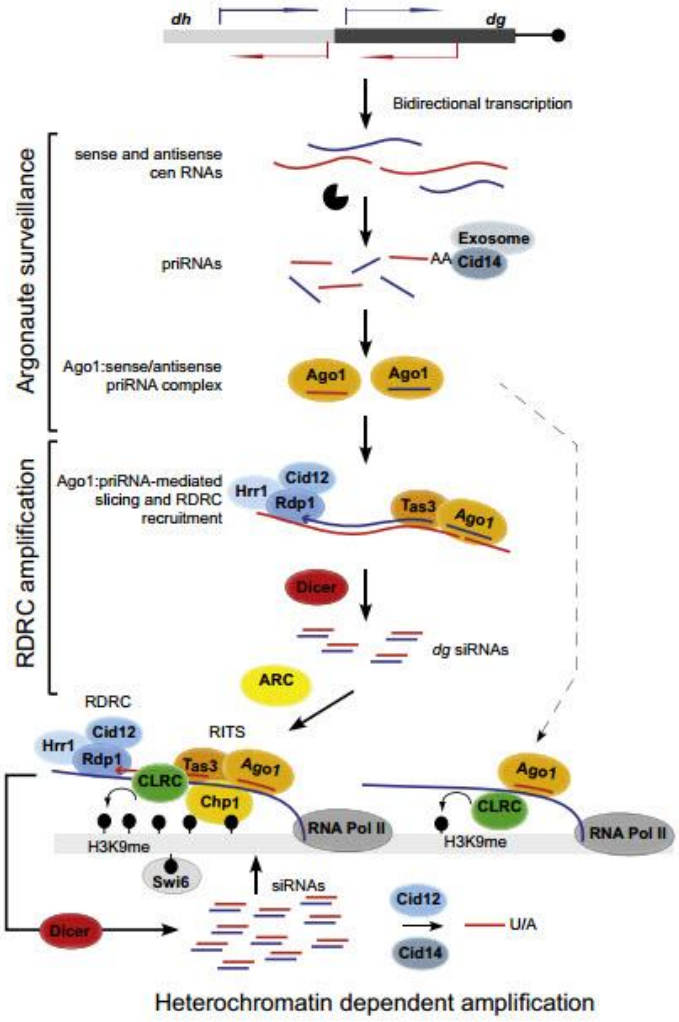

Figure 1.10 A fission yeast model for Dcr1-independent, Ago1-dependent pathway for the heterochromatin maintenance of H3K9me at the centromeric repeats (*dh*, *dg*).

The model proposed by Halic and Moazed suggests that the essential pathway to establish heterochromatin is depended on exosome-generated primal small RNAs (priRNAs) that act according to Argonaute (Ago1) to eventually recruit the RNA-dependent RNA polymarease complex (RDRC). In turn, via the action of Dicer (Dcr1)-produced *dg* small interfering RNAs (siRNAs), this results in the RNA-induced transcriptional silencing (RITS) complex, which mediate methylation of H3K9 by the Clr4-Rik1-Cul4 (CLRC) complex that forms the binding sites for Swi6 (HP1). The redundant pathway (shattered line) is dependent upon priRNAs and Ago1, but is independent of Dicer. The factors driving the redundant pathway have not been discovered yet (Halic and Moazed, 2010).

1.6.1 Evidence for a role for TRAX and Translin in RNAi

A recent study on *Drosophila* established that the TRAX/Translin complex works as a RNAi (RNA interference) regulator (Liu et al., 2009), where RNAi is a conservative mechanism controlling gene silencing (see below). In this study, *Translin* knockout flies exhibited RNAi malfunction. Lysates from the *Translin* mutants showed a 25% lower RISC (RNA-induced silencing complex) activity than in the wild-type; however, when recombinant TRAX and Translin were added to the lysate, the RISC activity was restored to normal levels. Therefore, the TRAX and Translin complex was renamed C3PO (component 3 promoter of RISC) (Liu et al., 2009). However, neither TRAX nor Translin has a significant function in *Neurospora* RNAi (Li et al., 2012).

RISC activation requires the transformation of RLC (RISC loading complex) to the activated RISC form. This process requires unwinding of duplex siRNAs (small interfering RNAs), followed by insertion of the guider strand onto Ago2. A siRNA-gel shift assay performed on *Drosophila* ovary extracts from a *Translin* mutant and wild-type showed that RISC levels were significantly reduced in the absence of C3PO, indicating a fundamental function for the complex in the transformation of RLC to activated RISC. C3PO is currently proposed to promote RISC activation by removing the siRNA passenger strand (Liu et al., 2009). C3PO exhibits high endoribonuclease activity against siRNA, but lower activity against double-stranded siRNA or ssDNA (Liu et al., 2009). Therefore, a model for the role of C3PO was suggested (Figure 1.11), where C3PO promotes RISC activation by removing the passenger strand. This action facilitates the loading of the guider strand onto Ago2. Therefore, all findings now strongly suggest that TRAX and Translin function in RNAi regulation (Liu et al., 2009). Another study has now supported a function for C3PO in the activation of human RISC and Ago2 (hAgo2) (Ye et al., 2011). Liu and co-workers (Liu et al., 2009) focused primarily on the function of C3PO in siRNA mediated RNA cleavage by removal of the siRNA passenger strand. They did not investigate miRNA mediated translation silencing, because their study focused only on *Drosophila* Ago2, whereas *Drosophila* Ago1 mediates miRNA translation silencing (Hammond et al., 2001; Okamura et al., 2004).

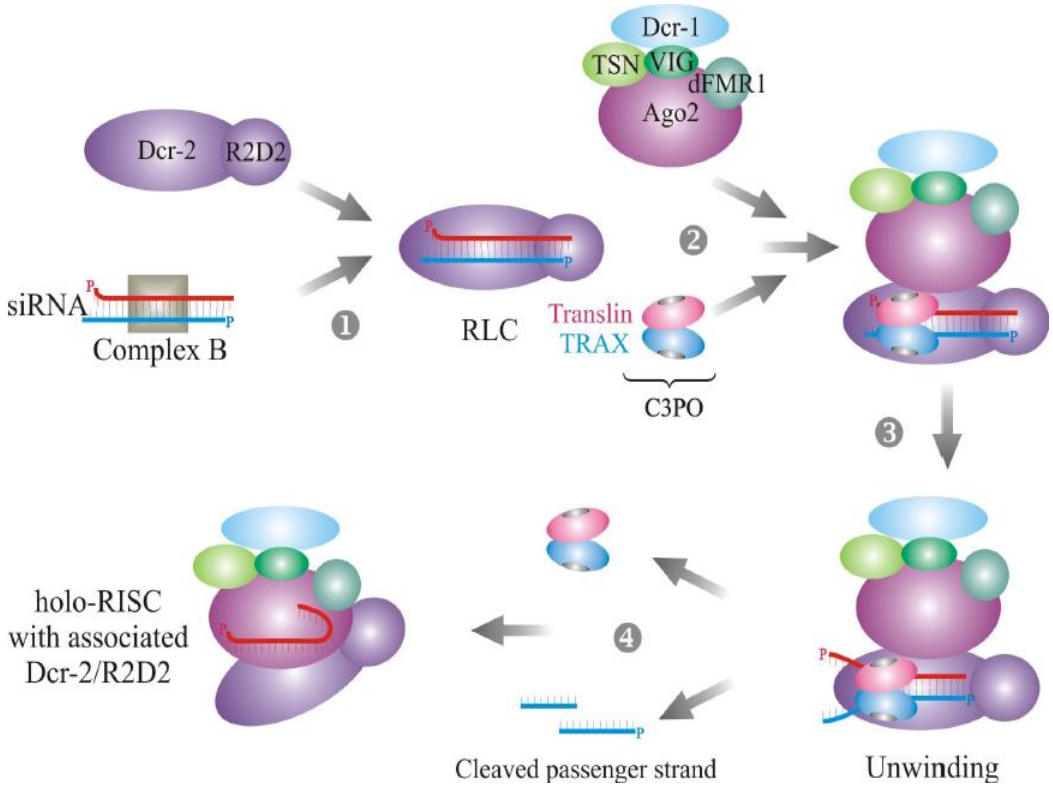

Figure 1.11 Schematic illustration of the model of the suggested role for C3PO in *Drosophila.*

Step 1: The duplex siRNA is translocated to the RLC complex (R2D2 and Dcr-2). Step 2: C3PO is joined to the RLC complex and the RISC complex Ago2, dFMR (*Drosophila* FMR), VIG (vasa intronic gene), TSN (Tudor-staphyloccal nuclease), Dcr-1. Step 3: C3PO enhances the removal of the passenger strand from duplex siRNA by its endoribonuclease capability. Step 4: The holoRISC invades the selected mRNAs. However, whether C3PO remains attached to holoRISC, as shown in this model, is not clear (reviewed in Jaendling and McFarlane, 2010).

1.6.2 Heterochromatin loci in *Schizosaccharomyces pombe*

The chromatin core component consists of repetitive nucleosomes. Each nucleosome has approximately 147 DNA base pairs, which form complexes with eight core histone proteins. These histone complexes include two copies each of histones H2A, H2B, H3 and H4 (reviewed in Goto and Nakayama, 2012). In addition, linker DNA is linked to nucleosomes by another histone, H1, which is attached to the core of the nucleosomes and stabilises the nucleoprotein complex (reviewed in Olsson and Bjerling, 2011). Chromatin condensation is regulated by histone post-translational modifications like methylation of H3 on lysine residues (e.g., K4, K9, K27, K36 and K79) and H4 on lysine residue K20, which activate or inactivate the transcription of genes surrounded by chromatin (Martin and Zhang, 2005).

An example of these modifications is the acetylation of H3 and H4, which leads to reshaping of the chromatin to a less-condensed form (euchromatin, transcriptionally active). However, methylation and hypoacetylation of H3 on K9 lead to reformation of the chromatin to its highly condensed form (heterochromatin, transcriptionally inactive); this modification of H3K9 is the core of heterochromatin formation due to binding to heterochromatin protein 1 (HP1) (in *S. pombe*, Swi6) (Gerace et al., 2010; Olsson and Bjerling, 2011). The Euchromatin regions are distinguished by methylation of lysine 4 of histone 3 (H3K4me) and acetylation of lysine 9 of histone 3 (H3K9ac). All these epigenetic modifications change the histone proteins at N-terminal regions, which are highly conserved regions in a broad range of eukaryotic species including fission yeast and humans (reviewed in Goto and Nakayama, 2012) (see Figure 1.12).

The heterochromatic regions in the *S. pombe* genome are well characterised and epigenetically regulated to be "silent", which means that genes in these regions remain in a silent state without expression. Moreover, any protein-coding gene genetically inserted into these regions should also be under the influence of the same epigenetically silent regulation (reviewed in Goto and Nakayama, 2012). Four major heterochromatin areas were identified in *S. pombe* genome: the centromeres and the telomeres of all chromosomes (*S. pombe* genome has just three chromosomes), the rDNA (ribosomal DNA repeats) and the mating type loci (reviewed in Djupedal and Ekwall, 2009; Klar, 2007). The nucleosomes at all of these heterochromatic regions are hypoacetylated and the H3K9 residues are extensively methylated. In fact, in *S. pombe*, the methylation of

H3K9 serves as a binding site for the four chromodomain proteins. These four chromodomain proteins are: Swi6 and Chp2, which are homologous to mammalian HP1, and Chp1 and Clr4 (Thon and Verhein-Hansen, 2000).

Both Swi6 and Chp2 are implicated in the maintenance of the heterochromatic region. Swi6 functions in the recruitment of cohesin to the centromeres and is involved in siRNA processing, which is crucial for heterochromatin maintenance at the centromeres. Chp2 is involved in transcriptional gene silencing (TGS) by contributing Clr3 subunits to deacetylate H3K14. Chp2 is also implicated in TGS by limiting the access of RNA pol II to the chromatin (Motamedi et al., 2008; Sugiyama et al., 2007). Chp1 is a component of the RITS complex and is bound to H3K9me, implicating it in RITS localisation along the chromatin (Verdel et al., 2004). Clr4 is an enzyme that methylates H3K9 in all heterochromatic regions. Heterochromatin spreading stops in cells with deleted Clr4 genes (Zhang et al., 2008).

In addition, as mentioned earlier, *S. pombe* requires RITS complex to mediate heterochromatin establishment at different heterochromatic loci in the genome. Recently, it was reported that Mmi1, an RNA-binding protein guides RITS to these specific meiotic gene mRNA targets (Hiriart et al., 2012). Mmi1 protein is associated to RNA surveillance machinery to degrade selective meiotic mRNAs which eventually shut off the selective meiotic genes by the Mmi1 pathway. This new discovery in fission yeast has suggested a mechanism for recruiting RNAi to selective meiotic genes and also proposed that RNAi is involved in the sexual differentiation control (Hiriart et al., 2012).

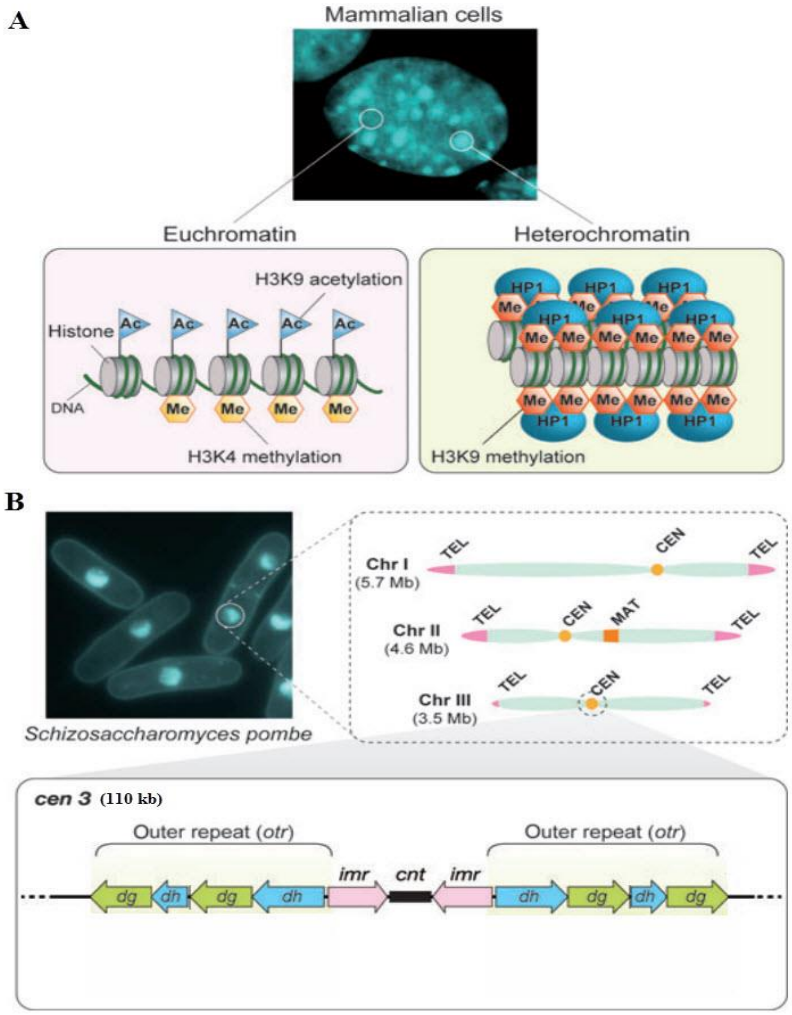

Figure 1.12 Schematic illustrations of the modifications to chromatin that lead either to heterochromatin or euchromatin formation. Some heterochromatic regions (*cen*, *mat* and *tel* loci) in *S. pombe* genome are also shown.

A. Heterochromatin is a highly condensed form of chromatin and appears as densely stained regions in the nucleus, as seen in mouse cells stained with DAPI. Heterochromatin is generated by histone modifications such as methylation of H3K9. In contrast, H3K9 acetylation and H3K4 methylation lead to euchromatin formation.
B. *S. pombe* has three chromosomes with different homochromatic regions (*cen*, *mat* and *tel* loci). Cells were stained by DAPI. At the lower panel, the centromeric regions are organised in distinguished regions, *cnt* and *imr*, that are flanked by the *otr* region that has two repetitive sequences (*dh* and *dg*) (adapted from Goto and Nakayama, 2012).

1.6.2 i Centromeres

Fission yeast centromeres, like *Drosophila* and mammalian centromeres, are characterised by highly repetitive DNA sequences (Doe et al., 1998; Morris and Moazed, 2007). The centromeres of *S. pombe* are divided into three regions. The *cnt* (the central core) is a non-repetitive domain where the kinetochore is assembled and the CenH3 containing nucleosomes are found. The other two regions, which are flanking regions of *cnt*, are characterised by repetitive inverted repeats and silent chromatins where Swi6 binding to H3K9me is induced by an RNAi mechanism (see previous). These two flanking regions are the *imr* (innermost repeats) and *otr* (outer repeats); the latter is divided into two types of sequences *dg* and *dh* (Pidoux and Allshire, 2004).

Heterochromatin in the centromere is characterised by H3K9 methylation, followed by Swi6 (HP1) protein attachment. Heterochromatin is initiated at the *otr* area and then spreads over the pericentromeric regions (reviewed in Grewal and Moazed, 2003). Insertion of the *ura4*$^{+}$ reporter gene insertion in the heterochromatic regions (*otr* and *imr*) leads to complete silencing of expression of this gene (Allshire et al., 1994).

The RNAi pathway is associated directly with centromeric heterochromatin formation and maintenance (Creamer and Partridge, 2011; Halic and Moazed, 2010). Deletion of any RNAi components prevents Swi6 localisation and H3K9 methylation (Volpe et al., 2002). The *dg* and *dh* DNA sequences in the *otr* region are transcribed by RNA polymerase II to produce noncoding transcripts, which are processed into sRNAs by the RNAi mechanism. Knockout of any RNAi component leads to accumulation of these noncoding RNAs and subsequently loss of the siRNAs (Motamedi et al., 2004; Volpe et al., 2002).

The histone methyltransferase Clr4 is required for processing of centromeric transcripts by RNAi. Knockout of Clr4 leads to upregulation of noncoding centromeric RNAs and loss of centromeric siRNAs (Halic and Moazed, 2010; Motamedi et al., 2004). In general, deletion of Swi6 or Clr4 or any RNAi components leads to defective silencing of marker genes that inserted in the *otr* regions (White and Allshire, 2008).

1.6.2 ii Mating types, telomeres and rDNA loci

Heterochromatic regions are found in *S. pombe* at mating-type loci, telomeres and rDNA. These regions are formed and maintained by complicated processes that involve DNA-binding proteins and the RNAi mechanism.

In *S. pombe*, three mating-type cassettes are recognised. The first, *mat1*, is an expressed domain that is maintained in the M (minus) or P (plus) state. The other two regions are *mat2-P* and *ma3-M,* which are silent domains. Mating-type switching occurs when a single-stranded DNA break occurs during DNA replication, and recombination subsequently occurs with a donor cassette of either *mat2-P* or *ma3-M*. The *mat2-P*, *ma3-M* and the area between them (*K* region) are heterochromatic regions (reviewed in Klar, 2007). Initiation of silencing depends on different DNA sequences, including the *cenH* region, which shares 96% sequence homology with the *dh* and *dg* repeats of the centromere. The *cenH* plays a role in heterochromatin assembly by acting as an RNAi-dependent nucleation point (Verdel and Moazed, 2005).

RNAi factors are implicated in creating heterochromatin at the mating-type loci (*mat2/3*) by recruiting the Clr4 H3K9 methyltransferase as they do in centromeres. A second pathway works by the binding of the transcription factors Pcr1 and Atf1. These transcription factors bind to the region between *mat3* and *cenH* and subsequently recruit Swi6 and Clr4 in an RNAi-independent fashion (Jia et al., 2004b). Knockout of any RNAi components has a silencing impact only when combined with knockout of *pcr1* or *atf1*; this suggests that Swi6 heterochromatin is maintained by two redundant pathways (Jia et al., 2004b).

At the telomeres, Taz1 (DNA-binding protein) is associated directly with repeat cassettes and recruits two proteins, Rif1 and Rap1, which are implicated in the control of telomeric clustering and length, and in the maintenance of the heterochromatic regions at the chromosomal ends (Kanoh and Ishikawa, 2001). Taz1 is recruited by Swi6 indirectly as well. On the other hand, heterochromatin maintenance at the telomeres does not require RNAi. Swi6 association with the telomere is not affected by deletion of any RNAi components; however, the combined deletion of $taz1^{+}$ and any RNAi components leads to the loss of Swi6 association with the telomere. This suggests that RNAi is implicated in heterochromatin formation but not in heterochromatin maintenance (Kanoh et al., 2005).

The eukaryotic Ribosomal DNA (rDNA) genes encode for ribosomal RNA (rRNA). The loci of these genes are heterochromatic regions that are organised as long tandem repeats in subtelomeric regions of Chromosome III. Insertion of reporter genes into rDNA loci silence them because of the heterochromatin position effect of these regions (Dubey et al., 2009). However, the fundamental function of heterochromatin at the rDNA locus could be to prevent the recombination at these regions and to prevent the loss of rDNA repeats (Kobayashi et al., 2004).

1.7 *Schizosaccharomyces pombe* and human cell lines as models for this study

The fission yeast, *S. pombe*, was isolated in the late 1890s; however, genetic studies on *S. pombe* only began in the late 1940s (Forsburg, 2005). Nowadays, this yeast is considered one of the workhorses of modern cell biology. It is a simple eukaryote and has only three chromosomes, which can be easily genetically manipulated. The genome of *S. pombe* is completely sequenced: it has 4979 genes and 14 Mb of DNA. Fifty genes in *S. pombe* are related to human diseases. Many genes are conserved in humans and *S. pombe*, but are missing in other model organisms (Wood et al., 2002). More importantly, the RNAi machinery, TRAX and Translin protein homologs are all found in *S. pombe* (Laufman et al., 2005; Martienssen et al., 2005). *S. pombe* has distinct heterochromatic regions in the centromere, telomeres, and mating-type loci, as well as rDNA, all of which have much similarity with epigenetic silencing systems in other organisms (Pidoux and Allshire, 2004). All these characteristics make *S. pombe* an excellent model for this study.

Three human cell lines are also used to prepare for future work: two colon cancer cell lines, SW480 and HCT116, and one human testicular germ cell tumour cancer line, NTER2. The work on these cell lines will provide preliminary data for further research.

1.8 The aim of this study

The aim of this study was to determine whether TRAX and Translin function in the regulation of heterochromatin regions via RNAi redundant pathways. The investigations focused on different heterochromatic regions the centromere, telomeres, and mating-type loci and rDNA. DNA damaging agents were used to determine the effect of TRAX and Translin deletion, together with other RNAi factors, on the DNA repair system. In addition, different human cell lines were used for preliminary analysis and preparation for future work on Translin and TRAX, along with RNAi components (Dicer and

Argonaute2). Understanding the role of Translin and TRAX in RNAi processes will help us to elucidate the distinct roles of these cancer-associated proteins.

CHAPTER 2

Material and Methods

2.1 Yeast and bacterial media recipes

Reagents for yeast, bacterial media and supplements were obtained from Sigma, Becton Dickinson (BD) and Fisher Scientific, unless otherwise stated. Enzymes and buffers were obtained from New England Biolabs (NEB), unless stated otherwise. All media were made in bulk and then sterilised by autoclaving at 10 psi for 20 mins. Media were stored in bottles, and agar was remelted in a microwave oven before use. All media were dissolved in distilled H_2O. Agar was omitted from liquid media (see Table 2.1).

For minimal media, amino acid supplements were added to a final concentration of 250 mg/l. All antibiotics were added to desired media at concentration of 100 µg/ml. Antibiotics used in this project included Geneticin (G418) (Sigma), Nourseothricin (Werner BioAgents) and Ampicillin (Sigma).

Table 2.1 Yeast and bacterial media recipes

YEA Yeast extract Glucose Agar	**(1 litre)** 5 g 30 g 14 g
YEL Yeast extract Glucose	**(1 litre)** 5 g 30 g
SPA Glucose Potassium dihydrogen orthophosphate Agar Vitamins (x1000)	**(1 litre)** 10 g 1 g 30 g 1 ml (added after autoclaving media)
NBA Nitrogen base Ammonium sulphate $(NH_4)_2SO_4$ Glucose Agar	**(1 litre)** 1.7 g 5 g 5 g 10 g

ME Malt extract Agar	**(1 litre)** 30 g 14 g
EMM2 Potassium hydrogen phthalate Di-sodium hydrogen phosphate Na_2HPO_4 Ammonium chloride NH_4Cl Glucose Vitamins (x1000) Minerals (x10,000) Salts (x50) Agar	**(1 litre)** 3 g 2.2 g 5 g 20 g 1 ml 0.1 ml 20 ml 14 g
LBA Tryptone Yeast extract Sodium chloride Agar Ampicillin (50mg/ml)	**(1 litre)** 10 g 5 g 10 g 14 g 2 ml
Vitamins (x1000) Pantothenic acid Nicotinic acid *myo*-inositol Biotin	**(1 litre)** 1 g 10 g 10 g 10 mg
Salts (x50) Magnesium chloride hexahydrate Calcium chloride dihydrate Potassium chloride Disodium sulphate	**(1 litre)** 52.5 g 0.735 g 50 g 2 g
Minerals (x10,000) Boric acid Manganese sulphate Zinc sulphate septahydrate Iron chloride hexahydrate Potassium iodide Molybdic acid Copper sulphate Citric acid	**(1 litre)** 5 g 4 g 4 g 2 g 1 g 0.4 g 0.4 g 10 g
After autoclaving add a few drops of 1:1:2 Chlorobenzene/dichloroethane/chlorobutane	

2.2 *traX, tsn1, dcr1* and a*go1* gene deletions using the PCR method

Four genes (*traX, tsn1, dcr1* and a*go1*) were deleted in *S. pombe* using the Bähler approach (Bähler et al., 1998). This involve the knockout cassettes which were amplified using PCR primers that include homologous (70-100 bp) to the ends of the desired gene to be deleted and the homologous (20 bp) to the DNA flanking region of the selectable marker cassettes. In some cases *kanMX6* cassette were used, in other cases *natMX6* or *ura4*$^{+}$ cassette were used. The different primer sequences are listed in Table 2.2. The primers were design using the Bähler lab genome regulation software:
http://www.bahlerlab.info/cgi-bin/PPPP/pppp_deletion.pl

All plasmids and primers were diluted 10-fold with 1x TE buffer [1.0 M Tris-HCl (pH 8.0) and 1.0 M EDTA] before use in PCR. For the *traX* gene deletion, each of the 50 µl PCR reactions contained: 1 µl DNA template (20 ng of plasmid DNA), 1 µl high fidelity Phusion polymerase (FINNZYMES), 1 µl 10x dNTPs, 1 µl each of forward and reverse primers at a concentration of 20 ng/ µl, 10 µl 5x Phusion™ HF buffer and 35 µl sterile distilled H_2O. The PCR programme was as follows: initial heating for 1 minute at 98ºC, followed by 30 cycles of 10 secs at 98ºC, 30 secs at 55ºC, and 20 secs at 72ºC. Final elongation was carried out for 5 mins at 72ºC. For the *dcr1* and *ago1* gene deletions, each of the 50 µl PCR reactions contained: 1 µl DNA template (20 ng of plasmid DNA), 1 µl high fidelity Phusion polymerase (FINNZYMES), 1µl 10x dNTPs, 1 µl each of forward and reverse primers at a concentration of 20 ng/ µl, 10 µl 5x Phusion™ GC buffer and 35 µl of sterile distilled H_2O. However, when using the *natMX6* cassette, the volume of water was reduced to 32.5 µl and 2.5 µl of DMSO was added to the reaction. The PCR programme was as follows: initial heating for 1 minute at 98ºC followed by 30 cycles of 10 secs at 98ºC, 30 secs at 59ºC and 1 minute 50 secs at 72ºC. Final elongation was performed for 5 mins at 72ºC. Several PCR reaction products were pooled and purified using phenol/chloroform (see Section 2.4). Each cassette was then transformed into the desired *S. pombe* strains by the Lithium Acetate (LiAc) method (see Section 2.5). All strains of *E. coli* and *S. pombe* that were used or constructed are listed in Tables 2.3 and 2.4.

Table 2.2 PCR primers used to delete *traX, tsn1, dcr1* and a*go1* genes

Primer name	Sequence	Location
TRAX-kan-F	5′-TAT AGA CTT ATA CAT TTA TAC CTT CCA CAC GGC TTT GCT GAA TTG AGG ATA TTA TAA AAC TTT AAC CGA ATT TGC CAA ATC GGA TCC CCG GGT TAA TTA A -3′	Forward primer for the kan ^{R} cassette for *traX* replacement
TRAX-kan-R	5′-ATT ATG ATT TTC AAA AGC TGC AAA ACA GAA AAA CTT TTA ATA AAC TAG TAA GGT GTC TGT CGA GAG CTG TCG ATC ATA TAT GAA TTC GAG CTC GTT TAA AC -3′	Reverse primer for the kan ^{R} cassette for *traX* replacement
Tsn-NatMX6-F	5′-TTA TTT GCA TAC TGA AAA CAT CAT TCG AAT ATC AAC ACT ACT CAA CAG CAT ACA TTA CAG ATT AAG TCG ACG GAT CCC CGG GTT AAT TAA-3′	Forward primer for the kan ^{R} cassette for *tsn1* replacement
Tsn-NatMX6-R	5′-ATA TTA AAA AAG CAA TTT TAT CGG CTC AAT TTT AGT CAA GCG TAC AGC TGG CAA ATA AAT TGT TAG CAA TGA ATT CGA GCT CGT TTA AAC-3′	Reverse primer for the kan ^{R} cassette for *tsn1* replacement
Dcr-pAW1-F	5′-ATA GCT TAG GAT TCA TTA TTT TTT AAG AGA CAA ATT TCT CGT CAA TTG AAT GAA ACC TTC CGC CTT TAT TTT CTT TTT GAC GGA TCC CCG GGT TAA TTA A-3′	Forward primer for the *ura4* cassette for *dcr1* replacement
Dcr-pAW1-R	5′-GCT TTG GAG ACC CAA ATT GAA AGT TTG AAA AGT TAC AAG GGC CGC GGT CAT AAA AAA TGA AAT ACT GTA TAT TTC AAG TCG AAT TCG AGC TCG TTT AAA C-3′	Reverse primer for the *ura4* cassette for *dcr1* replacement
DcrNatMX6-F	5′-ACA TAT GCA TGT TTA TTT GAA TAG CTT AGG ATT CAT TAT TTT TTA AGA GAC AAA TTT CTC GTC AAT TGA ATG AAA CCT TCC GCC TTT ATT TTC TTT TTG ACG GAT CCC CGG GTT AAT TAA-3′	Forward primer for the Nourseothricin ^{R} cassette for *dcr1* replacement
DcrNatMX6-R	5′-AAT ATC ACG AAA GGA TCC GTG CTT TGG AGA CCC AAA TTG AAA GTT TGA AAA GTT ACA AGG GCC GCG GTC ATA AAA AAT GAA ATA CTG TAT ATT TCA AGT CGA ATT CGA GCT CGT TTA AAC-3′	Reverse primer for the Nourseothricin ^{R} cassette for *dcr1* replacement

Ago-pAW1-F	5′-GGT TTG GTA TAT ATA AGC TTC CAA CCG CCA AAG CGA ATT GTC TTC AGC CAA CTC GTC CTT TAT GAT TCA GAG TGA GTA GGC GGA TCC CCG GGT TAA TTA A-3′	Forward primer for the *ura4* cassette for *ago1* replacement
Ago-pAW1-R	5′-TAA GGA AGT AAA AGT TGT GGG CAA TCC AGT AGT CAA TCG TAT ATC TAT TTC ATT ACT TAT TGC ATG CAA TCC ATC AAA CAG AAT TCG AGC TCG TTT AAA C-3′	Reverse primer for the *ura4* cassette for *ago1* replacement
AgoNatMX6-F	5′-TAT GAT GAG TCC TAA TCT AGG GTT TGG TAT ATA TAA GCT TCC AAC CGC CAA AGC GAA TTG TCT TCA GCC AAC TCG TCC TTT ATG ATT CAG AGT GAG TAG GCG GAT CCC CGG GTT AAT TAA-3′	Forward primer for the Nourseothricin ^{R} cassette for *ago1* replacement
AgoNatMX6-R	5′-AAA AAC AGA AGC AGA TTT AAT AAG GAA GTA AAA GTT GTG GGC AAT CCA GTA GTC AAT CGT ATA TCT ATT TCA TTA CTT ATT GCA TGC AAT CCA TCA AAC AGA ATT CGA GCT CGT TTA AAC-3′	Reverse primer for the Nourseothricin ^{R} cassette for *ago1* replacement

Table 2.3 *E. coli strains* and plasmids used in this project

Bangor strain number	***E. coli* strain and plasmid**	**Source**
BE9	pARC782 (*kanMX6 amp* ^{R})	McFarlane collection
BE180	pAW1 (*ura4*$^{+}$ *amp* ^{R})	D. Pryce
BE183	pYL16 (*natMX6 amp* ^{R})	E. Hartsuiker

Table 2.4 *S. pombe* strains used in this project

Strain Number	Genotype	Source
BP1	*h⁻ 972* (Wild type)	McFarlane collection
BP8	*h⁺* 975 (Wild type)	McFarlane collection
BP90	*h⁻ ade6-M26 ura4-D18leu1-32*	McFarlane collection
BP91	*h⁺ ade6-52 ura4-D18 leu1-32*	McFarlane collection
BP153	*h⁻ mis6-302*	McFarlane collection
BP187	*h⁻ mis4-242*	McFarlane collection
BP743	*h⁻ rad3-136*	McFarlane collection
BP846	*h⁺ ade6-M210 hop1::kanMX6*	McFarlane collection
BP1079	*h⁻ ade6-M26 ura4 -D18 leu1-32 tsn1::kanMX6*	McFarlane collection
BP1080	*h⁻ ade6-M26 ura4-D18 leu1-32 tsn1::kanMX6*	McFarlane collection
BP1089	*h⁻ ade6-M26 ura4 -D18 leu1-32 traX::kanMX6*	McFarlane collection
BP1090	*h⁻ ade6-M26 ura4 -D18 leu1-32 traX::kanMX6*	McFarlane collection
BP1162	*h⁺ bub1:: kanMX6 ura4-D18 leu1-32*	McFarlane collection
BP1731	*h⁺ ade6-M26 rec10-175 ::kanMX6*	McFarlane collection
BP2203	*h⁻ cntTM1(Nco1)::ura4⁺ ura4-DS/E leu1-32 ade6-M210*	McFarlane collection
BP2204	*h⁻ otrR1(Sph1)::ura4⁺ ura4-DS/E leu1-32 ade6-M210*	McFarlane collection
BP2221	*h⁻ ago1::G418ᴿ ade6-M210 ura4-DS/E leu1-32*	McFarlane collection
BP2292	*h⁹⁰ ade6-M26 ura4-D18 leu1-32*	McFarlane collection
BP2294	*h⁻ ade6-M210 ura4-D18 leu1-32 Ch16-23R*	McFarlane collection
BP2385	*h⁻ cntTM1(Nco1)::ura4⁺ ura4-DS/E leu1-32 ade6-M210 ago1::kanMX6*	McFarlane collection
BP2386	*h⁻ imr1(Nco1)::ura4⁺ ori1 ura4-DS/E leu1-32 ade6-M210 ago1::kanMX6*	McFarlane collection
BP2388	*h⁻ otrR1(Sph1)::ura4⁺ ura4-DS/E leu1-32 ade6-M210 ago1::kanMX6*	McFarlane collection

BP2406	*h⁻ ade6-M210 leu1-32 ura4-D18 Ch16-23R traX:: kanMX6*	This study
BP2407	*h^{90} ade6-M210 leu1-32 ura4-D18 traX:: kanMX6*	This study
BP2408	*h^{90} ade6-M210 leu1-32 ura4-D18 traX:: kanMX6*	This study
BP2409	*h⁺ ade6-52 ura4-D18 leu1-32 traX:: kanMX6*	This study
BP2410	*h⁺ ade6-52 ura4-D18 leu1-32 traX:: kanMX6*	This study
BP2411	*h⁻ cntTM1(Nco1)::ura4⁺ ura4-DS/E leu1-32 ade6-M210 traX::kanMX6*	This study
BP2412	*h⁻ cntTM1(Nco1)::ura4⁺ ura4-DS/E leu1-32 ade6-M210 traX::kanMX6*	This study
BP2413	*h⁻ otrR1(Sph1)::ura4⁺ ura4-DS/E leu1-32 ade6-M210 traX::kanMX6*	This study
BP2472	*h⁻ ade6-M210 leu1-32 ura4-D18 Ch16-23R ago1:: kanMX6*	McFarlane collection
BP2499	*h⁻ imr1(Nco1)::ura4⁺ ori1 ura4-DS/E leu1-32 ade6-M210 traX:: kanMX6*	This study
BP2506	*h⁻ imr1(Nco1)::ura4⁺ ori1 ura4-DS/E leu1-32 ade6-M210*	McFarlane collection
BP2704	*h⁺ rDNA::ura4⁺ ura4-DS/E ade6-M210*	McFarlane collection
BP2705	*h⁺ Ch16-m23::ura4⁺ TEL[72] ura4-DS/E leu1-32 ade6-M210 (Ch16 ade6-m216)*	McFarlane collection
BP2706	*h^{90} mat3-M (EcoRV)::ura4⁺ ura4-DS/E leu1-32 ade6-M210*	McFarlane collection
BP2714	*h⁺ rDNA::ura4⁺ ura4-DS/E ade6-M210 traX::kanMX6*	This study
BP2715	*h⁺ rDNA::ura4⁺ ura4-DS/E ade6-M210 traX::kanMX6*	This study
BP2716	*h⁺ Ch16-m23::ura4⁺ TEL[72] ura4-DS/E leu1-32 ade6-M210 (Ch16 ade6-m216) traX::kanMX6*	This study
BP2717	*h⁺ Ch16-m23::ura4⁺ TEL[72] ura4-DS/E leu1-32 ade6-M210 (Ch16 ade6-m216) traX::kanMX6*	This study
BP2718	*h^{90} mat3-M (EcoRV)::ura4⁺ ura4-DS/E leu1-32 ade6-M210 traX::kanMX6*	This study
BP2719	*h^{90} mat3-M (EcoRV)::ura4⁺ ura4-DS/E leu1-32 ade6-m210 traX::kanMX6*	This study
BP2720	*h⁺ rDNA::ura4⁺ ura4-DS/E ade6-M210 tsn1::kanMX6*	This study
BP2721	*h⁺ rDNA::ura4⁺ ura4-DS/E ade6-M210 tsn1::kanMX6*	This study
BP2722	*h+ Ch16-m23::ura4⁺ TEL[72] ura4-DS/E leu1-32 ade6-M210 (Ch16 ade6-m216) tsn1::kanMX6*	This study
BP2723	*h+ Ch16-m23::ura4⁺ TEL[72] ura4-DS/E leu1-32 ade6-M210 (Ch16 ade6-m216) tsn1::kanMX6*	This study
BP2724	*h^{90} mat3-M (EcoRV)::ura4⁺ ura4-DS/E leu1-32 ade6-M210 tsn1::kanMX6*	This study
BP2725	*h^{90} mat3-M (EcoRV)::ura4⁺ ura4-DS/E leu1-32 ade6-M210 tsn1::kanMX6*	This study
BP2746	*h⁻ ade6-M26 ura4-D18 leu1-32 dcr1::ura4⁺*	This study

BP2747	*h- ade6-M26 ura4-D18 leu1-32 dcr1::ura4+*	This study
BP2748	*h- ade6-M26 ura4-D18 leu1-32 tsn1:: kanMX6 dcr1::ura4+*	This study
BP2749	*h- ade6-M26 ura4-D18 leu1-32 tsn1:: kanMX6dcr1::ura4+*	This study
BP2750	*h- ade6-M26 ura4-D18 leu1-32 traX:: kanMX6 dcr1::ura4+*	This study
BP2751	*h- ade6-M26 ura4-D18 leu1-32 traX:: kanMX6 dcr1::ura4+*	This study
BP2757	*h- ade6-M26 ura4-D18 leu1-32 ago1::ura4+*	This study
BP2758	*h- ade6-M26 ura4-D18 leu1-32 ago1::ura4+*	This study
BP2759	*h- ade6-M26 ura4-D18 leu1-32 tsn1:: kanMX6 ago1::ura4+*	This study
BP2760	*h- ade6-M26 ura4-D18 leu1-32 tsn1:: kanMX6 ago1::ura4+*	This study
BP2761	*h- ade6-M26 ura4-D18 leu1-32 traX:: kanMX6 ago1::ura4+*	This study
BP2762	*h- ade6-M26 ura4-D18 leu1-32 traX:: kanMX6 ago1::ura4+*	This study
BP2811	*h- ade6-M26 ura4-D18 leu1-32 rec10:: kanMX6*	This study
BP2812	*h- ade6-M26 ura4-D18 leu1-32 rec10:: kanMX6*	This study
BP2813	*h- ade6-M26 ura4-D18 leu1-32 rec10:: kanMX6*	This study
BP2894	*h- ade6-M210 leu1-32 ura4-D18 Ch16-23R dcr1::ura4+*	This study
BP2895	*h- ade6-M210 leu1-32 ura4-D18 Ch16-23R dcr1::ura4+*	This study
BP2896	*h- ade6-M210 leu1-32 ura4-D18 Ch16-23R dcr1::ura4+*	This study
BP2897	*h- ade6-M210 leu1-32 ura4-D18 Ch16-23R traX:: kanMX6 dcr1::ura4+*	This study
BP2898	*h- ade6-M210 leu1-32 ura4-D18 Ch16-23R traX:: kanMX6 dcr1::ura4+*	This study
BP2899	*h- ade6-M210 leu1-32 ura4-D18 Ch16-23R tsn1:: kanMX6 dcr1::ura4+*	This study
BP2900	*h- ade6-M210 leu1-32 ura4-D18 Ch16-23R tsn1:: kanMX6 dcr1::ura4+*	This study
BP2973	*h- ade6-M210 leu1-32 ura4-D18 Ch16-23R ago1::ura4+*	This study
BP2974	*h- ade6-M210 leu1-32 ura4-D18 Ch16-23R ago1::ura4+*	This study
BP2975	*h- ade6-M210 leu1-32 ura4-D18 Ch16-23R traX:: kanMX6 ago1::ura4+*	This study
BP2976	*h- ade6-M210 leu1-32 ura4-D18 Ch16-23R traX:: kanMX6 ago1::ura4+*	This study
BP2977	*h- ade6-M210 leu1-32 ura4-D18 Ch16-23R tsn1:: kanMX6 ago1::ura4+*	This study
BP2978	*h- ade6-M210 leu1-32 ura4-D18 Ch16-23R tsn1:: kanMX6 ago1::ura4+*	This study
BP2985	*h- otrR1(Sph1)::ura4+ ura4-DS/E leu1-32 ade6-M210 dcr1:: natMX6*	This study

BP2986	*h- otrR1(Sph1)::ura4+ ura4-DS/E leu1-32 ade6-M210 dcr1:: natMX6*	This study
BP2987	*h- otrR1(Sph1)::ura4+ ura4-DS/E leu1-32 ade6-M210 traX::kanMX6 dcr1:: natMX6*	This study
BP2988	*h- otrR1(Sph1)::ura4+ ura4-DS/E leu1-32 ade6-M210 traX::kanMX6 dcr1:: natMX6*	This study
BP2989	*h- cntTM1(Nco1)::ura4+ ura4-DS/E leu1-32 ade6-M210 tsn1::kanMX6 dcr1:: natMX6*	This study
BP2990	*h- cntTM1(Nco1)::ura4+ ura4-DS/E leu1-32 ade6-M210 tsn1::kanMX6 dcr1:: natMX6*	This study
BP2991	*h- cntTM1(Nco1)::ura4+ ura4-DS/E leu1-32 ade6-M210 traX::kanMX6 ago1:: natMX6*	This study
BP2992	*h- cntTM1(Nco1)::ura4+ ura4-DS/E leu1-32 ade6-M210 traX::kanMX6 ago1:: natMX6*	This study
BP2993	*h- otrR1(Sph1)::ura4+ ura4-DS/E leu1-32 ade6-M210 traX::kanMX6 ago1:: natMX6*	This study
BP2994	*h- otrR1(Sph1)::ura4+ ura4-DS/E leu1-32 ade6-M210 traX::kanMX6 ago1:: natMX6*	This study
BP2995	*h- otrR1(Sph1)::ura4+ ura4-DS/E leu1-32 ade6-M210 tsn1::kanMX6 ago1:: natMX6*	This study
BP2996	*h- otrR1(Sph1)::ura4+ ura4-DS/E leu1-32 ade6-M210 tsn1::kanMX6 ago1:: natMX6*	This study
BP2997	*h- imr1(Nco1)::ura4+ ori1 ura4-DS/E leu1-32 ade6-M210 traX:: kanMX6 ago1:: natMX6*	This study
BP2998	*h- imr1(Nco1)::ura4+ ori1 ura4-DS/E leu1-32 ade6-M210 traX:: kanMX6 ago1:: natMX6*	This study
BP3001	*h- cntTM1(Nco1)::ura4+ ura4-DS/E leu1-32 ade6-M210 ago1:: natMX6*	This study
BP3002	*h- cntTM1(Nco1)::ura4+ ura4-DS/E leu1-32 ade6-M210 ago1:: natMX6*	This study
BP3003	*h- imr1(Nco1)::ura4+ ori1 ura4-DS/E leu1-32 ade6-M210 tsn1:: kanMX6 ago1:: natMX6*	This study
BP3004	*h- imr1(Nco1)::ura4+ ori1 ura4-DS/E leu1-32 ade6-M210 tsn1:: kanMX6 ago1:: natMX6*	This study
BP3005	*h- imr1(Nco1)::ura4+ ori1 ura4-DS/E leu1-32 ade6-M210 ago1:: natMX6*	This study
BP3006	*h- imr1(Nco1)::ura4+ ori1 ura4-DS/E leu1-32 ade6-M210 ago1:: natMX6*	This study
BP3024	*h- otrR1(Sph1)::ura4+ ura4-DS/E leu1-32 ade6-M210 tsn1::kanMX6 dcr1:: natMX6*	This study
BP3025	*h- otrR1(Sph1)::ura4+ ura4-DS/E leu1-32 ade6-M210 tsn1::kanMX6 dcr1:: natMX6*	This study
BP3026	*h- imr1(Nco1)::ura4+ ori1 ura4-DS/E leu1-32 ade6-M210 tsn1:: kanMX6 dcr1:: natMX6*	This study
BP3027	*h- imr1(Nco1)::ura4+ ori1 ura4-DS/E leu1-32 ade6-M210 tsn1:: kanMX6 dcr1:: natMX6*	This study
BP3028	*h- imr1(Nco1)::ura4+ ori1 ura4-DS/E leu1-32 ade6-M210 dcr1:: natMX6*	This study

BP3029	*h⁻ imr1(Nco1)::ura4⁺ ori1 ura4-DS/E leu1-32 ade6-M210 dcr1:: natMX6*	This study
BP3103	*h⁻ cntTM1(Nco1)::ura4⁺ ura4-DS/E leu1-32 ade6-M210 dcr1:: natMX6*	This study
BP3104	*h⁻ cntTM1(Nco1)::ura4⁺ ura4-DS/E leu1-32 ade6-M210 dcr1:: natMX6*	This study
BP3105	*h⁻ cntTM1(Nco1)::ura4⁺ ura4-DS/E leu1-32 ade6-M210 traX::kanMX6 dcr1:: natMX6 1*	This study
BP3106	*h⁻ cntTM1(Nco1)::ura4⁺ ura4-DS/E leu1-32 ade6-M210 traX::kanMX6 dcr1:: natMX6*	This study
BP3107	*h⁻ imr1(Nco1)::ura4⁺ ori1 ura4-DS/E leu1-32 ade6-M210 traX::kanMX6 dcr1:: natMX6*	This study
BP3108	*h⁻ imr1(Nco1)::ura4⁺ ori1 ura4-DS/E leu1-32 ade6-M210 traX:: kanMX6 dcr1:: natMX6*	This study
BP3109	*h⁻ otrR1(Sph1)::ura4⁺ ura4-DS/E leu1-32 ade6-M210 ago1:: natMX6*	This study
BP3110	*h⁻ otrR1(Sph1)::ura4⁺ ura4-DS/E leu1-32 ade6-M210 ago1:: natMX6*	This study
BP3111	*h⁻ cntTM1(Nco1)::ura4⁺ ura4-DS/E leu1-32 ade6-M210 tsn1::kanMX6 ago1:: natMX6*	This study
BP3112	*h⁻ cntTM1(Nco1)::ura4⁺ ura4-DS/E leu1-32 ade6-M210 tsn1::kanMX6 ago1:: natMX6 iso2*	This study
BP3150	*h⁻ leu1-32 ura4-D18 T2R1-30292::ura4⁺*	McFarlane collection
BP3151	*h⁻ leu1-32 ura4-D18 T2R1-7921::ura4⁺*	McFarlane collection
BP3152	*h⁻ leu1-32 ura4-D18 T2R1-7921::ura4⁺ dcr1::HYG*	McFarlane collection
BP3153	*h⁻ leu1-32 ura4-D18 T2R1-30292:: ura4⁺dcr1::HYG*	McFarlane collection
BP3154	*h⁺ rDNA::ura4⁺ ura4-DS/E ade6-M210 ago1:: natMX6*	This study
BP3155	*h^{90} mat3-M (EcoRV)::ura4⁺ ura4-DS/E leu1-32 ade6-M210 ago1:: natMX6*	This study
BP3156	*h⁺ rDNA::ura4⁺ ura4-DS/E ade6-M210 traX::kanMX6 ago1:: natMX6*	This study
BP3187	*h^{90} mat3-M (EcoRV)::ura4⁺ ura4-DS/E leu1-32 ade6-M210 traX::kanMX6 dcr1:: natMX6*	This study
BP3188	*h^{90} mat3-M (EcoRV)::ura4⁺ ura4-DS/E leu1-32 ade6-M210 traX::kanMX6 dcr1:: natMX6*	This study
BP3189	*h+ rDNA::ura4⁺ ura4-DS/E ade6-M210 tsn1::kanMX6 dcr1:: natMX6*	This study
BP3190	*h^{90} mat3-M (EcoRV)::ura4⁺ ura4-DS/E leu1-32 ade6-M210 tsn1::kanMX6 dcr1:: natMX6*	This study
BP3191	*h^{90} mat3-M (EcoRV)::ura4⁺ ura4-DS/E leu1-32 ade6-M210 tsn1::kanMX6 dcr1:: natMX6*	This study
BP3192	*h^{90} mat3-M (EcoRV)::ura4⁺ ura4-DS/E leu1-32 ade6-M210 traX::kanMX6 ago1:: natMX6*	This study
BP3193	*h⁺ rDNA::ura4⁺ ura4-DS/E ade6-M210 tsn1::kanMX6 ago1:: natMX6*	This study

BP3194	*h^{+} rDNA::ura4^{+} ura4-DS/E ade6-M210 tsn1::kanMX6 ago1:: natMX6*	This study
BP3195	*h^{90} mat3-M (EcoRV)::ura4^{+} ura4-DS/E leu1-32 ade6-M210 tsn1::kanMX6 ago1:: natMX6*	This study
BP3196	*h^{90} mat3-M (EcoRV)::ura4^{+} ura4-DS/E leu1-32 ade6-M210 tsn1::kanMX6 ago1:: natMX6*	This study
BP3206	*h^{-} leu1-32 ura4-D18 T2R1-30292::ura4^{+} ago1:: natMX6*	This study
BP3207	*h^{-} leu1-32 ura4-D18 T2R1-30292::ura4^{+} ago1:: natMX6*	This study
BP3208	*h^{-} leu1-32 ura4-D18 T2R1-7921::ura4^{+} ago1:: natMX6*	This study
BP3212	*h^{90} mat3-M (EcoRV)::ura4^{+} ura4-DS/E leu1-32 ade6-M210 dcr1:: natMX6*	This study
BP3213	*h^{+} rDNA::ura4^{+} ura4-DS/E ade6-M210 dcr1:: natMX6*	This study
BP3214	*h^{-} leu1-32 ura4-D18 T2R1-30292::ura4^{+} tsn1::kanMX6*	This study
BP3215	*h^{-} leu1-32 ura4-D18 T2R1-30292::ura4^{+} tsn1::kanMX6*	This study
BP3216	*h^{-} leu1-32 ura4-D18 T2R1-7921::ura4^{+} tsn1::kanMX6*	This study
BP3217	*h^{-} leu1-32 ura4-D18 T2R1-7921::ura4^{+} tsn1::kanMX6*	This study
BP3218	*h^{-} leu1-32 ura4-D18 T2R1-7921::ura4^{+} dcr1::HYG trsn1::kanMX6*	This study
BP3219	*h^{-} leu1-32 ura4-D18 T2R1-7921::ura4^{+} dcr1::HYG tsn1::kanMX6*	This study
BP3220	*h^{-} leu1-32 ura4-D18 T2R1-30292::ura4^{+} ago1::natMX6 tsn1::kanMX6*	This study
BP3221	*h^{-} leu1-32 ura4-D18 T2R1-30292::ura4^{+} ago1::natMX6 tsn1::kanMX6*	This study
BP3222	*h^{-} leu1-32 ura4-D18 T2R1-30292::ura4^{+} traX::kanMX6*	This study
BP3223	*h^{-} leu1-32 ura4-D18 T2R1-30292::ura4^{+} traX::kanMX6*	This study
BP3224	*h^{-} leu1-32 ura4-D18 T2R1-7921:: ura4^{+}traX::kanMX6*	This study
BP3225	*h^{-} leu1-32 ura4-D18 T2R1-7921::ura4^{+} traX::kanMX6*	This study
BP3226	*h^{-} leu1-32 ura4-D18 T2R1-7921::ura4^{+} dcr1::HYG traX::kanMX6*	This study
BP3227	*h^{-} leu1-32 ura4-D18 T2R1-7921:: ura4^{+}dcr1::HYG traX::kanMX6*	This study
BP3228	*h^{-} leu1-32 ura4-D18 T2R1-30292::ura4^{+} dcr1::HYG traX::kanMX6*	This study
BP3229	*h^{-} leu1-32 ura4-D18 T2R1-30292::ura4^{+} dcr1::HYG traX::kanMX6*	This study
BP3230	*h^{-} leu1-32 ura4-D18 T2R1-30292::ura4^{+} ago1:: natMX6 traX::kanMX6*	This study
BP3231	*h^{-} leu1-32 ura4-D18 T2R1-30292::ura4^{+} ago1:: natMX6 traX::kanMX6*	This study
BP3232	*h^{-} leu1-32 ura4-D18 T2R1-7921::ura4^{+} ago1:: natMX6 traX::kanMX6*	This study

BP3233	*h⁻ leu1-32 ura4-D18 T2R1-7921::ura4⁺ ago1:: natMX6 traX::kanMX6*	This study
BP3234	*h⁺ rDNA::ura4⁺ ura4-DS/E ade6-M210 traX::kanMX6 dcr1:: natMX6*	This study
BP3235	*h⁺ rDNA::ura4⁺ ura4-DS/E ade6-M210 traX::kanMX6 dcr1:: natMX6*	This study
BP3236	*h⁻ leu1-32 ura4-D18 T2R1-30292::ura4⁺ dcr1::HYG tsn1::kanMX6*	This study
BP3237	*h⁻ leu1-32 ura4-D18 T2R1-30292::ura4⁺dcr1::HYG tsn1::kanMX6*	This study
BP3238	*h⁻ leu1-32 ura4-D18 T2R1-7921:: ura4⁺ ago1:: natMX6 tsn1::kanMX6*	This study
BP3239	*h⁻ leu1-32 ura4-D18 T2R1-7921:: ura4⁺ago1:: natMX6 tsn1::kanMX6*	This study
BP3246	*h⁻ ade6-M26 ura4-D18 leu1-32 traX:: kanMX6 ago1::ura4⁺ tsn1::natMX6*	This study
BP3247	*h⁻ ade6-M26 ura4-D18 leu1-32 traX:: kanMX6 ago1::ura4⁺ tsn1::natMX6*	This study
BP3248	*h⁻ ade6-M26 ura4 -D18 leu1-32 traX::kanMX6 tsn1::natMX6*	This study
BP3249	*h⁻ ade6-M26 ura4 -D18 leu1-32 traX::kanMX6 tsn1::natMX6*	This study
BP3250	*h⁻ ade6-M26 ura4-D18 leu1-32 tsn1:: kanMX6 dcr1::ura4⁺ traX::natMX6*	This study
BP3251	*h⁻ ade6-M26 ura4-D18 leu1-32 tsn1:: kanMX6 dcr1::ura4⁺ traX::natMX6*	This study
BP3252	*h⁻ ade6-M26 ura4-D18 leu1-32 tsn1::kanMX6 traX::natMX6*	This study
BP3253	*h⁻ ade6-M26 ura4-D18 leu1-32 tsn1::kanMX6 traX::natMX6*	This study
BP3254	*h⁻ leu1-32 ura4-D18 T2R1-30292::ura4⁺ dcr1::natMX6*	This study
BP3255	*h⁻ leu1-32 ura4-D18 T2R1-30292::ura4⁺ dcr1::natMX6*	This study
BP3256	*h⁻ leu1-32 ura4-D18 T2R1-30292::ura4⁺ dcr1::natMX6*	This study
BP3257	*h⁻ leu1-32 ura4-D18 T2R1-30292::ura4⁺ dcr1::natMX6*	This study
BP3258	*h⁻ leu1-32 ura4-D18 T2R1-30292::ura4⁺ dcr1::natMX6*	This study
BP3259	*h⁻ leu1-32 ura4-D18 T2R1-30292::ura4⁺ traX::kanMX6 dcr1::natMX6*	This study
BP3260	*h⁻ leu1-32 ura4-D18 T2R1-30292::ura4⁺ traX::kanMX6 dcr1::natMX6*	This study
BP3261	*h⁻ leu1-32 ura4-D18 T2R1-30292::ura4⁺ traX::kanMX6 dcr1::natMX6*	This study
BP3262	*h⁻ leu1-32 ura4-D18 T2R1-30292::ura4⁺ traX::kanMX6 dcr1::natMX6*	This study

2.3 Plasmid extraction from *E. coli*

A Miniprep kit (QIAGEN) was used to extract plasmids from *E. coli* strains, following the manufacturer's protocol and using the buffers supplied with the kit. The *E. coli* strains were taken from a –80ºC freezer, and streaked on Luria Bertani Agar (LBA) (see Section 2.27) medium with ampicillin (100 mg/litre) and grown overnight at 37ºC. A single colony from the culture was inoculated into a Falcon tube containing 5 ml of liquid LB with ampicillin (100 mg/litre) and incubated overnight at 37ºC in an orbital shaking incubator. Cells were spun down for 5 min at 3,000 *g*, resuspended in 250 µl P1 buffer (containing RNase A), and then transferred to an Eppendorf tube. A 250 µl volume of P2 buffer (lysis buffer) was added to lyse the cells. The tube was inverted 4–5 times to thoroughly mix the contents, then 350 µl of N3 buffer (neutralising/binding buffer) was added to the tube and the tube was inverted 4–5 times again to thoroughly mix the contents. The tube was centrifuged for 10 min at 12,000 *g* and the pellet was discarded. The supernatant was transferred to a QIAprep tube (QIAGEN), which was then spun down for 30–60 secs at 12,000 *g*. The eluate was discarded and pellets were retained. The QIAprep tube was washed with 0.5 ml of PB buffer (washing buffer) and spun down for 30–60 secs at 12,000 *g*. The eluate was discarded and the pellet was retained. The QIAprep tube was washed with 0.75 ml of PE buffer and spun down for 30–60 secs at 12,000 *g*. The eluate was discarded and the plasmid was eluted from the filter by adding 50 µl of EB (elution buffer).

2.4 Phenol/ chloroform purification of DNA

An equal volume of phenol/chloroform and 0.1 M NaCl at a ratio of 1:1 was added to an Eppendorf tube containing the DNA solution, and the tube was then spun down at 12,000 g for 15 mins. The top aqueous layer was transferred to a new tube and a 3-fold volume of 100% ethanol was added. The tube was left at –80^{o}C for one hour to precipitate the DNA. The DNA was spun down at 12,000 *g* for 15 mins, washed with 70% ethanol, and the pellet was left on the lab bench to dry for 5 mins. The pellet was then resuspended in 40 µl of 1x TE buffer.

2.5 Chemical transformation of *S. pombe* cells using a DNA knockout cassette

A single colony of the *S. pombe* strain required for transformation was cultured in 100 ml of YEL (see Section 2.1) or selective media to a density of 1 X 10^7 cells per ml. The cells were centrifuged at 3,000 *g* for 5 mins, and then washed with an equal volume of sterile distilled water (sterile dH_2O). The cells were resuspended in 1 ml of sterile dH_2O, transferred to a 1.5 ml Eppendorf tube and then washed once with 1 ml of 0.1 M LiAc / 1x TE prewarmed to 30ºC. The cell pellet was then resuspended in LiAc/TE at a concentration of 2 X 10^9 cells / ml. A 100 µl volume of the concentrated cells was mixed with 2 µl of 10 mg/ml sheared herring testis DNA (Invitrogen), along with 10 µl of the DNA cassette solution to be used for the gene deletion. After 10 mins of incubation at room temperature, 260 µl of prewarmed (30ºC) 40% PEG / LiAc / TE (pH 7.3) was added to the cell mixture, mixed gently, and the cells were incubated for one hour in a water bath at 30ºC. A 43 µl volume of DMSO was added and cells were immediately heat shocked for 5 mins in another water bath at 42^{o}C. Cells were allowed to cool for 10 mins at room temperature, and then washed with 1 ml of sterile dH_2O. The cells were resuspended in 0.5 ml of sterile dH_2O, and the suspension was plated onto five YEA (see Section 2.27) plates or an appropriate solid medium (100 µl of suspension on each plate). The plates were incubated at 30^{o}C for roughly 18 hours. After lawns of cells were visible, plates were replicated onto a desired selective media and then incubated for 3–4 days at 30^{o}C.

2.6 Genomic DNA extraction

Single colonies were inoculated into 5 ml YEL and grown at 33^{o}C until saturated. Cells were harvested at 3,000 g, washed once with 1 ml of sterile dH_2O, centrifuged as described previously, and then resuspend in 1 ml of sterile dH_2O. Cells were transferred to 1.5 ml screw-cap tubes and harvested again by centrifugation. A 200 µl volume of Lysis Buffer (5 ml 10% SDS, 1 ml Triton-X100, 0.5 ml TE 100X , 5 ml 1M NaCl, and sterile dH_2O was added to reach 50 ml) was added along with 100 µl Chloroform, 100 µl Phenol and 0.3 grams of acid washed beads. Cells were disrupted by a Bead-Beater (FastPrep120, ThermoSavant.) for 30 secs and then spun down for 15 mins at 12,000 *g*. The top aqueous layer was removed and added to 1 ml 100% Ethanol. This was left at –20 ^{o}C for 1 hour and then centrifuged for 12 mins at 12,000 *g*. Pellets were washed with 1 ml 70% Ethanol, air-dried, and resuspended in 100 µl of 1x TE buffer.

2.7 Confirmation of gene knockout by PCR screening

Genomic DNA was extracted for the candidate knockout strains. Different "check primers", inside and outside the desired gene region, were designed along with primers inside the knockout cassettes as shown in Table 2.5. The PCR reaction conditions (for a 50 µl reaction) were 25 µl of BioMix red (BioLine), 1 µl of 20 ng/ µl each of forward and reverse primers, 1 µl of a 10% dilution of extracted genomic DNA in TE buffer and 22 µl sterile dH_2O. The PCR program was as follows: initial heating for 1 minute at 96ºC, followed by 25 cycles of 1 minute at 96ºC, 30 secs at XºC, and 72 ^{o}C as necessary (allowing 15–30 secs/kb). Final elongation was carried out for 5 mins at 72ºC. The annealing temperature (X) was varied, depending on the primers sets. The PCR products were run on a 1% agarose gel to visualise products size.

Table 2.5 Sequence of PCR check primers

Primer name	Sequence	Location
TRAX check-F	5′-CAA ATA GTC ATC TTG ATT TGC-3′	Upstream of *traX* ORF
TRAX check-R	5′-TCT AAC ATA TAG AAA GCA GCG-3′	Downstream of *traX* ORF
TRAX-int-F	5′-ATA AGA GGG AGA AAA TTA TTC G-3′	Forward primer inside *traX*
TRAX-int-R	5′-CTC CTC GGG AGG AGT TGC -3′	Reverse primer inside *traX*
TRAX-mid-F	5′-CTG ATG GAT TTC CTC TAC CC-3′	Forward primer inside *traX*
TRAX-mid-R	5′-GGA GAA CAG CAT TTC AAA AG-3′	Reverse primer inside *traX*
Tsn-F	5′-GAT CTA AAC AAC CCA AGC G-3′	Upstream of *tsn1* ORF
Tsn-R	5′-GCA TTC ATC ATA GGA CTG CC-3′	Downstream of *tsn1* ORF
Translin-int-F	5'-AAA CTG ACT GCA GAG GTC G-3'	Forward primer inside *tsn1*
Translin-int-R	5'-GAA CAC AGA GAT AGT ACT GC-3'	Reverse primer inside *tsn1*
Translin-mid-F	5′-CCC GGT TTT TCCAGA AGA G-3′	Forward primer inside *tsn1*
Translin-mid-R	5′-CGA AAT GTC TTC TTA AGG AG-3′	Reverse primer inside *tsn1*
Screencorrect-R	5′-CGG ATG TGA TGT GAG AAC TG-3′	Forward primer inside kan ^{R} cassette

Screentag-F	5′-CAG TTC TCA CAT CAC ATC CG-3′	Reverse primer inside kan ^{R} cassette
Dcr check-F	5′-AGT ATT CTG CTC GTG TGA TTG-3′	Upstream of *dcr1* ORF
Dcr check-R	5′-TGA TTG AAA CTC GAG ATG CTT TG-3′	Downstream of *dcr1* ORF
Dcr-int-F	5′-ATT CGA CGA ATG TCA TCA TGC-3′	Forward primer inside *dcr1*
Dcr-int-R	5′-AGA CGA TAT CAT CAG TCA CAC G-3′	Reverse primer inside *dcr1*
Dcr-mid-F	5′-TCC CTT AGT GTT TGT ACA AGC-3′	Forward primer inside *dcr1*
Dcr-mid-R	5′-TGG CAA CTT TAC GGG ATT TGC-3′	Reverse primer inside *dcr1*
pAW1-F	5′-AGT TTA ACT ATG CTT CGT CGG C-3′	Forward primer inside *ura4* cassette
pAW1-R	5′-ACA CGA CAT GTG CAG AGA TGC-3′	Reverse primer inside *ura4* cassette
NatMX6-F	5′-CAT GGG TAC CAC TCT TGA CG-3′	Forward primer inside Nourseothricin ^{R} cassette
NatMX6-R	5′-CTC AGT GGC AAA TCC TAA CC-3′	Reverse primer inside Nourseothricin ^{R} cassette
AgoNAS-F	5′-ACT TAT GTT GCG TTT GCG TGC-3′	Upstream of *ago1* ORF
AgoNAS-R	5′-AGC TAT CAA CAG TGG ATA GAG C-3′	Downstream of *ago1* ORF
Ago-int F	5′-AGG TAC TTG TTA GCT TCA TTC G-3′	Forward primer inside *ago1*
Ago-int R	5′-AGT ACC GAC ATT ATT GCG ATG C-3′	Reverse primer inside *ago1*
Ago-mid F	5′-TCA AAC TGC CAA CAT GAT CCG-3′	Forward primer inside *ago1*
Ago-mid R	5′-TCT CAA CAA AAG TAT CAT CGG C-3′	Reverse primer inside *ago1*
upupura4-F	5′-GAC AAT TCC AGG GAG ACA GC-3′	Upstream of *ura4* ORF
downura4-F	5′-CAA ACG CAA ACA AGG CAT CG-3′	Downstream of *ura4* ORF
imrura4-F	5′-ATT CAG AAA ATC ACC GGA GC-3′	Located upstream of *imr* sequence
imrura4-R	5′-TGC TTA GCA GTT GGT ACA ACG-3′	Located downstream of *imr* sequence
cntura4-F	5′-CAG AAG GTA TTA GTG GTC GG-3′	Located upstream of *cnt* sequence
cntura4-R	5′-CCA GAA CAA TAC AGA TTC GC-3′	Located downstream of *cnt* sequence
otrura4-F	5′-TCT GTT ATG TCA GTG CTT CG-3′	Located upstream of *otr* sequence

otrura4-R	5′-CAA GAC TGT TGT TGA GTG C-3′	Located downstream of *otr* sequence
ura4mid-R	5′-GTA TAA TAC CCT CGC CTG GC-3′	Reverse primer inside *ura4*

2.8 DAPI staining

A colony was taken with a sterile loop and then mixed in 7 µl of water in a small area on a slide and heat fixed at 70ºC. The slide was cooled for 1 minute before adding 3µl of 1X DAPI staining (1 µl/ml in Vectashield) and the sample was then covered with a 13 mm coverslip and sealed with nail polish. The slides were viewed with a fluorescent microscope and photos were taken for examination of cell morphology.

2.9 Minichromosome loss assay

Chl6 is a minichromosome which can be maintained in *S. pombe*. Ch16 is constructed from the centromere of chromosome III. This minichromosome has an *ade6-M216* allele; whereas, the chromosome III has an *ade6-M210* allele. The *ade6-M216* allele and *ade6-M210* allele are complementary and confer prototrophy. Therefore, when Ch16 is lost, cells lose the *ade6-M216* allele and colonies become red when grow in media licking adenine (Niwa et al., 1986). Therefore, a minichromosome loss assay was performed by streaking out the desired single and double mutants strains (contain Chl6) on minimal medium, NBA lacking adenine to force the cells to retain Ch16. Cells were incubated for 3-4 days at 30ºC. Three independent colonies were taken from each strain and inoculated into NBL medium lacking adenine. These cells were grown overnight in a shaker incubator at 30ºC. Serially diluted cells were plated out to approximately 100 colonies per plate onto YEA supplemented with adenine. Plates were incubated for two days at 30ºC until micro colonies were obtained. Nine independent micro colonies were inoculated into YEL with adenine and incubated overnight in a shaking incubator at 30ºC. A 1 ml volume was removed from each culture, spun down, and then washed with sterile dH_2O. The cells were serially diluted and plated out on unsupplemented YEA to get the desired number of colonies (100 colonies per plate). Plates were incubated at 30ºC and 35ºC for four days. The rates of loss of Ch16 were determined by calculating as the percentage of dark pink colonies.

2.10 Drop tests for drug sensitivity

A single colony from each *S. pombe* strain to be tested was cultured overnight in YEL at 30ºC and resuspended in sterile dH_2O to get approximately 5 x 10^6 cells/ml. The cells were serially diluted and 10 µl of each dilution was dropped gently onto plates containing fully supplemented YEA containing the drug to be tested. The drugs were prepared as stock solutions and the effective concentrations were titrated. Different concentrations were tested, as shown in Table 2.6.

Table 2.6 Drug concentrations

Drug	Concentration
Thiabendazole (TBZ) (Sigma)	10, 12.5, 15, 20, and 25 µg/ml
5-Fluoroorotic Acid (5-FOA) **(**ForMedium™**)**	100, 250,500,750 µg/ml and 1mg/ml
Trichostatin A (TSA) (Sigma)	25 and 30 µg/ml
Mitomycin C (Sigma)	0.15 mM
Hydroxyurea (H.U) (Sigma)	3 mM, 5 mM and 10 mM
Methyl Methanesulfonate (MMS) (Fluka Chemical)	0.0025%, 005% and 0.0075%
Camptothecin (Sigma)	0.5 µg/ml and 0.8 µg/ml
Phleomycin (InvivoGen)	1, 2.5, 5 and 10 µg/ml

Control plates contained fully supplemented YEA, but the drugs were replaced by the same volume of the appropriate drug solvent (i.e. either DMSO or H_2O). Each plate was inoculated with the desired strains in a straight line, as shown in Figure 2.1. Control plates were prepared for each experiment and incubated at desired temperatures for four days.

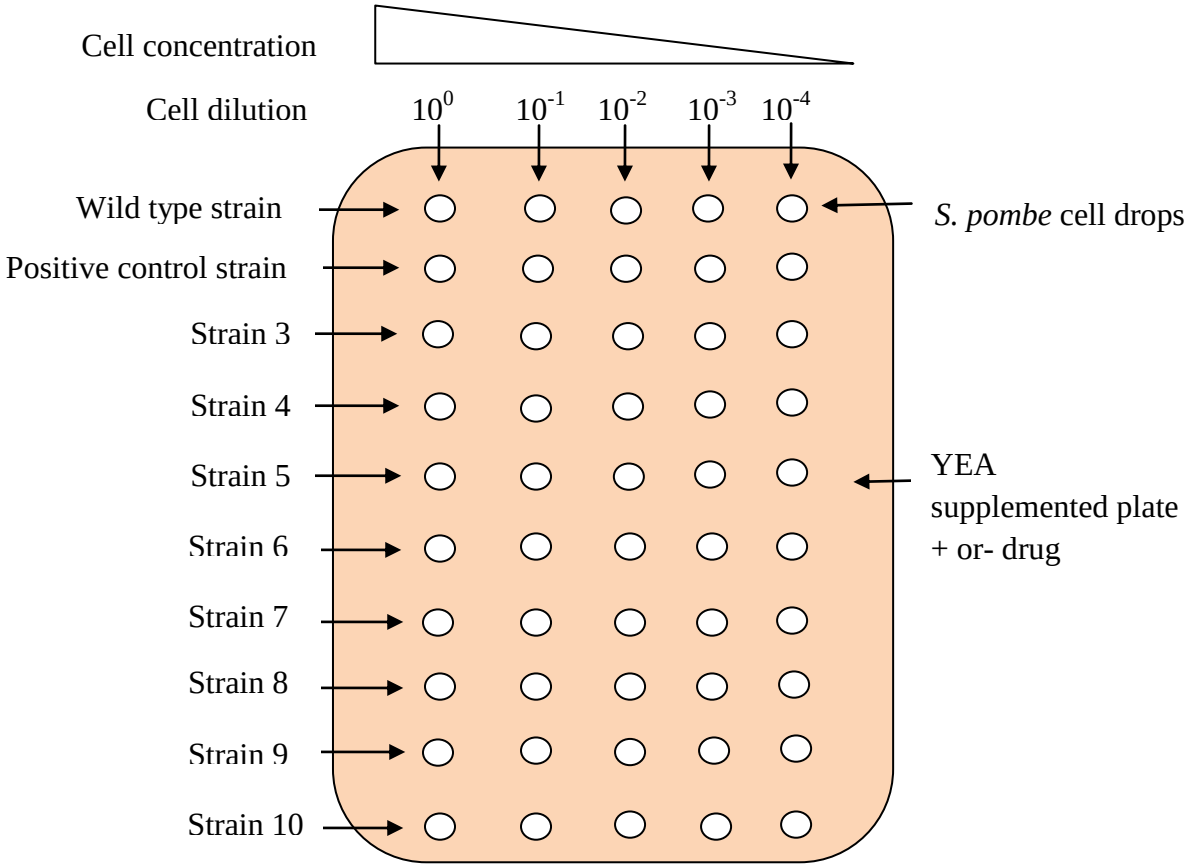

Figure 2.1 Arrangement of a square Petri dish for drop tests

Diagram demonstrates the arrangement of the drops (serial dilutions) of *S. pombe* cells in a square Petri dish. Drop tests were done to determine the effect of Thiabendazole and DNA damaging agents on cell survival. Each row represents a different *S. pombe* strain.

2.11 Ultraviolet (UV) irradiation of *S. pombe*

S. pombe strains to be tested were spotted as shown in Figure 2.1 onto fully supplemented YEA plates and incubated to dry for one hour at a 30°C incubator. Plates were then irradiated by an ultraviolet source (CL-1000 UV cross linker). Different exposure levels were tested (75, 150 and 300 J/m^2). The plates were incubated for 4 days at 30ºC and then cell growth was inspected.

2.12 Haemocytometer counting of yeast and human cells

Yeast cells were grown as required, and then 10 µl of culture was added under the end of the coverslip of a haemocytometer. The number of cells was counted using a light microscope (40X). Cells were counted on the first five squares in the first line. The average was then calculated and multiplied by 25 (because there are 25 squares in total). This total value was multiplied by 10^4 to obtain the numbers of cells per ml.

Human cells were grown as needed. Cells were washed with PBS, detached by trypsin (Sigma, T3924) treatment, and then the appropriate amount of medium was added to deactivate the trypsin. A 10 µl volume of culture was added under the end of the coverslip of the Haemocytometer. All cells in the 25 squares on the haemocytometer were counted using a light microscope (10X). The numbers of cells per ml were calculated as follows: The number of cells counted using the microscope was multiplied by 10^4. The number of cells per flask was then calculated based on the volume (in ml) of culture in the flask.

2.13 Whole cell protein extraction and western blotting of *S. pombe* cells

Anti-TRAX polyclonal antibody (TRAX18) was raised in guinea pigs and produced by Eurogentec, Liege, Belgium. The dilution for western blotting was 1:5000. The secondary antibody was goat anti-guinea pig IgG-HRP (Santa Cruz Biotechnology, sc-2438) diluted at 1:5000.

For whole-cell protein extracts and western blotting, single colonies were grown overnight in 5 ml YEL. The next day, 200 µl of culture was incubated in 50 ml YEL overnight. The cells were then harvested by spinning at 3,000 *g* for 5 mins and resuspended in 1.5 ml of ice cold STOP buffer (1 mM NaN_3, 10 mM EDTA (pH 8.15), 150 mM NaCl). The resuspension was transferred to a 1.5 ml screw cap tube and centrifuged at 3,000 *g* for 5 mins. The supernatant was discarded and 450 µl lysis buffer was added [one tablet of protease cocktail inhibitors (Roche) added to 10 ml RIPA buffer (Sigma-R0278)] and made up to 1 ml mark with glass beads (Sigma-G8772). The tube was placed in a Bead Beater (Thermo Savant) for 30 secs to rupture the cells, and then placed on ice for a further 30 secs. The tube was centrifuged at 12,000 *g* at 4^{o}C for 20 mins. The supernatant was collected in a new Eppendorf tube and the pellet was discarded. The tube was centrifuged again at 12,000 *g* at 4^{o}C for 10 mins. The cell lysate was collected in a new Eppendorf tube and stored at -80ºC until used. The protein

concentration was determined by the Bradford method to obtain approximately 30 µg of protein in 20 µl of fresh RIPA buffer, protein loading dye and reducing agent (Fermentas). The sample was boiled for 5 mins at 100ºC and loaded in a precast gel (Invitrogen-EC60352). The gel was run at 110 V for 10 min to get the samples to run into the resolving gel, and was then run at 200 V for about 45 mins. Four sheets of filter paper (7 x 10 cm for mini gels) and 1 sheet of Hybond PVDF membrane were cut; the filter papers were soaked in transfer buffer (0.2 M Tris, 1.92 M glycine) and the membrane was soaked in methanol. A blot sandwich was assembled in the following order: a Scotch Brite pad, 2 sheets of filter paper, the gel, the membrane, 2 sheets of filter paper and a Scotch Brite pad. The cassettes were placed in the transfer tank, which was filled with transfer buffer, and then run at 300 mA for about 1.5 hrs. The membrane was blocked for an hour on a shaker in 1x PBS containing 10% skimmed powdered milk and 0.5% of TWEEN. The membrane was probed overnight with primary antibody in 1x PBS, 10 % skim milk powder, and 0.5 % TWEEN and then washed in 1x PBS and 0.5% TWEEN for 5 mins. The membrane was then probed with a secondary antibody (usually conjugated HRP) and washed three times. The membrane was soaked in equal volumes of chemiluminescence (ECL, thermo scientific) solutions for 5 mins on a shaker. The membrane was then transferred to a cassette between two acetate sheets and taped down. In a dark room, a film was placed on the membrane and exposed for an appropriate time and then the film was developed. The membrane was washed in stripping buffer for about 15 mins and then stored in 1x PBS in a refrigerator.

2.14 Storage of *S. pombe* and bacterial strains

Single colonies were grown in 5 ml YEL until saturation was achieved. Glycerol was added to a final concentration of 30%, and the cells were stored at -80ºC. Strains were designated and the genotypes for each strain were recorded in the strains book.

2.15 Source of human cell lines

Table 2.7 Source of human cell lines

Cell line name	Cell line type	Source
HCT116	Human colon carcinoma	European collection of cell culture (ECACC)
SW480	Human colon adenocarcinoma	European collection of cell culture (ECACC)
NTERA-2	Human testicular germ cell tumour cancer	P.W. Andrew (University of Sheffield)

2.16 Human cell culture

The HCT116 cell line was grown in 1X McCoy's 5A medium + GlutaMAX™ (Invitrogen, GIBCO 36600) supplemented with 10% foetal bovine serum (FBS). The SW480 and NTERA-2 cell lines were grown in Dulbecco's modified Eagle's medium 1X (DMEM + GlutaMAX™) (Invitrogen, GIBCO 61965) supplemented with 10% FBS. All cells were maintained in a 37ºC incubator in 5% CO_2, except for NTERA-2 cells, which were maintained in a 37ºC incubator in 10% CO_2.

2.17 Human cell freezing

Human cells were cultured in a T75 flask until they reached the confluent stage. The medium was aspirated and the cells were washed with PBS buffer. A 1 ml volume of trypsin was added and the flask was incubated for 2 mins to detach the cells from the flask. 9 ml of medium was added to the cells and mixed well, and then the mixture was transferred to a 15 ml Falcon tube, and centrifuged at 1,000 *g* for 5 mins. The supernatant was aspirated and 1 ml of (10% DMSO, 90% FBS) was slowly added to the pellet and mixed gently. The cells were then transferred to a labelled Cryotube™ and incubated overnight at -80ºC. The tubes were then transferred to a liquid nitrogen container. Information was recorded in the cell culture book, including the name of the cell line, the person who did the work, dates and the passage number.

2.18 Human cell thawing

A cryotube was carefully removed from the liquid nitrogen container and the cells were thawed in water bath at 37ºC for 1 minute. The entire tube contents were then added to 5ml of media in a Falcon tube and mixed gently. The Falcon tube was spun down for 5 mins at 1,000 *g* and all supernatant was aspirated. Another 10 ml of media was added to the cells and gently mixed well. The cells were transferred to two T25 flasks so that each flask contained 5 ml of fresh medium and cells. The flasks were incubated overnight in a 37ºC incubator. The cells were trypsinised and transferred to T75 flasks.

2.19 Total human RNA extraction

Human cells were grown in 6 wells plates until they reached the confluent stage. The cells were then washed with cold PBS and 200 µl Trizol (Invitrogen) was added to all wells. The cells were scraped off and the resulting Trizol/cell lysates were transferred into 1.5 ml Eppendorf tubes. The tubes were centrifuged for 10 mins at 12,000 *g* at 4^{o}C, the supernatants were removed to new Eppendorf tubes and the pellets were discarded. A 200µl volume of chloroform was added to each tube and the tube was inverted 4-5 times. The tube was incubated at room temperature for 5 mins and then centrifuged for 15 mins at 12,000 *g*. The top aqueous layer was transferred to a new Eppendorf tube and 500 µl of isopropanol was added, and then mixed gently. The tube was incubated at room temperature for 10 mins and then centrifuged at 14,000 *g* for 25 mins. The supernatant was discarded and the pellet was placed on ice. 1 ml of 75% ethanol in DEPC treated water was added and mixed gently. The tube was centrifuged at 7,500 *g* for 5 mins, the supernatant was discarded and the pellet was air-dried for 5-10 mins. A 50 µl volume of DEPC treated water was added to the RNA pellet and the tube was incubated at 56^{o}C for 10 mins. The total RNA preparation was stored in a labelled tube at -80^{o}C.

2.20 cDNA synthesis

A SuperScript™ III first-strand synthesis kit (Invitrogen, Cat#18080-051) was used to synthesise a cDNA from total human RNA. The protocol used was as described by the manufacturer. All primers and reagents were supplied with the kit. Two sterile PCR tubes were prepared; the first tube contained (2 µg of total RNA, 1 µl of 50 µM oligo (dT), 1 µl of 10 mM dNTP mix, and then volume was made up to 10 µl by DEPC-treated water), this tube was incubated at 65^{o}C for 5 mins, then placed on ice for at least 1 min. The

second tube contained 2 µl 10X RT buffer, 4 µl 25 mM $MgCl_2$, 2 µl 0.1 M DTT, 1 µl RNaseOUT™, and 1 µl SuperScript™ III RT. The contents of the two tubes were mixed gently into one new tube, collected by a flash spin, and then incubated for 50 mins at 50ºC, followed by an incubation for 5 mins at 85^{o}C. The tubes were chilled on ice and then flash spun. One 1 µl of RNase H was added and incubated for 20 mins at 37ºC. At this stage, the resulting cDNA was stored at -20ºC.

2.21 Reverse transcription-PCR (RT-PCR)

The reaction conditions (for a 50 µl reaction) were as follows: 25 µl of BioMix red (BioLine), 1 µl of forward primer, 1 µl of reverse primer, 2 µl of cDNA and 21 µl of sterilised distilled water. The thermocycler program was as follows: the initial heating was for 1 minute at 96ºC, followed by 30 cycles of 30 secs at 96ºC, 30 secs at XºC, and 1 minute at 72^{o}C. Final elongation was carried out for 10 mins at 72ºC. The annealing temperature (X) was varied depending on the primers sets. The samples were run on a 1% agarose gel and images were recorded. Refer chapter 7 for RT-PCR primer details.

2.22 DNA Sequencing

The PCR products were purified by a Geneclean^{R} II kit before being sent for sequencing. The purification protocol was as described by the manufacturer. All DNA was sequenced in an out of house lab (Eurofins MWG operon, Germany).

2.23 Gene knockdown by RNAi assay for *TRAX, Translin, AGO2* and *DICER1* in human cell lines

A siRNA mixture was prepared in an Eppendorf tube for each sample by adding 0.6 µl of siRNA, 99.4 µl of media without FBS and 6 µl of HiPerFect Transfection Reagent (Cat# 301705, Qiagen). Each Eppendorf tube was vortexed and briefly centrifuged, then incubated at room temperature for 25 mins. A negative control mixture was prepared in a similar manner, but 0.6 µl of non-interference reagent (cat#1027284, Qiagen) was used instead of siRNA. Cells were seeded as required in 6 well plates in 2 ml of media. A 106 µl volume of siRNA mixture was added slowly in a clockwise rotation to each well and the wells were mixed by rotating. The 6 well plates were incubated at 37°C for 24 hours. Three hits were done for each well, with each hit lasting for 24 hour. Cells were then

harvested and western blots were used to detect gene knockdown. Four siRNAs were tested for each gene and the best knockdown was selected, as shown in chapter 7

2.24 Western blot and antibodies for human cell lines.

Whole cell proteins from human cells were extracted by the following steps: Cells were grown in 6 well plates as needed. Media were aspirated and cells were washed with PBS. A 200 µl volume of trypsin was added to each well to detach the cells and the plates were then incubated in a 37°C incubator for 2 mins. A 500 µl volume of medium was added to each well to deactivate the trypsin and the cells were mixed well and then transferred to Eppendorf tubes. The tubes were centrifuged for 5 mins at 3,000 *g* and the medium was aspirated. The cells were washed with PBS and then centrifuged again for 5 mins at 3,000 *g*. The PBS was aspirated and cells were resuspended in an equal volume of lysis buffer and Laemmli (loading) buffer (Sigma-S3401). The lysis buffer contained 0.5% Triton-100, 200 mM sodium chloride, 50 mM Tris-HCl (pH 7.4), 1 mM AEBSF [4-(2-aminoethyl)-benzenesulphonyl fluoride, Sigma-A8456] and one pill of protease inhibitor cocktail (Roche-11836170001). The whole cell lysates in Eppendorf tubes were boiled in a heating block at 100°C for 5 min and then loaded onto a precast gel (Invitrogen-EC60352). Western blotting was carried out as described previously (see Section 2.13). Primary and secondary antibodies for human western blots were as shown in chapter 7.

CHAPTER 3

Investigation of whether fission yeast TraX functions to regulated heterochromatin-mediated genome dynamics

3.1 Introduction

In *S. pombe*, the RNAi machinery pays an essential role in the formation and maintenance of heterochromatin (Castel and Martienssen, 2013). There are four relatively well characterised regions of heterochromatin in the *S. pombe* genome; these are the centromeres (one on each of three chromosomes), the telomeres, the *mat* locus and *rDNA* locus (see Section 1.6.2). The three centromeres are each divided into distinct sub regions and the heterochromatic region that is dependent upon the RNAi machinery is to be found flanking the central core (*cnt*) (Pidoux and Allshire, 2004).

S. pombe mutants that are defective in RNAi-mediated functions are compromised in their ability to form proper heterochromatin at centromeres, although there are redundant pathways functioning at other heterochromatic loci. This loss of centromeric heterochromatin results in defective function of the centromeres resulting in an increased chromosomal instability in these strains and a sensitivity to drugs which partially compromise chromosome segregation, such as the microtubule destabilising drug thiabendazole (TBZ). Recent work has indicated that both Translin and TRAX function to enhance the RNAi pathways in the mouse and fly, specifically mediating the removal of passenger strand from siRNAs (Liu et al., 2009; Ye et al., 2011). Moreover, a role in processing of tRNA precursors has been revealed in *Neurospora* and *tRNA* genes form chromatin boundary elements within the *S. pombe* centromeres (see Section 1.5.5). These combined finding raised the hypothesis that in the fission yeast these two proteins may function to maintain heterochromatic regions via the RNAi pathway, and thus control genome stability. However, previous analysis of *S. pombe tsn1* (Translin) and *traX* (TraX) null mutants did not reveal any sensitivity of these mutants to TBZ, indicating that these two genes do not provide unique functions within a pathways for maintaining centromeric function (via heterochromatin maintenance) (Jaendling et al., 2008). Given that the role for C3PO (Translin/TRAX) has been suggested to be an enhancing one, we speculated that subtle defects in heterochromatic function may have been missed in the previous study (Jaendling et al., 2008). The work described in this chapter addresses the

question of whether a loss of TraX function causes any defect on chromosome dynamics which might indicate a role for TraX in the regulation of heterochromatin within the fission yeast (note; the analysis of Translin-defective mutants was carried out by a co-worker and reported elsewhere).

3.2 Results

3.2.1 Construction of *traX* gene null mutants

Original studies of *tsn1*Δ mutants using strains generated using standard mating revealed a possible meiotic haploinsufficiency resulting in aberrant meiotic progeny (R. McFarlane, personal communication). For this reason, all strains used in this study were generated by direct deletion of genes in parental lines. No strains were generated by meiotic crosses.

The *traX*Δ knockout strains in this chapter were constructed using the Bähler approach (Bähler et al., 1998) (see Section 2.1). The *kanMX6* (Geneticin-resistance) cassette was amplified with PCR primers designed with 80 bp homologous to the flanks of the *traX* gene and 20 bp homologous to the DNA flanking region of the selectable marker *kanMX6* gene. The purified PCR product was then chemically transformed into the desired *S. pombe* strains (see Section 2.4) (Figure 3.1).

3.2.2 *traX* knockout screening by PCR

After transformation, *traX*Δ candidates were PCR screened to confirm *traX*Δ knockout using different sets of primers. External primers Trax check-F and Trax check-R should give a product size of 1747 bp for *traX*Δ and 963 bp for $traX^{+}$. Five primer pairs using at least one *traX* internal primer were also used to check the candidates. These should give no products for *traX*Δ candidates, while giving different product sizes for the $traX^{+}$ strains, as shown in Figure 3.2.

In addition, PCR screening was conducted with primers designed inside the *kanMX6* gene. These primers were named Screencorrect-R (ScrCor-R) and ScreenTag-F (ScrTag-F) (Figure 3).

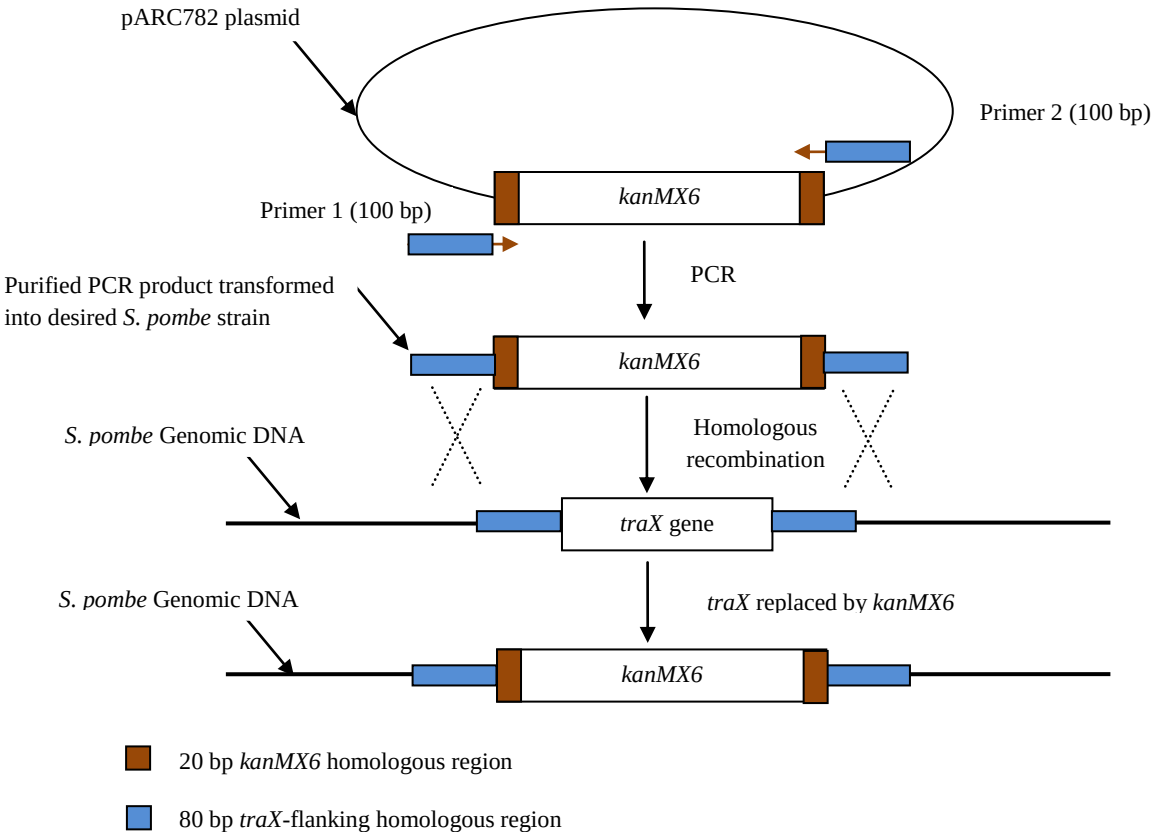

Figure 3.1 Diagram for *traX* gene knockout strategy

The pARC782 plasmid (pfa6A-kanMX6) was used as a template to amplify the *kanMX6* cassette, along with PCR primers designed with 80 bp homologous to the ends of the *traX* gene (blue box) and 20 bp homologous to *kanMX6* gene (brown box). The purified PCR product was chemically transformed into the desired *S. pombe* strains; the *traX* gene was replaced by a *kanMX6* cassette.

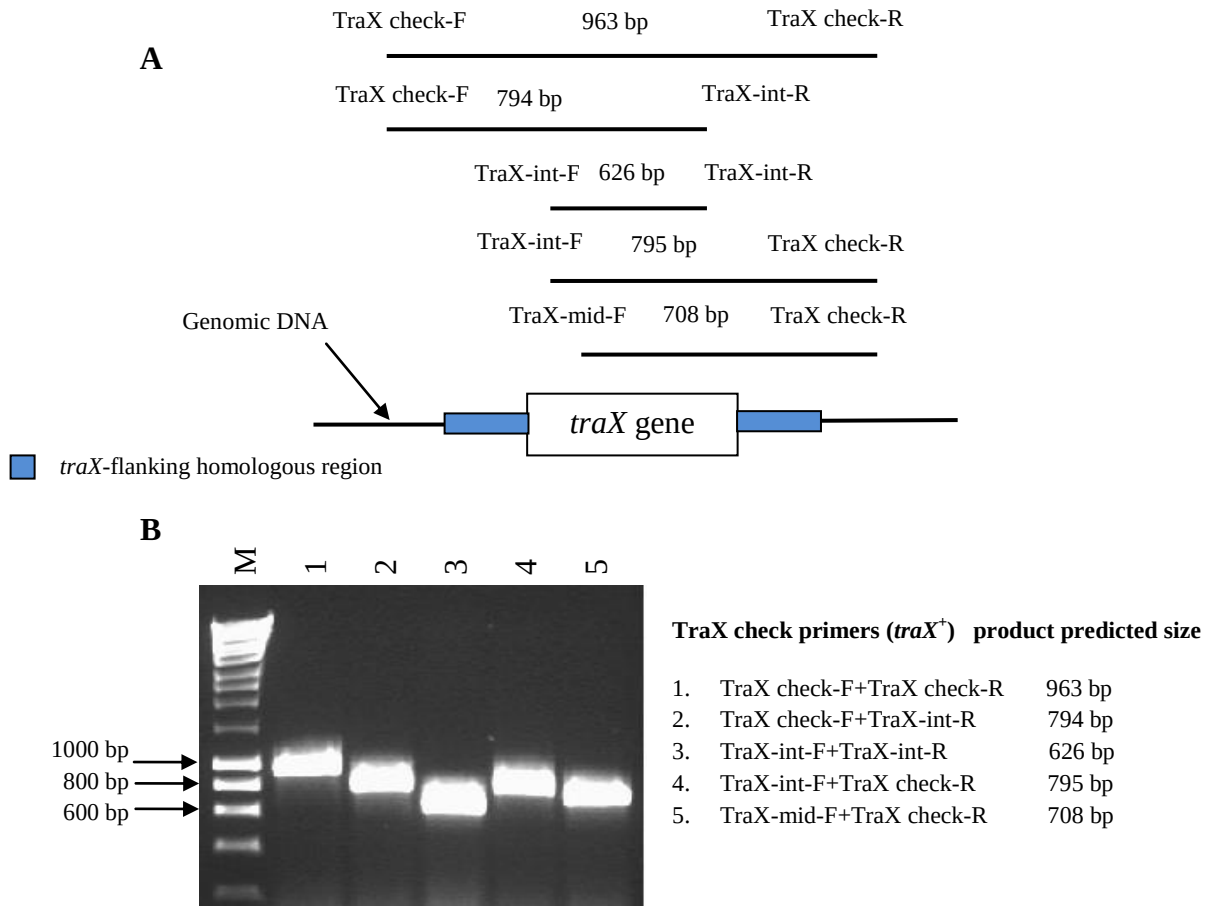

Figure 3.2 PCR checks on *traX*$^+$ strains.

A. The positions of the screening primer inside and outside of the *traX* gene region, together with the expected PCR product sizes.

B. PCR product sizes from the wild-type strain (*traX*$^+$) (BP90) obtained using five sets of screening primers. Primer set numbers 2, 3, 4 and 5 give no products for the successful *traX*Δ candidates, while primer set number 1 gives a product size of 963 bp for *traX*$^+$ and 1747 bp for *traX*Δ strains that are knocked out by the *kanMX6* cassette.

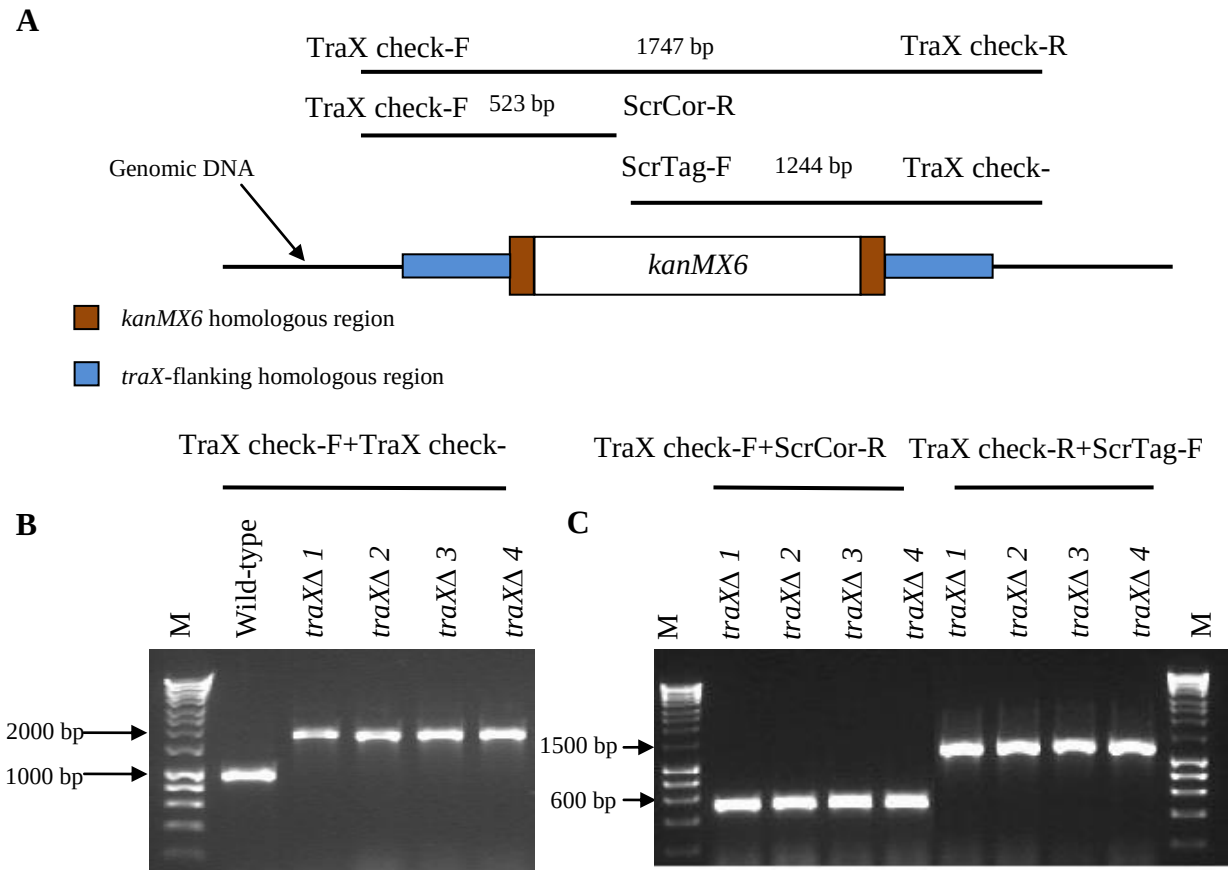

Figure 3.3 Examples of PCR screening of successful *traX*Δ candidates.

A. The positions of the checking primers inside and outside the *kanMX6* gene, together with the predicted PCR product sizes.

B. PCR products from wild-type (*traX*$^{+}$) (BP1) and *traX*Δ strains obtained using the external primers TraX check-F and TraX check-R, which give product sizes of 963 bp for the wild-type and 1747 bp for *traX*Δ candidates. The *traX*Δ strains (1, 2, 3 and 4) are (BP2413, BP2499, BP2411and BP2406), respectively.

C. PCR products for the *traX*Δ candidates obtained using the primers TraX check-F and ScrCor-R and TraX check-R and ScrTag-F, which give products of 523 bp and 1244 bp, respectively.

3.2.3 *traX* deletion confirmation by western blot

The absence of TraX protein in *traX*Δ mutants was confirmed by western blot analysis of whole cell protein extracts from *traX*Δ mutants (see Section 2.15). The western blot membranes were probed using anti-TraX polyclonal antibody (TRAX18) (Eurogentec, Liege, Belgium). The wild-type strain was used as a positive control and gave a band size of approximately 27 kDa for the TraX protein (TraX predicted mass is 26.7 kDa), while the *traX*Δ strains showed no band. In addition, the western blot membranes were stripped and then probed again against anti-α-Tubulin monoclonal antibody (Sigma, T6074), which gave a band size of approximately 50 kDa (α-Tubulin mass is approximately 50 kDa), which confirmed a uniform loading amount for all samples (Figure 3.4).

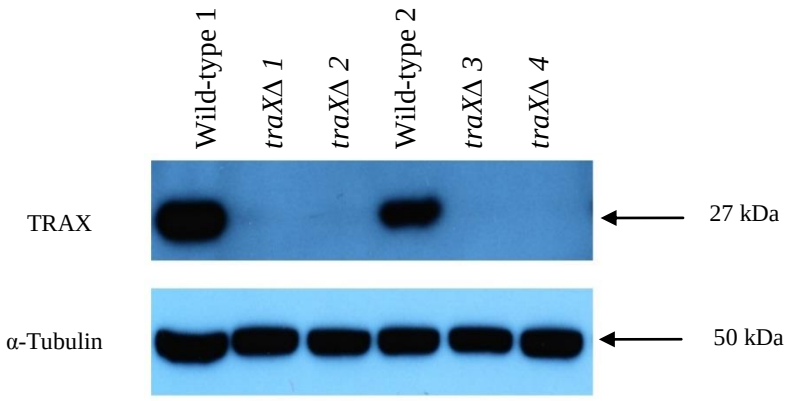

Figure 3.4 Examples of western blots for *traX*Δ strains

TRAX protein was present in wild-type strains and gave a band at approximately 27 kDa. The *traX*Δ strains did not have this 27 kDa protein. Anti-α-Tubulin (50 kDa) was used as a loading control. Wild type strains 1 and 2 are (BP1 and BP90), respectively; the *traX*Δ strains (1, 2, 3 and 4) are (BP2413, BP2499, BP2411 and BP2406), respectively.

3.2.4 Microtubule destabiliser drug thiabendazole (TBZ) sensitivity test

The heterochromatic regions of fission yeast are found in centromeres and other loci. Heterochromatin formation and maintenance at the centromere is associated directly with the functioning of the RNAi machinery. The regions of microtubule attachment to the chromosomes are centromeres. Cells with malfunctioning centromeres usually exhibit high sensitivity to TBZ destabilisation of spindle microtubules because the centromeres are attached to the mitotic spindle.

S. pombe was used as model organism because it possesses the RNAi machinery. Deletion of the RNAi component gene *ago1* disrupts chromosome segregation (Volpe et al., 2003). Therefore, *ago1*Δ was used as a positive control, along with the *bub1*Δ strain. *S. pombe* Bub1 is a kinetochore protein that is required for the mitotic checkpoint (Kadura et al., 2005). An earlier study by the McFarlane team (Jaendling et al., 2008) showed *tsn1*Δ strains had no sensitivity to TBZ.

To examine the possibility that the original study (Jaendling et al., 2008) had missed a subtle sensitivity to TBZ, different concentrations of TBZ were used, along with different treatment temperatures. This *traX*Δ strain is distinct from the one used by Jaendling et al. (2008) and observations here confirm the absence of any sensitivity to TBZ at different TBZ concentrations and temperatures (Figure 3.5). This suggests that deletion of *traX* alone does not affect chromosome segregation. The results confirm the previous study (Jaendling et al., 2008). A *tsn1*Δ strain was also tested and this too behaved as the *traX*Δ.

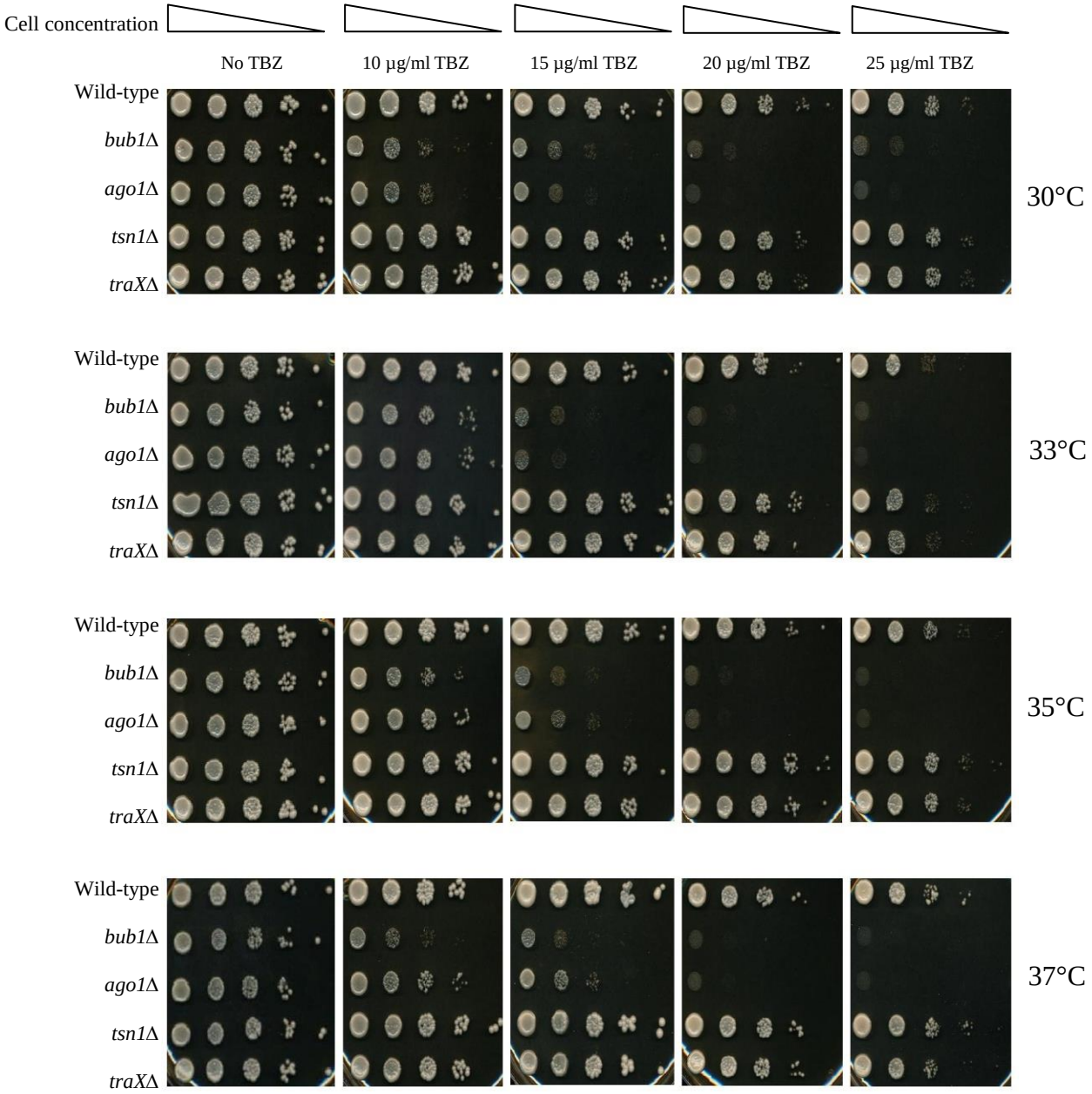

Figure 3.5 TBZ sensitivity drop tests of the *traX*Δ single mutant.

No increase in sensitivity to the microtubule destabilising agent thiabendazole (TBZ) was seen for *traX*Δ (BP1089) and *tsn1*Δ (BP1079) single mutants when compared to the wild-type (BP90). However, *bub1*Δ (BP1162) and *ago1*Δ (BP2221) strains exhibited sensitivity to TBZ. Five concentrations of TBZ were used and cells were tested at the following temperatures: 30°, 33°, 35° and 37°C.

3.2.5 Trichostatin A sensitivity tests

Trichostatin A (TSA) is a histone deacetylase inhibitor. Use of TSA prevents the re-establishment of the heterochromatic state in the absence of functional RNAi genes (Dawe, 2003), as the histone deacetylase enzymes are crucial for formation of the heterochromatic regions (Shahbazian and Grunstein, 2007). At present, TSA is being considered as an anticancer drug because it enhances apoptosis of cancerous cells (Chan et al., 2013; Suzuki and Miyata, 2005).

To question whether TraX functions in chromatin dynamics at non-centromeric regions, the effects of TSA on *traX*Δ strains were investigated using spot tests with 25 µg/ml of TSA at two temperatures, 30°C and 33°C. The *traX*Δ strain showed no increased sensitivity to the histone deacetylase inhibitor TSA when compared to the wild-type strain. A *mis6*Δ strain was used as positive control. Mis6 is a centromere associated fission yeast protein required for chromosome segregation (Saitoh et al., 1997). The *hop1::KanMX6* and *rec10::KanMX6* strains were used as it appears the *KanMX6* cassette gives a slight resistance to TSA. The *hop1* and *rec10* genes are meiosis-specific genes with no mitotic roles, so these serve as a good control for *KanMX6* gene. Apart from the *mis6*Δ strains, none of the strains tested exhibited sensitivity to TSA. (Note: the Translin-deficient cells, *tsn1*Δ were spotted for comparison) (Figure 3.6).

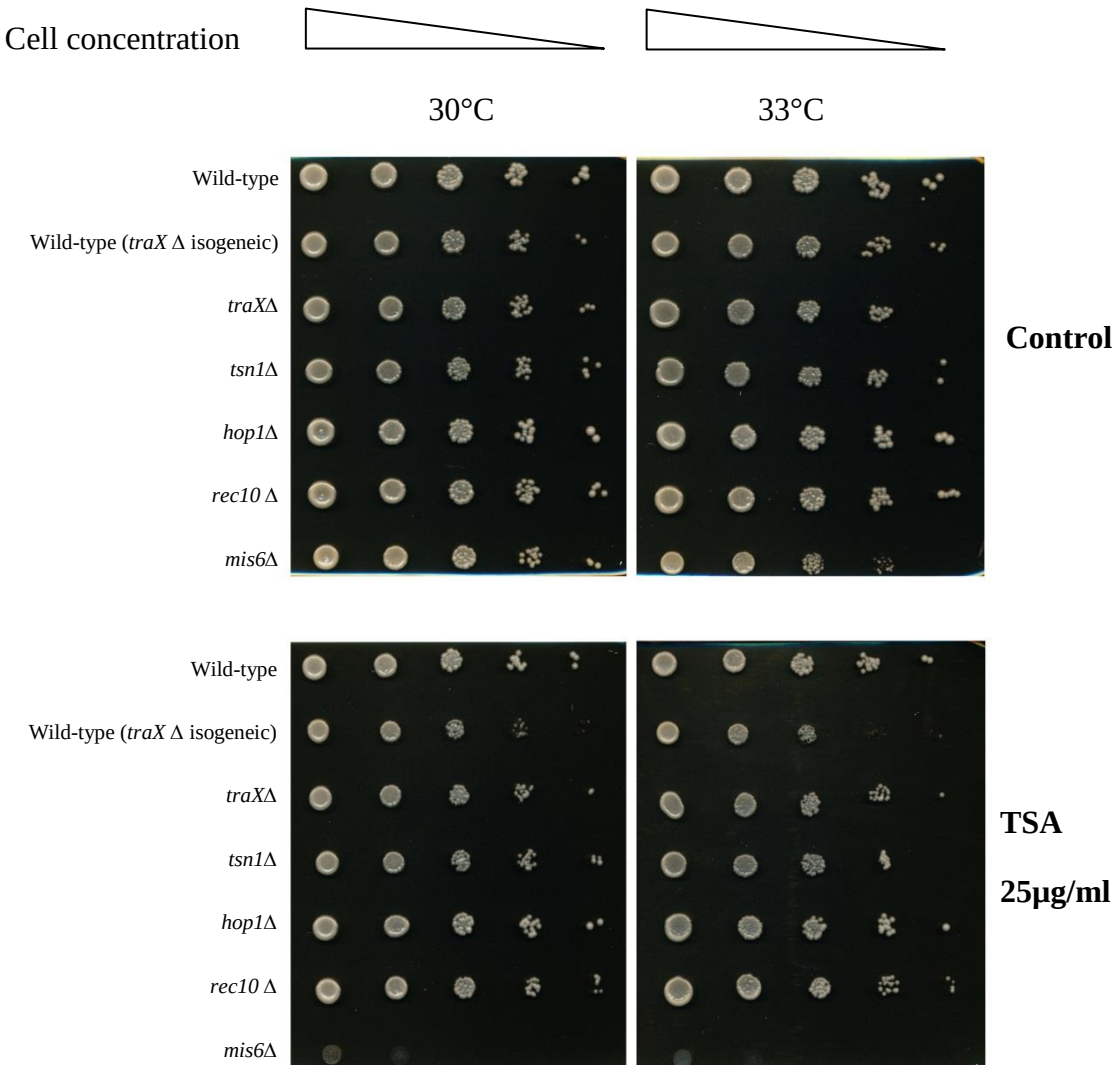

Figure 3.6 Trichostatin A spot tests of a *traX*Δ single mutant.

The histone deacetylase inhibitor TSA was used in YEA plates at concentration of 25 µg/ml. No increase in sensitivity to TSA was seen for *traX*Δ (BP1090), *tsn1*Δ (BP1080), *hop1*Δ (BP846) and *rec10*Δ (BP1731) single mutants. Two wild-type strains were used (BP1 and BP90, the latter is the isogeneic parent for the *traX*Δ strain). The *mis6*Δ (BP153) strain exhibited sensitivity to TSA and was used as a positive control. The concentration of TSA was 25 µg/ml and cells were tested at two temperatures: 30° and 33°C.

3.2.6 Minichromosome loss assays for the *traX*Δ mutant

The fission yeast minichromosome (Ch16) is an artificial centromere containing small chromosome derived from chromosome III (Niwa et al., 1986). Mitotic chromosome segregation is a complex process and requires the functioning of a large number of gene products. Sister chromatids are separated with great fidelity into two daughter nuclei by the complex spindle apparatus during anaphase. Heterochromatin regions in centromere are crucial for centromere function during this chromosome segregation (Volpe et al., 2003). Mutation of RNAi regulatory genes reduces the suppression of centromeric marker genes and leads to chromosome missegregation (Reddy et al., 2011).

Malfunctioning of the centromere and the missegregation of chromosomes can be investigated by calculating the rates of missegregation of artificial Ch16 chromosomes. Therefore, *traX*Δ strains were generated which carried the Ch16 minichromosome. These were used to investigate the effect of *traX* deletion on chromosome stability. Standard fluctuation analyses were carried out and the mean minichromosome loss percentage was derived from three independently generated median values from nine independent colonies (Figure 3.7). Data were obtained for chromosome stability at two growth temperatures 30° and 35°C. Deletion of the *traX* gene had no effect on minichromosome loss frequencies, suggesting it had no effect on chromosome segregation.

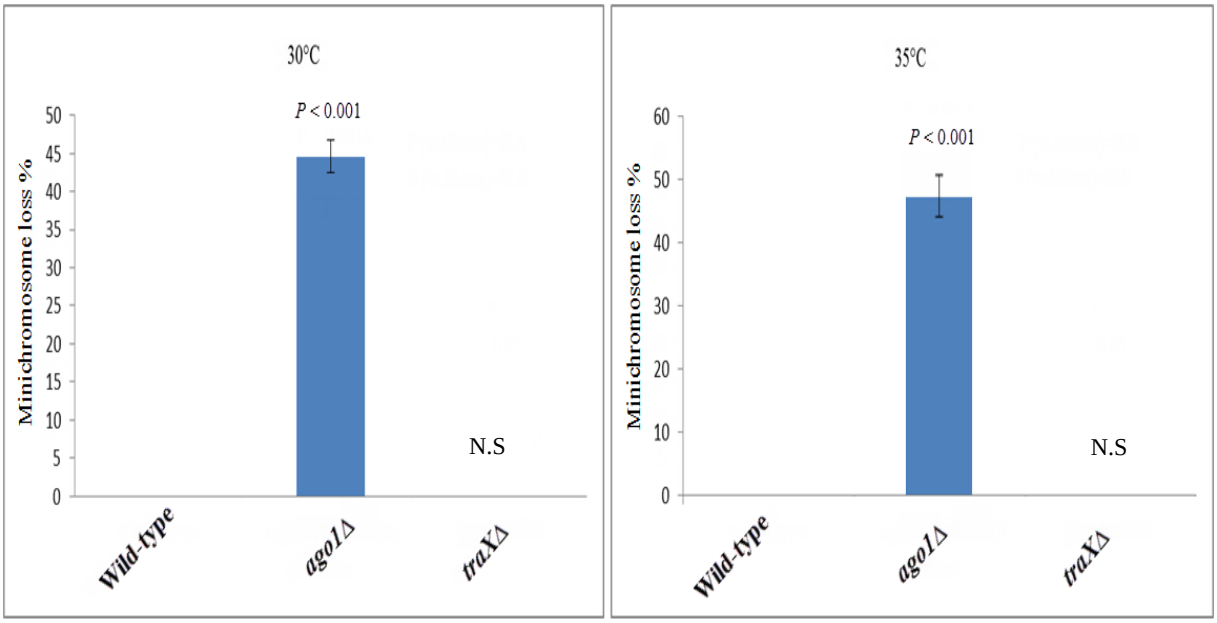

Figure 3.7 Minichromosome loss assays for a *traX*Δ single mutant.

The percentage of minichromosome loss in *traX*Δ and wild-type strains. The *ago::KanMX6* strain was used as a positive control. The percentage of minichromosome loss is taken from the mean of the median values from 3 repeats of 9 independent cultures. Strain designations are: wild-type (BP2294), *ago1*Δ (BP2472) and *traX*Δ is (BP2406). Error bars are standard deviations. *P* values were derived from a Student's *t*-test and show comparisons between wild-type and mutant *traX*Δ or *ago1*Δ strains. No significant difference was found between the *traX*Δ and wild-type strains. Cultures were tested at 30^{o} and 35^{o}C.

3.2.7 Investigation of gene silencing at different heterochromatic loci

We investigated the effect of *traX*Δ mutant on four heterochromatic regions of the *S. pombe* genome: the centromeres and the telomeres, the rDNA and the mating type locus. A *ura4*$^{+}$ marker gene was inserted into these heterochromatic regions where *ura4*$^{+}$ should be under the positional effect of heterochromatin, which maintains *ura4*$^{+}$ silencing. This was investigated using 5-FOA, which kills any strains that express *ura4*$^{+}$. Therefore, if *ura4*$^{+}$ remains silenced, cells are able to grow when treated with 5-FOA. On the other hand, if *ura4*$^{+}$ is activated in these regions, the cells will be sensitive and will die when treated with 5-FOA.

All stains that were constructed with *traX*Δ, along with other strains used in the 5-FOA spot tests, were PCR tested to ensure that the allele at the endogenous *ura4* locus on chromosome III was *ura4-DS/E*, which is a non-functional mutant, to avoid confusion with the *ura4*$^{+}$ inserted into the heterochromatin regions (Figure 3.8).

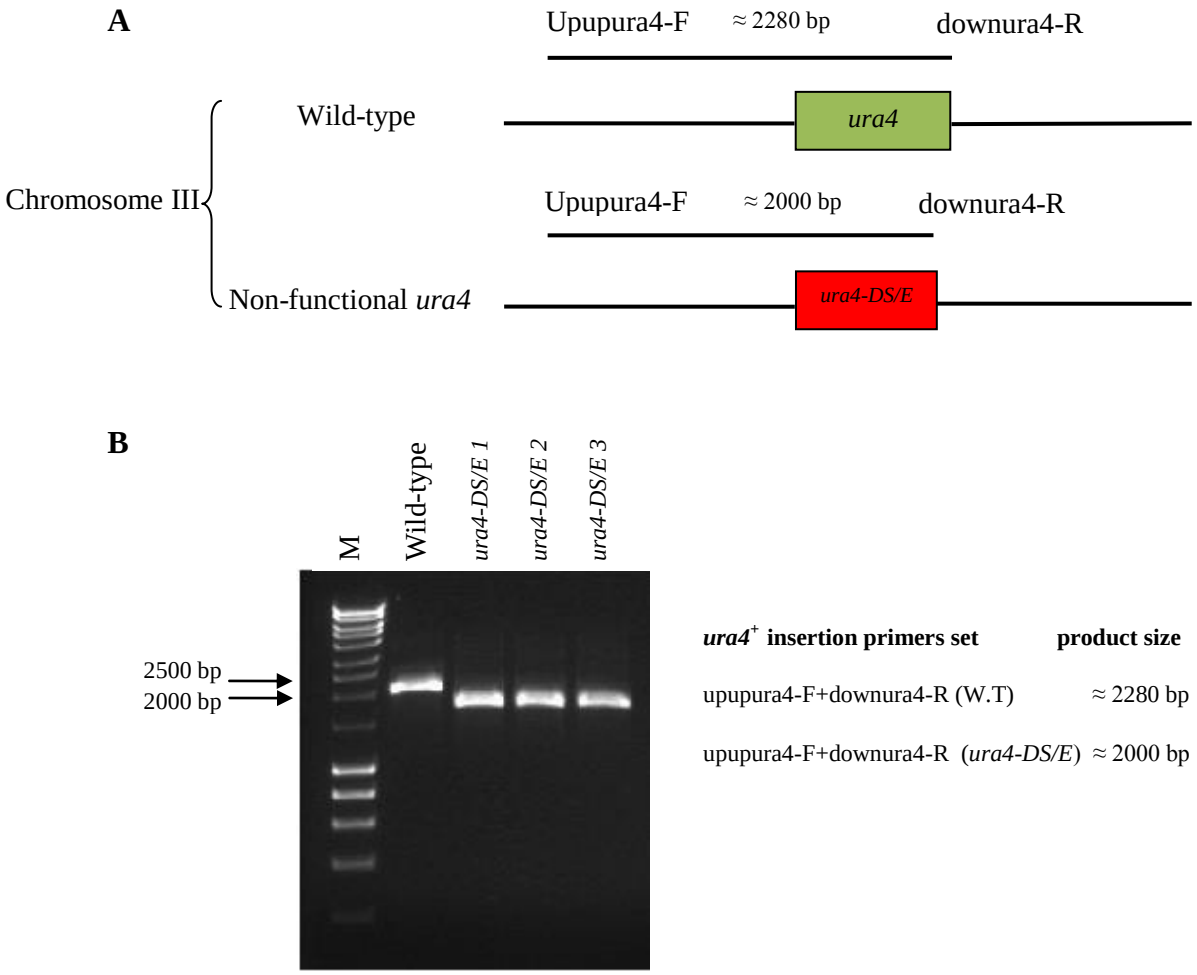

Figure 3.8 PCR screening of *ura4-DS/E* strains.

A. The positions of the checking primers outside the *ura4* gene, for wild-type strains (BP1) and non-functional *ura4-DS/E* strains (BP2411, BP2413 and BP2499), together with the approximate predicted PCR product sizes. The *ura4⁻DS/E* strains should show a size difference of 280 bp in the product.

B. PCR products from wild-type and *ura4-DS/E* strains obtained by using external primers upupura4-F and downura4-R, which give approximate product sizes of 2280 bp for the wild-type and 2000 bp for the *ura4-DS/E* strains.

3.2.7. i Analysis of centromeric gene silencing in the absence of TraX

Fission yeast centromeres are divided into three regions (for review see Section 1.7.1). The *cnt* region is where the kinetochore is assembled. The other two regions, which flank the *cnt*, are the *imr* and *otr*. The *otr* consists of two types of repeat sequence, *dg* and *dh* (Pidoux and Allshire, 2004). A potential role at for the *traX* gene in heterochromatin-mediated gene silencing at the centromere was investigated by deleting the *traX* gene in strains that carry the reporter gene *ura4*$^+$ inserted into these three heterochromatic regions (*cnt*, *otr* and *imr*) (Figure 3.9). No increased sensitivity to 5-FOA was noted in the *traX*Δ strains compared to the wild-type strains (Figure 3.10). The *ago1*Δ strains were used as a positive control because *ago1*Δ disrupts heterochromatin-mediated gene silencing. Cells were tested at 30°, 33°, 35° and 37°C.

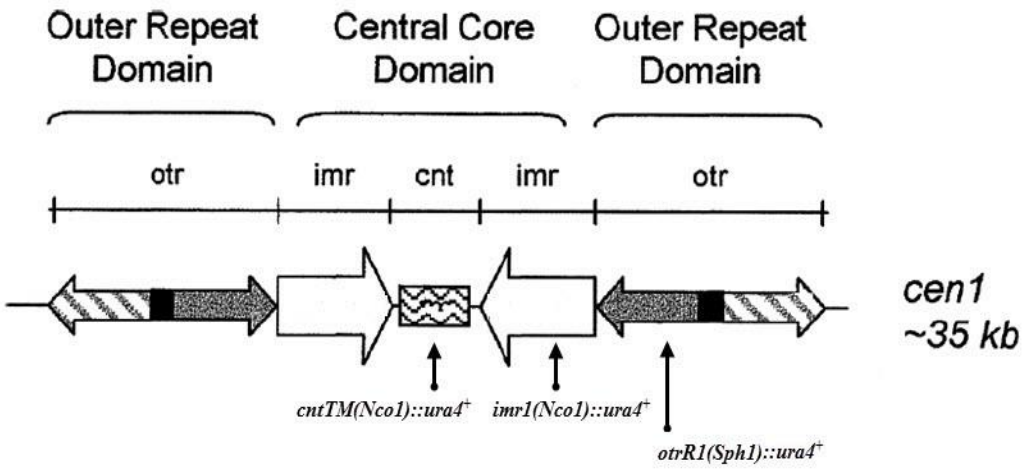

Figure 3.9 DNA structures of the fission yeast centromeres I, showing the *ura4*$^+$ gene insertion positions

The *ura4*$^+$ gene insertion positions in *cen1*. The (*cnt*) refers to the central core, (*imr*) refers to innermost repeats, and (*otr*) refers to outer repeats (adapted from Pidoux and Allshire, 2004).

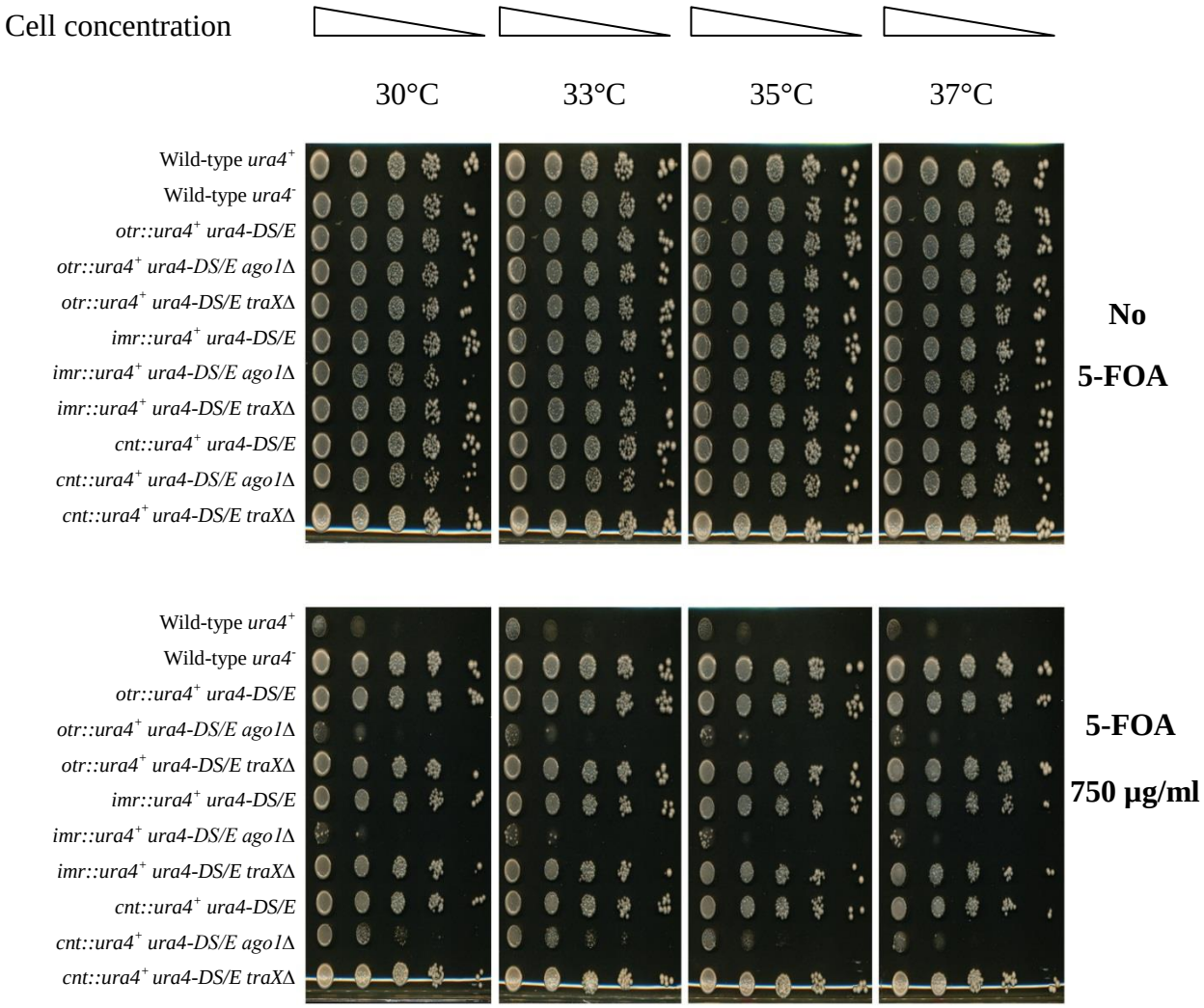

Figure 3.10 5-FOA spot tests of single mutants of *traX*Δ in strains with *ura4*$^+$ inserted into different loci in the centromere (*cnt, otr* and *imr*).

The strains were wild-types (BP1, which is *ura4*$^+$, and BP90, which is *ura4*$^-$) and wild-type *traX*Δ isogeneic strains for *otr*, *imr*, and *cnt* (BP2204, BP2506 and BP2203, respectively). The *ago1*Δ strains (BP2388, BP2386 and BP2385) were used as positive controls. The *traX*Δ strains were BP2413, BP2499 and BP2411. Cells were treated with 750 µg/ml of 5-FOA. No increase in sensitivity to 5-FOA was noticed in the *traX*Δ single mutants compared to *ago1*Δ strains. Cells were tested at 30°, 33°, 35° and 37°C.

3.2.7 ii Analysis of telomeric gene silencing in the absence of TraX

The telomeres are the ends of the chromosome and include heterochromatic repetitive DNA that are defined as subtelomeric regions (Dehé and Cooper, 2010). Maintenance of telomeres is important to avoid chromosome shortening during replication. The maintenance of telomeres is achieved by the telomerase enzyme (Schoeftner and Blasco, 2009). Telomeres contain nucleoproteins that prevent chromosomes ends from fusions or degradation (Weuts et al., 2012).

The RNAi machinery is important for heterochromatin formation at telomere regions (Kanoh et al., 2005). Heterochromatic telomeric DNA tandem repeats are found in fission yeast and also in mammalian genomes. The telomere position effect identified in telomeres is a phenomenon whereby any gene embedded in this heterochromatic tandem repeat region remains transcriptionally silenced (Bah and Azzalin, 2012; Pedram et al., 2006).

A potential role for the *traX* gene in heterochromatin-mediated gene silencing at the heterochromatin subtelomeric regions was analysed by constructing the fission yeast strains having the reporter gene *ura4*$^{+}$ inserted in subtelomeric heterochromatin regions with deletion of the *traX* gene. 5-FOA spot tests were applied at three temperatures: 30°, 33° and 35°C. No increased sensitivity to 5-FOA was noted in the *traX*Δ or *tsn1*Δ strains compared to the wild-type *ura4*$^{+}$ strain (Figure 3.11).

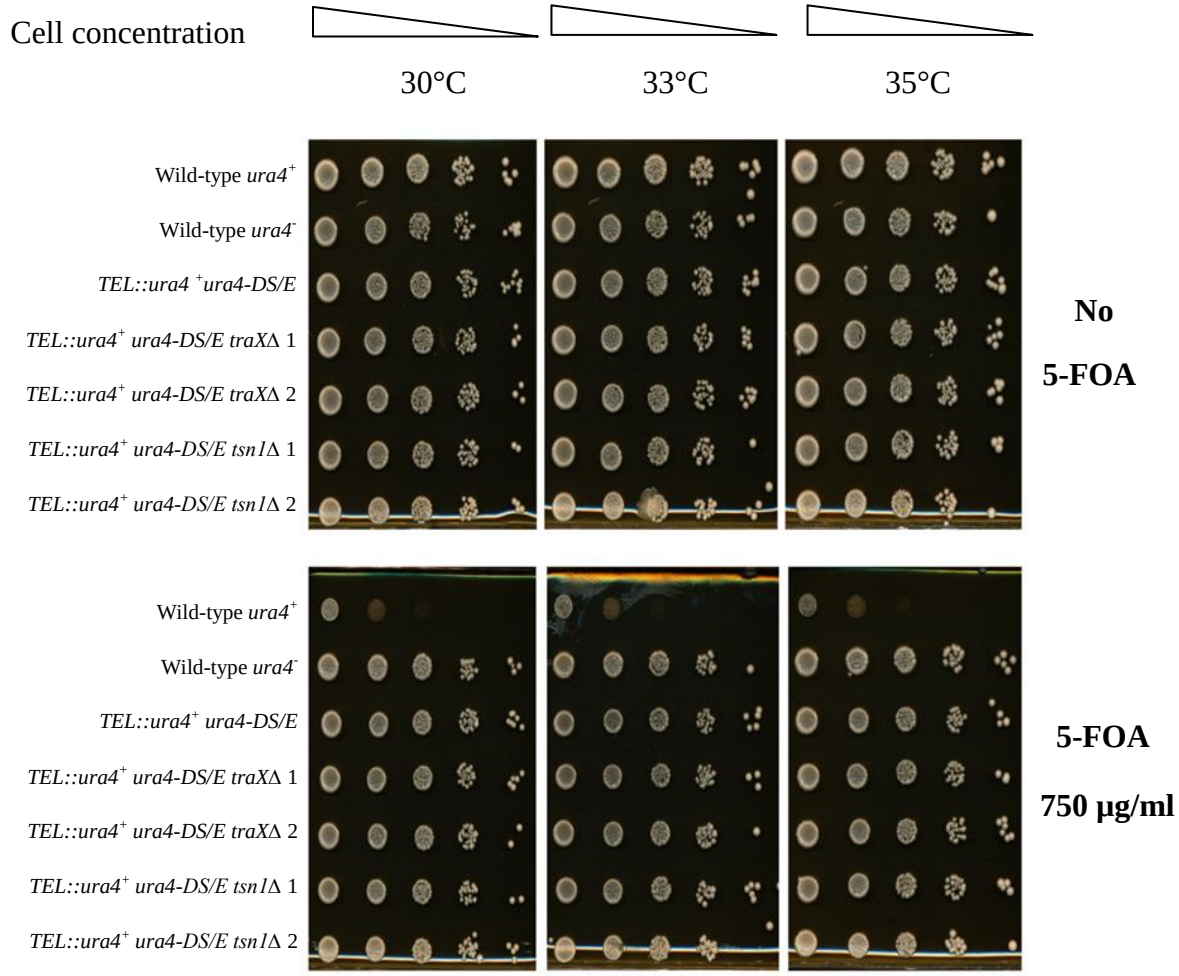

Figure 3.11 5-FOA spot tests of *traX*Δ *or tsn1*Δ single mutants of the *TEL::ura4*$^+$ strains.

The *traX*Δ single mutants (BP2716 and BP2717) and *tsn1*Δ single mutants (BP2722 and BP2723) showed no added sensitivity to 5-FOA when compared to the positive wild-type *ura4*$^+$ (BP1) strain. Wild-type *ura4*$^-$ (BP90) was used as a negative control. The *traX*Δ wild-type isogeneic strain was BP2705. Cells were tested at 30°, 33° and 35°C. The highest cell concentration (1x10^5 cells) was diluted (1:5) and spotted on YEA plates with and without 750 µg/ml 5-FOA. Plates were incubated for 4 days.

3.2.7 iii Analysis of gene silencing at the *mat* locus in the absence of TraX

S. pombe has three mating-type cassettes located on the long arm of chromosomes II (Egel, 2005). These cassettes are: *mat1P/M* (which means the mating type could be $P=h^+$ or $M=h^-$), *mat2-P* (h^+) and *ma3-M* (h^-). The latter two loci and the area between them (the *K* region) are heterochromatin regions, while the *mat1* locus is a euchromatin region that remains active to determine the state of the mating type (Hansen et al., 2011). Switching of the mating type is achieved when a single-stranded DNA break occurs during DNA replication and recombination subsequently happens with a donor cassette of either *mat2-P* or *mat3-M* (Figure 3.12). Mating-type switching can also occur under nitrogen starvation when the DNA recombination occurs between either of the donor cassettes into *mat1* (reviewed in Klar, 2007).

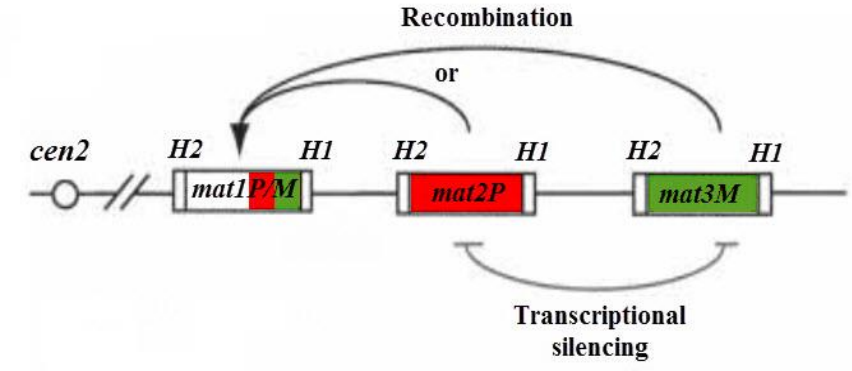

Figure 3.12 Mating-type switching on chromosome II in fission yeast

The three mating-type cassettes are located on chromosome II. During replication single-stranded DNA break can occur then the recombination (black arrow) is achieved by a donor cassettes either *mat2-P* or *mat3-M*. H1 and H2 are homology domains (adapted from Vengrova and Dalgaard, 2004).

Heterochromatin at *mat* is driven by either an RNAi-dependent or RNAi-independent, Atf1/Pcr1-dependent pathway (Jia et al., 2004b). A possible role for the *traX* gene in heterochromatin-mediated gene silencing at the mating-type locus was analysed by creating new *S. pombe* strains having the reporter gene *ura4*$^{+}$ inserted in the *mat3* locus, along with deletion of *traX* gene. These strains should retain their resistance to 5-FOA, unless the deletion of the *traX* gene disturbed heterochromatin regulation, allowing the *ura4*$^{+}$ gene to become transcriptionally active. The spot tests were conducted at three temperatures: 30°, 33° and 35°C. No increased sensitivity to 5-FOA was noted in the *traX*Δ or *tsn1*Δ strains when compared to the wild-type (*ura4*$^{+}$). Spot tests were conducted on supplemented YEA plates with and without 750 µg/ml 5-FOA. Plates were incubated for 4 days (Figure 3.13).

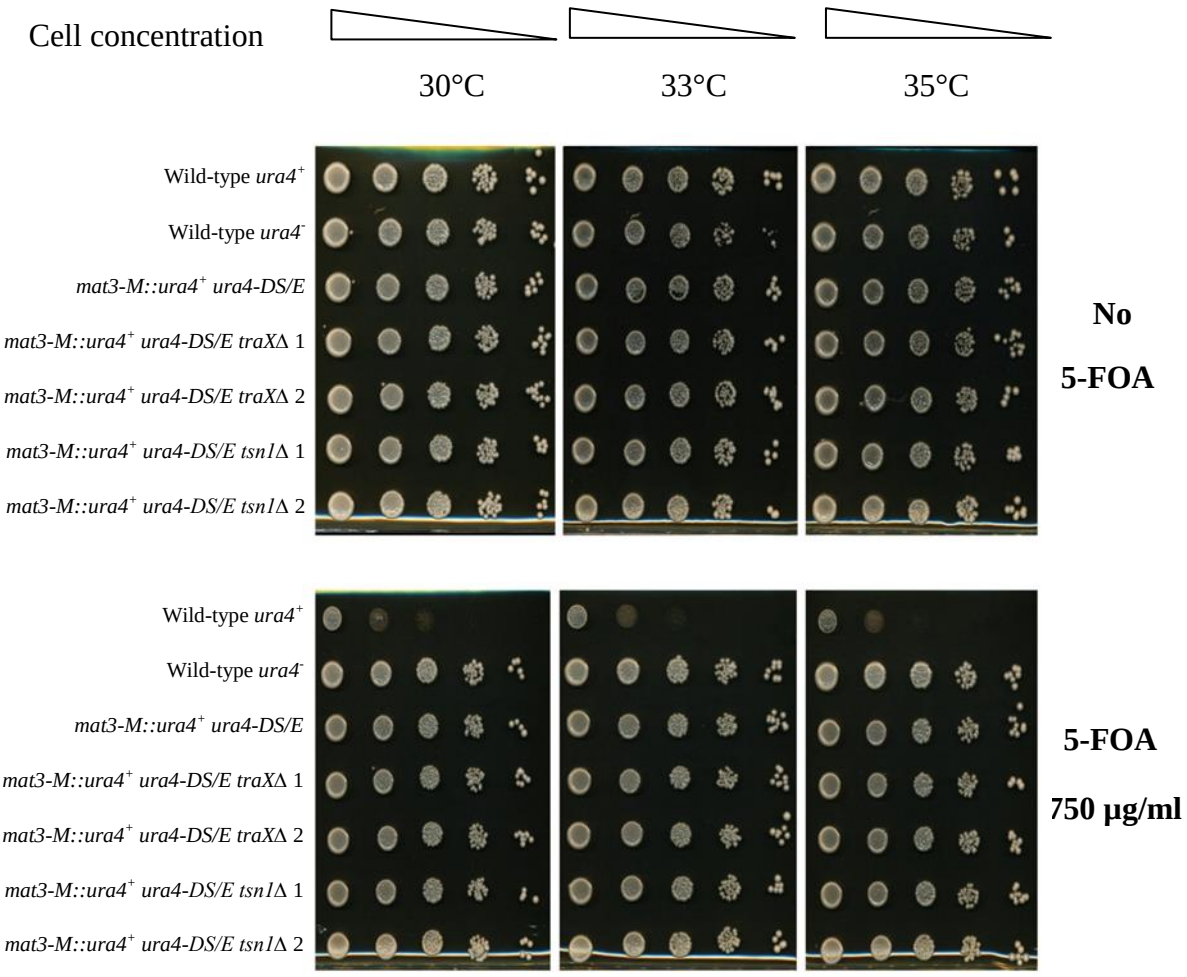

Figure 3.13 5-FOA spot tests of *traX*Δ or *tsn1*Δ single mutants of *mat3-M::ura4*$^+$ strains.

The *traX*Δ single mutants (BP2718 and BP2719) and *tsn1*Δ single mutants (BP2724 and BP2725) showed no added sensitivity to 5-FOA when compared to the positive wild-type *ura4*$^+$ (BP1). Wild-type *ura4*$^-$ (BP90) was used as a negative control. The *traX*Δ wild-type isogeneic was BP2706. Cells were tested at 30°, 33° and 35°C. Spot tests were conducted on YEA plates with or without 750 µg/ml 5-FOA. Plates were incubated for 4 days.

3.2.7 iv Analysis of gene silencing at the rDNA locus in the absence of TraX

The locus for ribosomal DNA (rDNA) in eukaryotic genomes is heterochromatic regions that are organised as clusters of long tandem repeats. These repeats of rDNA sequences encode ribosomal RNA, which is crucial for ribosomes (McStay and Grummt, 2008). The rRNAs are highly conserved in a broad range of species, from bacteria to humans (Kobayashi, 2011).

Reporter genes, such as *ura4*$^{+}$, inserted in rDNA regions show a transcription silencing effect because of the positional effects of these regions (Dubey et al., 2009). The heterochromatic rDNA regions are fragile sites in the genome. Therefore, the formation of heterochromatin at rDNA loci could be a mechanism for prevention of recombination at these regions (Kobayashi et al., 2004). A possible role for the *traX* gene in mediating silencing at the rDNA region was determined by constructing *traX*Δ strains that have *ura4*$^{+}$ inserted in the rDNA locus. Strains were spotted on supplemented YEA with 5-FOA and incubated for 4 days. No increased sensitivity to 5-FOA was noticed in the *traX*Δ mutants and *tsn1*Δ strains.

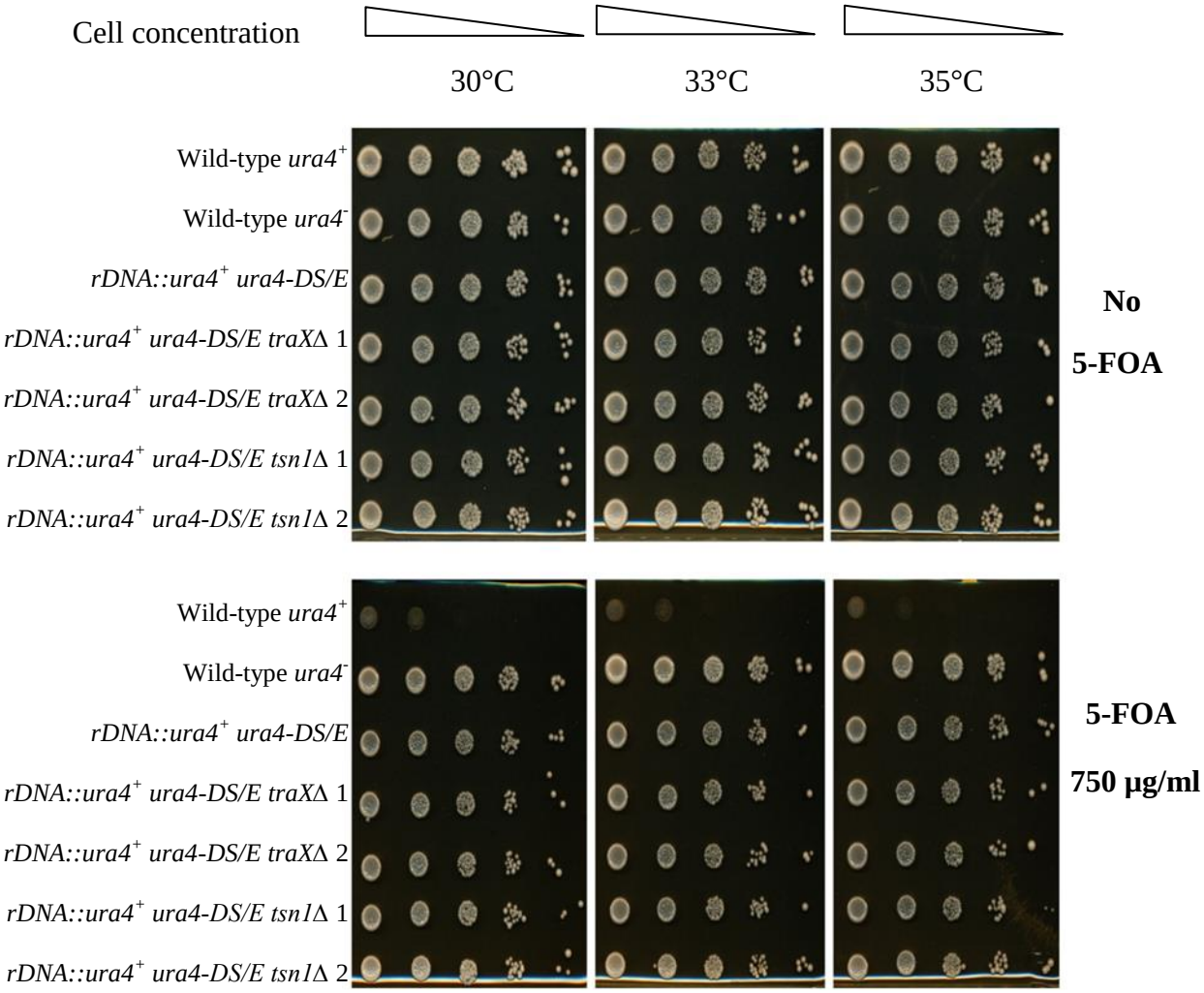

Figure 3.14 The 5-FOA spot tests of *traX*Δ or *tsn1*Δ single mutants of *rDNA::ura4*$^+$ strains.

The *traX*Δ single mutants 1 and 2 were BP2714 and BP2715, respectively and *tsn1*Δ single mutants were BP2720 and BP2721. All Single mutant strains either *traX*Δ or *tsn1*Δ showed no additional sensitivity to 5-FOA when compared to the positive wild-type *ura4*$^+$ (BP1). The negative wild-type *ura4*$^-$ was BP90. The *traX*Δ wild-type isogeneic was BP2704. Cells were tested at 30°, 33° and 35°C. The highest cell concentration (1x10^5 cells) was diluted (1:5) and spotted on YEA plates with and without 750 µg/ml 5-FOA. Plates were incubated for 4 days.

3.3 Discussion

3.3.1 The *traX*Δ single mutants are not sensitive to the microtubule inhibitor Thiabendazole (TBZ)

Translin-associated factor X (TRAX) and Translin proteins have been suggested to play an important role in the RNAi mechanism, which is central to the formation of heterochromatin regions such as the centromere. The heterochromatin in the centromere is a fundamental area for microtubule attachment during chromosome segregation. Translin was located at the centrosomes during metaphase and on the mitotic spindle, suggesting that Translin could be involved in chromosome segregation by accelerating microtubule organisation (Ishida et al., 2002). Fission yeast mutants that have defects in chromosome segregation, such as defective in kinetochore-microtubule attachment, are hypersensitive to the anti-microtubule drug TBZ (Murakami et al., 2007; Takahashi et al., 2011).

This chapter examined whether *traX*Δ (and *tsn1*Δ) single mutants are sensitive to the microtubule inhibitor TBZ. No increased sensitivity to TBZ was found in either *traX*Δ or *tsn1*Δ single mutants, which suggests that no direct function for these two proteins is required in either heterochromatin formation at the centromere or during chromosome segregation.

3.3.2 The *traX*Δ single mutants are not affected by Trichostatin A

The histone deacetylase enzymes play very important roles in heterochromatin formation at different regions (Yamada et al., 2005). Trichostatin A (TSA) is a histone deacetylase inhibitor that prevents re-establishment of the heterochromatic state by causing acetylation of H3K9 rather than methylation (Dawe, 2003). TSA is now used as an anticancer drug because it induces apoptosis of cancer cells (Chan et al., 2013). The TSA spot tests in the present study showed no increased sensitivity in the *traX*Δ (or *tsn1*Δ) single mutants, which again suggested that no direct link exists between TRAX and Translin proteins in heterochromatin establishment or maintenance in *S. pombe*.

3.3.3 No chromosome segregation instability for *traX*Δ single mutants

Chromosome segregation during cell division is achieved by a distinct mechanism. Errors in this mechanism may lead to instability of chromosome segregation and subsequently may cause genomic instability and ultimately the development of cancers (Draviam et al.,

2004). The centromere is a very important region for chromosome segregation during mitosis and meiosis. It is the region where the microtubule is attached to the kinetochore during sister chromatid segregation (Cutts et al., 1999). The centromere is one of the heterochromatic regions in the fission yeast genome and the RNAi machinery has been linked directly to centromeric function (Castel and Martienssen, 2013). Mutation of the RNAi genes causes defective heterochromatic silencing at the centromere (Reddy et al., 2011; Volpe et al., 2002). In the present study, deletion of the *traX* gene alone did not disturb chromosome segregation in the fission yeast single mutants. This suggests there is not a major primary role for TraX-dependent pathway in any function relating to chromosome stability maintenance.

3.3.4 No primary function for TraX in gene silencing at the centromere, telomeres, mating locus or rDNA region

As already described, the fission yeast genome contains different heterochromatin regions (the centromere, telomeres, mating locus and rDNA regions) (reviewed in Djupedal and Ekwall, 2009; Klar, 2007). Any active gene, such as *ura4*$^{+}$, placed into these regions should also remain silenced because it falls under the influence of the heterochromatin position effect (Goto and Nakayama, 2012). We hypothesised that TRAX (and Translin) plays a role in RNAi-mediated gene silencing in these heterochromatin regions, as these proteins were identified to have role in RNAi regulation in *Drosophila* (Liu et al., 2009). Our data show that *traX* gene deletion does not disturb the heterochromatin silencing of an active encoded-protein gene *ura4*$^{+}$ inserted into different heterochromatic regions. These finding suggests that deletion of the *traX* gene alone does not disrupt heterochromatin-mediated gene silencing.

3.4 Conclusions

The analysis of a single mutant of *traX*Δ (and to some degree, *tsn1*Δ) gives no evidence for a functional role in the genome regulation pathways controlled by RNAi. This contrast to the hypothesis, however, it supports the previous finding of Jaendling and co-workers (2008). Whilst a primary pathway does not appear to be perturbed, Halic and Moazed (2010) suggested a distinct secondary Dicer-independent pathway for heterochromatin formation. It might be the case that TraX (and Translin) function in secondary or redundant pathways; this hypothesis is tested in later chapters.

In *Neurospora* (Li et al., 2012) no role was found for Translin or TRAX in RNAi-like pathways. They found a predominant role in tRNA processing. It might be the case that *S. pombe tsn1* and *traX* do not have any RNAi function, but do function to regulate some unidentified mechanism such as tRNA processing. The data in this chapter certainly support the conclusion of no primary RNAi function for mediated genomic stability.

CHAPTER 4

Investigation of RNAi-defective in *traX* double and triple mutants

4.1 Introduction

As documented in Chapter 3, we found no defects in heterochromatin-mediated gene silencing and no evidence for increased genome instability in *traX*Δ single mutants. However, the TRAX-Translin complex (C3PO) is reported to function in facilitating the removal of the passenger strand during RNAi mediated gene silencing (Liu et al., 2009; Ye et al., 2011). In addition, TRAX and Translin serve in the endonucleolytically processing of immature RNAs, predominantly the processing of pre tRNAs to mature tRNA molecules (Li et al., 2012). These finding could indicate that these conserved proteins are involved in a range of biological functions resulting from their tRNA processing activity. Given the lack of a primary role in RNAi in *S. pombe*, we addressed the question of whether Tsn1 (Translin) and TraX (TRAX) might play a redundant role with RNAi regulators such as Dcr1 or Ago1.

S. pombe uses the RNAi machinery to maintain the heterochromatin state of key functional genomic regions such as centromeres, telomeres, mating-type loci and rDNA (reviewed in Djupedal and Ekwall, 2009; Klar, 2007). The RNAi machinery in the centromeres is linked directly to both heterochromatin assembly and maintenance (Creamer and Partridge, 2011). Deletion of RNAi component genes such as *dcr1* or *ago1* results in centromeric malfunction and disturbance of heterochromatin silencing (Carmichael et al., 2004; Volpe et al., 2002). In *S. pombe*, the *dcr1*Δ mutant is defective in the precentromic heterochromatin state, leading to chromosome missegregation, minichromosome instability and increased sensitivity to the microtubule poison TBZ (Reddy et al., 2011; Volpe et al., 2003).

In addition, Translin and TRAX proteins were implicated in responses to DNA damage. Mammalian Translin levels were increased in the nucleus after treatment with the DNA damaging agents mitomycin C and ionising radiation (Fukuda et al., 2008; Kasai et al., 1997). Moreover, mammalian TRAX interacted with the DNA binding protein C1D when cells were exposed to γ irradiation, which stops the binding of TRAX to Translin and formation of the Translin-TRAX complex and therefore the subsequent binding of this complex to DNA (Erdemir et al., 2002).

Given the above, we hypothesised that deletion of the *traX* gene, together with other RNAi regulator genes such as *ago1* and *dcr1* could expose a role for TraX protein in a redundant RNAi pathway to control genome stability. Therefore, we constructed a range of fission yeast double and triple mutants to test this hypothesis. A colleague within our group had already generated the double mutants *tsn1*Δ *ago1*Δ and *tsn1*Δ *dcr1*Δ. These mutants were used to expose a possible fundamentally important function for TraX and Tsn1 in *S. pombe*.

4.2 Results

4.2.1 Construction of *traX* double and triple mutant strains

All fission yeast strains were constructed using direct gene deletion, as described by Bähler and co-workers (Bähler et al., 1998). Four genes (*traX*, *tsn1*, *dcr1* and *ago1*) were deleted to construct the double mutants *traX*Δ *tsn1*Δ, *traX*Δ *ago1*Δ and *traX*Δ *dcr1*Δ and the triple mutants *traX*Δ *tsn1*Δ *ago1*Δ and *traX*Δ *tsn1*Δ *dcr1*. Three replacement cassettes were used: *kanMX6*, *natMX6* and *ura4*$^{+}$ (Hentges et al., 2005; Watson et al., 2008). The plasmids carrying the replacement cassettes were extracted from *E. coli* strains (see Table 2.3) and the cassettes were amplified using PCR with primers designed with 70-100 bp homologies to the sequence immediately upstream and downstream of the open reading frames (ORF) of the genes selected for deletion, together with 20 bp homology to the ends of the selectable replacement cassettes. The PCR product was then chemically transformed into the fission yeast genome, as described previously (see Section 2.5).

New strains and the parental strains used in Chapter 3 were used to construct the double and triple mutants investigated in this chapter. The pYL16 plasmid, which contains the *natMX6* resistance gene, was used as a replacement cassette for the *traX*Δ *tsn1*Δ *ago1*Δ and *dcr1*Δ genes. In addition, the pAW1 plasmid, which contains the *ura4*$^{+}$ gene, was used as a replacement cassette for the *ago1*Δ and *dcr1*Δ genes. PCR screenings were conducted to confirm gene deletion. Internal and external primers for each gene were designed. Examples of the PCR screenings, along with product sizes, are shown in Figures 4.1–4.9.

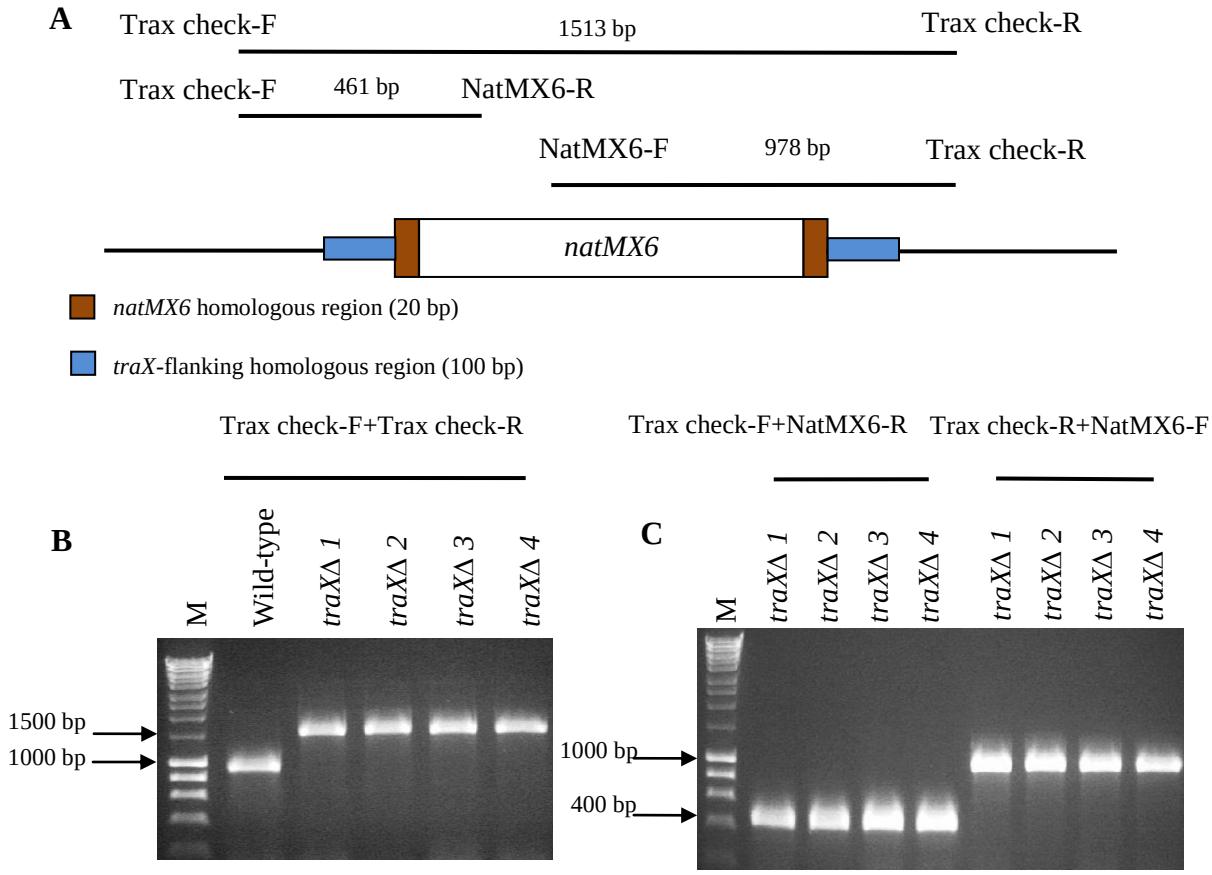

Figure 4.1 Examples of PCR screening of a successfully constructed *traX*Δ using the *natMX6* cassette.

A. The positions of the checking primers inside and outside the *natMX6* gene, together with the predicted PCR product sizes.

B. PCR products from wild-type (*traX*$^{+}$) (BP90) and *traX*Δ strains 1, 2, 3 and 4 (BP3250, BP3251, BP3252 and BP3523, respectively) obtained using the external primers Trax check-F and Trax check-R, which give a product size of 963 bp for the wild-type and 1513 bp for the *traX*Δ candidates with deletions due to the *natMX6* cassette.

C. PCR products for the *traX*Δ candidates obtained using the primers Trax check-F and NatMX6-R and Trax check-R and NatMX6-F, which give a product size of 461 bp and 978 bp, respectively.

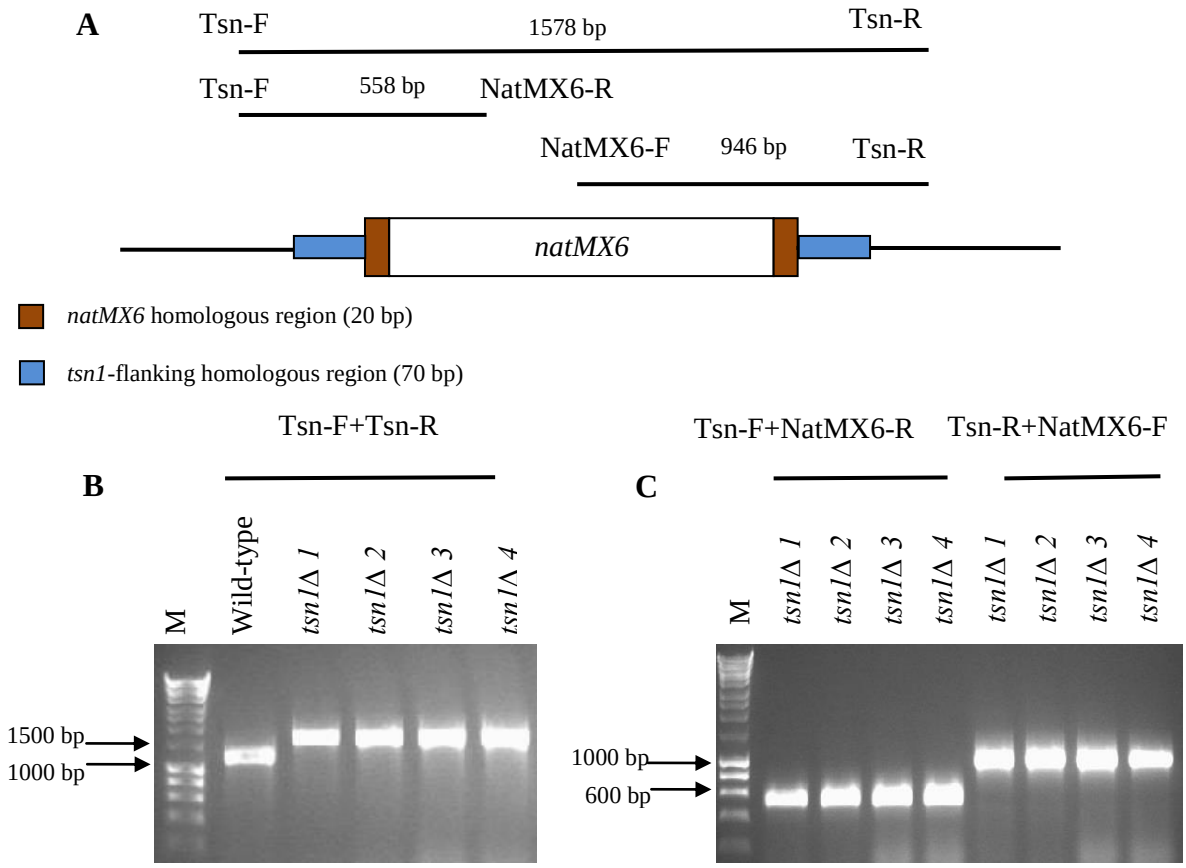

Figure 4.2 Examples of PCR screening of a successfully constructed *tsn1*Δ using the *natMX6* cassette.

A. The positions of checking primers inside and outside the *natMX6* gene, together with the predicted PCR product sizes.

B. PCR products from wild-type (*tsn1*$^{+}$) (BP1) and *tsn1*Δ1, 2, 3 and 4 strains (BP3246, BP3247, BP3248 and BP3249, respectively) obtained using the external primers Tsn-F and Tsn-R, which give a product size of 1218 bp for the wild-type and 1578 bp for the *tsn1*Δ candidates with deletions due to the *natMX6* cassette.

C. PCR products for the *tsn1*Δ candidates obtained using the primers Tsn-F and NatMX6-R and Tsn-R and NatMX6-F, which give a product size of 558 bp and 946 bp, respectively.

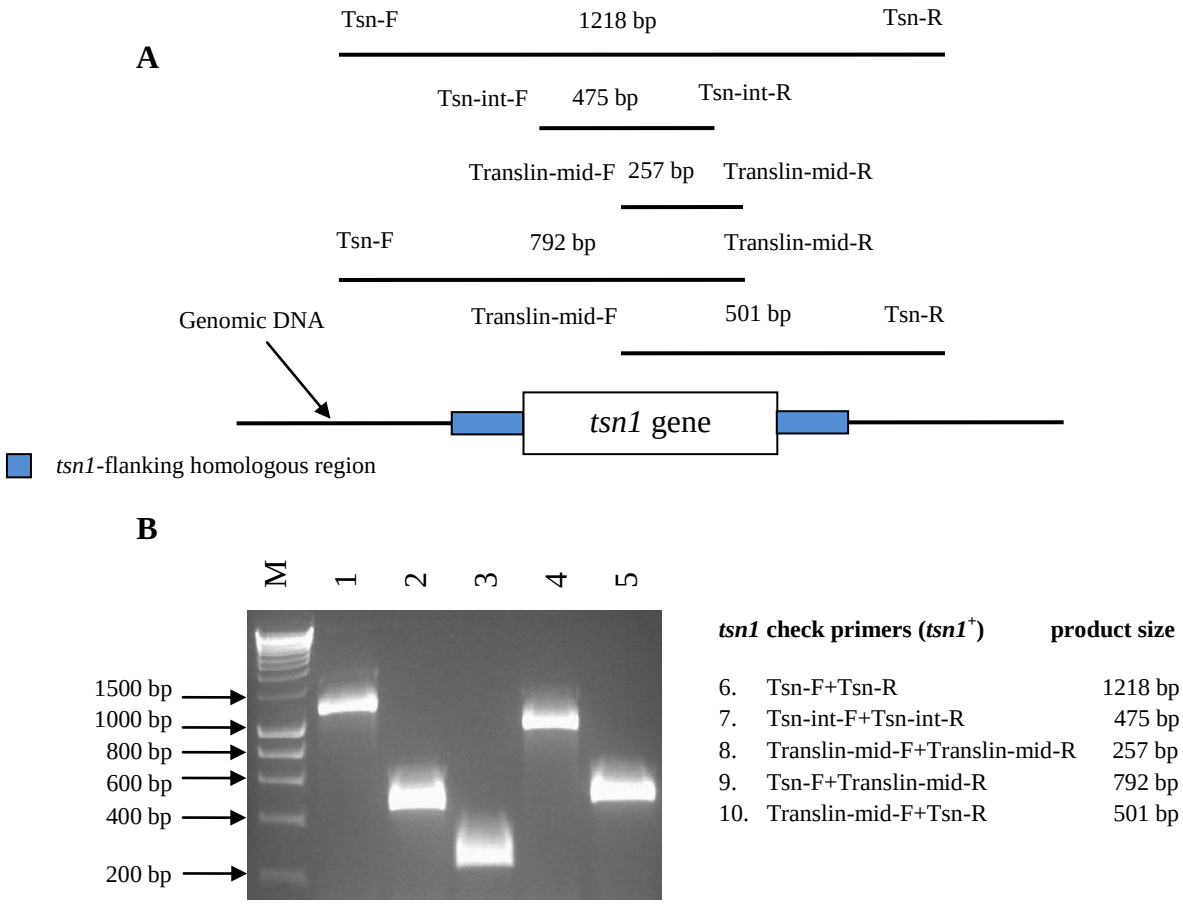

Figure 4.3 Examples of PCR checks on *tsn1*$^+$ strains.

A. The positions of the screening primer inside and outside of the *tsn1* gene, together with the predicted PCR product sizes.

B. PCR product sizes from wild-type strain (*tsn1*$^+$) (BP1) obtained using five sets of screening primers. Primer set numbers 2, 3, 4 and 5 give no products for the successful *tsn1*Δ candidates while primer set number 1 gave a product size of 1218 bp for *tsn1*$^+$ and 1578 bp for *tsn1*Δ strains with deletions due to the *natMX6* cassette.

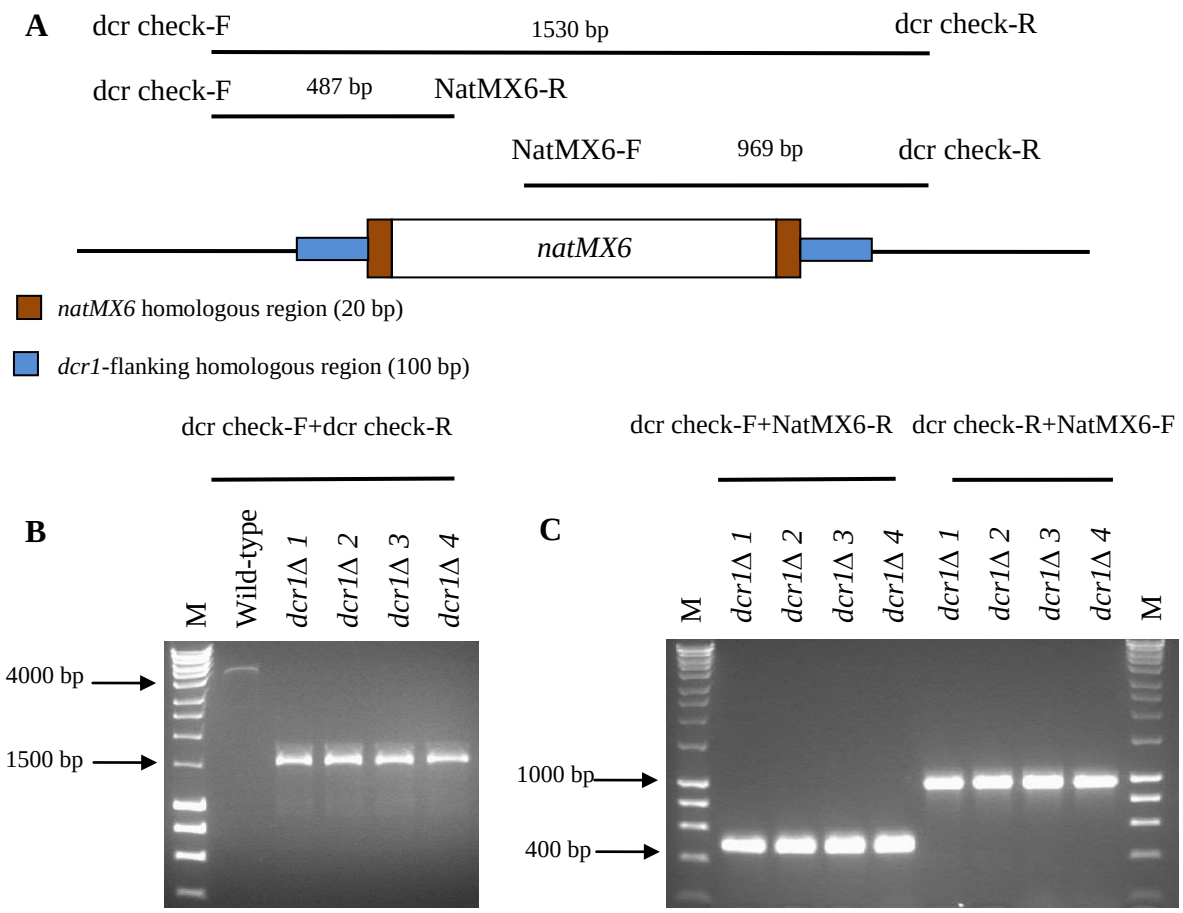

Figure 4.4 Examples of PCR screening of a successfully constructed *dcr1*Δ using the *natMX6* cassette.

A. The positions of checking primers inside and outside the *natMX6* gene, together with the predicted PCR product sizes.

B. PCR products from wild-type (*dcr1*$^{+}$) (BP1) and *dcr1*Δ 1, 2, 3 and 4 (BP3254, BP3255, BP3256 and BP 32567 respectively) strains obtained using the external primers dcr check-F and dcr check-R, which give a product size of 4409 bp for the wild-type and 1530 bp for the *dcr1*Δ candidates with deletions due to the *natMX6* cassette.

C. PCR products for the *dcr1*Δ candidates obtained using primers dcr1 check-F and NatMX6-R and dcr check-R and NatMX6-F, which give a product size of 487 bp and 969 bp, respectively.

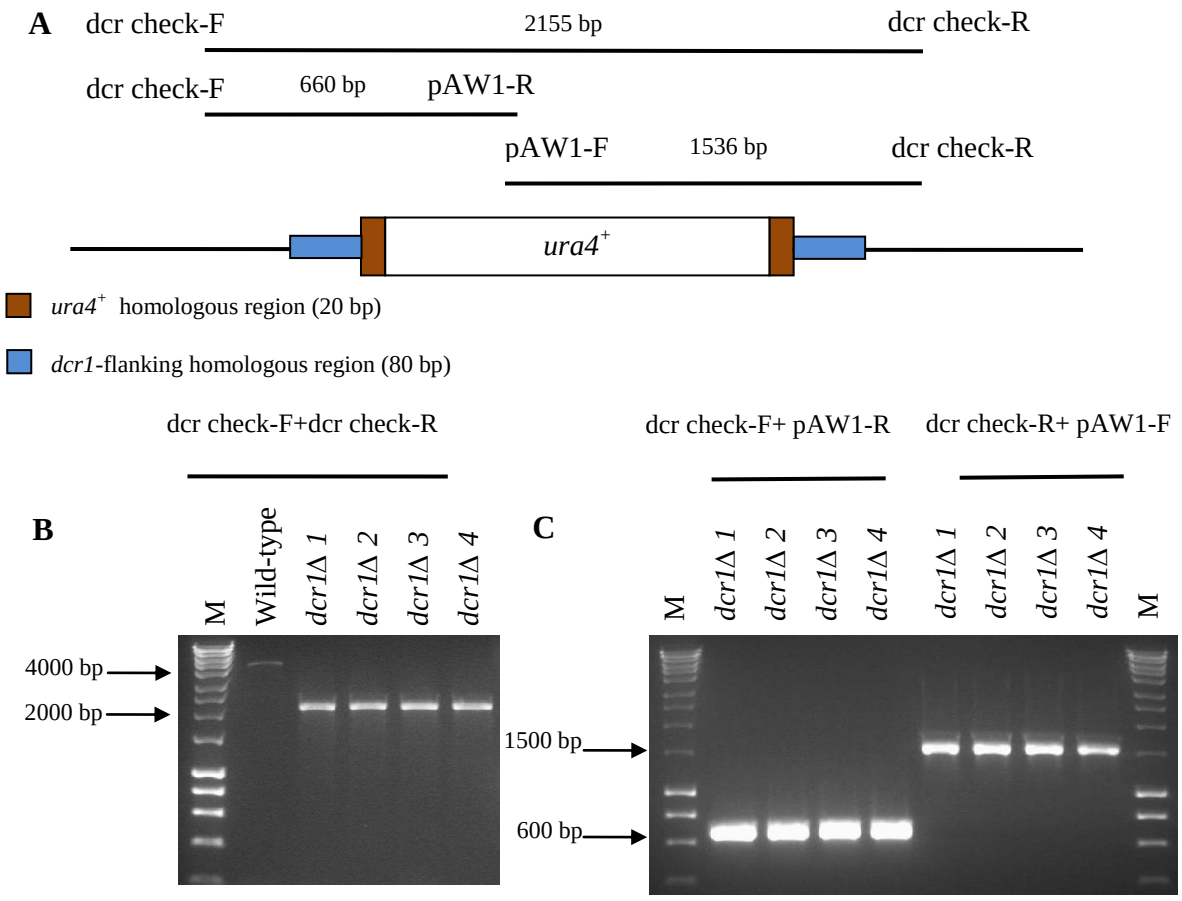

Figure 4.5 Examples of PCR screening of a successfully constructed *dcr1*Δ using the *ura4*$^+$ cassette.

A. The positions of checking primers inside and outside the *ura4* cassette, which was used to delete the *dcr1* gene, together with the predicted PCR product sizes.

B. PCR products from wild-type (*dcr1*$^+$) (BP1) and *dcr1*Δ1, 2, 3 and 4 strains (BP2746, BP2747, BP2748 and BP2749, respectively) obtained using the external primers dcr check-F and dcr check-R, which give a product size of 4409 bp for the wild-type and 2155 bp for the *dcr1*Δ candidates with deletions due to the *ura4*$^+$ cassette..

C. PCR products for the *dcr1*Δ candidates obtained using the primers dcr1 check-F and pAW1-R and dcr check-R and pAW1-F, which give a product size of 660 bp and 1536 bp, respectively.

A

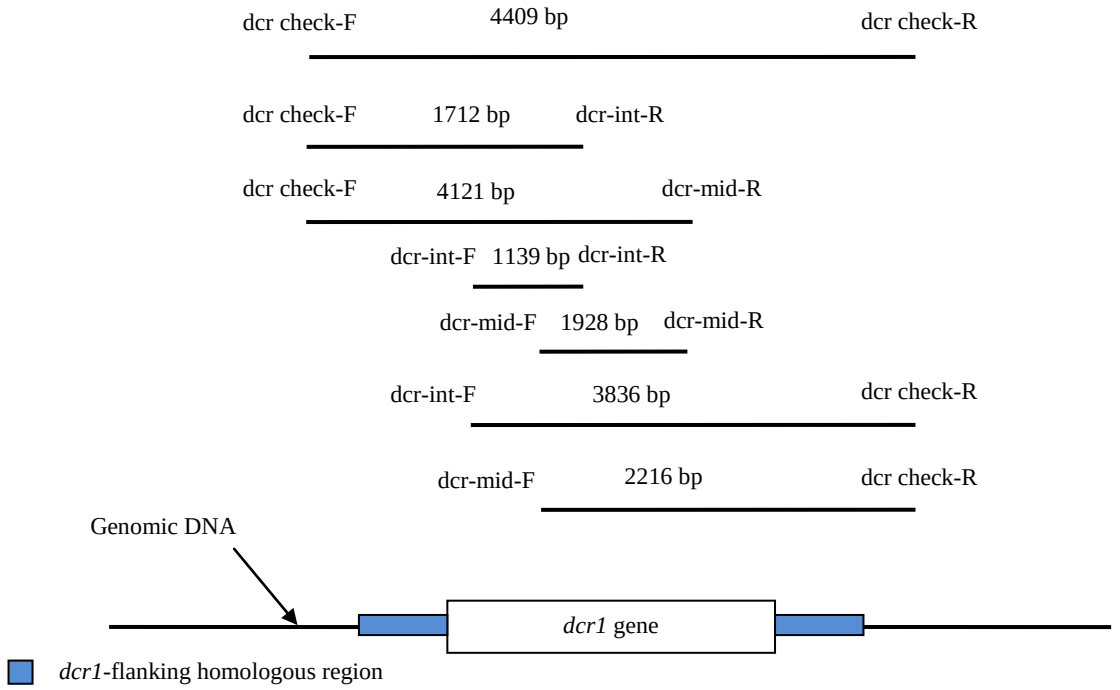

B

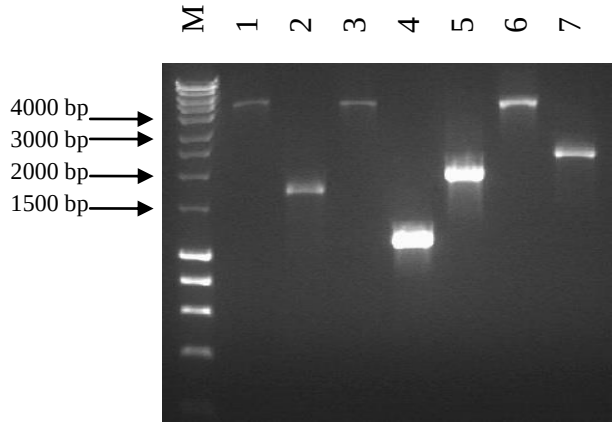

***dcr1* check primers (*dcr1*$^+$)**		**product size**
1.	dcr check-F+dcr check-R	4409 bp
2.	dcr check-F+dcr-int-R	1712 bp
3.	dcr check-F+dcr-mid-R	4121 bp
4.	dcr-int-F+dcr-int-R	1139 bp
5.	dcr-mid-F+dcr-mid-R	1928 bp
6.	dcr-int-F+dcr check-R	3836 bp
7.	dcr-mid-F+dcr check-R	2216 bp

Figure 4.6 Example of PCR checks on *dcr1*$^+$ strains.

A. The positions of the screening primers inside and outside of the *dcr1* gene, together with the expected PCR product sizes.

B. PCR product sizes from the wild-type strain (*dcr1*$^+$) (BP1) obtained using seven sets of screening primers. Primer set numbers 2, 3, 4, 5, 6 and 7 give no products for the successful *dcr1*Δ candidates, while primer set number 1 gives a product size of 4409 bp for *dcr1*$^+$ and 1530 bp for *dcr1*Δ strains, which had deletions due to the *natMX6* cassette or 2155 bp for deletions due to the *ura4*$^+$ cassette.

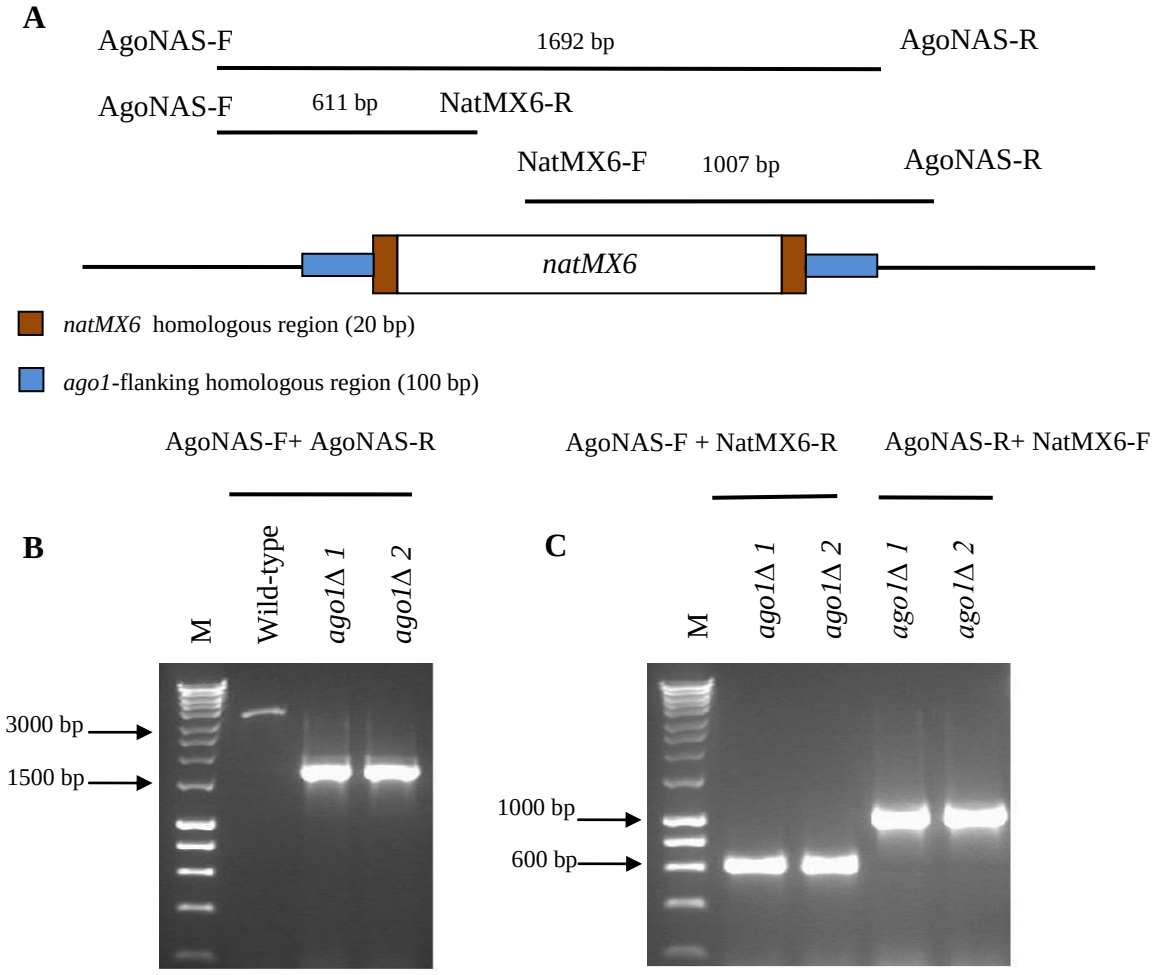

Figure 4.7 PCR screening of a successfully constructed *ago1*Δ using the *natMX6* cassette.

A. The positions of checking primers inside and outside the *natMX6* gene, together with the predicted PCR product sizes.

B. PCR products from the wild-type (*ago1*$^{+}$) (BP1) and *ago1*Δ 1 and 2 strains (BP3220 and BP3221, respectively) obtained using the external primers AgoNAS-F and AgoNAS-R, which give a product size of 3322 bp for the wild-type and 1692 bp for the *ago1*Δ candidates with deletions due to the *natMX6* cassette.

C. PCR products for the *ago1*Δ candidates obtained using the primers AgoNAS-F and NatMX6-R and AgoNAS-R and NatMX6-F, which give a product size of 611 bp and 1007 bp, respectively.

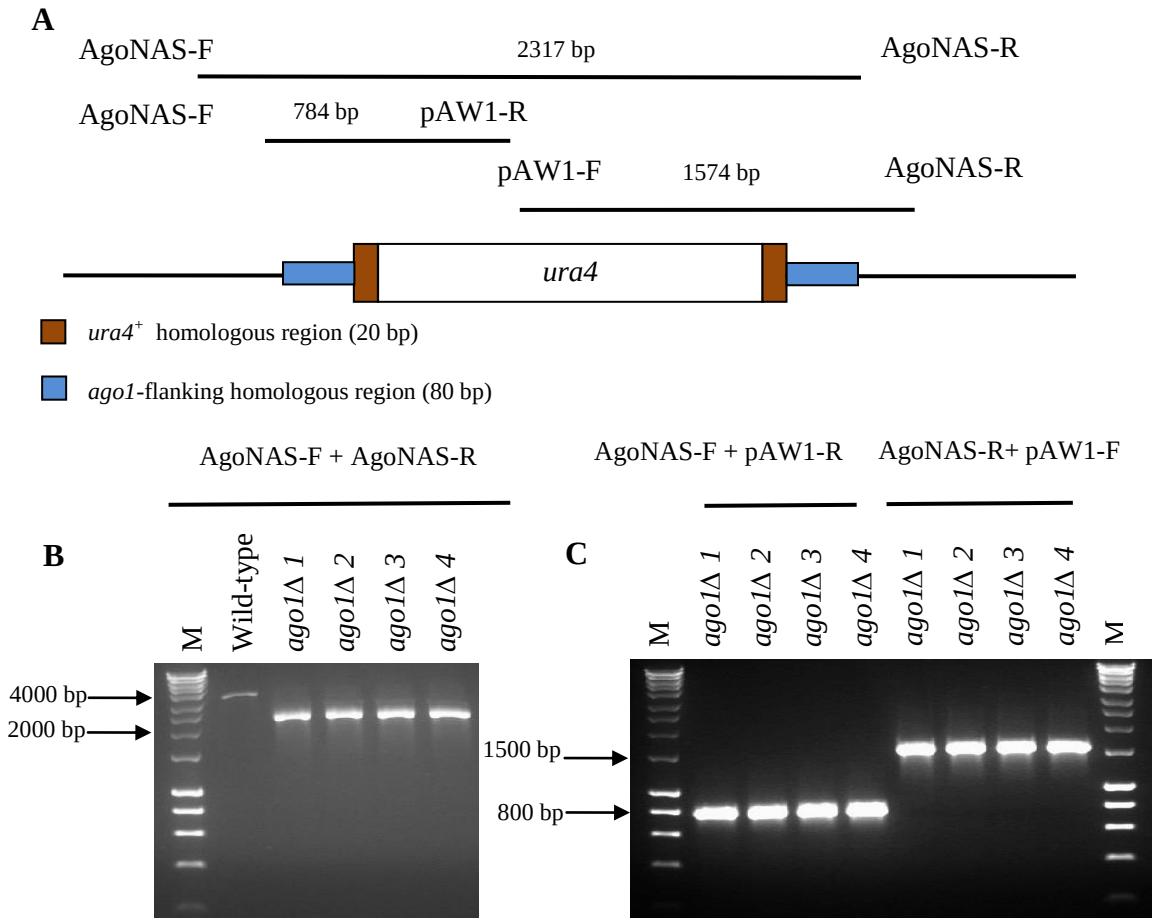

Figure 4.8 Examples of PCR screening of a successfully constructed *ago1*Δ using the *ura4*$^+$ cassette.

A. The positions of the checking primers inside and outside the *ura4* cassette, which was used to delete the *ago1* gene, together with the predicted PCR product sizes.

B. PCR products from the wild-type (*ago1*$^+$) (BP1) and *ago1*Δ1, 2, 3 and 4 strains (BP2757, BP2758, BP2759 and BP2760, respectively) obtained using the external primers AgoNAS-F and AgoNAS-R, which give a product size of 3322 bp for the wild-type and 2317 bp for the *ago1*Δ successful candidates with deletions due to the *ura4*$^+$ cassette.

C. PCR products for the *ago1*Δ candidates obtained using primers AgoNAS-F and pAW1-R and AgoNAS-R and pAW1-F, which give product sizes of 784 bp and 1574 bp, respectively.

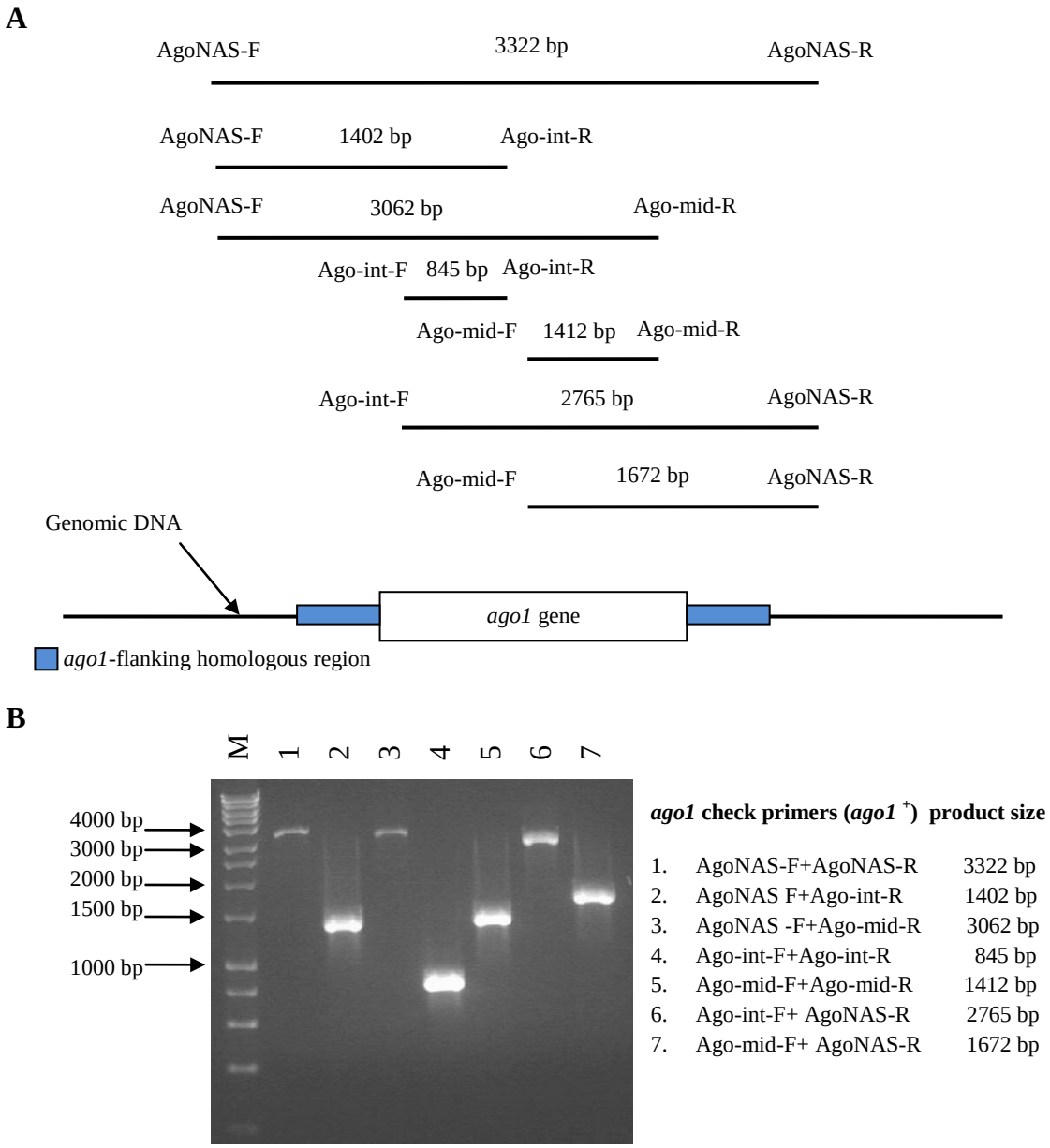

Figure 4.9 Examples of PCR checks on *ago1*$^+$ strains.

A. The positions of the screening primers inside and outside of the *ago1* gene, together with the expected PCR product sizes.

B. PCR product sizes from the wild-type strain (*ago1*$^+$) (BP1) obtained using seven sets of screening primers. Primer set numbers 2, 3, 4, 5, 6 and 7 give no products for the successful *ago1*Δ candidates, while primer set number 1 gave a product size of 3322 bp for *ago1*$^+$ and 1692 bp for the *ago1*Δ strains with deletions due to the *natMX6* cassette or 2317 bp with deletions due to the *ura4*$^+$ cassette.

4.2.2 Thiabendazole sensitivity tests on *traX*Δ double and triple mutants revels a possible function for TraX and Tsn1.

During cell division, the microtubules dramatically change their morphology with the assembly of the mitotic spindle (Sato and Toda, 2010). Faithful chromosome segregation requires that the microtubules attach to kinetochores at the centromeres of both sisters chromatids so that the chromosomes are pulled toward the spindle poles (Kawashima et al., 2011).

Thiabendazole (TBZ) is a microtubule-destabilising drug which has the capability to inhibit microtubule function (Sato and Toda, 2010). Cells with malfunctions of centromere activity exhibit high sensitivity to TBZ (Reddy et al., 2011; Volpe et al., 2003). Fission yeast has conserved RNAi machinery that is required for heterochromatic centromere formation and maintenance (Verdel et al., 2004; Volpe et al., 2002). Therefore, cells that are deficient in the RNAi pathway are also defective in heterochromatin formation at the centromere; this renders these cells hypersensitive to TBZ. The TRAX-Translin complex (C3PO) is implicated in the functioning of the RNAi machinery in humans and *Drosophila* (Liu et al., 2009; Ye et al., 2011). Therefore, we tested our *traX*Δ/ RNAi double and triple mutants for TBZ sensitivity, in order to investigate whether double and/or triple mutants have altered sensitivity to TBZ.

For all TBZ sensitivity drop analysis, cells were cultured to density of approximately 5 x 10^6 cells/ml. The cells were serially diluted and 10 µl of each dilution was spotted onto plates containing fully supplemented YEA containing TBZ (15 µg/ml) and onto supplemented YEA plates without TBZ as controls. All plates were incubated for four days at a range of temperatures.

4.2.2.i Analysis of *traX*Δ *tsn1*Δ double mutant

Four *traX*Δ *tsn1*Δ double mutants were generated using *kanMX6* and *natMX6* cassettes. All of them show no sensitivity to TBZ (15 µg/ml) at all temperatures tested (Figure 4.10).

4.2.2ii Tsn1 provides a redundant function to Dcr1

The *tsn1*Δ *dcr1*Δ double mutant showed increased sensitivity to TBZ when compared to the *dcr1*Δ single mutant (Figure 4.11). This new finding suggests that Tsn1 functions in a dcr1-independent pathway. In addition, the triple mutant *traX*Δ *tsn1*Δ *dcr1*Δ showed no further increases in sensitivity to TBZ when compared to the *tsn1*Δ *dcr1*Δ double mutant (Figure 4.12).

4.2.2iii TraX suppresses a Translin –dependent, Ago1-independent pathway

The *traX*Δ *ago1*Δ double mutant showed marked resistance to TBZ when compared to the *ago1*Δ single mutant. However, the triple mutant of *traX*Δ *tsn1*Δ *ago1*Δ showed the same sensitivity to TBZ as seen with the *ago1*Δ single mutant (Figure 4.11-4.13). These findings provide clear evidence for an interaction of TRAX and Translin with the RNAi regulators Ago1 and Dcr1.

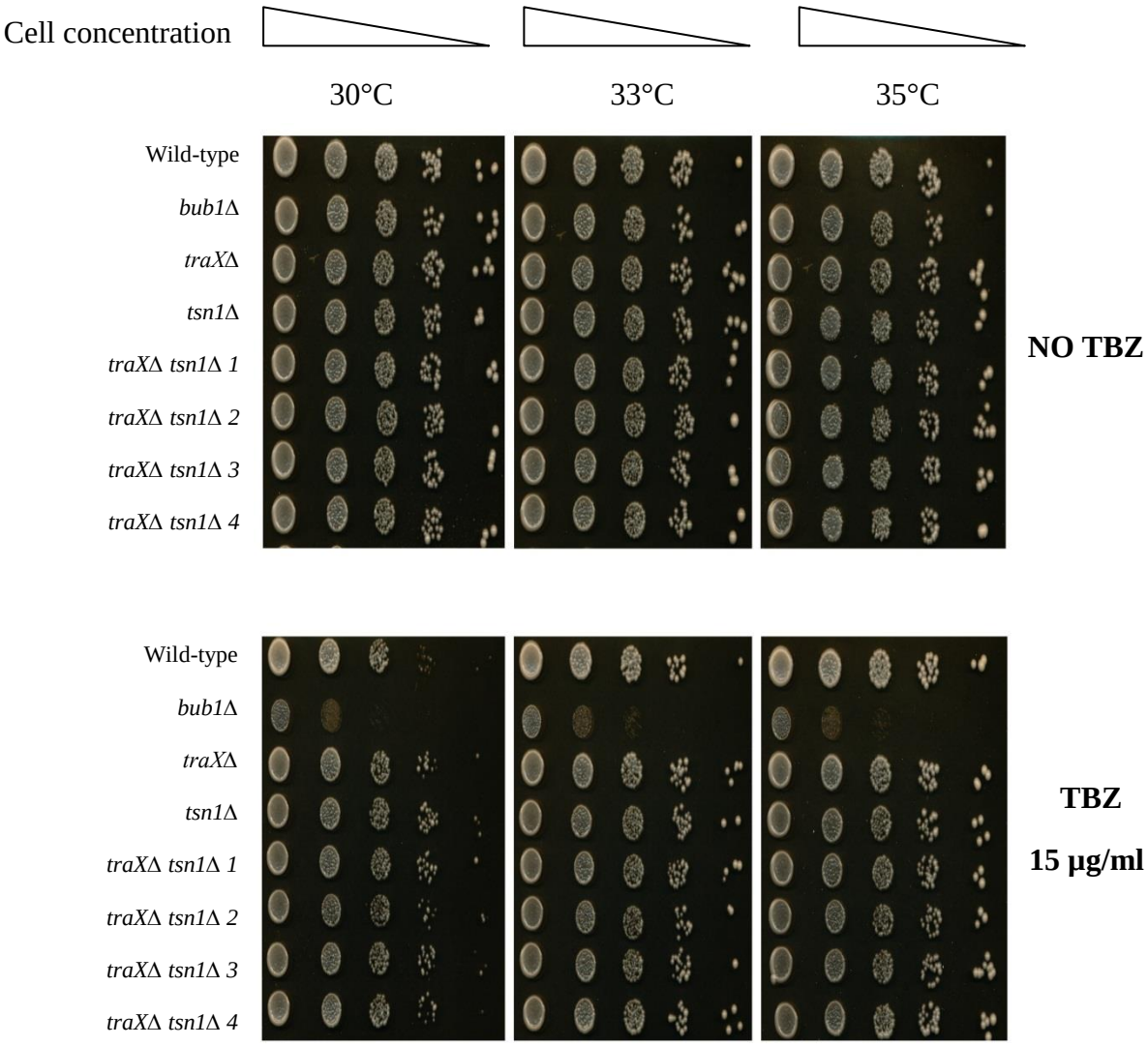

Figure 4.10 TBZ sensitivity tests for *traX*Δ *tsn1*Δ double mutants.

Double mutants of *traX*Δ *tsn1*Δ 1, 2, 3 and 4 (BP3248, BP3249, BP3252 and BP3253 respectively) showed no increased sensitivity to TBZ (15 µg/ml). Four *traX*Δ *tsn1*Δ double mutant strains were constructed using *kanMX6* and *natMX6* cassettes on *traX*Δ *tsn1*Δ *1* and *2* strains, and vice versa for the *trax*Δ *tsn1*Δ 3 and 4 strains. The *bub1*Δ (BP1162) strain was used as a positive control. The wild-type is BP90, *traX*Δ is BP1089, and *tsn1*Δ is BP1079. Three temperatures were tested: 30°, 33° and 35°C.

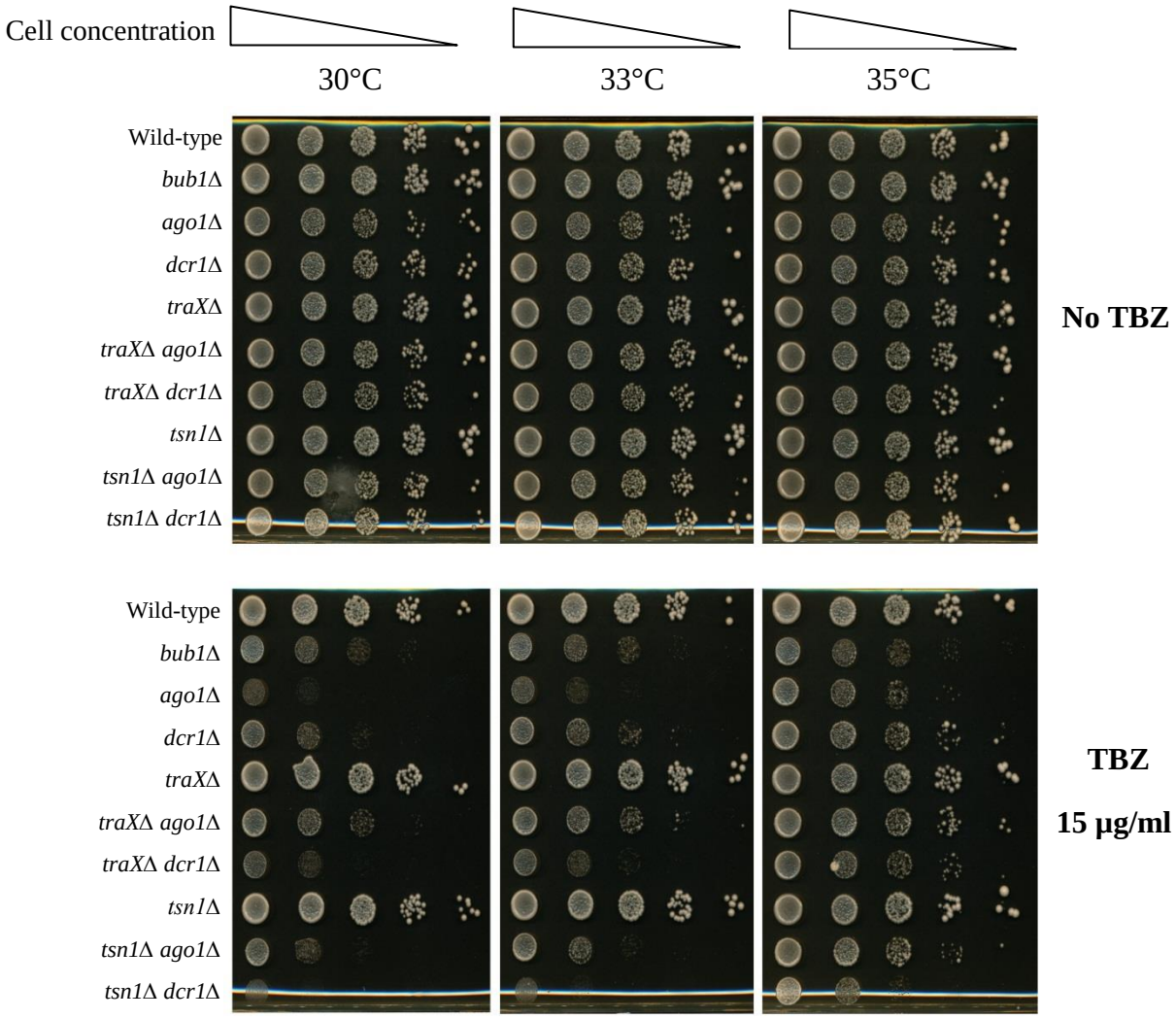

Figure 4.11 TBZ sensitivity tests for *traX*Δ *ago1*Δ, *traX*Δ *dcr1*Δ, *tsn1*Δ *ago1*Δ and *tsn1*Δ *dcr1*Δ double mutants.

Double mutants of *traX*Δ *ago1*Δ, *traX*Δ *dcr1*Δ, *tsn1*Δ *ago1*Δ and *tsn1*Δ *dcr1*Δ are BP2761, BP2750, BP2760 and BP2749, respectively. The *traX*Δ *ago1*Δ double mutant showed marked resistance to TBZ (15 µg/ml) when compared to the *ago1*Δ single mutant (BP2757). Whilst the *traX*Δ *dcr1*Δ double mutants demonstrated no/little sensitivity differences when compared to the *dcr1*Δ single mutant (BP2746). The *tsn1*Δ *dcr1*Δ double mutant showed increased sensitivity when compared to the *dcr1*Δ single mutant. The *tsn1*Δ *ago1*Δ double mutant exhibited no alteration in sensitivity relate to the *ago1*Δ single mutant. The *bub1*Δ (BP1162) strain was used as a positive control. The wild-type is BP90, *traX*Δ is BP1089 and *tsn1*Δ is BP1079. Three temperatures were tested: 30°, 33° and 35°C.

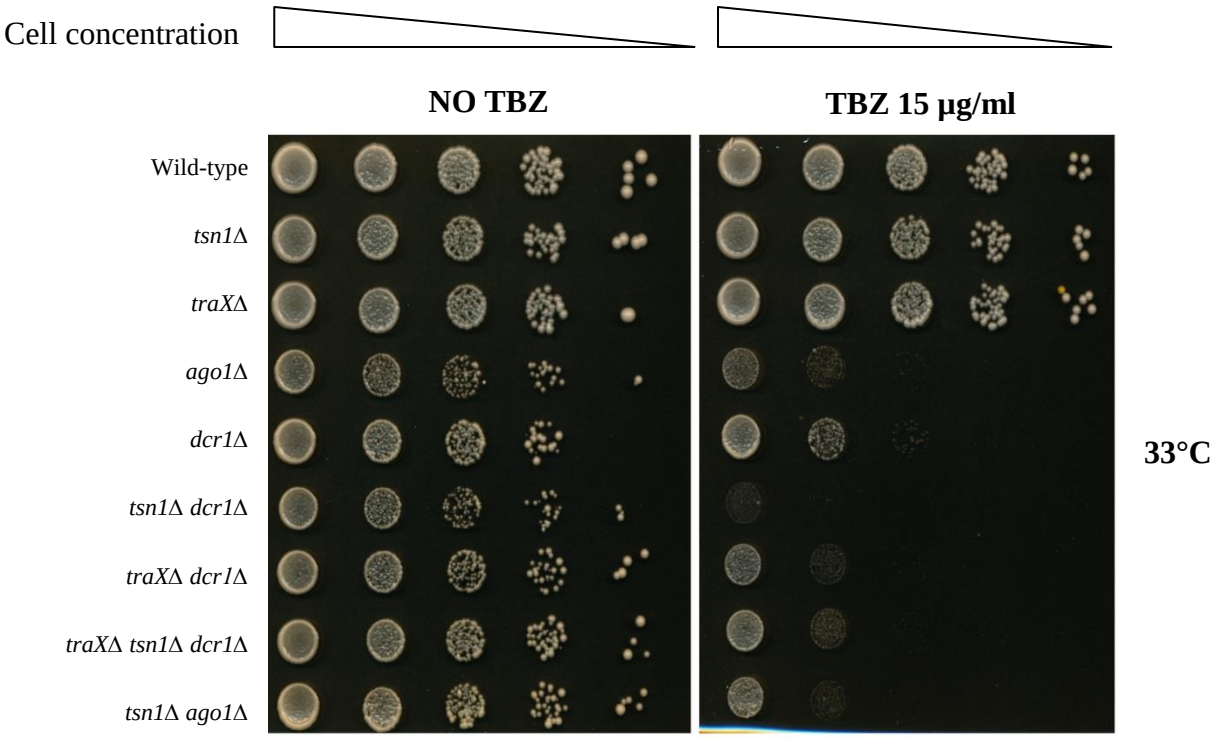

Figure 4.12 TBZ sensitivity tests for *traX*Δ *tsn1*Δ *dcr1*Δ triple mutants.

Given that *tsn1*Δ *dcr1*Δ (BP2749) shows greater sensitivity to TBZ (15 µg/ml) than is seen with the *dcr1*Δ single mutant (BP2746), we tested triple mutants of *traX*Δ *tsn1*Δ *dcr1*Δ (BP3250) to investigate whether deletion of *traX*Δ affects this sensitivity. The triple mutant of *traX*Δ *tsn1*Δ *dcr1*Δ and the double mutant of *traX*Δ *dcr1*Δ (BP2750) had equal TBZ sensitivity to that seen with the *dcr1*Δ single mutant. In addition, the TBZ sensitivity of the *tsn1*Δ *ago1*Δ (BP2760) double mutant was the same as that of the *ago1*Δ single mutant (BP2757), as shown previously. The *tsn1*Δ single mutant is BP1080, the *traX*Δ single mutant is BP1090 and wild-type is BP90. Plates were incubated for four days at 33°C.

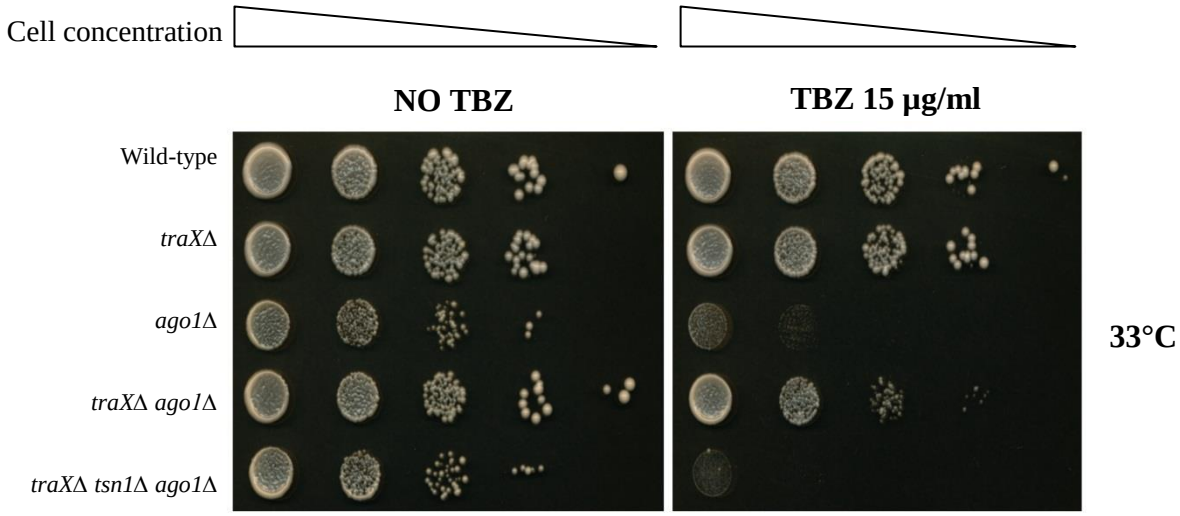

Figure 4.13 TBZ sensitivity tests for *traX*Δ *tsn1*Δ *ago1*Δ triple mutants

Given that *traX*Δ *ago1*Δ (BP2761) shows greater resistance to TBZ (15 µg/ml) than seen with the *ago1*Δ single mutant (BP2757), we tested triple mutants of *traX*Δ *tsn1*Δ *ago1*Δ (BP3246) to investigate whether deletion of *tsn1*Δ affects this resistance activity. The triple mutant was as sensitive as the *ago1*Δ single mutant to TBZ. This shows that Translin can substitute for the loss of Argonaute, but that this activity is suppressed in the presence of TRAX. The *traX*Δ single mutant is BP1090 and wild-type is BP90. Plates were incubated for four days at 33°C.

4.2.3 Minichromosome loss assays for the *traX*Δ *dcr1*Δ and *traX*Δ *ago1*Δ double mutants

The minichromosome loss assay was used to determine the chromosome segregation stability, which is related to RNAi defects in the *traX*Δ *ago1*Δ and *traX*Δ *dcr1*Δ double mutants. The *traX*Δ *ago1*Δ double mutant strains showed considerable resistance to TBZ relative to the *ago1*Δ (Figure 4.11-4.13), so the minichromosome assay was used to determine whether this was associated with chromosome stability in the absence of TBZ. The *S. pombe* minichromosome Ch16 is an artificial chromosome 530 kb in length, which is derived from chromosome III. This minichromosome is stable during cell division; however, 0.2% of Ch16 is normally lost from all cells during cell division (Allshire et al., 1995). The *ade6-M216* allele (on Ch16) and *ade6-M210* allele (on chromosome III) are complementary and confer prototrophy, which results in white colonies when grown on limiting adenine (adenine auxotroph grow as red colonies on limiting adenine). Therefore, when Ch16 is lost, cells lose the *ade6-M216* allele and colonies become red when grown in media with limiting adenine, due to the disruption of the adenine biosynthetic way (Niwa et al., 1986). Chromosome segregation instability leads to minichromosome loss which results in visualisation of red colonies or red/white sectored colonies. If Ch16 loss happens within the colony, the colony will become sectored so that half of the colony will contain no minichromosome and will form a red sector, while the other half that retains the Ch16 will form a white sector. Examples are shown in Figure 4.14. We investigated the percentage of minichromosome loss using fluctuation assays (see Section 2.9). The numbers of completely red colonies (i.e. colonies that had lost Ch16 in liquid culture) were counted and this number was then divided by the total number of all colonies to obtain the minichromosome loss frequency. Median values from 9 independent cultures were calculated. This experiment was repeated three times for each strain and mean values of the medians represented the percentage of minichromosome loss. The *traX*Δ *ago1*Δ double mutants showed a significant increase in minichromosome stability when compared to the *ago1*Δ single mutant, which was consistent with the TBZ phenotype (Figure 4.15). Interestingly, the *ago1*Δ mutant exhibits greater minichromosome instability than the *dcr1*Δ. In addition, the *tsn1*Δ *dcr1*Δ double mutant showed a significant increase of minichromosome instability compared to the *dcr1*Δ single mutant, which is also consistent with the TBZ phenotype (Z. Al-shehri, PhD thesis, Bangor University).

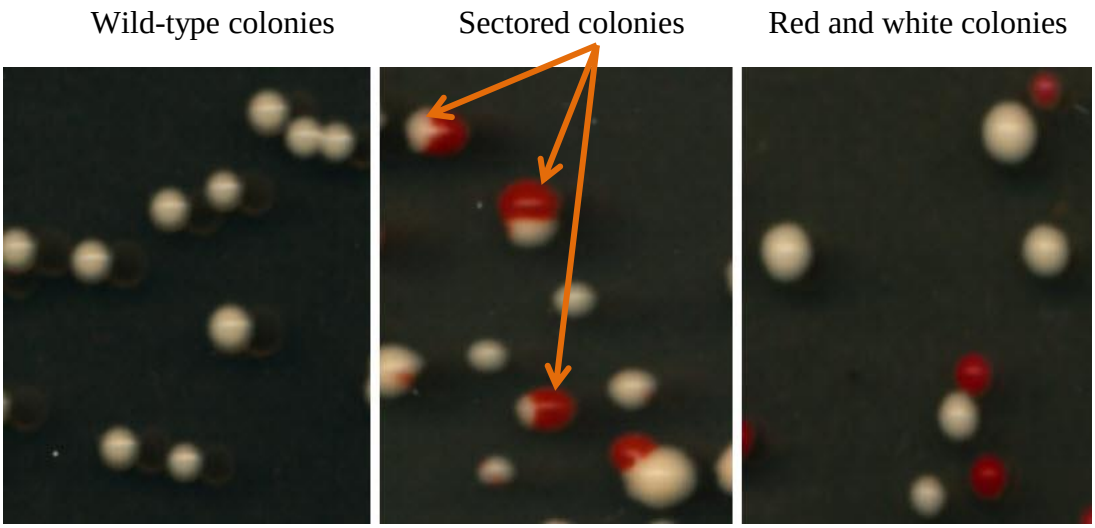

Figure 4.14 Examples of minichromosome phenotypes

The wild-type strain (BP2294) retains the minichromosome during cell division; therefore, colonies are white (left hand panel). Other strains that lose the minichromosome completely become red (right hand panel). If Ch16 loss occurs within the colony, the colony will become sectored, as shown in the middle panel. Plates were incubated for four days at 30°C, and then the images were recorded.

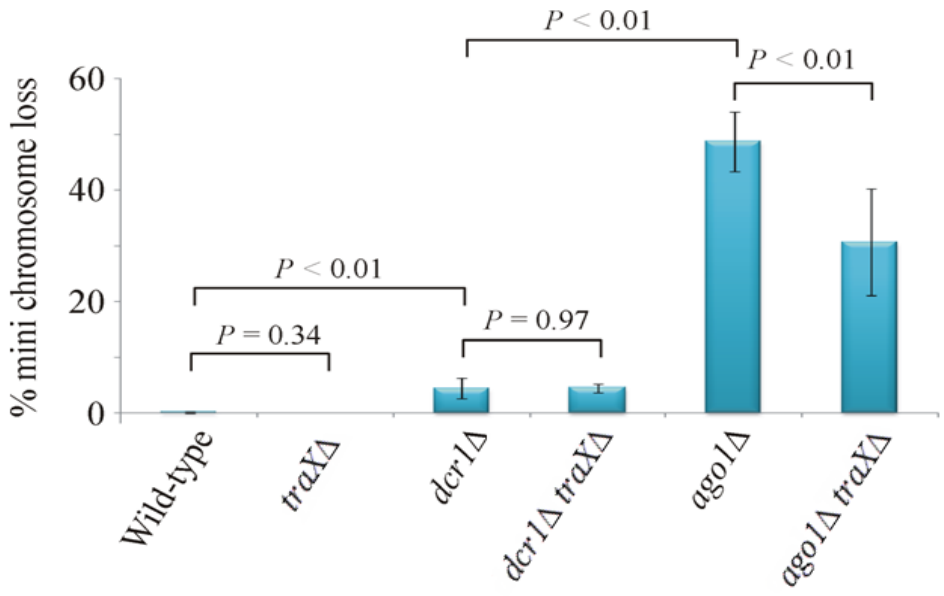

Figure 4.15 Minichromosome loss assay

The *traX*Δ *ago1*Δ (BP2975) double mutant shows significantly increased minichromosome stability when compared to the *ago1*Δ (BP2973) single mutant, which has higher levels of minichromosome instability than the *dcr1*Δ (BP2894) single mutant. This finding is consistent with the TBZ sensitivity assays. In addition, the minichromosome instability of the *dcr1*Δ single mutant is the same as that of the *traX*Δ *dcr1*Δ (BP2897) double mutant. The *traX*Δ single mutant is BP2406 and the wild-type is BP2294. *P* values were derived by the Student *t*-test. Error bars are standard deviations. Cultures were tested at 30°C.

4.2.4 Sensitivity analysis for DNA damaging agents

The data presented in this chapter suggests a Translin-dependent pathway which is redundant with Ago1 and suppressed by TraX. Translin and TRAX have been implicated in DNA repair pathways. Given this, we postulated that the genome stability phenotypes observed were due to altered DNA damage responses. Therefore, we investigated whether the *traX*Δ *ago1*Δ, *traX*Δ *dcr1*Δ, *tsn1*Δ *dcr1*Δ and *tsn1*Δ *ago1*Δ double mutants exhibited altered sensitivity to DNA damaging agents. The *rad3*Δ (check point defective) mutant strain was used as a positive control. Different DNA damaging agents were used, including hydroxyurea (HU), which is a DNA replication inhibitor (Figure 4.16); camptothecin, which is a DNA topoisomerase inhibitor (Figure 4.17); mitomycin C, which is a potent DNA crosslinker (Figure 4.18); methyl methanesulphonate (MMS), which is an alkylating agent (Figure 4.19); phleomycin, which generates DNA strand breaks (Figure 4.20); and ultraviolet irradiation (UV) (Figure 4.21). No increased or decreased sensitivity was observed in any of the double mutants tested. *tsn1*Δ and *traX*Δ single mutants exhibited levels of response similar to the wild-type, consistent with previous work (Jaendling et al., 2008). The *ago1*Δ and *dcr1*Δ single mutants appear to be less sensitive to higher concentration of phleomycin at higher temperature (Figure 4.20) and whilst this is interesting, it does not explain the observations made with *TraX*Δ and *tsn1*Δ mutants.

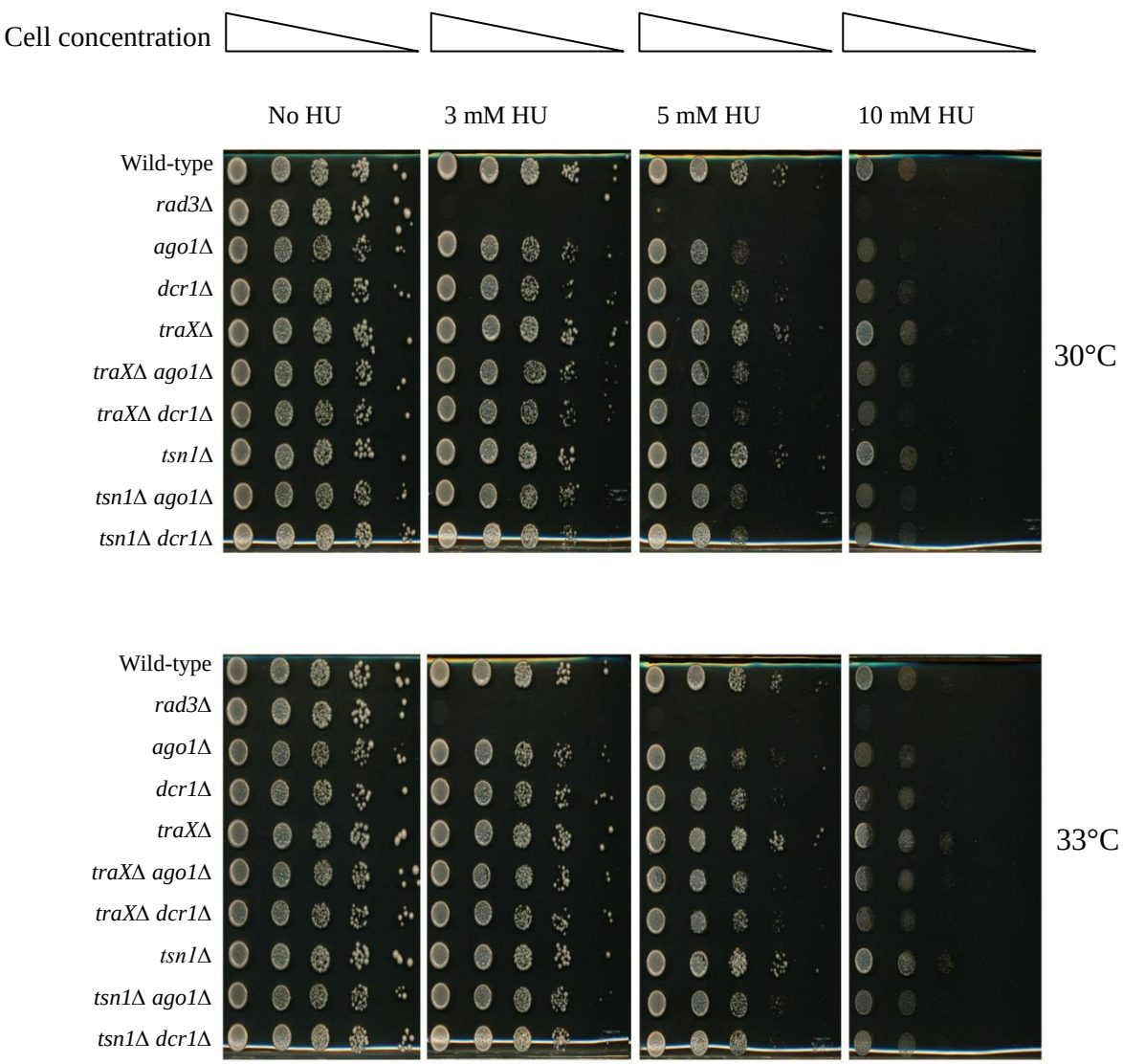

Figure 4.16 Hydroxyurea (HU) sensitivity spot tests.

Non-specific sensitivity to HU for the double mutants *traX*Δ *ago1*Δ, *traX*Δ *dcr1*Δ, *tsn1*Δ *ago1*Δ, and *tsn1*Δ *dcr1*Δ (BP2761, BP2750, BP2760 and BP2749, respectively) compared to the wild-type strain (BP90). The single mutant strains *ago1*Δ, *dcr1*Δ, *traX*Δ and *tsn1*Δ are BP2757, BP2746, BP1090 and BP1080, respectively. The *rad3*Δ (BP743) was used as a postive control. Plates were incubated for four days and tested at 30° and 33°C.

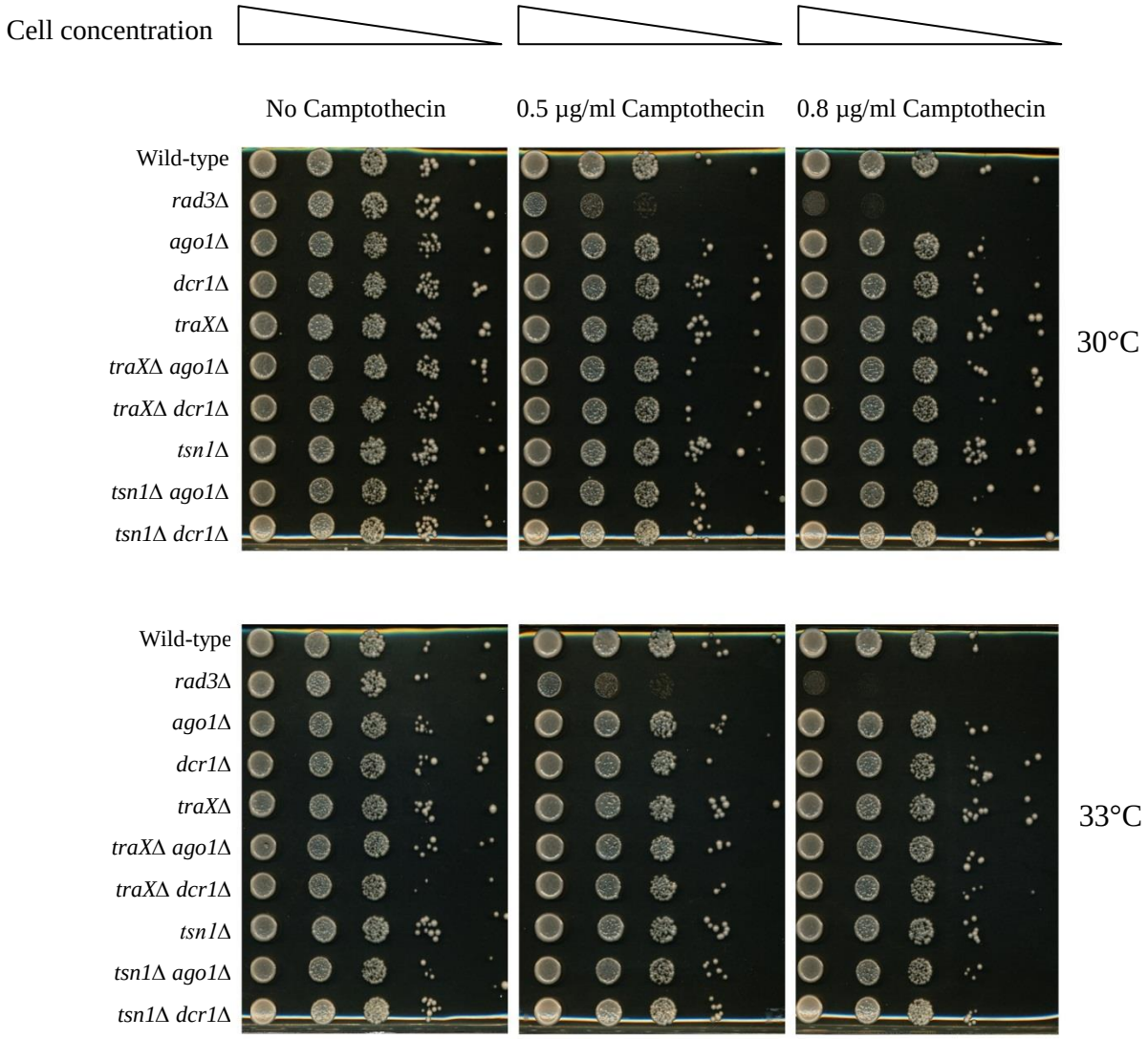

Figure 4.17 Camptothecin sensitivity spot tests.

Non-specific sensitivity to camptothecin for the double mutants *traX*Δ *ago1*Δ, *traX*Δ *dcr1*Δ, *tsn1*Δ *ago1*Δ, and *tsn1*Δ *dcr1*Δ (BP2761, BP2750, BP2760 and BP2749, respectively) compared to the wild-type strain (BP90). The single mutant strains *ago1*Δ, *dcr1*Δ, *traX*Δ and *tsn1*Δ are BP2757, BP2746, BP1090 and BP1080, respectively. The *rad3*Δ (BP743) was used as a postive control. Plates were incubated for four days and tested at 30° and 33°C.

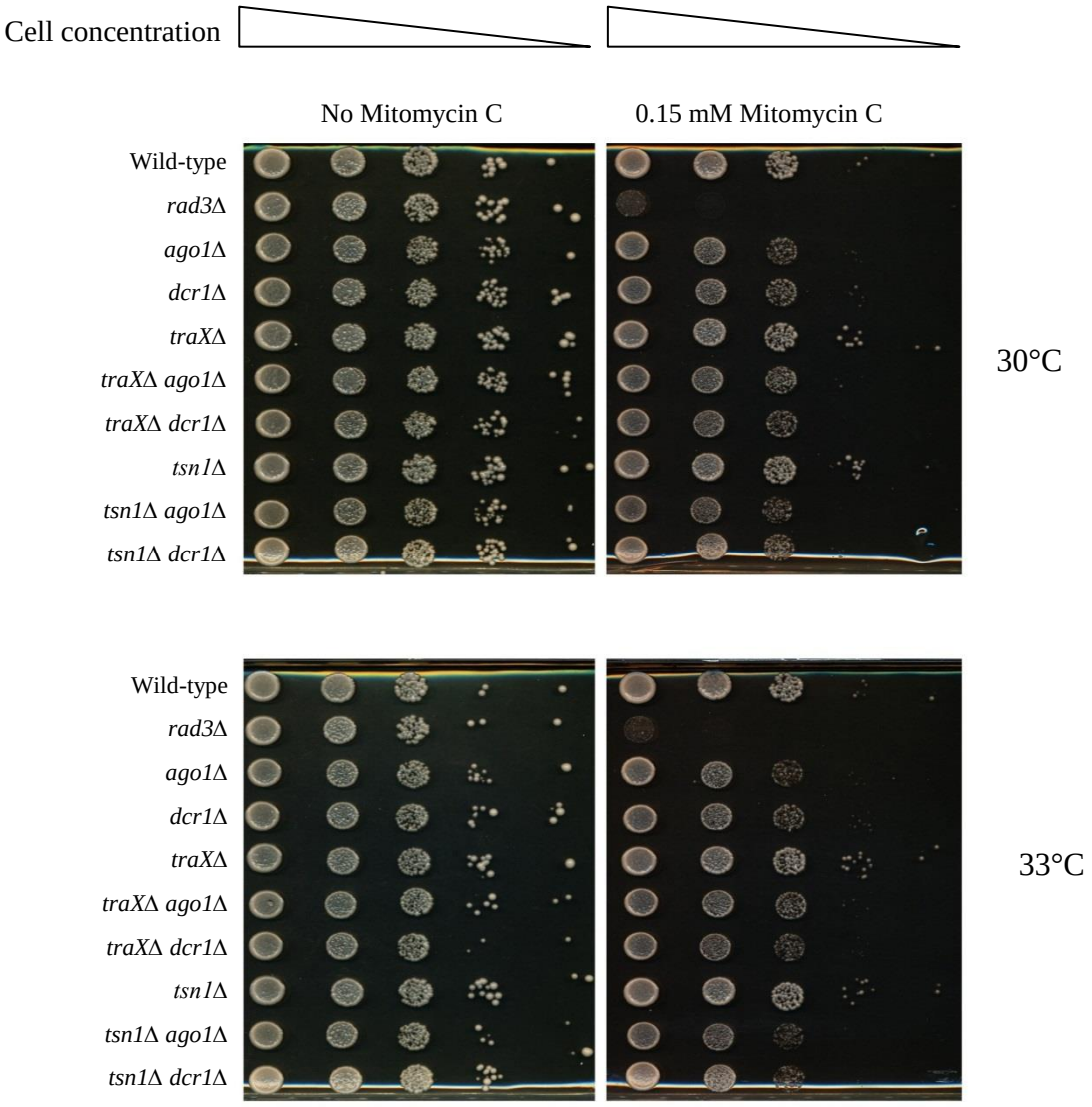

Figure 4.18 Mitomycin C sensitivity spot tests.

Non-specific sensitivity to mitomycin C for the double mutants *traX*Δ *ago1*Δ, *traX*Δ *dcr1*Δ, *tsn1*Δ *ago1*Δ, and *tsn1*Δ *dcr1*Δ (BP2761, BP2750, BP2760 and BP2749 respectively) compared to the wild-type strain (BP90). The single mutant strains *ago1*Δ, *dcr1*Δ, *traX*Δ and *tsn1*Δ are BP2757, BP2746, BP1090 and BP1080, respectively. The *rad3*Δ (BP743) was used as a postive control. Plate were incubated for four days and tested at 30° and 33°C.

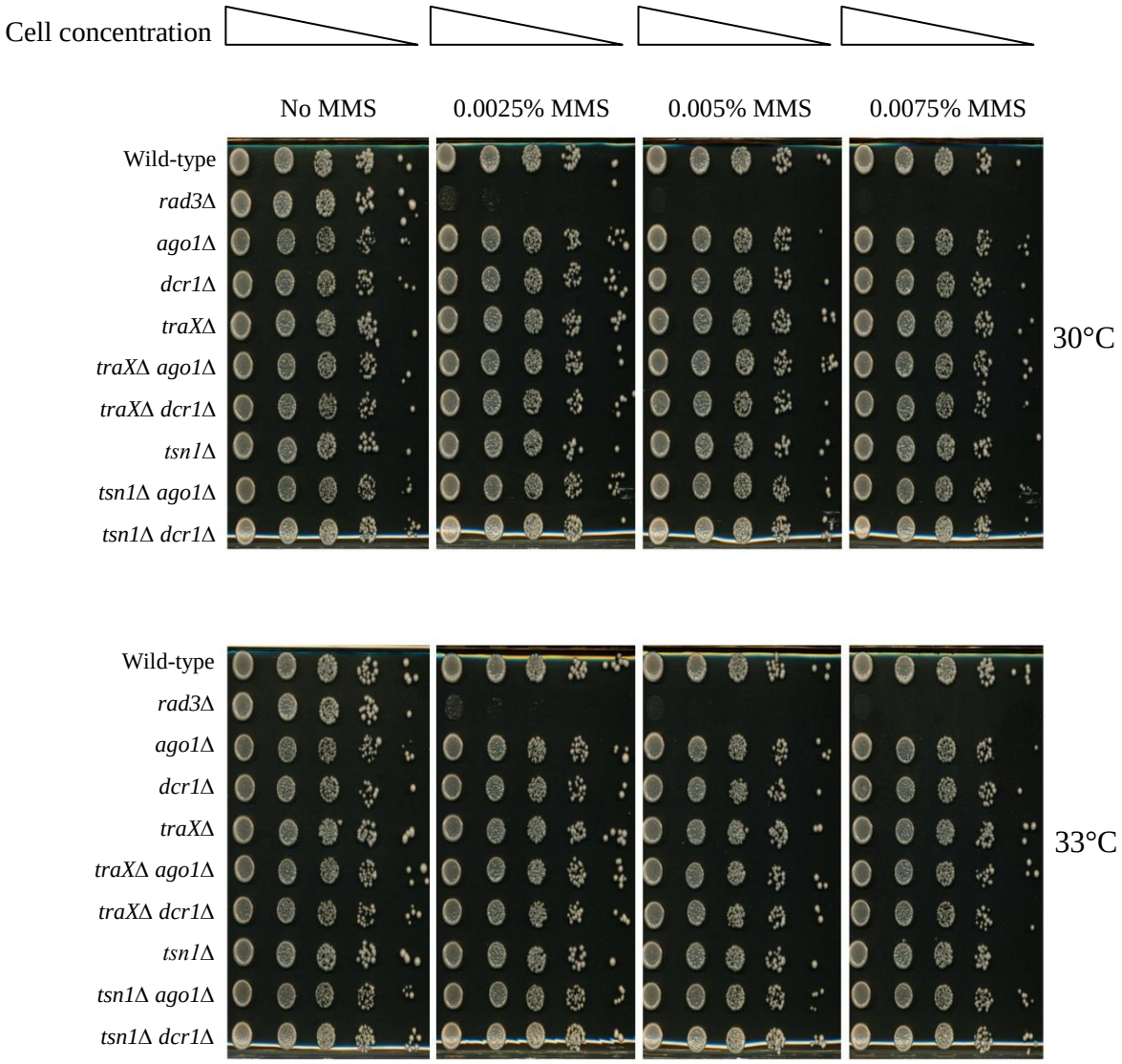

Figure 4.19 Methyl methanesulphonate (MMS) sensitivity spot tests.

Non-specific sensitivity to MMS for the double mutants *traX*Δ *ago1*Δ, *traX*Δ *dcr1*Δ, *tsn1*Δ *ago1*Δ, and *tsn1*Δ *dcr1*Δ (BP2761, BP2750, BP2760 and BP2749, respectively) compared to the wild-type strain (BP90). The single mutant strains *ago1*Δ, *dcr1*Δ, *traX*Δ and *tsn1*Δ are BP2757, BP2746, BP1090 and BP1080, respectively. The *rad3*Δ (BP743) was used as a postive control. Plates were incubated for four days and tested at 30° and 33°C.

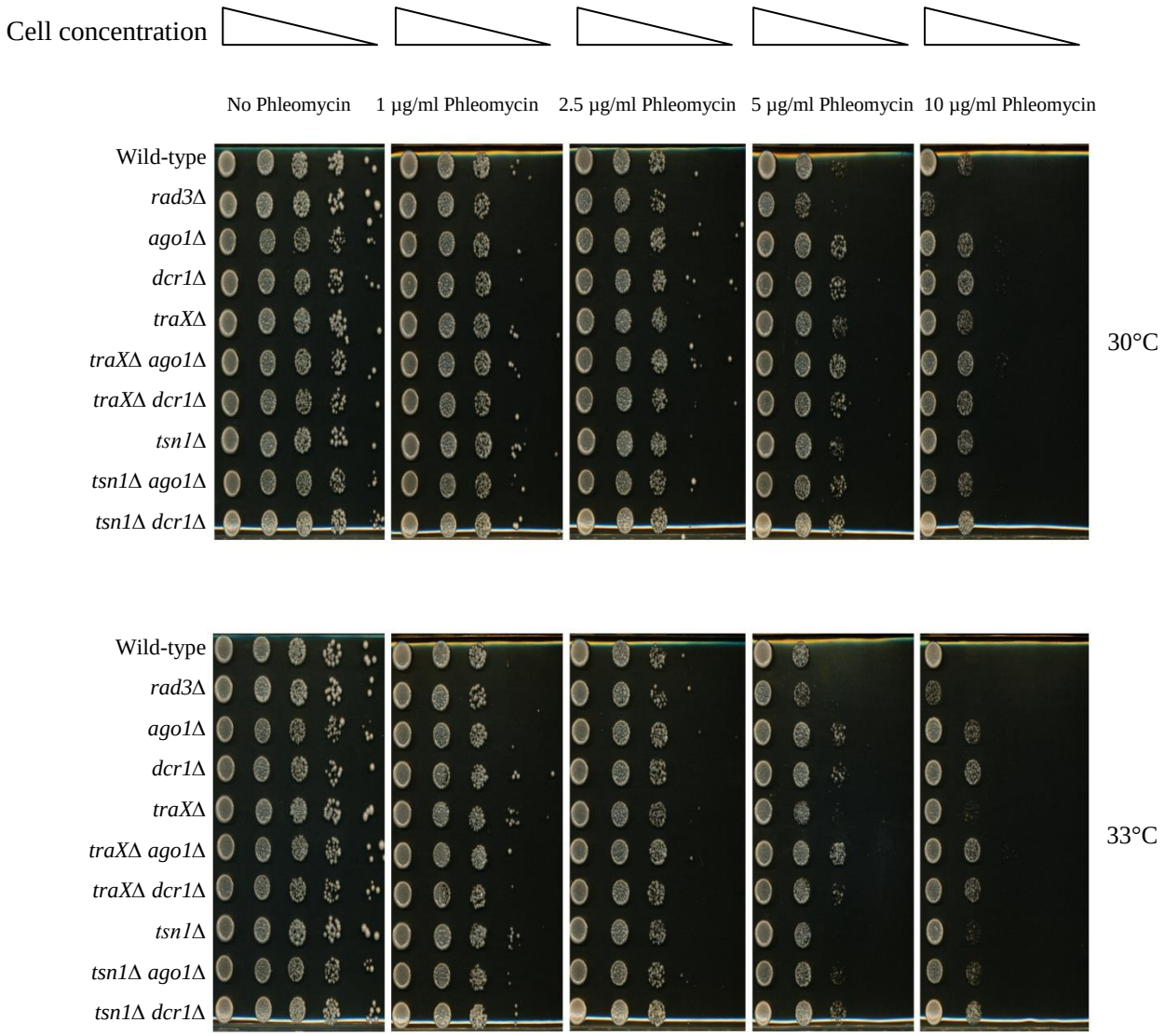

Figure 4.20 Phleomycin sensitivity spot tests.

Non-specific sensitivity to phleomycin for the double mutants *traX*Δ *ago1*Δ, *traX*Δ *dcr1*Δ, *tsn1*Δ *ago1*Δ, and *tsn1*Δ *dcr1*Δ (BP2761, BP2750, BP2760 and BP2749, respectively) compared to the wild-type strain (BP90). The single mutant strains *ago1*Δ, *dcr1*Δ, *traX*Δ and *tsn1*Δ are BP2757, BP2746, BP1090 and BP1080, respectively. The *rad3*Δ (BP743) was used as a postive control. Plates were incubated for four days and tested at 30° and 33°C.

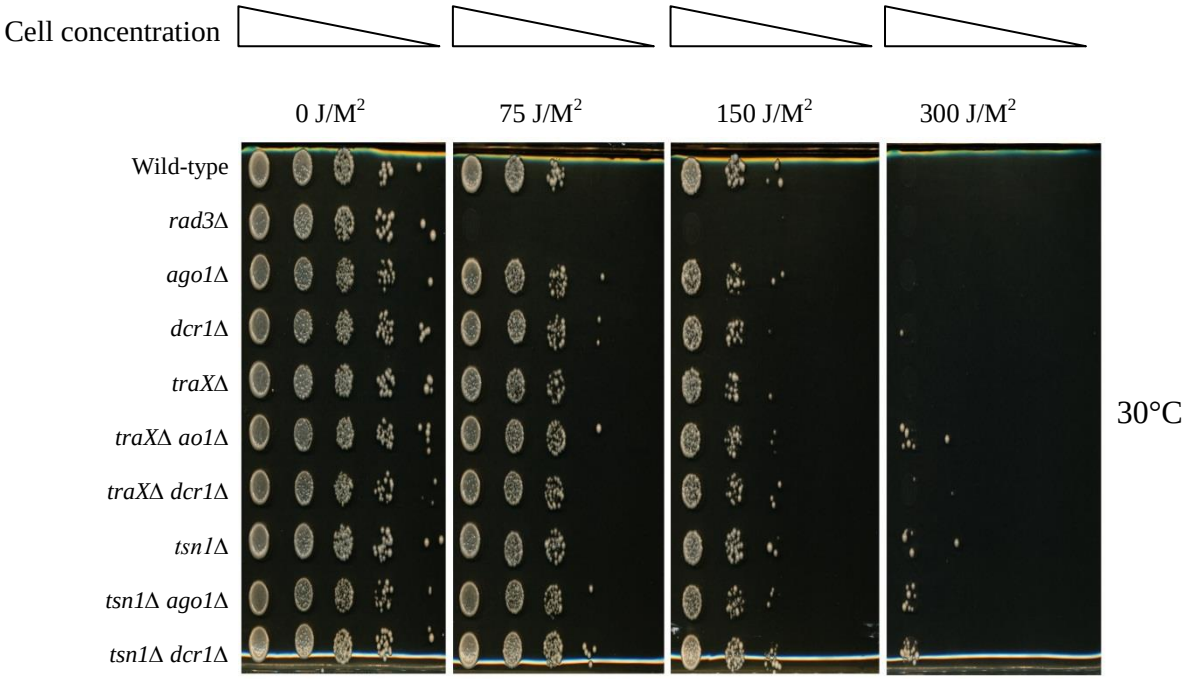

Figure 4.21 Ultraviolet (UV) irradiation sensitivity spot tests.

Non-specific sensitivity to UV for the double mutants *traX*Δ *ago1*Δ, *traX*Δ *dcr1*Δ, *tsn1*Δ *ago1*Δ, and *tsn1*Δ *dcr1*Δ (BP2761, BP2750, BP2760 and BP2749, respectively) compared to the wild-type strain (BP90). The single mutant strains *ago1*Δ, *dcr1*Δ, *traX*Δ and *tsn1*Δ are BP2757, BP2746, BP1090 and BP1080, respectively. The *rad3*Δ (BP743) was used as a postive control. Plates were incubated for four days and tested at 30°C.

4.3 Discussion

4.3.1 A Dicer-independent role for Translin in maintaining genome stability.

The *tsn1*Δ *dcr1*Δ double mutant exhibit increased TBZ sensitivity relative to the *dcr1*Δ single mutant. This indicates that Translin functions in a Dicer-independent pathway that promotes tolerance of microtubule dysfunction. A co-worker in the McFarlane group (Z. Al-shehri, PhD thesis, Bangor University) has also demonstrated that a *dcr1Δ tsn1Δ* double mutant exhibit increased mini chromosome loss relative to the *dcr1Δ* single mutant; indicting the TBZ sensitivity phenotype reflects chromosome instability. The *ago1*Δ mutant exhibits greater sensitivity to TBZ than does the *dcr1*Δ mutant and this is not further increased upon loss of Translin. These findings indicate that Translin functions in a pathway that is redundant with Dicer activity.

Recently, Halic and Moazed proposed a possible Dcr1-independent, Ago1-dependent pathway that involves RNAs to trigger heterochromatin formation. They reported that H3K9me of the heterochromatin region was not reduced in a *dcr1*Δ mutant to the same degree of *ago1*Δ mutant. So, a model was suggested for Dcr1-independent, Ago1-dependent pathway in fission yeast for formation of H3K9me in the centromere (Halic and Moazed, 2010). In addition, it has been suggested that *Neurospora* and *C. elegance* have dicer-independent pathways (Castel and Martienssen, 2013). The data described here support this and suggest that the *S. pombe* Dicer-independent pathway is Translin-dependent. Figure 4.22 is an adaptation of the model of Halic and Moazed in which they propose an Ago1-dependnet, Dcr1-independent pathway. Our work indicates that this other function could indeed be provided by Tsn1 (Translin) (Figure 4.22). However, when centromeric heterochromatin-dependent gene silencing was tested in a *dcr1Δ tsn1Δ* double mutant, no increase in deregulation of silencing was observed casting some doubt on this simple model (Z. Al-shehri, PhD thesis, Bangor University).

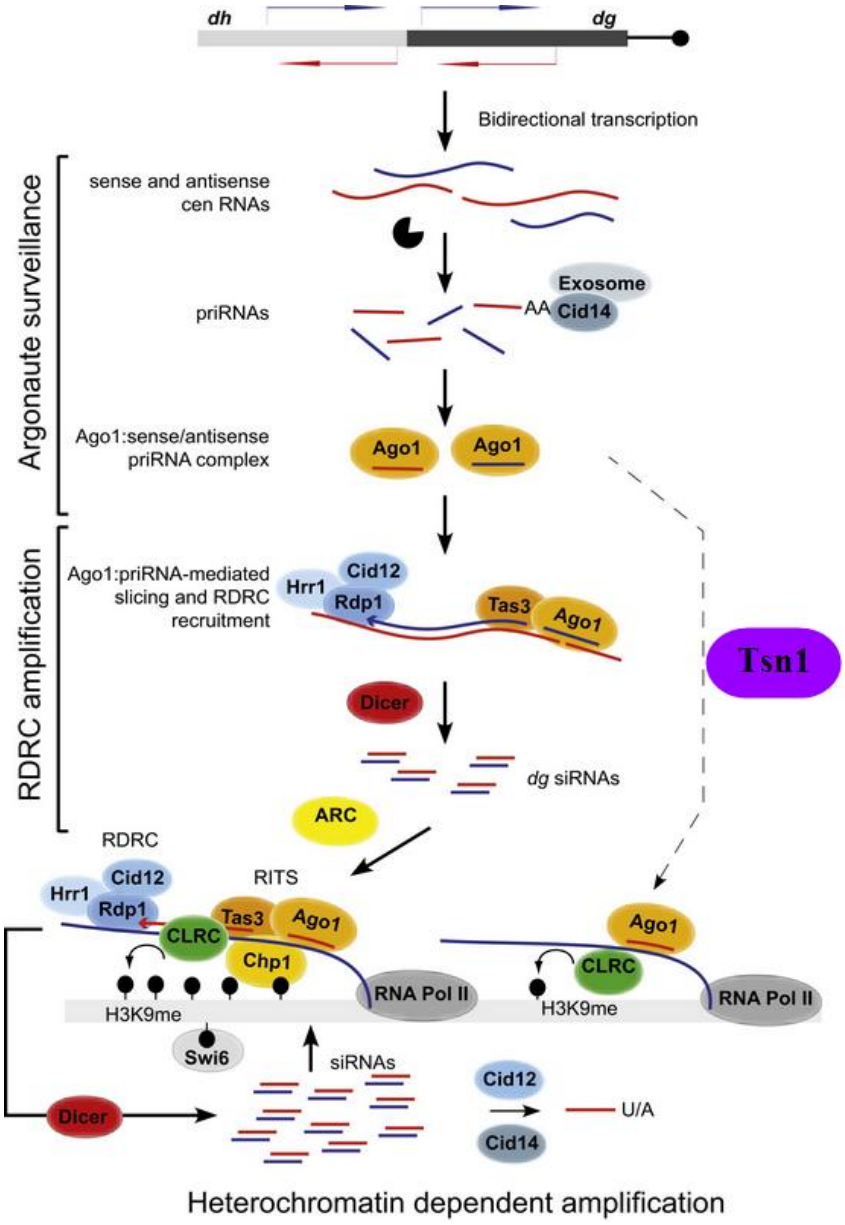

Figure 4.22. A model suggesting Translin functions in an Ago1-dependent, Dcr1-independent auxiliary pathway for functional centromere maintenance.

This model is an adaptation of the model of Halic and Moazed (2010) in which they infer a Dcr1-independent pathway to maintain functional centromeric heterochromatin. The data presented here indicate this function could be provided by Translin (Tsn1). In the normal pathway Dcr1 functions to generate siRNA molecules that become taken up by the Ago1 complex to ultimately mediate gene silencing.

4.3.2. TraX suppresses an Ago1-independent pathway for maintenance of genome stability.

Mutants of genes encoding RNAi regulators (*dcr1*Δ*, ago1*Δ) exhibit sensitivity to the microtubule destabilising drug TBZ (Carmichael et al., 2004; Volpe et al., 2003), whereas *tsn1*Δ and *traX*Δ null mutants do not (Jaendling et al., 2008). Remarkably, the loss of TraX function suppresses the *ago1*Δ sensitivity to TBZ, indicating that another activity can substitute for Ago1 function, which is normally repressed by TraX. Given the close association between Translin and TraX, we tested whether this other activity was mediated by Translin, a triple *ago1*Δ *traX*Δ *tsn1*Δ mutant was tested and shown to be as TBZ sensitive as the *ago1*Δ single mutant. This indicates that Translin can provide a function to substitute for the loss of Argonaute, but that this activity is normally suppressed in the presence of TraX.

Together these observations suggest that not only does Translin drive a Dicer-independent pathway, but that in the absence of TraX it can drive a largely Ago1-independent pathway for tolerating microtubule dysfunction. This is an important new function for Translin, one which is regulated by TraX. Whether this Translin-dependent pathway functions via control of centromeric heterochromatin remains unknown, but this possibility is explored in the next chapter.

4.3.2 The *traX*Δ *ago1*Δ double mutants increase chromosomal stability

Loss of TraX increases chromosomal stability in the absence of Argonaute. The *ago1*Δ mutants have higher levels of minichromosome instability than the *dcr1*Δ single mutant and this is consistent with Halic and Moazed model which infers an additional Dicer-independent, Argonaute-dependent pathway (which is consistent with the observed TBZ sensitivities presented here). However, concomitant deletion of *traX*Δ and *ago1*Δ in a strain leads to a partial reduction of this high *ago1*Δ chromosome instability, which again is consistent with the findings of the TBZ sensitivity assays. This indicates that the loss of TraX function restores chromosome stability to the *ago1*Δ*,* and the TBZ sensitivity data indicate this is Translin-dependent.

4.3.3 Chromosome stability dynamics controlled by TraX and Tsn1 Are not linked to DNA damage recovery.

We tested *traX*Δ and *tsn1*Δ and RNAi regulator gene double mutants on DNA damaging agents to ask the question, could changes to genome instability and TBZ sensitivities be due to dysfunction of DNA repair pathways?

TRAX and Translin have been implicated in the DNA damage response (Fukuda et al., 2008; Kasai et al., 1997). Therefore, we tested six DNA damaging agents, including HU, camptothecin, mitomycin C, MMS, phleomycin and UV. However, we found no sensitivity changes for any of the single or double mutants including *traX*Δ *ago1*Δ and *traX*Δ *dcr1*Δ, *tsn1*Δ *dcr1*Δ and *tsn1*Δ *ago1*Δ double mutants. Therefore, TRAX and Translin may not appear to function in DNA damage recovery in *S. pombe*. This suggests the chromosome stability changes observed in the double mutants is not related to changes in DNA damage recovery pathways.

4.3.4 Unexplored potential alteration in microtubules dynamics in the absence of TraX

Murine Translin has been shown to bind microtubules, although this function appears to be linked to mRNA transport/regulation rather than microtubule function *per se* (Han et al., 1995a; Ohashi et al., 2000; Wu and Hecht, 2000). Given this, we cannot fully dismiss the possibility that loss of TraX alters microtubule dynamics in such a way as to moderate genome stability. This would need to result in a suppression of the genome instability observed in an *ago1Δ* mutant; how this might work remains unknown, but TraX might exert a microtubule destabilising influence which could be linked to mRNA transport. However, there currently remains no evidence for this in *S. pombe* and the *traXΔ* single mutant does not exhibit a greater TBZ tolerance than *traX* proficient cells.

4.4 Conclusions

1 TRAX functions to repress an Argonaute by-pass pathway.

2 Translin has an activity capable of substituting for that of Argonaute for genome stability maintenance in the absence of TraX.

3 The role played by TRAX in maintaining genome stability is not essential for mediating responses to DNA damage.

CHAPTER 5

Analysis of gene silencing at different heterochromatic regions in TraX- and RNAi-deficient cells

5.1 Introduction

Heterochromatic regions have a fundamental role in gene regulation, genomic stability and chromosome segregation (Trewick et al., 2007). The heterochromatic regions in *S. pombe* are distributed in the centromeres and the telomeres of all three chromosomes, the rDNA repeats and the mating locus. The three centromeric regions differ in size and occupy 40 (*cen1*), 55 (*cen2*) and 110 (*cen3*) kilo base pairs of inverted DNA repeats (Allshire, 2001). The telomeres are found on both ends of all three chromosomes and include clusters of DNA tandem repeats, which are characterised by a transcriptionally silenced state (Bah and Azzalin, 2012). The rDNA locus includes highly repetitive DNA where are many *rRNA* genes are located as tandem repeats; these are also transcriptionally silent (Kobayashi et al., 2004). Of the three gene cassettes at the mating type locus, two are transcriptionally silent and one is active (reviewed in Klar, 2007). In fission yeast, the RNAi factors Dcr1 and Ago1 are required for the silencing of heterochromatin as well as for H3K9me at centromere and mating type region (Grewal and Jia, 2007) (see Section 1.6).

All heterochromatic regions are epigenetically regulated to remain in a silent state without expression. Reporter genes, such as *ura4*$^{+}$, inserted into these regions should also be under the influence of the same epigenetically silent regulation (Goto and Nakayama, 2012). In Chapter 4, we found greater resistance to TBZ for the *traX*Δ *ago1*Δ double mutant than for the *ago1*Δ single mutant. Moreover, the *traX*Δ *ago1*Δ double mutant showed a significant increase in minichromosome stability when compared to the *ago1*Δ single mutant. *ago1*Δ cells have compromised centromeric function which is thought to be caused by failure in pericentromeric heterochromatin (Castel and Martienssen, 2013). Given this, we speculated that the *traX*Δ *ago1*Δ strain has restored or partially restored heterochromatin at the pericentromeric regions and/or other heterochromatic loci.

Double mutants strains of *traX*Δ *ago1*Δ and *traX*Δ *dcr1*Δ were constructed and confirmed by PCR screening in strains that had the reporter gene *ura4*$^{+}$ inserted in different heterochromatin regions, such as centromeric regions (*cnt, imr, otr*), the subtelomeric

region, the mating-type locus and the rDNA regions. The *ura4*$^{+}$ should be retained in a silent state unless the double mutation is able to disturb the heterochromatin regulation. Therefore, these strains will normally grow on 5-FOA. However, when the heterochromatin state is deregulated, the *ura4*$^{+}$ is expressed and the strains become sensitive to 5-FOA. The working hypothesis in this chapter is that the silencing level is greater for the *traX*Δ *ago1*Δ double mutant than for the *ago1*Δ single mutant.

5.2 Results

5.2.1 Analysis of centromeric gene silencing in the absence of TraX and Ago1 functions.

Cancers could occur as result of deregulation of centromeric integrity, which subsequently affect chromosome segregation and lead to chromosomal instability and cancers (Manning et al., 2010). Fission yeast has three chromosomes containing three complex centromeres (Ekwall et al., 1999). Each one of these centromeres is divided into three regions: the *cnt* (the central core), the *imr* (inner most repeats) and *otr* (outer repeats); the latter is divided into *dg* and *dh* sequences (Pidoux and Allshire, 2004).

The effect of *traX* deletion on centromeric gene silencing in the absence of RNAi regulation was investigated by constructing double mutants strains of *traX*Δ *ago1*Δ and *traX*Δ *dcr1*Δ using the selectable marker *kanMX6* and *natMX6* cassettes and confirmed by PCR screening. These strains have the reporter gene *ura4*$^{+}$ introduced into the three centromeric regions *cnt*, *imr* and *otr* in centromere 1 (Figure 5.1). These strains were then tested to examine the sensitivity to 5-FOA at three temperatures (30°, 33° and 35°C).

5.2.1.i Analysis of *cnt1::ura4*$^+$ strains

The *traX*Δ single mutant showed full transcriptional repression of reporter gene *ura4*$^+$ inserted into the central core (*cnt1*) (Chapter 3), indicating a fully functional heterochromatic silencing. The *ago1*Δ and *dcr1*Δ single mutants showed sensitivity to 5-FOA (500 µg/ml) indicating a deregulation of silencing. However, no alterations were apparent in sensitivity levels of the *traX*Δ *ago1*Δ and *traX*Δ *dcr1*Δ double mutants relative to *ago1*Δ and *dcr1*Δ single mutants. Three temperatures were tested (Figure 5.2). Further analysis was done at lower concentration of 5-FOA (300 and 400 µg/ml) (Figure 5.3).

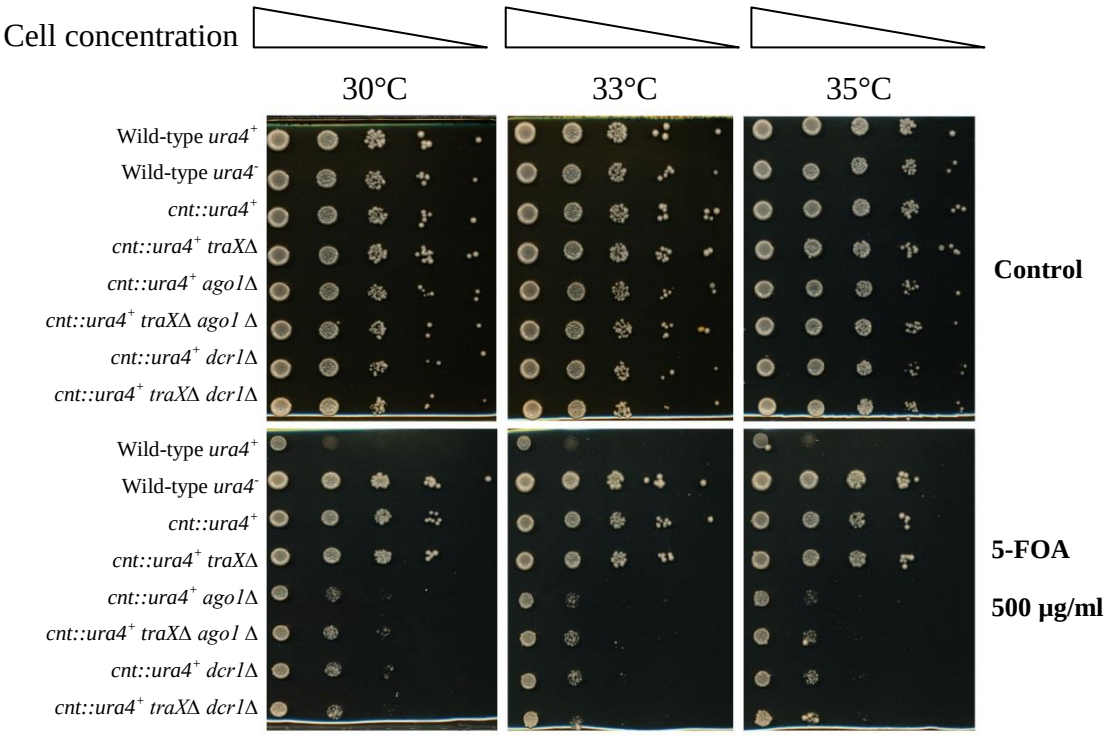

Figure 5.2 The 5-FOA spot tests of double mutants (*traX*Δ *dcr1*Δ) and (*traX*Δ *ago1*Δ) of *cnt::ura4*$^+$ strains.

The wild-type *ura4*$^+$ is (BP1), wild-type *ura4*$^-$ is (BP90), the parent mutant strain is (BP2203), *traX*Δ is (BP2411), *ago1*Δ is (BP3001) and *dcr1*Δ is (BP3103). No increase in sensitivity to 5-FOA (500 µg/ml) was seen in the single mutant *traX*Δ. The *ago1*Δ and *dcr1*Δ single mutants are sensitive to 5-FOA. However, no alterations in sensitivity was seen in the double mutants *traX*Δ *dcr1*Δ (BP3105) or *traX*Δ *ago1*Δ (BP2991) comparing to *ago1*Δ and *dcr1*Δ single mutants. Cells were tested at 30°, 33° and 35°C.

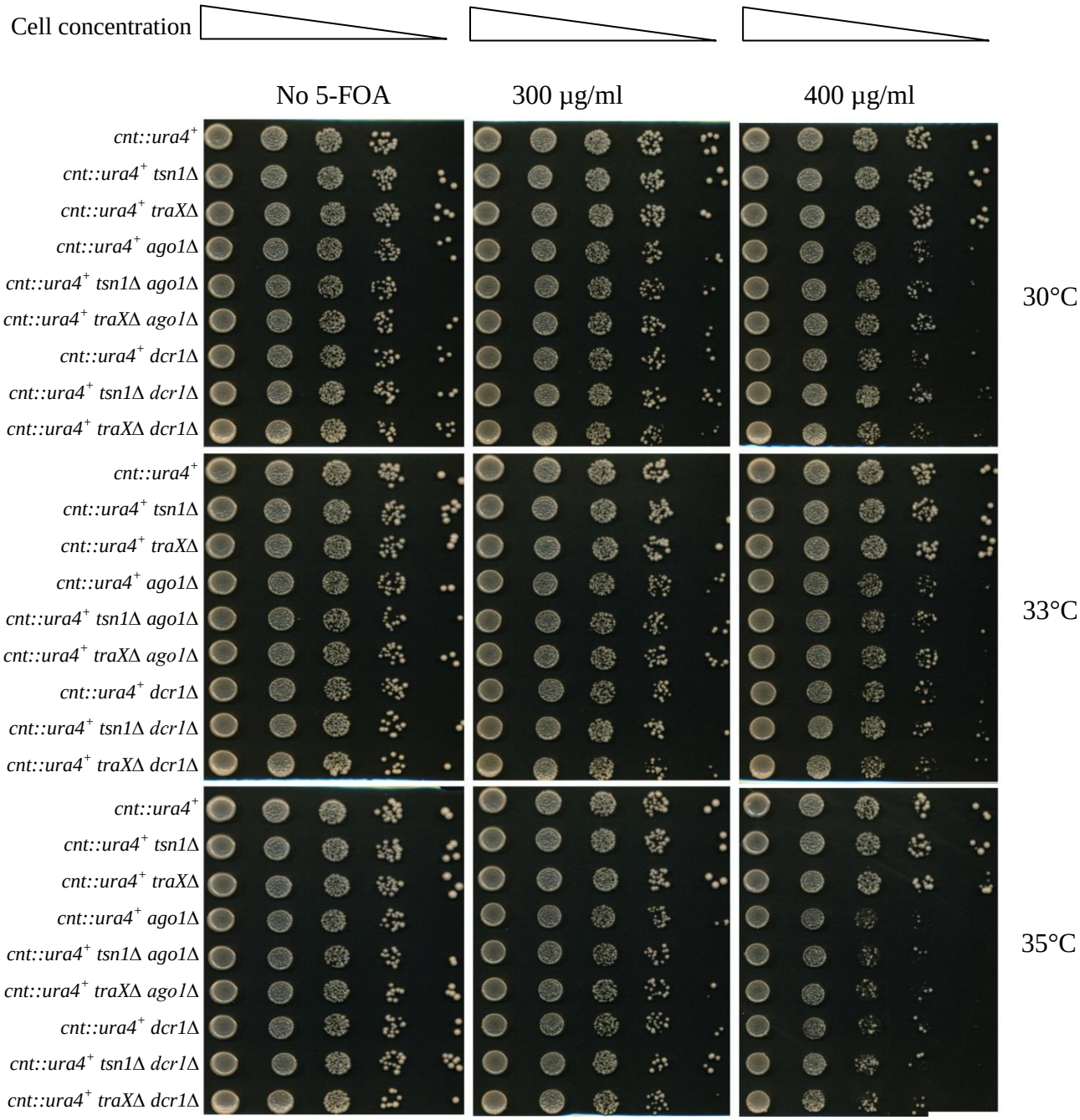

Figure 5.3 The 5-FOA spot tests of double mutants of *cnt::ura4*$^+$ strains at lower concentrations (300 and 400 µg/ml)

The parent mutant strain is (BP2203), *tsn1*Δ is (BP2418) *traX*Δ is (BP2411), *ago1*Δ is (BP3001) and *dcr1*Δ is (BP3103). No increase in sensitivity to 5-FOA (300 and 400 µg/ml) was seen in the single mutants *tsn1*Δ and *traX*Δ. The *ago1*Δ and *dcr1*Δ single mutants are sensitive to 5-FOA. However, no alterations in sensitivity was seen in the double mutants *tsn1*Δ *ago1*Δ (BP3111), *traX*Δ *ago1*Δ (BP2991), *tsn1*Δ *dcr1*Δ (BP2989) and *traX*Δ *dcr1*Δ (BP3105) comparing to *ago1*Δ and *dcr1*Δ single mutants. Cells were tested at 30°, 33° and 35°C.

5.2.1.ii Analysis of *imr::ura4*$^{+}$ strains

The *traX*Δ single mutant showed full transcriptional repression of the reporter gene *ura4*$^{+}$ inserted into an *imr* repeat (Chapter 3), indicating a fully functional heterochromatic silencing. The *ago1*Δ and *dcr1*Δ single mutants showed sensitivity to 5-FOA (500 µg/ml), indicating a deregulation of silencing. However, no alterations were apparent in sensitivity levels of the *traX*Δ *ago1*Δ and *traX*Δ *dcr1*Δ double mutants relative to *ago1*Δ and *dcr1*Δ single mutants. Three temperatures were tested (Figure 5.4). Further analysis was done at lower concentration of 5-FOA (300 and 400 µg/ml) (Figure 5.5).

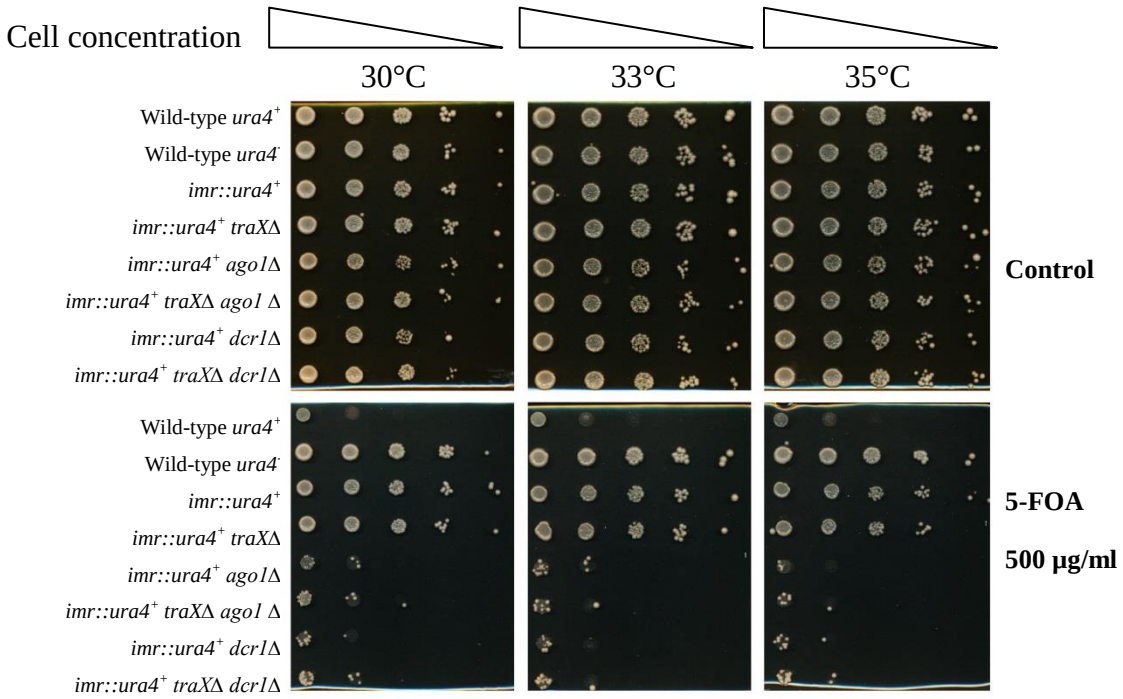

Figure 5.4 The 5-FOA spot tests of double mutants (*traX*Δ *dcr1*Δ) and (*traX*Δ *ago1*Δ) of *imr::ura4*$^{+}$ strains.

The wild-type *ura4*$^{+}$ is (BP1), wild-type *ura4*$^{-}$ is (BP90), the parent mutant strain is (BP2506), *traX*Δ is (BP2499), *ago1*Δ is (BP3005) and *dcr1*Δ is (BP3028). No measurable increase in sensitivity to 5-FOA (500 µg/ml) was seen in the single mutant *traX*Δ. The *ago1*Δ and *dcr1*Δ single mutants are sensitive to 5-FOA. However, no alterations in sensitivity was seen in the double mutants *traX*Δ *dcr1*Δ (BP3107) or *traX*Δ *ago1*Δ (BP2997) relative to *ago1*Δ and *dcr1*Δ single mutants. Cells were tested at 30°, 33° and 35°C.

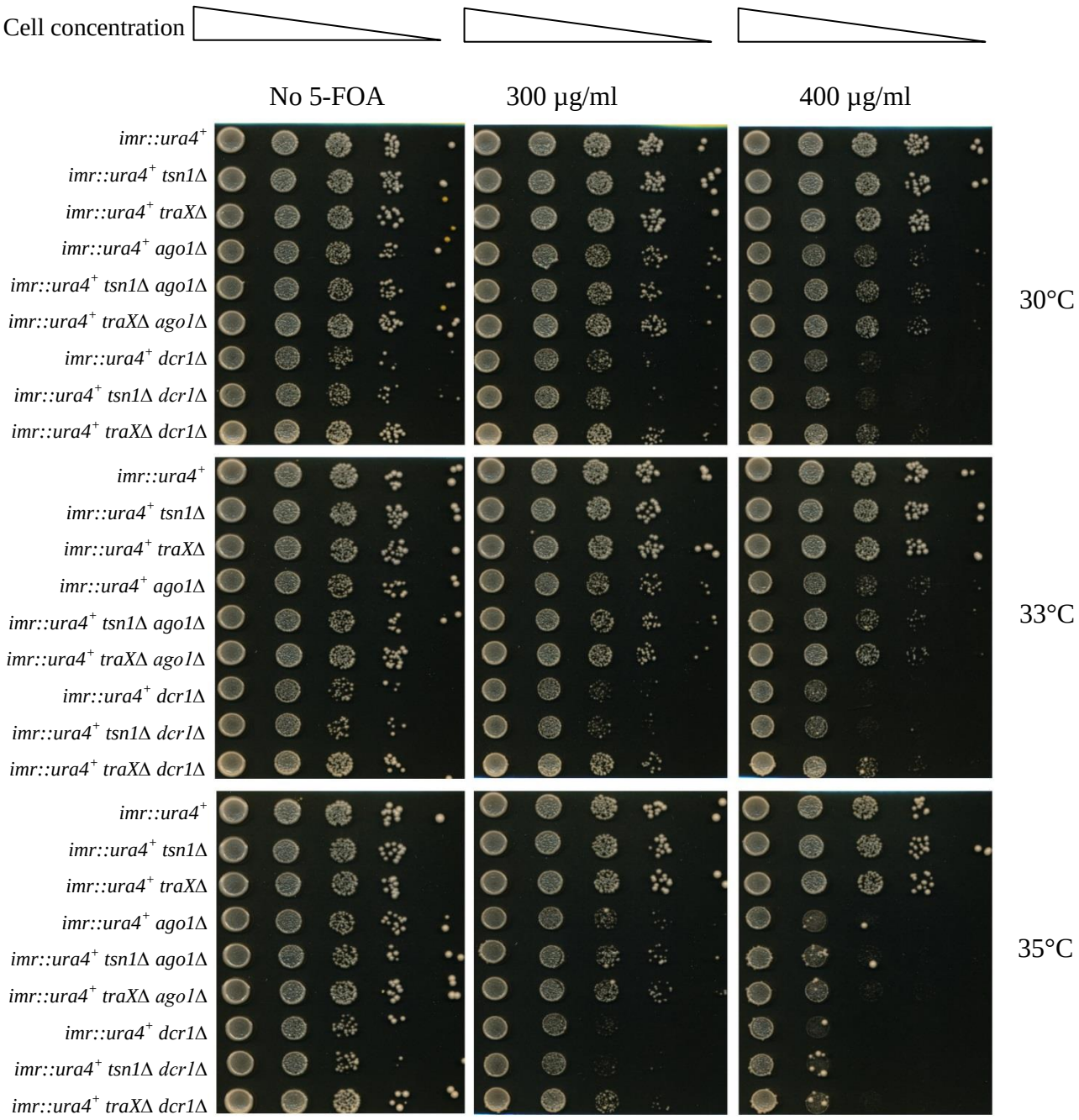

Figure 5.5 The 5-FOA spot tests of double mutants of *imr::ura4*$^+$ strains at lower concentrations (300 and 400 µg/ml).

The parent mutant strain is (BP2506), *tsn1*Δ is (BP2500), *traX*Δ is (BP2499), *ago1*Δ is (BP3005) and *dcr1*Δ is (BP3028). No increase in sensitivity to 5-FOA (300 and 400 µg/ml) was seen in the single mutants *tsn1*Δ and *traX*Δ. The *ago1*Δ and *dcr1*Δ single mutants are sensitive to 5-FOA. However, no alterations in sensitivity was seen in the double mutants *tsn1*Δ *ago1*Δ (BP3003), *traX*Δ *ago1*Δ (BP2997), *tsn1*Δ *dcr1*Δ (BP3026), and *traX*Δ *dcr1*Δ (BP3107) relative to *ago1*Δ and *dcr1*Δ single mutants. Cells were tested at 30°, 33° and 35°C.

5.2.1.iii Analysis of *otr::ura4*$^{+}$ strains

The *traX*Δ single mutant showed full transcriptional repression of the reporter gene *ura4*$^{+}$ inserted into an *otr* repeat (Chapter 3), indicating a fully functional heterochromatic silencing. The *ago1*Δ and *dcr1*Δ single mutants showed sensitivity to 5-FOA (500 µg/ml) indicating a deregulation of silencing. However, no alterations were apparent in sensitivity levels of the *traX*Δ *ago1*Δ and *traX*Δ *dcr1*Δ double mutants relative to *ago1*Δ and *dcr1*Δ single mutants. Three temperatures were tested (Figure 5.6). Further analysis was done at lower concentration of 5-FOA (300 and 400 µg/ml) (Figure 5.7).

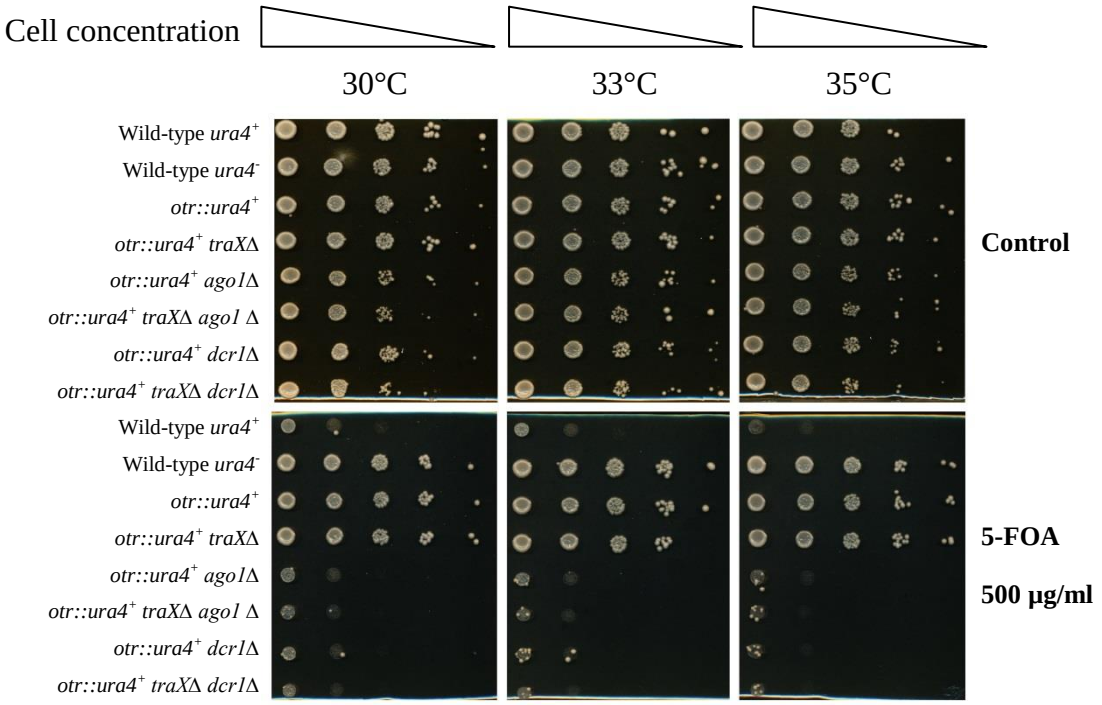

Figure 5.6 The 5-FOA spot tests of double mutants (*traX*Δ *dcr1*Δ) and (*traX*Δ *ago1*Δ) of *otr::ura4*$^{+}$ strains.

The wild-type *ura4*$^{+}$ is (BP1), wild-type *ura4*$^{-}$ is (BP90), the parent mutant strain is BP2204, *traX*Δ is BP2413, *ago1*Δ is BP3109 and *dcr1*Δ is BP2985. No increase in sensitivity to 5-FOA (500 µg/ml) was seen in the single mutant *traX*Δ. The *ago1*Δ and *dcr1*Δ single mutants are sensitive to 5-FOA. However, no alterations in sensitivity were seen in the double mutants *traX*Δ *dcr1*Δ (BP2987) or *traX*Δ *ago1*Δ (BP2993) relative to *ago1*Δ and *dcr1*Δ single mutants. Cells were tested at 30°, 33° and 35°C.

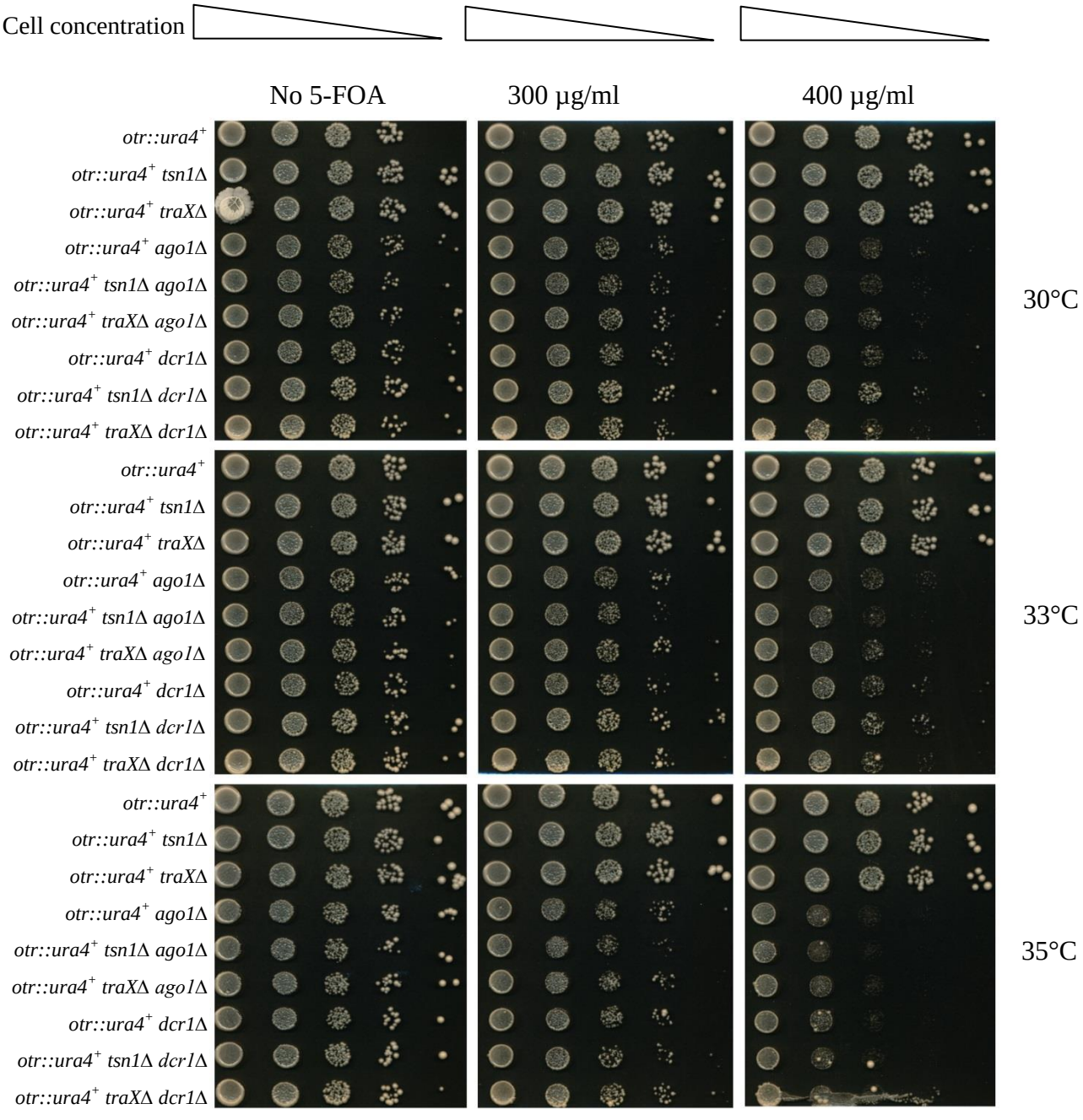

Figure 5.7 The 5-FOA spot tests of double mutants of *otr::ura4*$^{+}$ strains at lower concentrations (300 and 400 µg/ml).

The parent mutant strain is (BP2204), *tsn1*Δ is (BP2420), *traX*Δ is (BP2413), *ago1*Δ is (BP3110) and *dcr1*Δ is (BP2985). No increase in sensitivity to 5-FOA (300 and 400 µg/ml) was seen in the single mutants *tsn1*Δ and *traX*Δ. The *ago1*Δ and *dcr1*Δ single mutants are sensitive to 5-FOA. However, no alterations in sensitivity was seen in the double mutants *tsn1*Δ *ago1*Δ (BP2995), *traX*Δ *ago1*Δ (BP2993), *tsn1*Δ *dcr1*Δ (BP3024), and *traX*Δ *dcr1*Δ (BP2987) comparing to *ago1*Δ and *dcr1*Δ single mutants. Cells were tested at 30°, 33° and 35°C

5.2.2 Analysis of subtelomeric gene silencing in the absence of TraX and RNAi functions.

The heterochromatic regions at the telomeres contain DNA tandem repeats which have a fundamental role in protecting the linear chromosome ends (Poon and Mekhail, 2012). In *S. pombe*, the Swi6 (HP1) protein establishes telomeric heterochromatin regions independently of the RNAi machinery by the telomere-binding protein Taz1 (Kanoh et al., 2005). Any reporter genes inserted into these subtelomeric heterochromatin regions, such as *ura4*$^{+}$, will retain transcriptional silence unless deregulation of these regions occurs (Yankulov, 2011).

No suppression of pericentromeric silencing was observed in the *ago1*Δ *traX*Δ double mutant suggestion the suppression of the a*go1*Δ TBZ sensitivity was caused by another factor. To explore whether this was associated with subtelomeric silencing, appropriate strains were constructed using the Bähler method and PCR verified. The effect of double mutants *traX*Δ *ago1*Δ and *traX*Δ *dcr1*Δ on subtelomeric gene silencing was investigated by generating double mutants in strains which had *ura4*$^{+}$ inserted at approximately 7 kilo base pairs from the telomeres (*TEL-7421::ura4*$^{+}$). These strains were then tested to examine the sensitivity to 5-FOA at three temperatures (30°, 33° and 35°C). No measurable loss of silencing was observed in any strain except for the positive control wild-type *ura4*$^{+}$ (Figure 5.8).

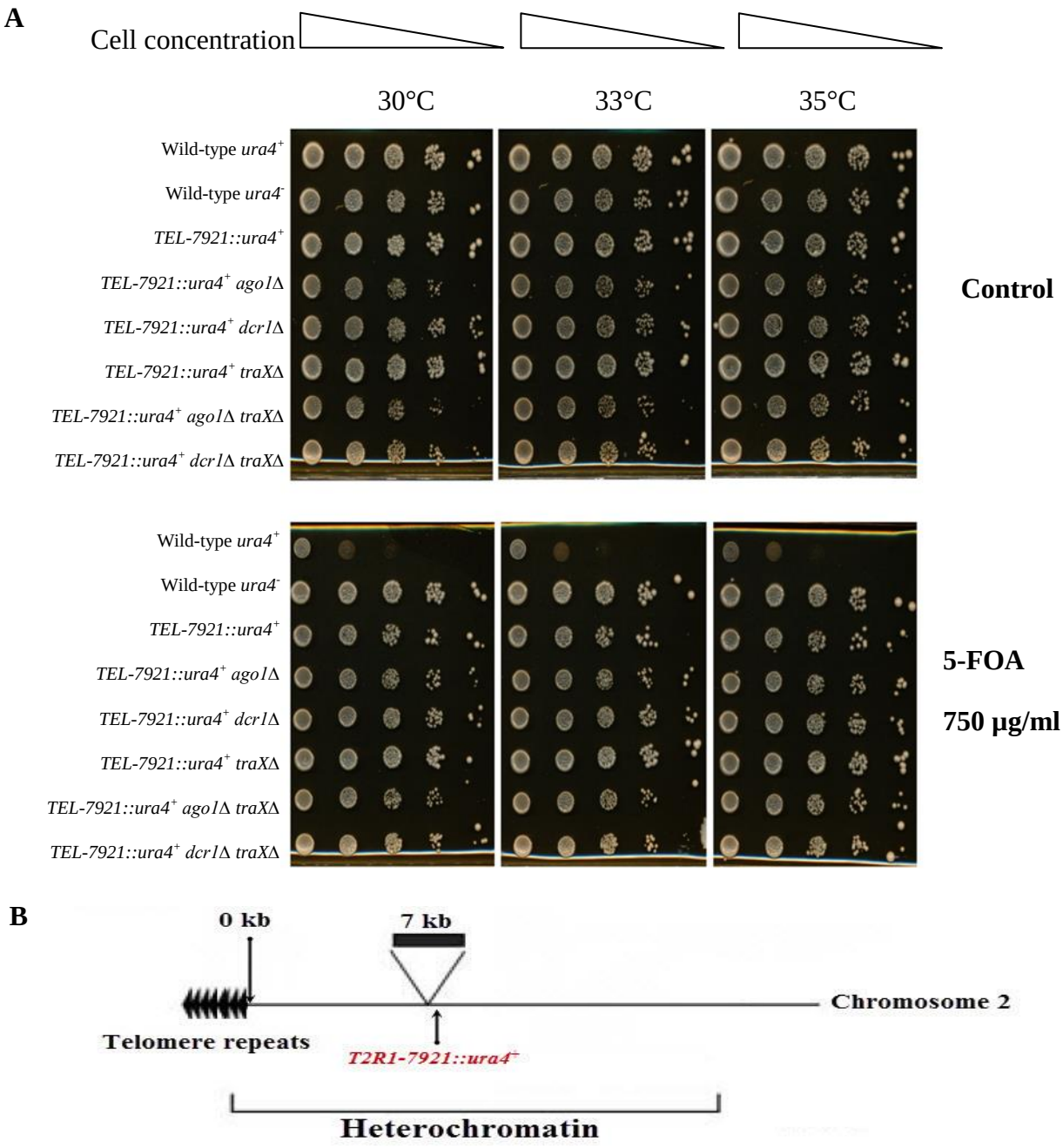

Figure 5.8 The 5-FOA spot tests of double mutants (*traX*Δ *ago1*Δ) and (*traX*Δ *dcr1*Δ) of *TEL-7921::ura4*$^+$.

A. The wild-type *ura4*$^+$ is (BP1), wild-type *ura4*$^-$ is (BP90), and the parent mutant strain is (BP3151). None of the single *traX*Δ (BP3224), *ago1*Δ(BP3208), *dcr1*Δ (BP3152) or double mutants *traX*Δ *ago1*Δ (BP3232) and *traX*Δ, *dcr1*Δ (BP3226) strains have increased sensitivity to 5-FOA (750 µg/ml). Cells were tested at 30^o, 33^o and 35^{o}C.

B. A schematic representation of subtelomere locus (chromosome 2, right arm) and inserted *ura4*$^+$ marker gene at 7921 base pairs from the telomere (adapted from Dohke et al., 2008).

5.2.3 Analysis of *mat* locus gene silencing in the absence of TraX and RNAi functions.

The mating-type locus elements *mat2-P* and *mat3-M* are heterochromatic regions that are characterised by H3K9me, which is recruited by the RNAi machinery (Bayne et al., 2010). Additionally, an RNAi-independent pathway which functions through the stress response regulators, Atf1-Pcr1 serves to mediate heterochromatin function (Jia et al., 2004a). Mating-type switching occurs when a single-stranded DNA break occurs during DNA replication, and recombination subsequently occurs with a donor cassette of either *mat2-P* or *ma3-M* (reviewed in Klar, 2007). The fission yeast mating-type locus is characterised by a well-defined structure, which allows analysis of how heterochromatic histone modification affects gene expression (Hansen et al., 2011).

Given that, there was no alteration to heterochromatin silencing in telomeres or centromeres, *mat* locus heterochromatin mediated silencing was tested. The possible effects of the double mutants *traX*Δ *ago1*Δ and *traX*Δ *dcr1*Δ on *mat* locus gene silencing were investigated by generating double mutants in strains that had *ura4*$^{+}$ inserted (*mat3-M::ura4*$^{+}$). These strains were then tested to examine the sensitivity to 5-FOA at three temperatures (30°, 33° and 35°C). No measurable loss of silencing was observed in any strain except for the positive control wild-type *ura4*$^{+}$ (Figure 5.9).

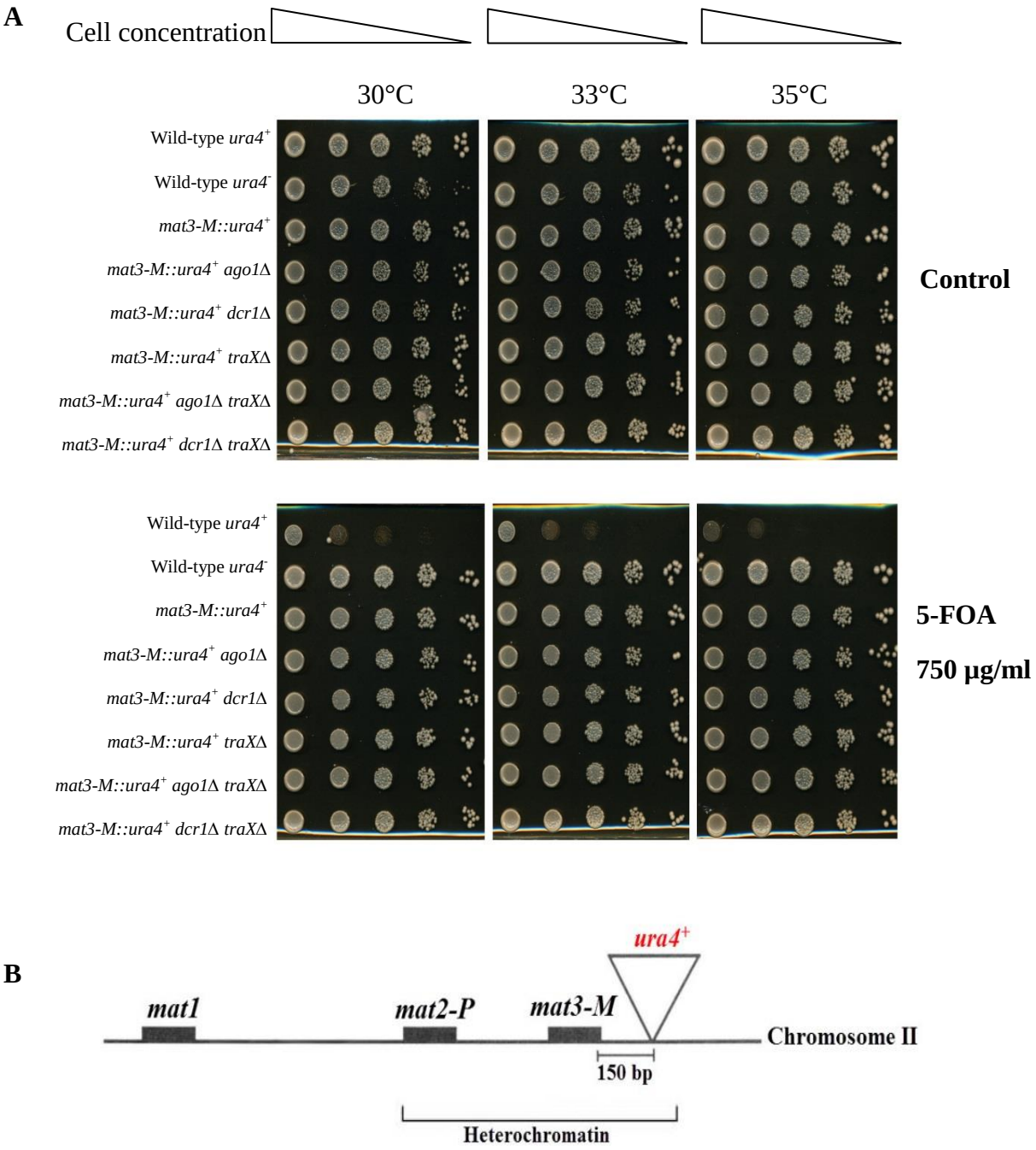

Figure 5.9 The 5-FOA spot tests of double mutants (*traX*Δ *ago1*Δ) and (*traX*Δ *dcr1*Δ) of *mat3::ura4*$^+$ strains.

A. The wild-type *ura4*$^+$ is (BP1), wild-type *ura4*$^-$ is (BP90), and the parent mutant strain is (BP2706). No increase in sensitivity to 5-FOA (750 µg/ml) was seen compared to single *traX*Δ (BP2718), *dcr1*Δ (BP3212), *ago1*Δ (BP3155) or the double mutants *traX*Δ *ago1*Δ (BP3192) or *traX*Δ *dcr1*Δ (BP3187). Cells were tested at 30°, 33° and 35°C.

B. A schematic representation of inserted *ura4*$^+$ marker gene at 150 base pairs from the *mat3-M* (chromosome 2) (dapted from Thon and Klar, 1992).

5.2.4 Analysis of *rDNA* locus gene silencing in the absence of TraX and RNAi functions

Ribosomal DNA (*rDNA*) genes are found in the subtelomeric regions of Chromosome III of *S. pombe.* These are heterochromatic regions found clustered as families of long tandem repeats. The fundamental function of heterochromatin at the rDNA locus could be to prevent recombination at these regions and to prevent the loss of rDNA repeats (Kobayashi et al., 2004).

The rDNA region remains the only extensive heterochromatic region that had not been tested in the double mutant. Marker genes such as *ura4*$^{+}$ inserted into rDNA loci silence at these loci because of the heterochromatin position effect of these regions (Dubey et al., 2009). Therefore, the possible effects of double mutants *traX*Δ *ago1*Δ and *traX*Δ *dcr1*Δ on rDNA locus gene silencing were investigated by generating double mutants in strains that had *ura4*$^{+}$ inserted (*rDNA::ura4*$^{+}$). These strains were then tested to examine the sensitivity to 5-FOA at three temperatures (30°, 33° and 35°C). Generally, no measurable loss of silencing was observed in any strain except for the positive control wild-type *ura4*$^{+}$ (Figure 5.10). However, a subtle increase in 5-FOA sensitivity appears to be apparent at 35°C in the *traX*Δ *dcr1*Δ double mutant, although it is limited.

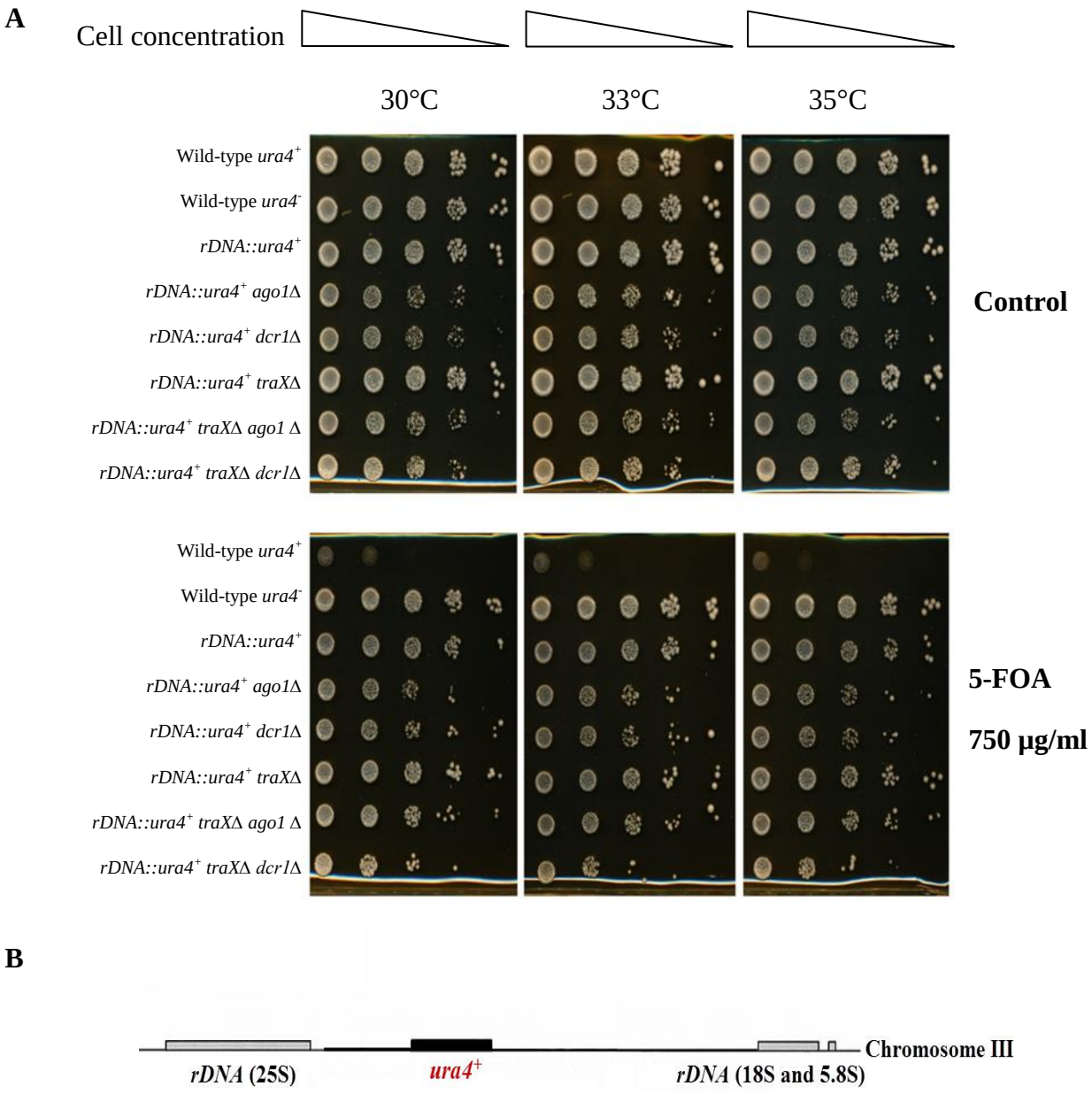

Figure 5.10 The 5-FOA spot tests of double mutants (*traX*Δ *dcr1*Δ) and (*traX*Δ *ago1*Δ) of *rDNA::ura4*$^+$ strains.

A. The wild-type *ura4*$^+$ is (BP1), wild-type *ura4*$^-$ is (BP90), and the parent mutant strain is (BP2704). No increase in sensitivity to 5-FOA (750 µg/ml) was seen in the single mutants *traX*Δ (BP2714), *ago1*Δ(BP3154), *dcr1*Δ (BP3213) or in the double mutants *traX*Δ *dcr1*Δ (BP3234) or *traX*Δ *ago1*Δ (BP3156). Cells were tested at 30°, 33° and 35°C.

B. A schematic representation of inserted *ura4*$^+$ marker gene at *rDNA* (chromosome III) (adapted from Thon and Verhein-Hansen, 2000).

5.2.5 Mating-type tests in *traX*Δ mutant

The life cycle of *S. pombe* includes haploid and diploid phases (Davis and Smith, 2001). The cell cycle involves meiosis to produce haploid gametes, which is a crucial step for production of genetically individual cells that could mate with opposite mating type cells. Under starvation conditions, two haploid *S. pombe* cells of opposite mating types are conjugated to form diploid cells, which then undergo sporulation to produce four spores (ascospores) (reviewed in Klar, 2007) (Figure 5.10). However, *S. pombe* does not mate in rich media. *S. pombe* normally grows as haploid cells that have three mating-type cassettes containing four mating-type genes within the maiting type locus: *mat1* (transcriptionally active), *mat2P* (h^+) and *mat3M* (h^-) (the latter two are both transcriptionally silent) (Hansen et al., 2011). RNAi recruit chromatin modification to form heterochromatin at the mating loci by facilitating H3K9me establishment (Bayne et al., 2010).

In fission yeast, the wild-type h^{90} strains can switch between h^- and h^+ mating type; this can occur once in every three cell divisions (Yamamoto et al., 1997). Cells in the sporulation phase secrete a starch-like product that can be detected using iodine vapours. When the spores are stained with iodine vapours to a dark black colour, this indicates high levels of mating and spore formation. However, when the cells remains light coloured, this indicates that no mating has occurred (Shankaranarayana et al., 2003).

The effect of *traX* gene deletion on mating-type switching ability was investigated in the h^{90} strains by deleting the *traX* gene in strains required for this test using the *kanMX6* cassette and the deletion was confirmed by PCR. The *traX*Δ h^{90} strain showed a similar switch in the *mat* cassettes to that seen in the positive control h^{90} strain (Figure 5.11). In addition, fission yeast mating resulted in the formation of asci with four equally sizes spores, which were investigated by light and fluorescence microscopy and showed the same morphology as asci from the positive control h^{90} strain (Figure 5.12). Strains were tested at three temperatures (25°, 30° and 35°C) with the same results.

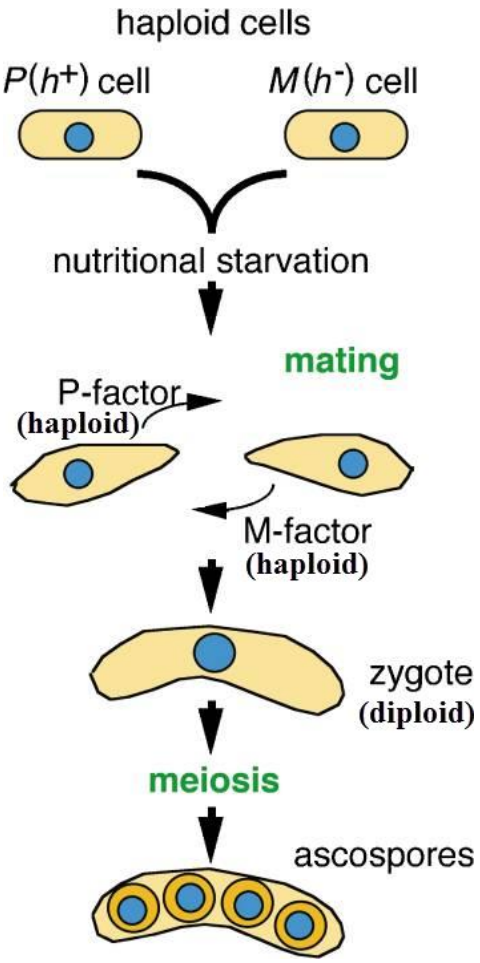

Figure 5.10 Diagram of mating and meiosis in *S. pombe*

Under nutritional starvation, haploid cells of *P* (h^+) and *M* (h^-) mating-type stop vegetative growing and start mating. Cells of *P* and *M* mating-types communicate via pheromones, and then conjugate to form a zygote (diploid), which undergoes meiosis to produce four spores in the ascus (ascospores) (adapted from Yamamoto, 2010).

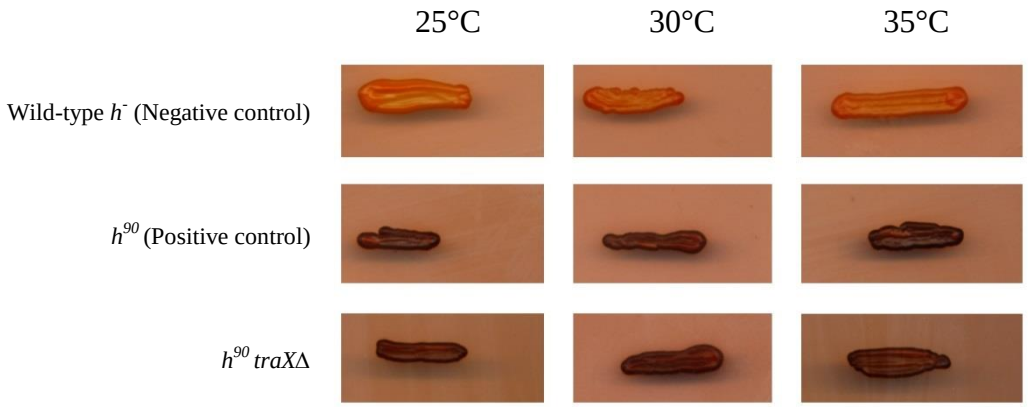

Figure 5.11 Examination of mating type switching by iodine staining experiment.

The wild-type h^- strain is (BP1) and the positive control strain h^{90} is (BP2292). The h^{90} *traX*Δ strain is (BP2407). Examination shows no effect of *traX* deletion on mating type of the h^{90} strain. Iodine staining of mating cells shows a range from light colour for wild-type, and dark colour for h^{90} stains. Strains were sporulated on supplemented SPA media for three days and then exposed to iodine vapour for 5 minutes. Matings were carried out at different temperatures (25°, 30° and 35°C).

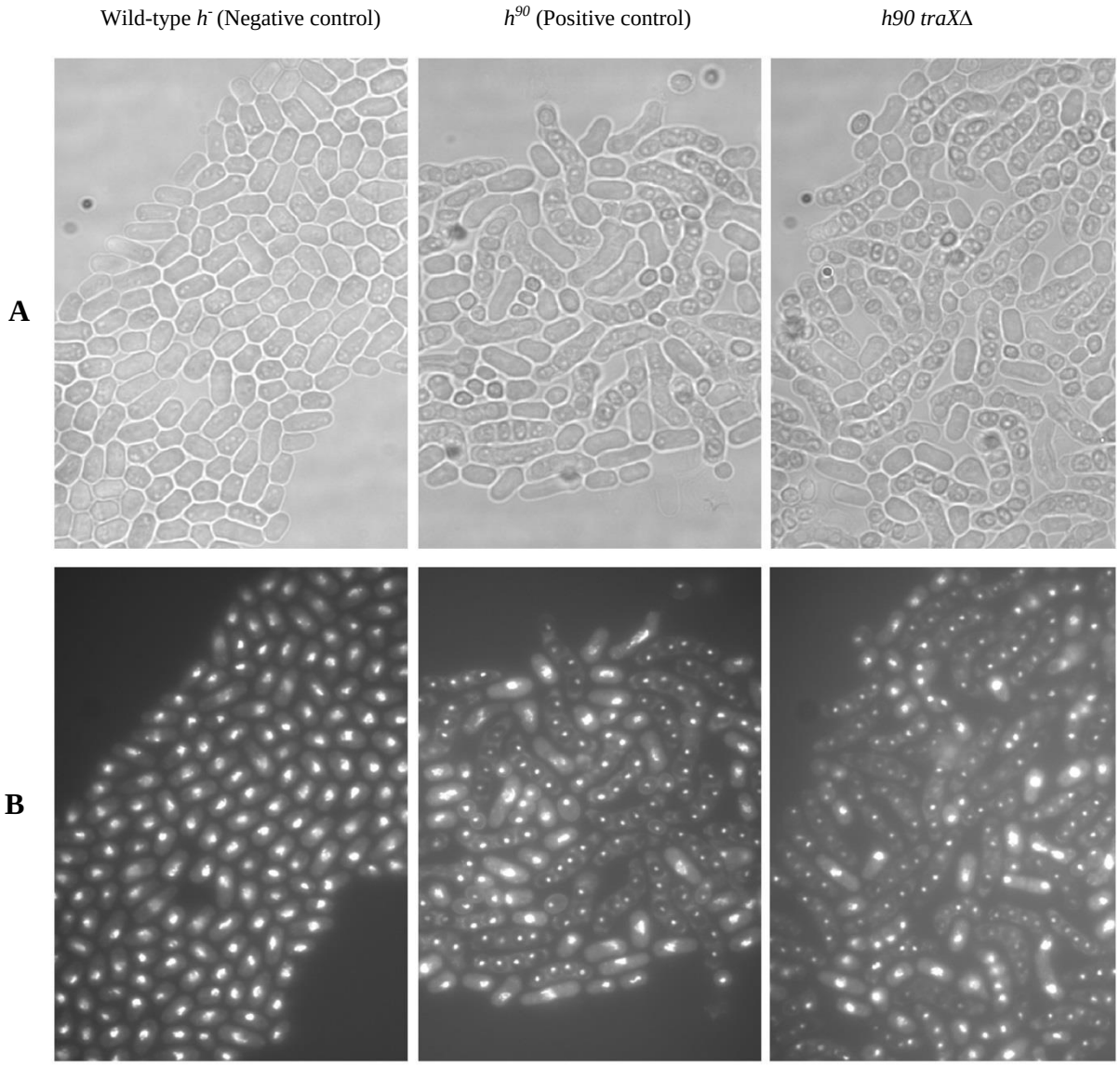

Figure 5.12 Microscopic examination of cells and asci morphology.

The wild-type h^- strain is (BP1) and the positive control strain h^{90} is (BP2292). The h^{90} *traX*Δ strain is (BP2407).

A. Cells and asci viewed with a light microscope.

B. Cells and asci with DAPI staining. The examination shows normal asci morphology for the *trax* deleted h^{90} strain. Strains were sporulated on supplemented SPA media for three days at 30°C. Similar results were seen at 25° and 35°C (not shown).

5.3 Discussion

5.3.1 Loss of TraX function does not alter centromeric gene silencing.

Fission yeast centromeres are transcriptionally silenced, and are fundamental heterochromatic regions required for cell segregation. We found that *traX*Δ *ago1*Δ double mutants exhibited a greater resistance to TBZ than the *ago1*Δ single mutant (Chapter 4). A similar result was seen in mini chromosome loss assays, where the *traX*Δ *ago1*Δ double mutant showed significantly less mini chromosome loss when compared to the *ago1*Δ single mutant (Chapter 4), indicating a possible link to the RNAi machinery. This observation suggested the potential operation of an auxiliary pathway in centromeric heterochromatin maintenance which is suppressed by TraX. However, the results in the present chapter show this not to be the case because no additional alterations in centromeric silencing were observed in the double mutant *traX*Δ *ago1*Δ or *traX*Δ *dcr1*Δ in three centromeric regions *cnt1*, *imr1* and *otr1*. This result is remarkable as previous work suggests that Ago1-defecient cells have TBZ sensitivity and genome instability due to dysfunction of centromeric heterochromatin (Castel and Martienssen, 2013). However, mutating the TraX pathway partially represses the *ago1*Δ genome instability phenotype (Chapter 4). Additionally, we demonstrate the suppression of the *ago1*Δ mutant phenotype in a *traX*Δ mutant is Translin-dependent. However, whilst Translin (in the absence of TraX) can support a pathway that partially suppresses the chromosome instability of the *ago1*Δ, the work in this chapter demonstrates that this does not work via restoring increased centromeric heterochromatin gene silencing. This is remarkable as it uncouples centromeric heterochromatic status from chromosome stability; i.e. the chromosome instability in the *ago1*Δ mutant is not caused solely by loss of centromeric heterochromatin as this remains unaltered in the *traX*Δ *ago1*Δ double mutant and yet genome instability is repressed relative to the *ago1*Δ mutant. This suggests the sensitivity of *ago1*Δ mutant to TBZ might be caused by defects in another unknown pathway which is compensated for by Translin activity in the absence of TraX.

5.3.2 No effect of loss of TraX function on subtelomeric gene silencing

Heterochromatin regions at telomeric regions are involved in maintaining telomere integrity (Wong, 2010). Fission yeast heterochromatin formation at subtelomeric regions is an RNAi independent, Taz1-dependent pathway (Kanoh et al., 2005). Reporter genes

that are introduced into subtelomeric regions remain transcriptionally silent (Bah and Azzalin, 2012). The 5-FOA sensitivity tests on the double mutant strains *traX*Δ *ago1*Δ and *traX*Δ *dcr1*Δ with *ura4*$^{+}$ inserted in the subtelomeric region did not indicate any alteration in gene silencing. This suggests that the *ago1*Δ phenotype suppression does not relate to telomeric heterochromatin dynamics, despite the function of TRAX and Translin having previously been inferred to play a role in telomere dynamics (reviewed in Jaendling and McFarlane, 2010).

5.3.3 No effect of loss of TraX function on *mat* locus gene silencing

Fission yeast heterochromatic regions at mating-type loci *mat2-P* and *mat3-M* are transcriptionally silenced; however, *mat1* is transcriptionally active and is not considered a heterochromatic region (Hansen et al., 2011). At the *mat* locus two pathways are responsible for heterochromatin-mediated gene silencing. These are the RNAi pathway and the stress activated ATF/CREB pathway (Jia et al., 2004a). The 5-FOA sensitivity tests on the double mutants strains *traX*Δ *ago1*Δ and *traX*Δ *dcr1*Δ with *ura4*$^{+}$ inserted in the *mat3* locus did not indicate any alteration to gene silencing. This observation is linked to mating switching as well as the lack of any defect or morphology change in the *traX*Δ strains.

5.3.4 No effect of loss of TraX function on *rDNA* locus gene silencing

The rDNA locus is a heterochromatic region in the subtelomere that contains a long tandem repeat of DNA in chromosome III. Reporter genes such as *ura4*$^{+}$ inserted into rDNA loci lead to silencing (Dubey et al., 2009). The 5-FOA sensitivity tests on double mutants strains *traX*Δ *ago1*Δ and *traX*Δ *dcr1*Δ that have *ura4*$^{+}$ inserted in rDNA region showed no alteration to gene silencing. This indicates that the *traX*Δ double mutant does not affect gene silencing at the rDNA locus.

5.4 Conclusion

The evidence from the previous chapter resulted in the suggestion that loss of TraX function “released” Translin to partially substitute for Ago1 in an *ago1*Δ background. This lead to the hypothesis that Translin, in the absence of TraX, could partially restores heterochromatin function at the centromeres and thus partially restore chromosome segregation potential. Surprisingly, this was not the case and here we provide important new evidence to partly uncouple the chromosome instability phenotype of an *ago1*Δ

mutant from centromeric heterochromatin dysfunction. This opens up the possibility there is another pathway controlling chromosome stability that is Ago1-dependent. The dependence on Ago1 to mediate this pathway can be partly repressed by loss of TraX function, possibly by enabling Tsn1 to function in a 'TraX-free environment' as TraX may normally associate with Tsn1 to block this activity.

CHAPTER 6

Interpretation and discussion of related transcription data

6.1 Introduction

Thus far this study has revealed some key novel findings. One of the main observations is that a pathway exists that can partially substitute for the loss of Ago1 to support stable chromosome segregation. Under normal laboratory conditions this pathway is repressed by the activity of the Translin binding partner protein TraX, as mutation of the *traX* gene is required for the activation of this pathway in an Ago1-deficient background. Interestingly, the pathway does not appear to act by reverting the dysfunction of centromeric heterochromatin generated by the loss of Ago1 function as marker genes placed within the silenced centromeric regions remain de-repressed. This leads to the proposal that there is another, as yet uncharacterised function for Ago1 which is not directly related to the regulation of heterochromatin-mediated silencing in the centromeric regions. When this pathway is perturbed it results in genome instability. It is this pathway that is normally repressed by TraX and appears to be Tsn1-dependent.

Given that TraX and Translin have been implicated in RNA dynamics in a range of organisms (reviewed in Jaendling and McFarlane, 2010; Li et al., 2012) we postulated that the hypothetical pathway suppressed by TraX related to some aspect of RNA metabolism. To address this, a systematic approach was taken to analyse the whole transcriptome of various mutants to provide insight into what the Ago1-independent, Tsn1-dependent pathway might be and how it is normally repressed by TraX function. A whole genome approach was taken and *S. pombe* tiled genome arrays were used to analyse the transcriptional profile of both DNA strands in appropriate mutants.

6.2 Data interpretation

6.2.1 Microarray strategy

For whole transcriptome analysis Affymetrix GeneChip *S. pombe* Tiling 1.0FR Arrays were used. The RNA isolation, labelling and array reading were carried out by our collaborators (M. Bühler's Group, Friedrich Miescher Institute for Biomedical Research, Switzerland) as previously described (Emmerth et al., 2010). All strains were analysed in triplicate on different days. Data analysis was carried out by a colleague (Julia Feichtinger; currently based at the Technical University Graz, Austria) by means of the wave Tiling R package (Beuf et al., 2012). The genotypes of the strains analysed in this study are given in Table 6.1.

Table 6.1 Strains analysed by tiled genome arrays.

Relevant strain genotype*	**Strain numerical designation**	**Bangor strain designations**
Wild-type (wt)	1	BP90
ago1Δ	2	BP2757
traXΔ	4	BP1090
ago1Δ traXΔ	5	BP2761
tsn1Δ traXΔ	7	BP3248
tsn1Δ traXΔ ago1Δ	8	BP3246
tsn1Δ	10	BP1080

Note: other strains (e.g., *dcr1Δ tsn1Δ* and *dcr1Δ*) were analysed, but this was outside the remit of this study. *For full genotype see Materials and Methods (Chapter 2).

6.2.2 Transcriptome comparisons

In all cases, only transcripts with log 2-fold change (lg2FC) ≥ 1.0 and P values of < 0.05 are shown (Stouffer, 1949). Data files are located in the electronic Appendices (see e-Appendix files Array Data 1.xls and Array Data 2.xls).

6.2.2.i. wt vs. *ago1*Δ

As anticipated, a large number of transcript was altered in the *ago1Δ* strain (see Appendix file Array Data 3.xls and 4.xls). However, there are two relevant points to note. Firstly, is the fact that the normally silent sub-telomeric RecQ-like genes *tlh1* and *tlh2* were not up regulated in the *ago1Δ* strain relative to the wt. Secondly, is the fact that the *rif1* gene is highly up regulated. The importance of these two observations will become apparent (see below).

6.2.2.ii wt *vs. traX*Δ

The only change in the *traX*Δ strain is a remarkable one. The sub-telomeric RecQ-like genes *tlh1* and *tlh2* are both significantly up regulated. Figure 6.1 shows this up regulation for *tlh2* (SPBCPT2R1.08c). This is the most right hand region of chromosome II and is immediately adjacent to the right hand telomere. Figure 6.2 shows this region of the genome. The gene starts at position 4,526,885 and the 5' upstream pseudogene ends at position 4,526,884, the preceding 5' nucleotide. The transcript analysis data indicate that the pseudo gene is not activated in the *traX*Δ mutant, nor are any other adjacent genes, indicating the up regulation is strictly limited to the *tlh2* gene in the *traX*Δ strain; this indicates that the up regulation is not caused by a global de-repression of transcription in this region.

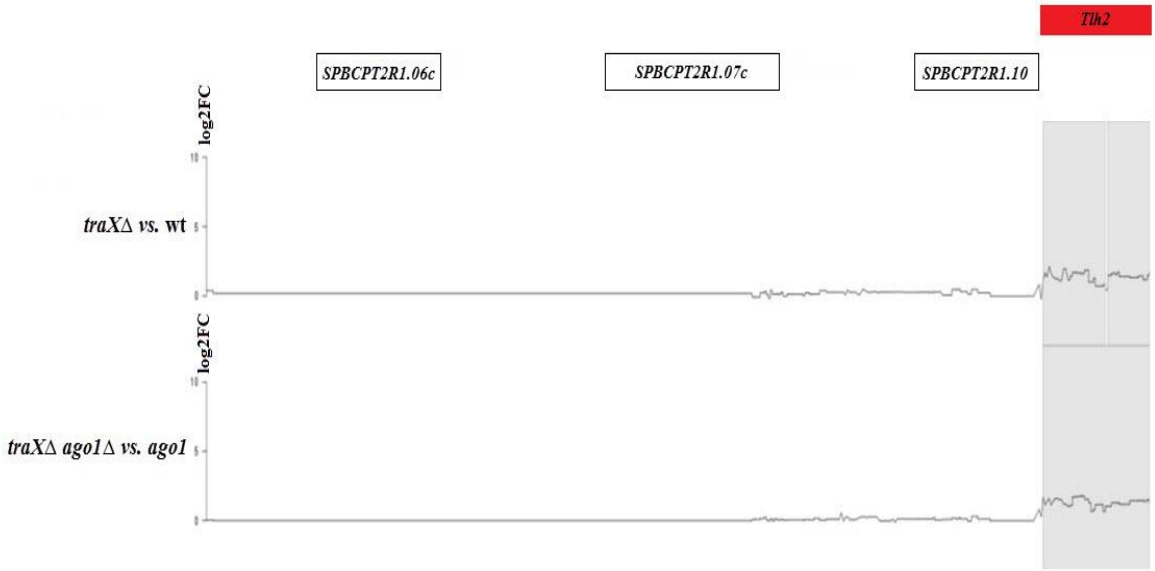

Figure 6.1 plot profile for the reverse strands showing the right hand region of chromosome II.

The upper rectangle boxes represent genes, the *SPBCPT2R1.10* is pseudogene adjacent to *tlh2*, (see Figure 6.2); *tlh2* is represented by the red rectangle box which starts immediately to the right of SPBCPT2R1.10 and corresponds to the grey activated regions. The two reverse strand plots shown below are for a *traX*Δ *vs.* wt pair wise plot (4-1) and a *traX*Δ *ago1*Δ *vs. ago1*Δ pair wise plot (5-2). The grey boxes indicate regions that are ≥ the statistical threshold (lg2FC ≥ 1.0, P < 0.05).

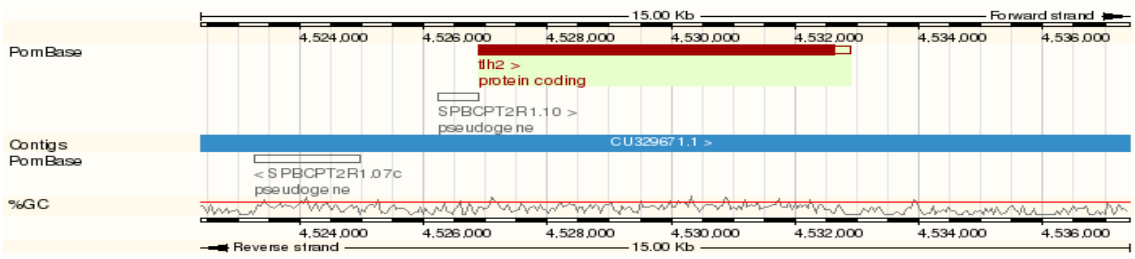

Figure 6.2 Map of the right hand region of *S. pombe* chromosome II.

The *tlh2* gene is shown as a burgundy rectangle and the position of the 5' up stream pseudogene (SPBCPT2R1.10) is marked.

6.2.2.iii wt *vs. tsn1*Δ

Unlike the *traX*Δ strain, there was no statistically meaningful alteration at the threshold set of any transcript in the *tsn1*Δ strain relative to the wt (excluding the *tsn1* transcript and a ncRNA transcript from the opposite strand within the gene). However, there was a slight up regulation of both *tlh1* and *tlh2*, but both fell below the statistical thresholds set ($lg2FC \geq 1.0$, $P < 0.05$); TraX proteins levels are diminished in a *tsn1*Δ mutant, but not obliterated; as the *tsn1*Δ mutant has *tlh1* and *tlh2* weakly up regulated, this is consistent with a loss of some, but not all TraX in the *tsn1*Δ mutant.

6.2.2.iv. *ago1*Δ *vs. ago1*Δ *traX*Δ

There are only a few statistically meaningful changes in the double mutant relative to the single mutant (these are shown in Table 6.2):

i. The *tlh2* gene is up regulated in the double mutant (as in the *traX*Δ single mutant).

ii. The *rif1* gene (global regulator of origin firing) and its associated ncRNA gene are partially down regulated in the double mutant compared to the *ago1*Δ single mutant [*rif1* is strongly up regulated in the *ago1*Δ single mutant compared to the wt (see above)].

iii. Two adjacent genes (SPAC186.02 and SPAC186.05) have expression altered in the double mutant (one up one down) and they reside in a region close to the telomere on the right hand end of Chromosome I that appears to be rich in ncRNA genes.

iv. A non-coding RNA (SPNCRNA.1255) is down regulated in the double mutant.

Table 6.2 Changes in *ago1*Δ *vs. ago1*Δ *traX*Δ (excluding *ago1, traX* or opposite strand transcripts)

Systematic ID	Standard name	Status in *ago1Δ traXΔ* relative to *ago1Δ*	lg2FC	Notes
SPBCPT2R1.08c	*tlh2*	↑	1.05	Sub-telomeric RecQ-like gene; Chr II- right
SPAC6F6.17	*rif1*	↓*	-1.04	Origin / telomere regulator
SPNCRNA.852	*rif1*-antisense ncRNA	↓*	-1.04	
SPAC186.02c	Unassigned	↑	1.02	Hydroxyacid dehydrogenase (predicted)
SPAC186.05c	Unassigned	↓	-1.13	TMEM165 homologue
SPNCRNA.1255	Unassigned	↓	-1.01	Intergenic ncRNA; Chr III

*Note: *rif1* is significantly activated in the *ago1*Δ single mutant compared to wt (lg2FC value 0f 3.41; the change in the *ago1*Δ *traX*Δ strain relative to the wt is 2.40), so the reduction here simply reflects a reduced elevation.

6.2.2.v *ago1*Δ *traX*Δ *vs. ago1*Δ *tsn1*Δ *traX*Δ

There are only a few statistically meaningful (lg2FC ≥ 1.0) changes from the double to the triple mutant (shown in Table 6.3):

i. *abc4* is up regulated, but this is the gene adjacent to *tsn1* and it seems reasonable to surmise this up regulation is due to the disruption of *tsn1* (although this activation was not observed in the *tsn1*Δ single mutant and might be a consequence of an altered chromatin structure in the *ago1*Δ *traX*Δ background). The genome structure showing the location of *abc4* is given in Figure 6.3.

ii. A predicted RNA binding protein gene (SPAC22E12.02) and the adjacent gene (SPAC22E12.03; transcribed in the opposite direction and overlapping) are activated.

iii. A predicted centromeric (*cenII*) ncRNA is activated.

iv. Two adjacent genes with convergent transcription (SPCC965.06 and *gst2*) are activated.

Table 6.3 Changes in *ago1*Δ *traX*Δ *vs. ago1*Δ *traX*Δ *tsn1*Δ (excluding *ago1, traX, tsn1* or opposite strand transcripts)

Systematic ID	Standard name	Status in *ago1*Δ *traX*Δ *tsn1*Δ relative to *ago1*Δ *traX*Δ	lg2FC	Notes
SPAC30.04c	*abc4*	↑	1.77	Adjacent to *tsn1*
SPAC22E12.02	Unassigned	↑	1.05	Predicted RNA binding protein
SPAC22E12.03c	Unassigned	↑	1.05	Transcribed from opposite strand to above gene.
SPNCRNA.365	Unassigned	↑	1.12	Predicted centromeric ncRNA (*cenII*)
SPCC965.06	Unassigned	↑	1.30	Predicted potassium channel
SPCC965.07c	*gst2*	↑	1.25	Glutathione S-transferase; adjacent to above gene, but transcribed in opposite direction.

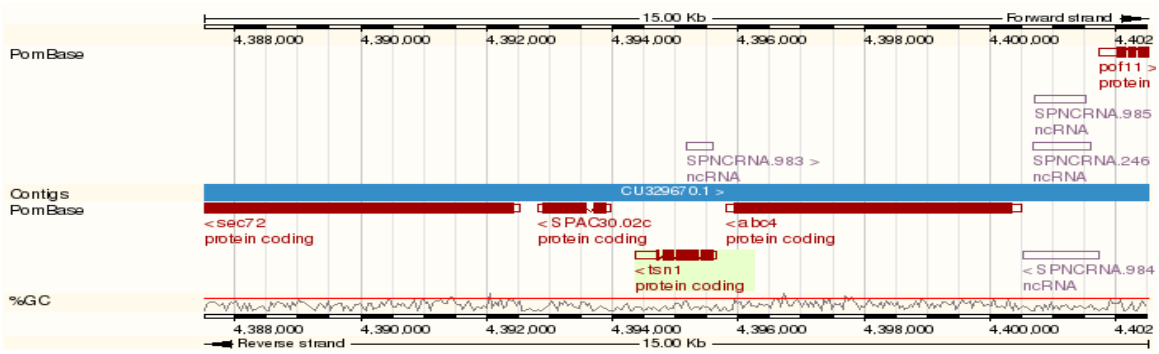

Figure 6.3 The genome structure showing the position of the *abc4* gene.

The *abc4* gene is immediately adjacent to the *tsn1* gene.SPNCRNA.983 is a non-coding RNA (ncRNA) transcribed from the opposite strand to *tsn1*; as this ncRNA is deleted when *tsn1* is deleted the transcript abundance goes down in a *tsn1*Δ strain. (Derived from PombeBase; http://www.pombase.org/).

6.3. Discussion

Here the data for an extensive micro array analysis of the transcriptomes of various strains with the aim of exposing the changes in the genomic transcriptional landscape arising due to mutation of *traX*. Whilst this analysis revealed very few changes in response to *traX* deletion, this should not come as a surprise as the *traXΔ* single mutant does not exhibit any major phenotype (indeed, studies in the McFarlane group reveal no measurable phenotype in this mutant; Jaendling et al., 2008). The only significant change in the *traXΔ* mutant relative to the wt was the activation of the two sub-telomerically encoded RecQ-like genes, which are normally silenced. These genes showed a mild up regulation in the *tsn1Δ* mutant, but this fell below the statistical threshold used here; this might reflect the fact that TraX is depleted in the *tsn1Δ* mutant and so this weak up regulation is due to partial depletion of TraX.

6.3.1. Tlh1 and Tlh2: suppressors of an Ago1 deficiency?

The function of the *tlh1* and *tlh2* genes remains unknown. Tlh1 and Tlh2 proteins are 100% identical along the majority of their length, with Tlh1 having the final 19 amino acids missing. This suggests that this paralogue pair arose due to a relatively recent gene duplication event. An attempt to elucidate the function by over expressing the gene in *S. pombe* cells essentially failed as a full length version could not be cloned (Mandell et al., 2005). Interestingly, the study carried out here found no alteration to the expression profile of either gene in the *ago1Δ* strain whereas Mandell and co-workers (2004) used non-quantitative RT-PCR to demonstrate one (or both) of the putative RecQ-like helicase gene(s) was expressed in both *dcr1Δ* and *ago1Δ* cells (Mandell et al., 2004). These opposing observations could support a role for the Tlh proteins in suppressing the negative effects of loss of Ago1 function, as the strains used by Mandell and co-workers (2004) might have acquired expression of one (or both) *tlh* gene(s) to provide a survival advantage in the absence of Ago1 and/or Dcr1; the primary deleted strains used here have not acquired this expression yet. Clearly, loss of TraX activates *tlh* genes and this correlates to a suppression of the chromosomal instability phenotype of the *ago1Δ* mutant.

The findings here lead to the hypothesis that expression of *tlh* can override the defects of loss of Ago1. This could be readily tested by cloning *tlh2* (the full length *tlh* version) in

an *ago1Δ* strain. If the hypothesis is correct, that *tlh2* expression alone is responsible for the enhanced genome stability in the *ago1Δ* background when *traX* is mutated, then these cells will be less sensitive to TBZ than the *ago1Δ* mutant with a vector alone. This experiment needs completing as it was beyond the time frame of this study.

How might TraX regulate *tlh1/2*? This cannot be deduced from the current study. However, the tight physical limits to the *tlh2* up regulation (i.e. no flanking genes are up regulated; see Figure 6.2) demonstrate that this does not operate via a regional de-regulation of transcriptional suppression. Instead, it suggests that this is a specific transcriptional up regulation response which activates *tlh2* in a highly targeted fashion. Alternatively, *tlh2* activation may occur via the removal of a post-transcriptional function which destroys *tlh2* mRNA in a TraX-dependent fashion; interestingly, TraX has been demonstrated to possess RNAse activity opening up the speculative suggestion that TraX functions to specifically degrade *tlh2* (and possibly *tlh1*) mRNAs. At this stage neither of these possibilities can be excluded and further experimentation is required.

What is the significance of the TraX regulation of *tlh1/2* up regualtion? Firstly, it is clear that these data seem to uncouple the functions of Tsn1 and TraX, as loss of Tsn1 only results in only a mild up regulation of *tlh1/2* that is below statistically accepted norms for array data sets; this is most likely due to a depletion of TraX levels. This is also supported by the finding that deletion of *tsn1* does not result in the same suppression of the *ago1Δ* phenotype as generated by the depletion of *traX* and so the levels of *tlh1/2* expression in the *tsn1Δ* mutant are insufficient to suppress the *ago1Δ* defect, if indeed *tlh1/2* expression is the suppressing factor. It is clear that one of the primary functions of TraX (or possibly the only function) is to regulate, via repression, *tlh1/2* expression. Whether this is a direct regulation remains to be determined, but the wt-like phenotype of the *traXΔ* mutant suggests a very specialist function for TraX. Indeed, we hypothesis that these data support the idea that *tlh1/2* only require activation under some as yet uncharacterised, specific conditions (possibly a stress of some kind), and that TraX acts as a regulatory trigger for their rapid activation when they are required.

6.3.2. Could *rif1* levels play a role?

The comparison of the *ago1Δ* and *ago1Δ traXΔ* strains revealed that the levels of *rif1* gene transcripts are reduced in the double mutant relative to the single mutant and that the

same is true for an associated ncRNA. However, *rif1* transcription is not elevated in the *traXΔ* single mutant relative to the wt. This paradox is resolved when one realises that *rif1* transcription is greatly up regulated in the *ago1Δ* single mutant (see Section 6.2.2.i). A comparison of the transcript levels of wt *vs*. *ago1Δ traXΔ* double mutant reveals that *rif1* is elevated in the double mutant, but not to the same degree as the *ago1Δ* single mutant, so the apparent reduction between the *traXΔ ago1Δ* double mutant relative to the *ago1Δ* single mutant is in fact a reduced elevation of *rif1* and not a reduction relative to wt levels (i.e. the levels of *rif1* transcription in the *ago1Δ traXΔ* are still higher than the levels in the wt).

It could be the case that the highly elevated expression of *rif1* in the *ago1Δ* mutant results in the genome instability. Rif1 controls origin of replication firing and telomere dynamics (Hayano et al., 2012; Kanoh and Ishikawa, 2001; Miller et al., 2005). Too much Rif1 could simply disrupt normal chromosomal dynamics resulting in a chromosome stability defect. The loss of TraX in an *ago1Δ* background causes the levels of *rif1* transcription to be reduced (not back to wt levels), and this might be sufficient to alleviate the negative effects of elevated *rif1* expression. This hypothesis is an appealing one and one that can be readily tested in one of two ways. Firstly, over expression of *rif1* in a wt cell should cause *ago1Δ*-like levels of chromosomal instability and TBZ sensitivity. Secondly, deletion of *rif1* should suppress (partly, at least) the chromosomal instability of an *ago1Δ* mutant. Again, these experiments now need to be done to test this hypothesis.

6.3.3. Loss of Tsn1 overrides the beneficial effects on Ago1 deficient cells which have lost TraX.

Deletion of *tsn1* results in an *ago1Δ traXΔ* background reverting to a high level of TBZ sensitivity. The original explanation for this was that loss of TraX resulted in the ‘freeing’ of Tsn1 to override the need for Ago1 (see previous chapters). However, this idea was cast into doubt by the finding that TraX and Ago1 deficient cells retained high levels of centromeric silencing dysfunction, and thus the genome instability phenotype is partly uncoupled from the dysfunction of centromeric heterochromatin-medicated gene silencing. This suggested that if Tsn1 was substituting for Ago1, it was not a direct replacement that could ensure normal centromeric heterochromatin.

Indeed, the micro array analysis has revealed a very different story. There are few further changes when *tsn1* is deleted in the *ago1Δ traXΔ* background. Certainly *tlh1/2* levels are not reduced relative to the double mutant (not even below the threshold levels); this suggests loss of Tsn1 does not revert the repression by removing the RecQ-like helicase. Secondly, *rif1* levels do not change (not even below the threshold levels), so it seems unlikely that loss of Tsn1 results in an additional elevation in Rif1. So what could cause the reversion to a TBZ sensitive state? Well one change is the up regulation of a predicted RNA binding protein gene (SPAC22E12.02), it could be the activation of this gene that now imposes TBZ sensitivity on the Ago1/TraX defective cells. This is easily tested in one of two ways. Firstly, SPAC22E12.02 could be over expressed in the *ago1Δ traXΔ* double mutant; if the hypothesis is correct, and SPAC22E12.02 expression is the cause of the phenotype, then this should confer TBZ sensitivity to the *ago1Δ traXΔ* double mutant. Secondly, deletion of SPAC22E12.02 in the triple mutant should revert the strain to a less sensitive state. These simple experiments remain to be done and so these hypotheses remain to be tested.

6.4. Conclusions.

1. TraX functions to repress *tlh* gene expression, but not other genes adjacent to *tlh* genes.

2. Translin deficient cells have no large scale statistically meaningful changes to gene expression.

3. *rif1* gene expression is greatly up regulated in an *ago1Δ* mutant.

4. Suppression of the *ago1Δ* TBZ sensitivity phenotype by loss of TraX is coincident with up regulation of *tlh2* expression and a relative down regulation of *rif1* expression (relative to the *ago1Δ* mutant).

5. Re-sensitisation of the *ago1Δ traXΔ* strain to TBZ by deletion of *tsn1* is associated with few transcriptional changes, but the up regulation of expression of a predicted RNA binding protein gene might point to a novel RNA binding function that is normally repressed by Tsn1.

CHAPTER 7

Preliminary analysis and preparation for future work on TRAX and Translin functions in human cell lines

7.1 Introduction

Several functions have been suggested for TRAX and Translin in different species including *S. pombe*, *Drosophila*, *Neurospora*, mice and humans (see Chapter 1), which might reflect differences in the interactions of Translin and TRAX with each other in these species or perhaps the evolution of different functions in different organisms. For instance, in mouse brain neurons, TRAX and Translin form a complex that is proposed to have a role in dendrite RNA processing (Finkenstadt et al., 2000). Many studies on humans have linked distinct neurological disorders with the *TRAX* gene, in support of a relationship between TRAX/Translin and mRNA processing in the human brain (Cannon et al., 2005; Hennah et al., 2005; Okuda et al., 2010; Palo et al., 2007; Schosser et al., 2009; Thomson et al., 2005). Recently, the TRAX-Translin complex (known as C3PO) has been reported to play an important role in enhancing the RNAi machinery in humans and *Drosophila*, where it serves as an endonuclease that activates the RNA-induced silencing complex (RISC) by removing the passenger strand of the siRNA duplex (Liu et al., 2009; Ye et al., 2011). Interestingly, *Saccharomyces cerevisiae* has neither a Translin nor a TRAX orthologue (Laufman et al., 2005) and it also lacks the RNAi machinery, which supports the proposed relationship between these proteins and RNAi (as reviewed by Jaendling and McFarlane, 2010). In *Neurospora*, the TRAX-Translin protein complex reportedly functions in tRNA possessing (Li et al., 2012). In *S. pombe* cells, *traX* and *tsn1* knockout has been reported to cause a slightly increased rate of cell proliferation (Laufman et al., 2005), although this phenotype has not been observed by our group (Jaendling et al, 2008).

The *Drosophila* model recently revealed an interesting discovery, wherein the Dcr-2 and R2D2 proteins recruited duplex siRNA (guide-passenger) to Ago2 to activate RISC formation. The process of RISC assembly consists of loading the duplex siRNA (guide-passenger) into Ago2, with subsequent dissociation of the RNA passenger strand from Ago2 through a process involving C3PO (Liu et al., 2009). However, humans have four AGO proteins (AGO1, AGO2, AGO3 and AGO4), but only AGO2 has the slicer activity necessary for *in vivo* RNAi-mediated gene silencing (Liu et al., 2004; Meister et al.,

2004). Reconstruction of the human RISC complex using C3PO and AGO2, in the absence and presence of DICER1, has demonstrated a crucial role of C3PO in activating the human RISC complex (Ye et al., 2011).

Our investigations of TraX and Translin functions in the *S. pombe* model revealed the interesting feature of Translin as suggested in Chapter 4, whereas Tsn1 provides a redundant function to Dcr1 and TraX suppresses a Translin–dependent, Ago1-independent pathway. The question therefore arises as to whether this same finding also holds up in human cells. The fundamental purpose of the work proposed in human cell lines is to investigate whether the same process that exists in *S. pombe* also operated in humans, as this is the ultimate goal of this line of research.

The key tools required for performing human experimental work are specific antibodies for performing western blot studies. Therefore, we have generated anti-human TRAX and anti-human Translin antibodies (out of house) and analysed them. In addition, we have also validated most of the commercially available human antibodies against TRAX, Translin, DICER1 and Ago2 proteins. One of the aims of this chapter is to perform an equivalent study to that of the *S. pombe* TBZ sensitivity experiment in human cell lines. We propose to use vinblastine, which is a microtubule destabilising agent that is active in human cells (Nakamura et al., 1993). We have successfully knocked down the *TRAX, Translin, DICER1* and *AGO2* genes in human cell lines, which is an important step for determining whether human cells depleted for AGO2 and TRAX are less sensitive to vinblastine than the AGO2 only depleted cells. Hence, future work will focus on single knockdown of *TRAX, Translin, DICER1* and *AGO2* and double knockdown *Translin DICER1, Translin AGO2, TRAX DICER1* and *TRAX AGO2* to investigate cell viability with and without the vinblastine agent. In other words, we are looking to parallel the work done in *S. pombe* but now in human cells.

Three human cell lines were chosen as models of human TRAX and Translin for future work (Figure 7.1). This chapter represents a preliminary step into the human work.

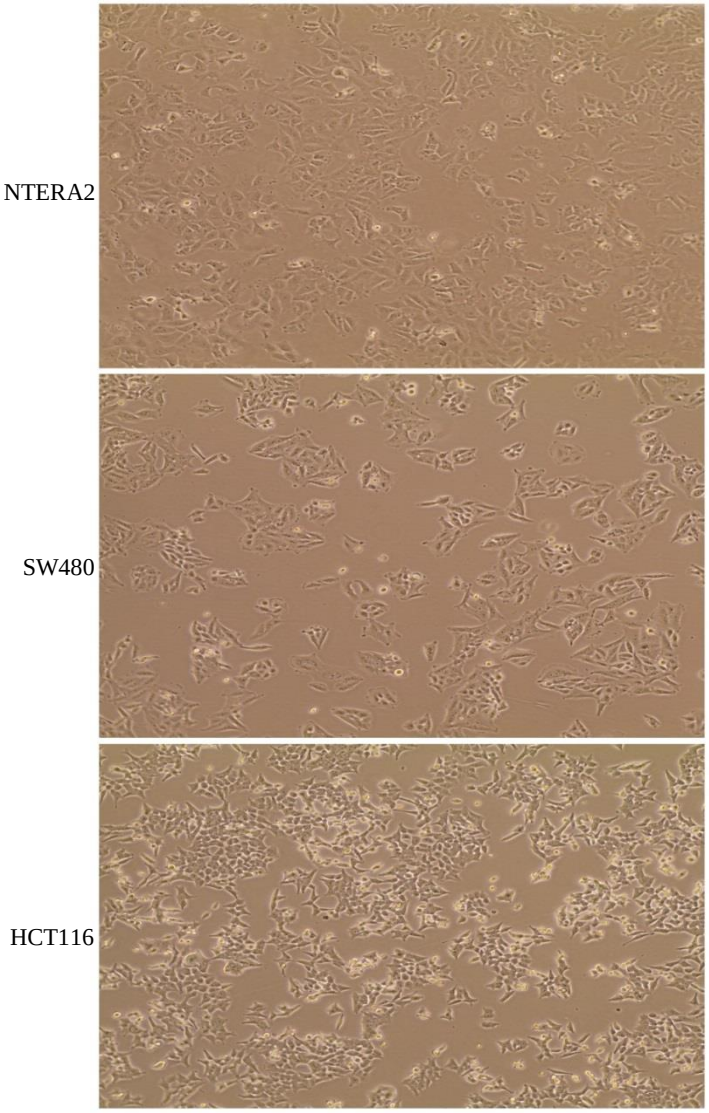

Figure 7.1 Three human cancer cell lines viewed with the light microscope

Human testicular germ cell tumour cancer (NTERA2), human colon adenocarcinoma cells (SW480) and human colon carcinoma cells (HCT116) at the sub-confluent stage viewed with a light microscope.

7.2 Results

7.2.1 cDNAs construction and RT-PCR for *TRAX, Translin, DICER1* and *AGO2* genes

We investigated whether all of the chosen cancer cell lines expressed *TRAX, Translin, DICER1* and *AGO2* genes by isolating total RNA from each cell line, as described previously (see Section 2.19) and constructing cDNAs for each (see Section 2.20). Primers for each cDNA were designed as shown in Table (7.1). Subsequently, RT-PCR was applied to identify gene expression in the selected cell lines (Figure 7.2). The RT-PCR products were purified by a Geneclean^{R} II kit before being sent for sequencing outside the lab (Eurofins MWG). All sequenced products matched the cDNA sent.

Table 7.1 RT-PCR screening primers

TRAX-H.S-F	5′-CCA TCG AGC CAT TAC TAC AG-3′	Forward primer inside Human *TRAX* cDNA
TRAX-H.S-R	5′-AGG TAA TCG ACA GGT GTG AC-3′	Reverse primer inside Human *TRAX* cDNA
TSN-H.S-F	5′-CTG TGA GCG AGA TCT TCG TG -3′	Forward primer inside Human *TSN* cDNA
TSN-H.S-R	5′-TGC TGC CAA GAA GAC CAA GC-3′	Reverse primer inside Human *TSN* cDNA
H.S DICER1-F	5′-CAC GAG TCA CAA TCA ACA CG-3′	Forward primer inside Human *DICER1* cDNA
H.S DICER1-R	5′-CAG GAG AGT ACA TTC ATC GC-3′	Reverse primer inside Human *DICER1* cDNA
H.S-AGO2-F	5′-AGC GTT TTA CAA GGC ACA GC-3′	Forward primer inside Human *AGO2* cDNA
H.S-AGO2-R	5′-AGG TAT GGC TTC CTT CAG C-3′	Reverse primer inside Human *AGO2* cDNA

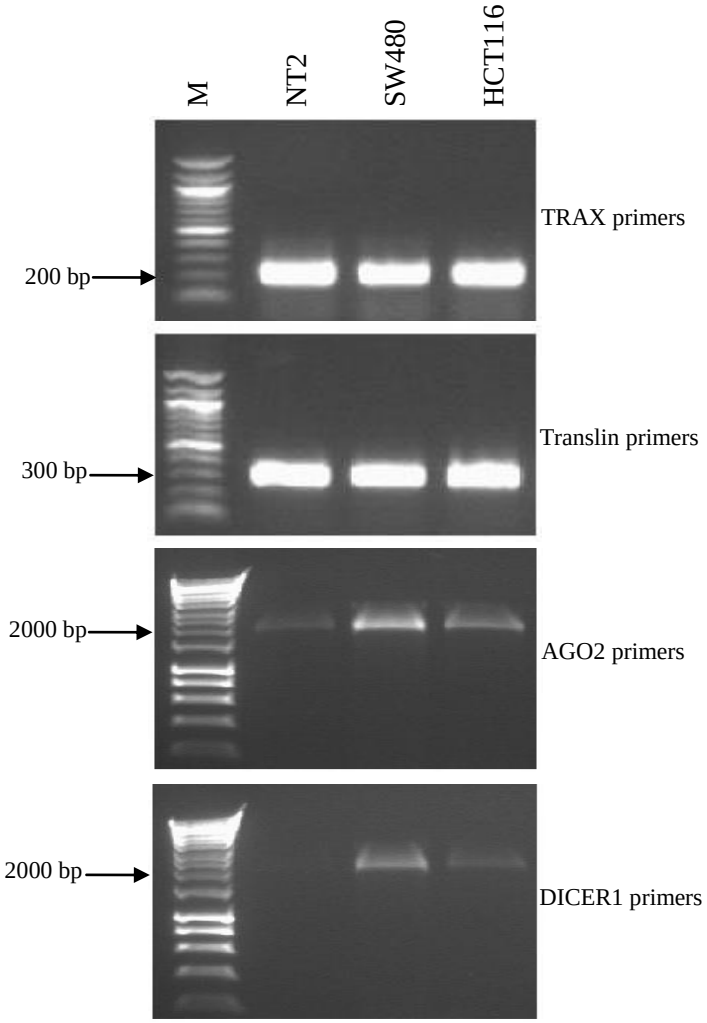

Screening primer sets	product predicted size
TRAX-H.S-F+TRAX-H.S-R	216 bp
TSN-H.S-F+TSN-H.S-R	240 bp
H.S DICER1-F+H.S DICER1-R	1847 bp
H.S-AGO2-F + H.S-AGO2-R	1724 bp

Figure 7.2 RT-PCR for human cDNAs of *TRAX*, *Translin*, *AGO2* and *DICER1* in three cancer cell lines

Agarose gels show the RT-PCR products for *TRAX*, *Translin*, *AGO2* and *DICER1* cDNAs in all three cell lines. *DICER1* expression was not evident in the NTERA2 cell line.

7.2.2 Generation of TRAX and Translin antibodies

Polyclonal anti-human TRAX and anti-human Translin antibodies were generated (out of house by the Eurogente). The anti-TRAX polyclonal antibody was raised in guinea pigs through inoculation with the synthetic peptides FSUKTEMIDQEEGI (TRAX-1) and RKHDNFPHNQRRE (TRAX-2) (Figure 7.3). The anti-Translin antibody was raised in rabbits through inoculation with the synthetic peptides CDSLRKRYDGLKYD (Translin-1) (Figure 7.4) and CKTKFPAEQYYRFHE (Translin-2). Western blots results showed multi cross-reactivity for TRAX-1 for all three selected cell lines. Translin-1 antibody showed specificity for Translin-1 at approximately 26 kDa, with multi cross reactivity for all three cell lines. However, TRAX-2 and Translin-2 give no bands at all.

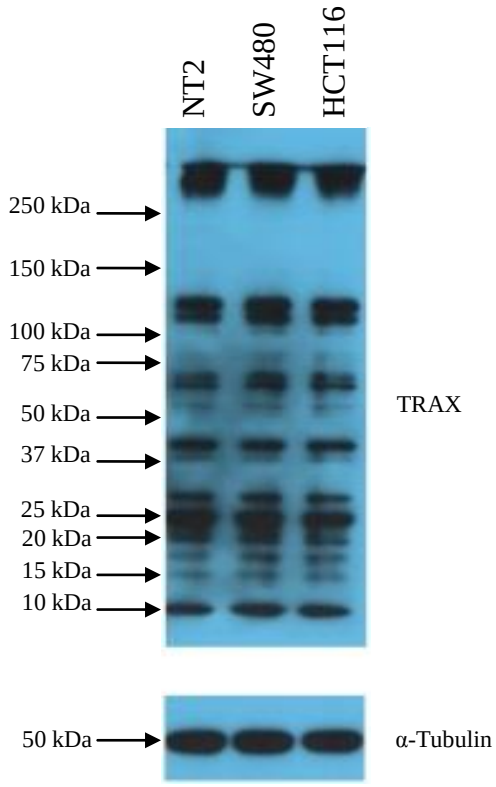

Figure 7.3 Western blots using anti-human TRAX-1 antibody in three cell lines

The molecular mass of human TRAX is predicted to be 33 kDa. Western blots show no specificity for TRAX-1 antibody, with multi cross reactivity occurring for all three cell lines tested. Anti- α-Tubulin (50 kDa) was used as a loading control.

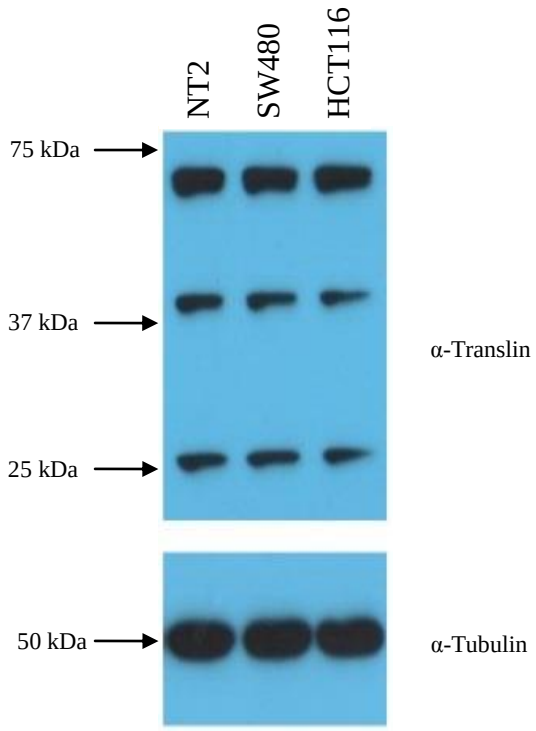

Figure 7.4 Western blots using anti-human Translin-1 antibody in three cell lines.

The molecular mass of human Translin is predicted to be 26 kDa. Western blots show bands for Translin-1 antibody at approximately 26 kDa, with multi cross reactivity for all three cell lines tested. Anti- α-Tubulin (50 kDa) was used as a loading control.

7.2.3 Commercial antibodies against human TRAX, Translin, DICER1 and AGO2.

Most of the commercial antibodies against human TRAX, Translin, DICER1 and AGO2 proteins were titrated and validated. The best specific primary antibodies for the four proteins of interest are as shown in Table 7.2 using the secondary antibody shown in Table 7.3. Western blotting was performed as described previously (see Section 2.24).

Table 7.2 Primary antibodies

Antibody	Clonality	Host	Company	Cat. No	WB dilution
Anti-TRAX	Monoclonal	Mouse	Abcam	Ab58642	1:200
Anti-Translin	Polyclonal	Rabbit	Abcam	Ab71775	1:500
Anti-DICER1	Monoclonal	Mouse	Millipore	04-721	1:10,000
Anti-DICER1	Polyclonal	Rabbit	Novus Biologicals	NBP1-06520	1:2000
Anti-AGO2	Monoclonal	Mouse	Millipore	04-642	1:2000
Anti-AGO2	Monoclonal	Rabbit	Cell Signaling	C34C6	1:1000
Anti-Tubulin	Monoclonal	Mouse	Sigma	T6074	1:5000

Table 7.3 Secondary antibodies

Antibody	Stock concentration	Company	Cat. No	WB dilution
Donkey anti-mouse	0.8 mg/ml	Jackson Immunoresearch	715-035-150	1:25,000
Donkey anti-rabbit	0.8 mg/ml	Jackson Immunoresearch	711-005-152	1:25,000

Abbreviations for Tables 7.2 and 7.3 WB: western blot.

7.2.4 Gene knockdown by RNAi assay for *TRAX*, *Translin*, *AGO2* and *DICER1* in human cell lines

All siRNAs used for gene knockdown were obtained from Qiagen (Table 7.4). The protocol for gene knockdown was described previously (see Section 2.23). Cells were seeded as required in 6-well plates containing 2 ml of media. Three hits of siRNA were applied before the cells were harvested. Western blots were used to detect gene knockdown and also to confirm the antibody specificity. Four siRNAs were tested for each gene and the best knockdown was selected, as shown in Table 7.4. Western blotting confirmed the knockdown of the four genes, as shown in Figure 7.3.

Table 7.4 siRNAs

Gene symbol	siRNA name	Cat#	siRNA type	Stock conc.
TRAX	Hs_TSNAX_6	SI04201883	Predesigned	10 µM
Translin	Hs_TSN_5	SI04347497	Predesigned	10 µM
DICER1	Hs_DICER1_11	SI02655492	Predesigned	10 µM
AGO2	Hs_EIF2C2_5	SI03065461	Predesigned	10 µM

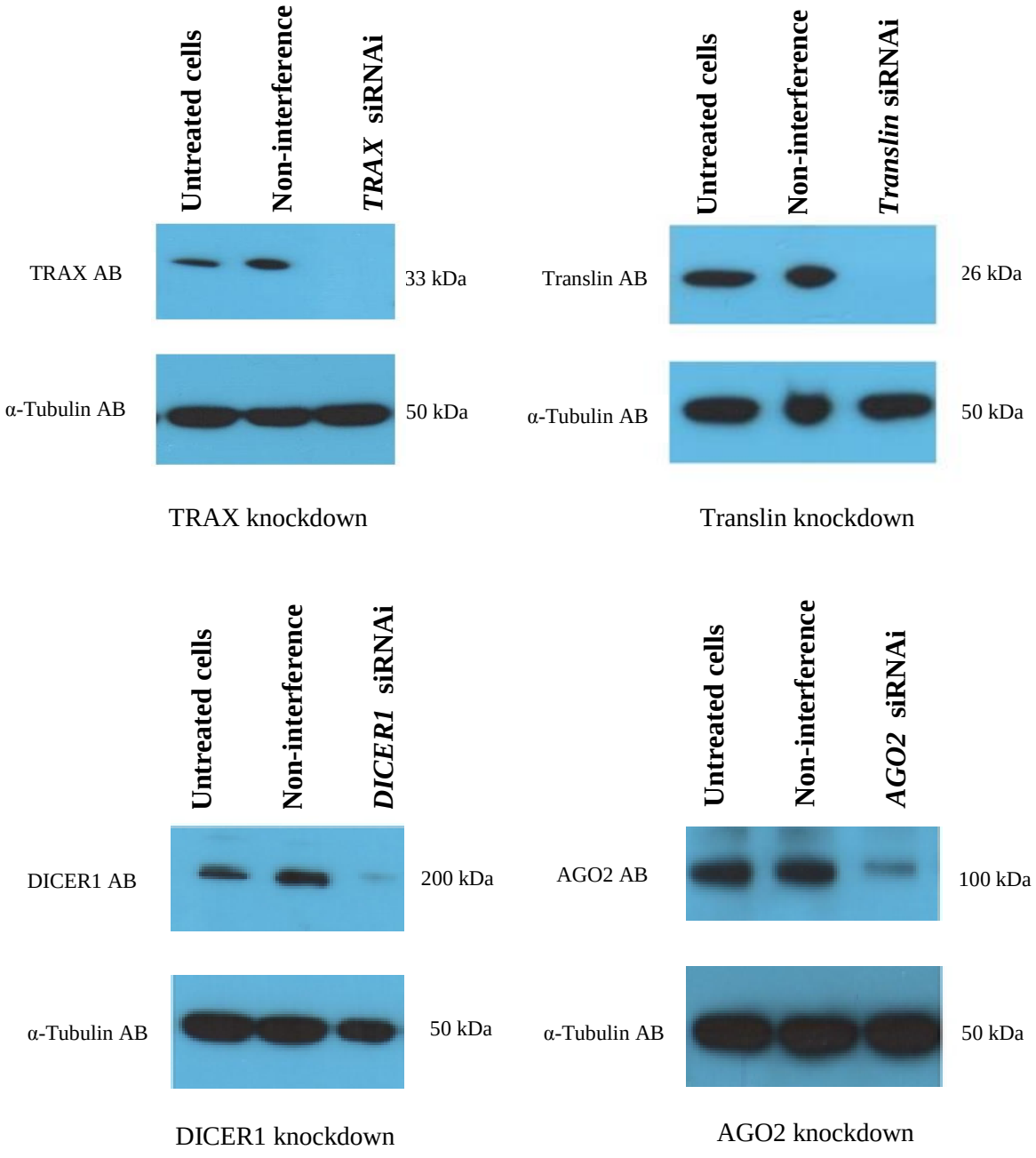

Figure 7.5 Western blot analyses of knockdown of *TRAX*, *Translin*, *DICER1* and *AGO2* genes.

Knockdown of the *TRAX*, *Translin*, *DICER1* and *AGO2* genes in the SW480 cell line was achieved using siRNAi assays α-Tubulin was used as a loading control to confirm the protein amount loaded in each well.

7.3 Discussion and future work

The RT-PCR results confirmed that the SW480 cell line expresses the *TRAX, Translin, DICER1* and *AGO2* genes. In addition, the doubling time for this cell line is approximately every 38 hours, which allows sufficient time for siRNA to knock down the desired genes. On the other hand, the RT-PCR results show that *DICER1* expression was not measurable in NTERA2 cell line when compared to other cell lines tested. The HCT116 cell line has all four genes expressed but its doubling time is rapid (every 16 hours). Therefore, we suggest that SW480 is a good human cell line for future use as a model for studying TRAX and Translin with RNAi factors DICER1 and AGO2.

TRAX and Translin Antibodies were generated out of house by the Eurogentec Company. However, these antibodies appear to give multi-cross reactivity. Therefore, we have validated all of the commercially available antibodies against TRAX and Translin in addition to DICER1 and AGO2 antibodies and we provide recommendations for the best antibodies with best dilutions for use in future work, as presented in Table 7.2.

All genes were successfully knocked down by siRNAi assays, including *TRAX, Translin, DICER1* and *AGO2* genes. All successful siRNAis for knockdown are mentioned, together with their catalogue numbers, in Table 7.4. Therefore, we recommend using these siRNAis to perform future single knockdowns (*TRAX*, *Translin*, *DICER1* and *AGO2*) and double knockdowns (*Translin DICER1, Translin AGO2, TRAX DICER1* and *TRAX AGO2*) to investigate cell viability with and without the vinblastine agent, i.e. the parallel experiments to those performed in *S. pombe* works to investigate whether the same observation will be made in human cells as we noticed in *S. pombe*.

CHAPTER 8

Final Discussion

8.1 Introduction

Human Translin was first isolated as a protein that had the ability to bind to specific DNA sequences associated with the breakpoint junctions of leukaemia chromosomal translocations (Aoki et al., 1995). It was independently identified in the mouse as an RNA binding protein that was proposed to be specific to the testis and the brain, although this was later found to be enrichment in these tissues (Han et al., 1995c; Wu et al., 1997). These distinct routes for Translin identification in mammals set the scene for over a decade of studies that set out to elucidate the underlying biochemical and biological function of Translin and the partner protein TRAX (reviewed in Jaendling and McFarlane, 2010). These resulted in these two proteins being implicated in a diverse range of biological processes from neuronal mRNA transport through to DNA damage recovery and recombination mechanisms (reviewed in Jaendling and McFarlane, 2010). At the centre of these findings was the ability of Translin to bind to both RNA and DNA, although the biological substrates remain largely elusive. Additionally, it was demonstrated in both mammals and yeast that the stability of TRAX was largely dependent upon Translin and that depletion of Translin resulted in a large reduction in the levels of TRAX; the conservation of this biochemical characteristic from unicellular yeast through to mammals was suggestive of the conservation of a fundamentally important biological role. However, the importance of this function remained unclear and the finding that loss of Translin function in mouse, fly and fission yeast appeared to result in little, if any, measurable phenotypic change seemed to indicate a specialist function or a function that had in fact become redundant.

It was not until just prior to the onset of this current study that a major breakthrough was made into elucidating the underlying function of Translin and TRAX. Liu and co-workers (2009) purified a biochemical activity that was capable of stimulating the activity of the RNAi machinery of *Drosophila in vitro*; they termed this complex C3PO and found that Translin and TRAX were the only constituent proteins. This indicated that Translin and TRAX functioned as enhancers of the RNAi pathways and this was extended to demonstrate this was true in mammals too (Liu et al., 2009). The role played by C3PO was to assist in the removal of the passenger strand of duplex siRNAs presented to

Argonaute complexes enabling Argonaute to have a guide strand RNA free of a passage strand, thus enabling it to associate with target mRNAs (Liu et al., 2009). The link to RNAi addressed the outstanding question of why the budding yeast did not possess orthologues of Translin and/or TRAX, as the budding yeast does not possess an RNAi pathway.

During the course of this current study a further key finding was revealed by work predominantly in *Neurospora crassa*, but supported in mammals. Li and co-workers (2012) found that *N. crassa* and mammalian C3PO played a role in processing a specific group of RNA molecules, largely tRNA precursors. They did not find a measurable role for C3PO in *N. crassa* RNAi regulation. This led them to postulate that the many different functions attributed to Translin and TRAX in different organisms arose due to a fundamental failure to process immature tRNAs resulting in a broad spectrum of defects.

So, at the onset of this study or during the course of this study two key functions for Translin and TRAX were unveiled pointing to a function in general and important RNA processing pathways. However, loss of these pathways had at best limited negative influence on organisms ranging from mouse through to the fission yeast (reviewed in Jaendling and McFarlane, 2010). The only plausible explanation for this was that these pathways were relatively minor or that they were redundant with other more essential pathways. Indeed, it might be that Translin and TRAX function in very specific, condition-dependent pathways, or even tissue specific pathways. In complex eukaryotes there is evidence that Translin functions in a tissue-specific fashion to drive a DNA damage recovery pathway specifically in hematopoietic stem cells in the bone marrow (Fukuda et al., 2008). Moreover, in humans, failures in a specific intra neuronal trafficking of BDNF mRNA mediated by Translin has been associated with autism spectrum disorders (Chiaruttini et al., 2009), indicating a highly specific mRNA processing function has evolved in at least some cells/tissues.

Despite this new finding, some key questions remained, not least of which was why cells defective in Translin and or TRAX exhibit relatively few or no negative phenotypic changes. To address this the study reported here set out to take these new findings and use a fundamental experimental model system, the fission yeast, to elucidate the basic functional role of TRAX, and to some degree Translin (this study accompanied a parallel sister study with a greater focus on Translin). The study set out with the core hypothesis

that TRAX, and /or Translin played a role associated with the RNAi regulatory pathways in fission yeast. Moreover, whilst this study focussed on TRAX and a parallel study focussed mostly on Translin, it was hypothesised that their functions were intimately associated as the stability of fission yeast TRAX is largely dependent upon Translin (Jaendling et al., 2008). Surprisingly, distinct functional roles for Translin and TRAX in *S. pombe* have been revealed; the phenotypes of the *tsn1*Δ mutants revealed are not comparable to the phenotypes of the *traX*Δ mutants indicating that whilst TraX is largely depleted in the *tsn1*Δ cells, the residual TraX must play a functional role. Thus, this work not only goes a good way to pointing to a new functional role for TraX, at least in *S. pombe*, it also serves to partly uncouple the functions of these two associated and conserved proteins.

8.2 Tsn1 and TraX do not play a primary role in RNAi-mediated heterochromatin control or RNA regulation

Previous studies from the McFarlane group had indicated that there was no readily apparent defect in the phenotype of *traX*Δ or *tsn1*Δ null mutants (Jaendling et al., 2008); although others had reported mild growth defects (Laufman et al., 2005). Indeed, the previous work from the McFarlane group had indicated that there was no sensitivity to the microtubule destabilizing drug TBZ and this work was full supported here following a more detailed study of this phenotype. Mutants that are defective in RNAi regulation in fission yeast are often defective in centromeric heterochromatin maintenance and exhibits sever sensitivity to TBZ (as illustrated within this study). The fact that the *tsn1*Δ and *traX*Δ single mutants exhibit no measureable TBZ sensitivity indicates that if they are involved in RNAi regulation, it is not to the same degree as key regulators in this pathway, such as Ago1. Indeed, from the work described here it should be argued that there is no evidence for any primary role in RNAi for either gene.

The more detailed study of the single mutants carried out here did not reveal any evidence for a primary function in any pathway. Additionally, the microarray analysis of the *tsn1*Δ mutant supports the notion that *tsn1* does not play a major primary role in processing of any major species of RNA. Comparison for the array profile for wild-type cells relative the *tsn1*Δ profile revealed no significant changes at the lg2FC level which is the widely accepted threshold for meaningful change.

However, the analysis of the transcriptional data for the *traX*Δ mutant in comparison with the isogenic wild-type profile indicated that there was a significant change in the expression of the RecQ-like helicase genes, *tlh1* and *tlh2*, which are located sub telomerically on one arm of chromosomes I and II (Mandell et al., 2004; Mandell et al., 2005). This is intriguing, as the function of these two RecQ-like helicase genes remains unknown. In the *traX*Δ mutant both are significantly up regulated and both are thought to be largely transcriptionally silent under normal laboratory growth conditions. This up regulation does not appear to reflect a general de-regulation of transcriptional silencing in the subtelomeric regions as these genes are the only genes to be elevated in their expression in the *traX*Δ cells. So, whilst the array analysis does not support a general role for RNA (including tRNA) regulation in the *tsn1*Δ or *traX*Δ mutants, TraX does appear to function to specifically repress the levels of *tlh1* and *tlh2* mRNA within the cell. The functional significance of this is discussed below, however, it is clear that expression of *tlh1* and *tlh2* in the *traX*Δ single mutant does not result in any measurable phenotype indicating that elevated levels of *tlh1/2* mRNA does not confer measurable dysfunction on the cells (it remains unknown whether these mRNAs are translated to produce protein).

One key point to be made from the above point is that this is the first observation to separate the function of TraX and Tsn1. Indeed, it could also provide evidence to indicate that the low levels of TraX which are retained in the *tsn1*Δ cells is functional as the *tsn1*Δ mutant does not exhibit the same up regulation of *tlh1/2* as observed in the *traX*Δ null mutant. This re-opens the question of why Tsn1 is required to regulate TraX, a question that remains unaddressed by this current study.

8.3Translin functions in an auxiliary pathway to Dicer

Having found no measurable phenotype for *traX*Δ and *tsn1*Δ single mutants we hypothesised that Tsn1 and TraX may function in an auxiliary pathway to the RNAi pathway. Previously it has been demonstrated that the TraX component of the C3PO complex has RNAse activity (Liu et al., 2009); moreover, a Dcr1-independent, Ago1-dependent part of the central RNAi pathway has been postulated for RNAi-mediated centromeric heterochromatin regulation in *S. pombe* (Halic and Moazed, 2010). From this we set out to make double mutants of *tsn1*Δ and *traX*Δ with mutants in the RNAi pathway, either *ago1*Δ or *dcr1*Δ.

The main hypotheses set out within this study were aimed at elucidating the function of TraX. The study of Translin in *S. pombe* was largely carried out by a colleague. The finding that revealed a disconnection of function of TraX and Tsn1 has to some degree justified this approach. However, during the course of this study it was essential to evaluate the function of Translin too, if only to serve as a confirmation of results obtained by the parallel study.

Two striking observations were made by this work. Firstly, the *dcr1*Δ single mutant does not exhibit the same degree of TBZ sensitivity or mini chromosome instability as the *ago1*Δ mutant. This supports the model that in the central RNAi pathway the function provided by Dcr1 is partly redundant with another factor (Halic and Moazed, 2010). The second observation is that the *dcr1*Δ *tsn1*Δ double mutant is more TBZ sensitive than the *dcr1*Δ single mutant alone and that the double mutant exhibits greater mini chromosome instability. These observations indicate that Tsn1 might provide the Dcr1-independent function alluded to by Halic and Moazed (2010). This is illustrated in the model shown in Figure 8.1 (adapted from Al-Shehri). This observation is all the more striking as the *dcr1*Δ *traX*Δ double mutant does not appear to show such a clear added sensitivity, further supporting a model indicating a disconnection of the TraX and Tsn1 function in fission yeast.

The micro array data for the *dcr1*Δ *tsn1*Δ and other mutant comparison were not made as part of this study and the late time at which the array data were obtained precluded any in depth comparison to be presented in this thesis. These analyses will be done in due course. However, it is clear from these genetic analyses that the requirement for Tsn1 is only apparent when Dcr1 function is lost, as the Dcr1 competent *tsn1*Δ mutants do not exhibit any phenotype to indicate an RNAi defect.

8.4 Loss of TraX activates a repressor of Ago1 deficiency

As discussed, the loss of TraX has no observable influence on the cellular activity of fission yeast cells (Jaendling et al., 2008). However, the array analysis indicates that the *tlh1/2* gene become transnscriptionally active in the *traX*Δ background and this appears to be a gene-specific activation and it is not as evident in a *tsn1*Δ mutant. Despite this, no phenotype is associated with *tlh1/2* activation, certainly not in the absence of TraX. Moreover, the loss of *traX* in the *dcr1*Δ background does not appear to have the same

increase in genome instability as the *tsn1*Δ *dcr1*Δ mutant. These observations become all the more remarkable when considering the suppression of the *ago1*Δ genome instability phenotype by the loss of *traX* function, which is quite a marked phenotype, as exemplified by the almost full suppression of the *ago1*Δ TBZ sensitivity phenotype.

Added to this, the triple mutant, *ago1*Δ *traX*Δ *tsn1*Δ reverts to TBZ sensitivity similar to the *ago1*Δ single mutant. The most appealing means of explaining this is to postulate that upon loss of TraX, Tsn1 was released to provide function that could substitute for that of Ago1. This would fit with a mechanism in which loss of TraX enabled Tsn1 not only to serve as an alternative for Dcr1, but also for an alternative for the central core of the RNAi pathway which normally requires Ago1. However, the microarray data seem to raise other very different and more complex possibilities.

Whilst there are few changes, two notable observations come to light from the microarray data when comparing the *ago1*Δ single mutant and the *ago1*Δ *traX*Δ double mutant (which has enhanced genome stability). Firstly, there is the activation of the *tlh2* gene, as seen in the *traX*Δ single mutant. Secondly, there is a reduction in the expression of *rif1*, a gene that is required to regulate the proper timing of DNA replication origins (Hayano et al., 2012) and which also has a minor role in telomere regulation in *S. pombe* (Miller et al., 2005). These two observations could be of great importance in understanding the role of RNAi pathways in *S. pombe*. Firstly, it might be the case that the RecQ-like Tlh helicase activity (if it is proven to have helicase activity) could suppress the instability of the Ago1-deficiency. If this is the case, then this suggests a link between Ago1 loss and a dysfunction in a helicase activity. The RecQ family member helicase in *S. pombe*, Rqh1, is required for maintaining genome stability (Win et al., 2005) and so loss of Ago1-could potentially have a negative influence on the activity of Rqh1, either directly or indirectly. To test the importance of the expression of *tlh2* in the suppression of the *ago1*Δ genome instability the *tlh2* gene could be over expressed in the *ago1*Δ background. If *tlh2* expression is the factor driving the enhanced chromosome stability in the *ago1*Δ *traX*Δ double mutant, *tlh2* expression should mimic the observations made when *traX* is deleted in the *ago1*Δ background. This should be considered a trivial experiment, but a previous Attempt to clone full length *tlh2* for functional analysis failed as the gene sequence results in clone instability within *E. coli* cells (Mandell et al., 2005). However, a second attempt to clone *tlh2* should be made given the potential importance of this observation.

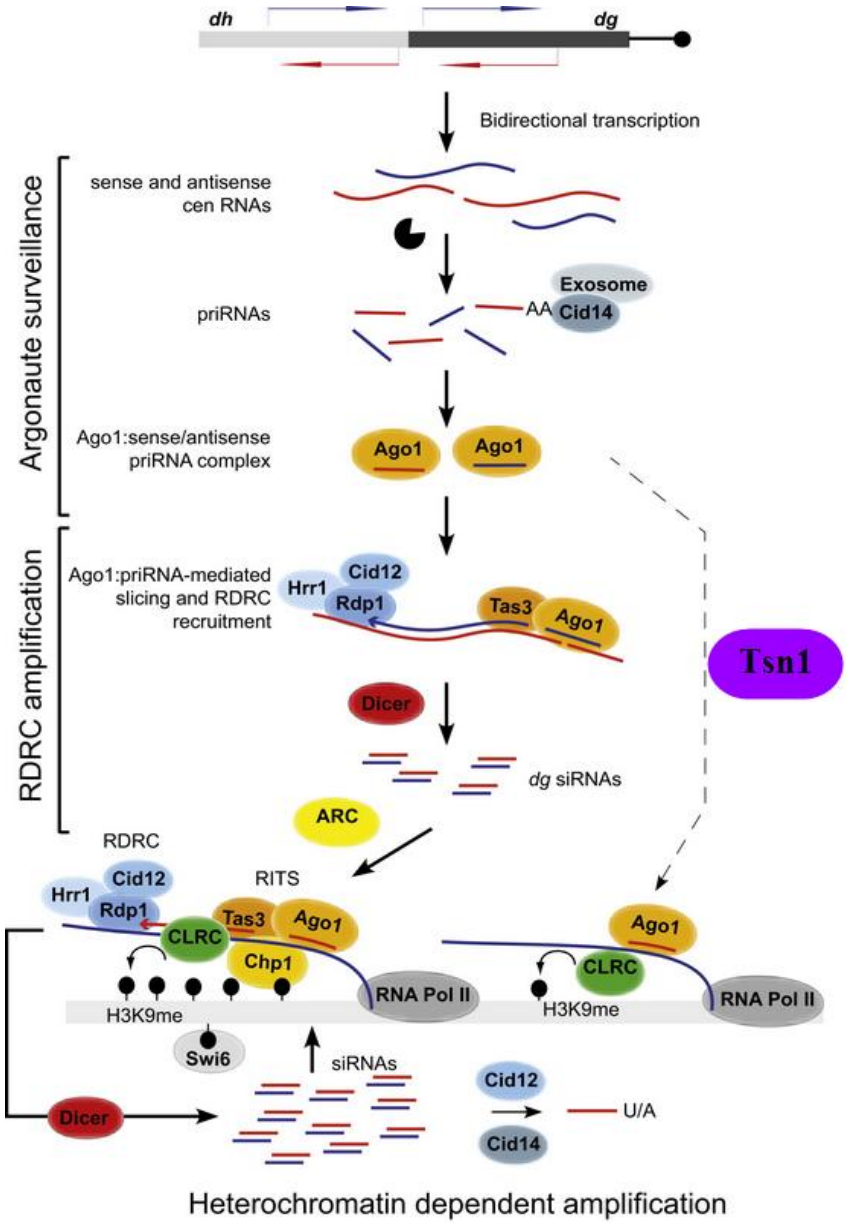

Figure 8.1 Model for proposed role of Tsn1 in the absence of Dcr1.

Halic and Moazed (2010) proposed a model in which the requirement for Dicer in the core RNAi pathway for centromeric heterochromatin formation could be partially bypassed. They suggested a secondary function that could make the need for Dicer redundant (dashed line). The analysis of the *dcr1*Δ *tsn1*Δ suggests that this other pathway could be Tsn1-dependent.

The second factor might be the reduced level of *rif1* expression in the *ago1*Δ *traX*Δ relative to the *ago1*Δ single mutant. As noted in Chapter 6, *rif1* gene expression becomes greatly elevated in *ago1*Δ single mutant and this elevation is reduced when *traX* is mutated, but does not fall back down to wild-type levels as a comparison of *rif1* expression in the *ago1*Δ *traX*Δ double mutant compared to the wild-type reveals an elevation in *rif1* expression, but not to the same level as in the *ago1*Δ single mutant. The primary role of Rif1 protein seems to be linked to regulation of replication origin firing (Hayano et al., 2012). Elevation of *rif1* expression could conceivably alter replication origin kinetics. Partial suppression of the elevated *rif1* expression by loss of TraX might alleviate this disruption of origin firing and restore a replication programme more in line with proper chromosome stability. Alternatively, the elevated Rif1 protein might drive telomeric instability and this is suppressed when *traX* mutation reduced *rif1* expression. Which of these possibilities is correct, if either, will need further investigation. How TraX might function to regulate *rif1* expression is unclear and it seems to only apply to the *ago1*Δ mutant when *rif1* is over expressed as no change to *rif1* expression is observed in the *traX*Δ single mutant. The possibility that *rif1* expression reduction drives the suppression of the *ago1*Δ genome instability phenotype needs to be tested. The simplest way to do this would be to mutate *rif1* in an *ago1*Δ background; if the *ago1*Δ *rif1*Δ rescued the sensitivity to TBZ of the *ago1*Δ single mutant, then it could be concluded that *rif1* levels play a role in the chromosomal instability of the *ago1*Δ.

There are other changes seen when comparing the transcriptional profiles of *ago1*Δ with the *ago1*Δ *traX*Δ strains. For example, the change to a ncRNA (see Chapter 6); however, it is not so easy to develop a model as to why this is important and it is simpler to test the *rif1* and *tlh2* models first. It might be that all the changes observed contribute to some degree and that all are linked to an inherent regulator role for TraX which is triggered when Ago1 becomes dysfunctional. In theory this might be an important developmental or conditional response; that is, Ago1 function might become inactivated under certain conditions and TraX becomes deactivated too, thus triggering the auxiliary pathway. If this is the case, then to date there is no evidence to point to a specific set of conditions or developmental programme when such a scenario might occur.

Lastly, the suppression of the genome instability of the *ago1*Δ mutant by mutation of *traX* is reversed by mutation of *tsn1*. Initially it was thought that this indicated that Tsn1, in the

absence of TraX, could serve to bypass the need for Ago1 and this might be the case. However, the transcription microarray data reveal a tantalising observation. When comparing the *ago1*Δ *traX*Δ double mutant (suppressed TBZ sensitivity) with the *ago1*Δ *traX*Δ *tsn1*Δ triple mutant (full TBZ sensitivity) a new gene becomes activated, *SPAC22E12.01*. This gene encodes a predicted RNA binding protein of unknown function. This opens up the possibility that this gene encodes a protein that can substitute for TraX function and restore the genome instability to the levels seen in the *ago1*Δ single mutant. This hypothesis can be readily tested in two ways. Firstly the *SPAC22E12.01* gene could be deleted in the triple mutant back ground; if this additional deletion now re-suppressed the TBZ sensitivity of the triple mutant then this would suggest that the RNA binding protein could indeed be substituting for TraX function. Secondly, the *SPAC22E12.01* gene could be over expressed in the *ago1*Δ *traX*Δ double mutant; if this resulted in restoration of the TBZ sensitivity, then this would suggest it was the activation of this gene which was compensating for the loss of TraX. How Tsn1 might regulate *SPAC22E12.01* expression is not clear, but it is suggestive of a complex regulatory network aimed at controlling genome stability when Ago1 becomes deactivated. As discussed above, it is unclear whether such an event is part of the normal life cycle of fission yeast when subjected to specific, unknown conditions.

8.5 Uncoupling Ago1 genome instability from centromeric heterochromatin

One of the dramatic findings to come from this work is that observation discussed above, that loss of TraX can suppress the genome instability of the *ago1*Δ mutant. It is widely accepted that the genome instability of the *ago1*Δ mutant is caused by a dysfunction in the centromeric heterochromatin rendering the centromeres partially compromised (not fully as cell division can still occur in the absence of Ago1). However, the work described here makes an important observation as the *ago1*Δ *traX*Δ double mutant has a partially restored genome stability relative to the *ago1*Δ mutant and yet the centromeric heterochromatin remains deregulated and transcriptionally active to the same degree as seen in the *ago1*Δ single mutant (as measured by gene silencing assays and the fact that comparisons of microarray data between *ago1*Δ and *ago1*Δ *traX*Δ does not indicate extensive re-silencing of the centromeric repeat regions that are under the regulation of heterochromatic structures). This is a remarkable observation as it uncouples the centromeric heterochromatin defect of the *ago1*Δ mutant from the genome instability

phenotype. So, whilst defective heterochromatin might play some role in contributing to chromosomal instability, it is certainly not the full cause (and might not be the main cause). It points to another defect in Ago1-deficient cells being the cause of some or all of the genome instability. What that other defect might be remains unknown, but studying the role of *rif1* levels and loss of a function that can be suppressed by the RecQ-like potential helicase Tlh2 seems an appropriate place to start to look.

8.6 Closing remarks

Translin and TraX have provided a puzzle over the last 15 years and only recently has insight into their core biological function become apparent with the finding of a link to RNA processing of both tRNAs and small RNAs in the RNAi pathway (Li et al., 2012; Liu et al., 2009). They have been implicated in a wide range of functions and the suggestion has been put forward that they have evolved distinct tissue and species specific functions based on core biochemical activities associated with nucleic acid metabolism. In this study the fission yeast has yielded new insight into these two closely related proteins. Not only has new insight to their function been gained, but the study alludes to a new activity for the central RNAi regulator Ago1. Moreover, the widely accepted close functional relationship between Translin and TraX is cast into doubt as there is clear evidence for distinct roles in the fission yeast.

This work demonstrated that there is an auxiliary pathway that appears to serve as a backup to core Ago1-dependent RNAi pathway. Evidence has been presented to suggest that this might link Ago1 function to chromosome stability through the regulation of Rif1 levels or the control of some replicative or recombinogenic process which can be substituted for by the tlh2 RecQ-like helicase. This finding needs further exploration to reveal the new function of Ago1 now that genome stability regulation has been uncoupled from centromeric heterochromatin.

These findings from fission yeast point to an important and previously uncharacterised function for Translin and TraX. The biological relevance of this pathway remains unclear, as the single *traX*Δ and *tsn1*Δ mutants exhibit no defect in mitotic growth under normal laboratory conditions. A major proposal to come from this study is that there is a set of conditions in which the Ago1-mediated RNAi pathways becomes partially compromised and that TraX regulates a secondary ‘backup’ pathway (possibly via *tlh1/2* or *rif1* control)

to enable the cell to cope with these conditions. If such conditions exist, for example some form of stress, then further studies will be needed to elucidate what they may be. Lastly, how this work correlates to the functional role of TRAX and Translin in human cells and how this might be altered in a tissue-specific manner remains to be explored. Within this work programme the foundations to addressing these questions have been laid. Moreover, the fundamental question of what links TRAX and Translin to chromosomal translocations in cancers and how this relates to RNA metabolism remains unclear from this work and is an important open question for the future.

References

Abeysinghe, S. S., Chuzhanova, N., Krawczak, M., Ball, E. V., and Cooper, D. N. (2003). Translocation and gross deletion breakpoints in human inherited disease and cancer I: Nucleotide composition and recombination-associated motifs. Human mutation *22*, 229-244.

Agarwal, S., Tafel, A., and Kanaar, R. (2006). DNA double-strand break repair and chromosome translocations. DNA repair *5*, 1075-1081.

Aharoni, A., Baran, N., and Manor, H. (1993). Characterization of a multisubunit human protein which selectively binds single stranded d (GA) nand d (GT) nsequence repeats in DNA. Nucleic acids research *21*, 5221-5228.

Allshire, R. (2001). Dissecting fission yeast centromeres via silencing.

Allshire, R. C., Javerzat, J. P., Redhead, N. J., and Cranston, G. (1994). Position effect variegation at fission yeast centromeres. Cell *76*, 157-169.

Allshire, R. C., Nimmo, E. R., Ekwall, K., Javerzat, J.-P., and Cranston, G. (1995). Mutations derepressing silent centromeric domains in fission yeast disrupt chromosome segregation. Genes & Development *9*, 218-233.

Aoki, K., Inazawa, J., Takahashi, T., Nakahara, K., and Kasai, M. (1997a). Genomic structure and chromosomal localization of the gene encoding translin, a recombination hotspot binding protein. Genomics *43*, 237-241.

Aoki, K., Ishida, R., and Kasai, M. (1997b). Isolation and characterization of a cDNA encoding a Translin-like protein, TRAX. FEBS letters *401*, 109-112.

Aoki, K., Suzuki, K., Sugano, T., Tasaka, T., Nakahara, K., Kuge, O., Omori, A., and Kasai, M. (1995). A novel gene, Translin, encodes a recombination hotspot binding protein associated with chromosomal translocations. Nature genetics *10*, 167-174.

Atlas, M., Head, D., Behm, F., Schmidt, E., Zeleznik-Le, N., Roe, B., Burian, D., and Domer, P. (1998). Cloning and sequence analysis of four t (9; 11) therapy-related leukemia breakpoints. Leukemia *12*, 1895-1902.

Badge, R. M., Yardley, J., Jeffreys, A. J., and Armour, J. A. L. (2000). Crossover breakpoint mapping identifies a subtelomeric hotspot for male meiotic recombination. Human molecular genetics *9*, 1239-1244.

Bah, A., and Azzalin, C. M. (2012). The telomeric transcriptome: From fission yeast to mammals. The international journal of biochemistry & cell biology.

Bähler, J., Wu, J., Longtine, M., Shah, N., McKenzie, A., Steever, A., Wach, A., Philippsen, P., and Pringle, J. (1998). Heterologous modules for efficient and versatile PCR-based gene targeting in Schizosaccharomyces pombe. Yeast Chichester England *14*, 943-951.

Bandyopadhyay, R., Heller, A., Knox-DuBois, C., McCaskill, C., Berend, S., Page, S., and Shaffer, L. (2002). Parental origin and timing of de novo Robertsonian translocation formation. The American Journal of Human Genetics *71*, 1456-1462.

Bath, K. G., and Lee, F. S. (2006). Variant BDNF (Val66Met) impact on brain structure and function. Cognitive, Affective, & Behavioral Neuroscience *6*, 79-85.

Bayne, E. H., White, S. A., Kagansky, A., Bijos, D. A., Sanchez-Pulido, L., Hoe, K.-L., Kim, D.-U., Park, H.-O., Ponting, C. P., and Rappsilber, J. (2010). Stc1: a critical link between RNAi and chromatin modification required for heterochromatin integrity. Cell *140*, 666-677.

Beuf, K. D., Pipelers, P., Andriankaja, M., Thas, O., Inzé, D., Crainiceanu, C., and Clement, L. (2012). Analysis of tiling array expression studies with flexible designs in Bioconductor (waveTiling). BMC bioinformatics *13*, 234.

Birchler, J. A., Pal Bhadra, M., and Bhadra, U. (2000). Making noise about silence: repression of repeated genes in animals. Current Opinion in Genetics & Development *10*, 211-216.

Blagosklonny, M. V. (2011). Cell cycle arrest is not senescence. Aging (Albany NY) *3*, 94.

Bray, J. D., Chennathukuzhi, V. M., and Hecht, N. B. (2002). Identification and characterization of cDNAs encoding four novel proteins that interact with translin associated factor-X. Genomics *79*, 799-808.

Bray, J. D., Chennathukuzhi, V. M., and Hecht, N. B. (2004). KIF2Aβ: A kinesin family member enriched in mouse male germ cells, interacts with translin associated factor-X (TRAX). Molecular reproduction and development *69*, 387-396.

Budirahardja, Y., and Gönczy, P. (2009). Coupling the cell cycle to development. Development *136*, 2861-2872.

Callebaut, I., Malivert, L., Fischer, A., Mornon, J., Revy, P., and De Villartay, J. (2006). Cernunnos interacts with the XRCC4· DNA-ligase IV complex and is homologous to the yeast nonhomologous end-joining factor Nej1. Journal of Biological Chemistry *281*, 13857.

Cannon, T. D., Hennah, W., van Erp, T. G. M., Thompson, P. M., Lonnqvist, J., Huttunen, M., Gasperoni, T., Tuulio-Henriksson, A., Pirkola, T., and Toga, A. W. (2005). Association of DISC1/TRAX haplotypes with schizophrenia, reduced prefrontal gray matter, and impaired short-and long-term memory. Archives of general psychiatry *62*, 1205.

Carmichael, J. B., Provost, P., Ekwall, K., and Hobman, T. C. (2004). ago1 and dcr1, two core components of the RNA interference pathway, functionally diverge from rdp1 in regulating cell cycle events in Schizosaccharomyces pombe. Molecular biology of the cell *15*, 1425-1435.

Castel, S. E., and Martienssen, R. A. (2013). RNA interference in the nucleus: roles for small RNAs in transcription, epigenetics and beyond. Nature Reviews Genetics *14*, 100-112.

Chaldakov, G., Tonchev, A., and Aloe, L. (2009). NGF and BDNF: from nerves to adipose tissue, from neurokines to metabokines. Rivista di psichiatria *44*, 79.

Chalk, J. G., Barr, F. G., and Mitchell, C. D. (1997). Translin recognition site sequences flank chromosome translocation breakpoints in alveolar rhabdomyosarcoma cell lines. Oncogene *15*, 1199.

Chan, S. T., Yang, N. C., Huang, C. S., Liao, J. W., and Yeh, S. L. (2013). Quercetin Enhances the Antitumor Activity of Trichostatin A through Upregulation of p53 Protein Expression In Vitro and In Vivo. PloS one *8*, e54255.

Chennathukuzhi, V., Morales, C. R., El-Alfy, M., and Hecht, N. B. (2003a). The kinesin KIF17b and RNA-binding protein TB-RBP transport specific cAMP-responsive element modulator-regulated mRNAs in male germ cells. Proceedings of the National Academy of Sciences *100*, 15566-15571.

Chennathukuzhi, V., Stein, J., Abel, T., Donlon, S., Yang, S., Miller, J., Allman, D., Simmons, R., and Hecht, N. (2003b). Mice deficient for testis-brain RNA-binding protein exhibit a coordinate loss of TRAX, reduced fertility, altered gene expression in the brain, and behavioral changes. Molecular and cellular biology *23*, 6419.

Chennathukuzhi, V., Stein, J. M., Abel, T., Donlon, S., Yang, S., Miller, J. P., Allman, D. M., Simmons, R. A., and Hecht, N. B. (2003c). Mice deficient for testis-brain RNA-binding protein exhibit a coordinate loss of TRAX, reduced fertility, altered gene expression in the brain, and behavioral changes. Molecular and cellular biology *23*, 6419-6434.

Chiarle, R., Zhang, Y., Frock, R. L., Lewis, S. M., Molinie, B., Ho, Y. J., Myers, D. R., Choi, V. W., Compagno, M., and Malkin, D. J. (2011). Genome-wide translocation sequencing reveals mechanisms of chromosome breaks and rearrangements in B cells. Cell *147*, 107-119.

Chiaruttini, C., Vicario, A., Li, Z., Baj, G., Braiuca, P., Wu, Y., Lee, F., Gardossi, L., Baraban, J., and Tongiorgi, E. (2009). Dendritic trafficking of BDNF mRNA is mediated by translin and blocked by the G196A (Val66Met) mutation. Proceedings of the National Academy of Sciences *106*, 16481.

Cho, Y. S., Chennathukuzhi, V. M., Handel, M. A., Eppig, J., and Hecht, N. B. (2004). The relative levels of translin-associated factor X (TRAX) and testis brain RNA-binding protein determine their nucleocytoplasmic distribution in male germ cells. Journal of Biological Chemistry *279*, 31514-31523.

Chou, J., and Roizman, B. (1994). Herpes simplex virus 1 gamma (1) 34.5 gene function, which blocks the host response to infection, maps in the homologous domain of the genes expressed during growth arrest and DNA damage. Proceedings of the National Academy of Sciences *91*, 5247-5251.

Chu, W. K., and Hickson, I. D. (2009). RecQ helicases: multifunctional genome caretakers. Nature Reviews Cancer *9*, 644-654.

Claussen, M., Koch, R., Jin, Z., and Suter, B. (2006). Functional characterization of Drosophila Translin and Trax. Genetics *174*, 1337.

Creamer, K. M., and Partridge, J. F. (2011). RITS—connecting transcription, RNA interference, and heterochromatin assembly in fission yeast. Wiley Interdisciplinary Reviews: RNA *2*, 632-646.

Cross, F. R., Buchler, N. E., Skotheim, J. M., Cross, F. R., Buchler, N. E., and Skotheim, J. M. (2011). Evolution of networks and sequences in eukaryotic cell cycle control. Philosophical Transactions of the Royal Society B: Biological Sciences *366*, 3532-3544.

Cutts, S. M., Fowler, K. J., Kile, B. T., Hii, L. L. P., O'Dowd, R. A., Hudson, D. F., Saffery, R., Kalitsis, P., Earle, E., and Choo, K. (1999). Defective chromosome segregation, microtubule bundling and nuclear bridging in inner centromere protein gene (Incenp)-disrupted mice. Human molecular genetics *8*, 1145-1155.

Davis, J. D., and Lin, S. Y. (2011). DNA damage and breast cancer. World journal of clinical oncology *2*, 329.

Davis, L., and Smith, G. R. (2001). Meiotic recombination and chromosome segregation in Schizosaccharomyces pombe. Proceedings of the National Academy of Sciences *98*, 8395-8402.

Dawe, R. K. (2003). RNA interference, transposons, and the centromere. The Plant Cell Online *15*, 297-301.

Dehé, P. M., and Cooper, J. P. (2010). Fission yeast telomeres forecast the end of the crisis. FEBS letters *584*, 3725-3733.

Devon, R., Taylor, M., Millar, J., and Porteous, D. (2000). Isolation and characterization of the mouse translin-associated protein X (Trax) gene. Mammalian Genome *11*, 395-398.

Dillon, L. W., Burrow, A. A., and Wang, Y. H. (2010). DNA instability at chromosomal fragile sites in cancer. Current genomics *11*, 326.

Djupedal, I., and Ekwall, K. (2009). Epigenetics: heterochromatin meets RNAi. Cell Research *19*, 282-295.

Doe, C. L., Chow, C., Mellor, E. J., Wang, G., Fricker, M. D., and Singh, P. B. (1998). The fission yeast chromo domain encoding gene chp1+ is required for chromosome segregation and shows a genetic interaction with alpha-tubulin. Nucleic acids research *26*, 4222-4229.

Doherty, A., and Jackson, S. (2001). DNA repair: how Ku makes ends meet. Current Biology *11*, R920-R924.

Dohke, K., Miyazaki, S., Tanaka, K., Urano, T., Grewal, S. I., and Murakami, Y. (2008). Fission yeast chromatin assembly factor 1 assists in the replication-coupled maintenance of heterochromatin. Genes to Cells *13*, 1027-1043.

Draviam, V. M., Xie, S., and Sorger, P. K. (2004). Chromosome segregation and genomic stability. Current Opinion in Genetics & Development *14*, 120-125.

Dubey, R. N., Nakwal, N., Bisht, K. K., Saini, A., Haldar, S., and Singh, J. (2009). Interaction of APC/C-E3 ligase with Swi6/HP1 and Clr4/Suv39 in heterochromatin assembly in fission yeast. Journal of Biological Chemistry *284*, 7165-7176.

Ebersole, T., Kim, J. H., Samoshkin, A., Kouprina, N., Pavlicek, A., White, R. J., and Larionov, V. (2011). tRNA genes protect a reporter gene from epigenetic silencing in mouse cells. Cell Cycle *10*, 2779-2791.

Egel, R. (2005). Fission yeast mating-type switching: programmed damage and repair. DNA repair *4*, 525-536.

Ekwall, K., Cranston, G., and Allshire, R. C. (1999). Fission yeast mutants that alleviate transcriptional silencing in centromeric flanking repeats and disrupt chromosome segregation. Genetics *153*, 1153-1169.

Emmerth, S., Schober, H., Gaidatzis, D., Roloff, T., Jacobeit, K., and Bühler, M. (2010). Nuclear retention of fission yeast dicer is a prerequisite for RNAi-mediated heterochromatin assembly. Developmental Cell *18*, 102-113.

Erdemir, T., Bilican, B., Oncel, D., Goding, C. R., and Yavuzer, U. (2002). DNA damage-dependent interaction of the nuclear matrix protein C1D with translin-associated factor X (TRAX). Journal of cell science *115*, 207-216.

Eymin, B., and Gazzeri, S. (2010). Role of cell cycle regulators in lung carcinogenesis. Cell adhesion & migration *4*, 114-123.

Ferguson, D., and Alt, F. (2001). DNA double strand break repair and chromosomal translocation: lessons from animal models. Oncogene *20*, 5572.

Finkenstadt, P. M., Kang, W. S., Jeon, M., Taira, E., Tang, W., and Baraban, J. M. (2000). Somatodendritic localization of Translin, a component of the Translin/Trax RNA binding complex. Journal of neurochemistry *75*, 1754-1762.

Fire, A., Xu, S., Montgomery, M., Kostas, S., Driver, S., and Mello, C. (1998). Potent and specific genetic interference by double-stranded RNA in Caenorhabditis elegans. Nature *391*, 806-811.

Forsburg, S. (2005). The yeasts Saccharomyces cerevisiae and Schizosaccharomyces pombe: models for cell biology research. Gravit Space Biol *18*, 3-10.

Foster, I. (2008). Cancer: A cell cycle defect. Radiography *14*, 144-149.

Fukuda, Y., Ishida, R., Aoki, K., Nakahara, K., Takashi, T., Mochida, K., Suzuki, O., Matsuda, J., and Kasai, M. (2008). Contribution of Translin to Hematopoietic Regeneration after Sublethal Ionizing Irradiation. Biological & pharmaceutical bulletin *31*, 207-211.

Gajecka, M., Glotzbach, C. D., and Shaffer, L. G. (2006a). Characterization of a complex rearrangement with interstitial deletions and inversion on human chromosome 1. Chromosome Research *14*, 277-282.

Gajecka, M., Pavlicek, A., Glotzbach, C. D., Ballif, B. C., Jarmuz, M., Jurka, J., and Shaffer, L. G. (2006b). Identification of sequence motifs at the breakpoint junctions in three t (1; 9)(p36. 3; q34) and delineation of mechanisms involved in generating balanced translocations. Human genetics *120*, 519-526.

Galagan, J. E., Calvo, S. E., Borkovich, K. A., Selker, E. U., Read, N. D., Jaffe, D., FitzHugh, W., Ma, L. J., Smirnov, S., and Purcell, S. (2003). The genome sequence of the filamentous fungus Neurospora crassa. Nature *422*, 859-868.

Gerace, E. L., Halic, M., and Moazed, D. (2010). The Methyltransferase Activity of Clr4 Suv39h Triggers RNAi Independently of Histone H3K9 Methylation. Molecular cell *39*, 360-372.

Gollin, S. (2007). Mechanisms leading to nonrandom, nonhomologous chromosomal translocations in leukemia. (Elsevier).

Goto, D. B., and Nakayama, J. (2012). RNA and epigenetic silencing: Insight from fission yeast. Development, growth & differentiation.

Grabarz, A., Barascu, A., Guirouilh-Barbat, J., and Lopez, B. S. (2012). Initiation of DNA double strand break repair: signaling and single-stranded resection dictate the choice between homologous recombination, non-homologous end-joining and alternative end-joining. American Journal of Cancer Research *2*, 249.

Grawunder, U., Wilm, M., Wu, X., Kulesza, P., Wilson, T., Mann, M., and Lieber, M. (1997). Activity of DNA ligase IV stimulated by complex formation with XRCC4 protein in mammalian cells. Nature *388*, 492-495.

Grewal, S. I. S., and Elgin, S. C. R. (2002). Heterochromatin: new possibilities for the inheritance of structure. Current Opinion in Genetics & Development *12*, 178-187.

Grewal, S. I. S., and Jia, S. (2007). Heterochromatin revisited. Nature Reviews Genetics *8*, 35-46.

Grewal, S. I. S., and Moazed, D. (2003). Heterochromatin and epigenetic control of gene expression. Science Signalling *301*, 798.

Gupta, G., Kale, A., and Kumar, V. (2012). Molecular Evolution of Translin Superfamily Proteins Within the Genomes of Eubacteria, Archaea and Eukaryotes. Journal of molecular evolution.

Gupta, G. D., and Kumar, V. (2012). Identification of Nucleic Acid Binding Sites on Translin-Associated Factor X (TRAX) Protein. PloS one *7*, e33035.

Hake, S. (2003). MicroRNAs: a role in plant development. Current Biology *13*, R851-R852.

Haldar, D., and Kamakaka, R. T. (2006). tRNA genes as chromatin barriers. Nature Structural & Molecular Biology *13*, 192-193.

Halic, M., and Moazed, D. (2009). Transposon silencing by piRNAs. Cell *138*, 1058-1060.

Halic, M., and Moazed, D. (2010). Dicer-independent primal RNAs trigger RNAi and heterochromatin formation. Cell *140*, 504-516.

Hall, I. M., Shankaranarayana, G. D., Noma, K., Ayoub, N., Cohen, A., and Grewal, S. I. S. (2002). Establishment and maintenance of a heterochromatin domain. Science *297*, 2232-2237.

Hammond, S. M., Boettcher, S., Caudy, A. A., Kobayashi, R., and Hannon, G. J. (2001). Argonaute2, a link between genetic and biochemical analyses of RNAi. Science Signalling *293*, 1146.

Han, J., Yiu, G., and Hecht, N. (1995a). Testis/Brain RNA-Binding Protein Attaches Translationally Repressed and Transported mRNAs to Microtubules. Proceedings of the National Academy of Sciences of the United States of America *92*, 9550-9554.

Han, J. R., Gu, W., and Hecht, N. B. (1995b). Testis-brain RNA-binding protein, a testicular translational regulatory RNA-binding protein, is present in the brain and binds to the 3'untranslated regions of transported brain mRNAs. Biology of reproduction *53*, 707-717.

Han, J. R., Yiu, G. K., and Hecht, N. B. (1995c). Testis/brain RNA-binding protein attaches translationally repressed and transported mRNAs to microtubules. Proceedings of the National Academy of Sciences *92*, 9550-9554.

Hanahan, D., and Weinberg, R. A. (2011). Hallmarks of cancer: the next generation. Cell *144*, 646-674.

Hannon, G. J. (2003). RNAi: A guide to gene silencing: Cold Spring Harbor Laboratory Pr).

Hansen, K. R., Hazan, I., Shanker, S., Watt, S., Verhein-Hansen, J., Bähler, J., Martienssen, R. A., Partridge, J. F., Cohen, A., and Thon, G. (2011). H3K9me-independent gene silencing in fission yeast heterochromatin by Clr5 and histone deacetylases. PLoS Genetics *7*, e1001268.

Hartmann, R. K., Gößringer, M., Späth, B., Fischer, S., and Marchfelder, A. (2009). The making of tRNAs and more–RNase P and tRNase Z. Progress in molecular biology and translational science *85*, 319-368.

Hasegawa, T., and Isobe, K. (1999). Evidence for the interaction between Translin and GADD34 in mammalian cells. Biochem Biophy Acta *1428*, 161-168.

Hasegawa, T., Xiao, H., Hamajima, F., and Isobe, K. (2000). Interaction between DNA-damage protein GADD34 and a new member of the Hsp40 family of heat shock proteins that is induced by a DNA-damaging reagent. Biochemical Journal *352*, 795.

Hayano, M., Kanoh, Y., Matsumoto, S., Renard-Guillet, C., Shirahige, K., and Masai, H. (2012). Rif1 is a global regulator of timing of replication origin firing in fission yeast. Genes & Development *26*, 137-150.

He, L., and Hannon, G. J. (2004). MicroRNAs: small RNAs with a big role in gene regulation. Nature Reviews Genetics *5*, 522-531.

Hefferin, M. L., and Tomkinson, A. E. (2005). Mechanism of DNA double-strand break repair by non-homologous end joining. DNA repair *4*, 639-648.

Heitz, E. (1928). Das Heterochromatin der Moose. I. Jahrb. wiss. Bot. 69: 762-818. 1931, Die ursache der gesetzmassingen Zahl, Lage, Form und Grosse pflanzlicher Nukleolen. Planta *12*, 775-844.

Helleday, T., Lo, J., van Gent, D. C., and Engelward, B. P. (2007). DNA double-strand break repair: from mechanistic understanding to cancer treatment. DNA repair *6*, 923-935.

Hennah, W., Tuulio-Henriksson, A., Paunio, T., Ekelund, J., Varilo, T., Partonen, T., Cannon, T., Lönnqvist, J., and Peltonen, L. (2005). A haplotype within the DISC1 gene is associated with visual memory functions in families with a high density of schizophrenia. Molecular psychiatry *10*, 1097-1103.

Hentges, P., Van Driessche, B., Tafforeau, L., Vandenhaute, J., and Carr, A. M. (2005). Three novel antibiotic marker cassettes for gene disruption and marker switching in Schizosaccharomyces pombe. Yeast *22*, 1013-1019.

Hiriart, E., Vavasseur, A., Touat-Todeschini, L., Yamashita, A., Gilquin, B., Lambert, E., Perot, J., Shichino, Y., Nazaret, N., and Boyault, C. (2012). Mmi1 RNA surveillance machinery directs RNAi complex RITS to specific meiotic genes in fission yeast. The EMBO journal *31*, 2296-2308.

Holthausen, J., Van Loenhout, M., Sanchez, H., Ristic, D., van Rossum-Fikkert, S., Modesti, M., Dekker, C., Kanaar, R., and Wyman, C. (2011). Effect of the BRCA2 CTRD domain on RAD51 filaments analyzed by an ensemble of single molecule techniques. Nucleic acids research *39*, 6558-6567.

Hosaka, T., Kanoe, H., Nakayama, T., Murakami, H., Yamamoto, H., Nakamata, T., Tsuboyama, T., Oka, M., Kasai, M., and Sasaki, M. S. (2000). Translin binds to the sequences adjacent to the breakpoints of the TLS and CHOP genes in liposarcomas with translocation t (12; 6). Oncogene *19*, 5821.

Houtgraaf, J., Versmissen, J., and van der Giessen, W. (2006). A concise review of DNA damage checkpoints and repair in mammalian cells. Cardiovascular Revascularization Medicine *7*, 165-172.

Huisinga, K. L., Brower-Toland, B., and Elgin, S. C. R. (2006). The contradictory definitions of heterochromatin: transcription and silencing. Chromosoma *115*, 110-122.

Ishida, R., Okado, H., Sato, H., Shionoiri, C., Aoki, K., and Kasai, M. (2002). A role for the octameric ring protein, Translin, in mitotic cell division. FEBS letters *525*, 105-110.

Iwasaki, O., Tanaka, A., Tanizawa, H., Grewal, S. I. S., and Noma, K. (2010). Centromeric localization of dispersed Pol III genes in fission yeast. Molecular biology of the cell *21*, 254-265.

Jackson, S. P., and Bartek, J. (2009). The DNA-damage response in human biology and disease. Nature *461*, 1071-1078.

Jacob, E., Pucshansky, L., Zeruya, E., Baran, N., and Manor, H. (2004). The human protein translin specifically binds single-stranded microsatellite repeats, d (GT) n, and G-strand telomeric repeats, d (TTAGGG) n: a study of the binding parameters. Journal of molecular biology *344*, 939-950.

Jaendling, A., and McFarlane, R. (2010). Biological roles of translin and translin-associated factor-X: RNA metabolism comes to the fore. Biochem J *429*, 225-234.

Jaendling, A., Ramayah, S., Pryce, D., and McFarlane, R. (2008). Functional characterisation of the Schizosaccharomyces pombe homologue of the leukaemia-associated translocation breakpoint binding protein translin and its binding partner, TRAX. Biochimica et Biophysica Acta (BBA)-Molecular Cell Research *1783*, 203-213.

Jefford, C., and Irminger-Finger, I. (2006). Mechanisms of chromosome instability in cancers. Critical reviews in oncology/hematology *59*, 1-14.

Jia, S., Noma, K.-i., and Grewal, S. I. (2004a). RNAi-independent heterochromatin nucleation by the stress-activated ATF/CREB family proteins. Science Signalling *304*, 1971.

Jia, S., Noma, K., and Grewal, S. I. S. (2004b). RNAi-independent heterochromatin nucleation by the stress-activated ATF/CREB family proteins. Science Signalling *304*, 1971.

Jones, M. J. K., and Jallepalli, P. V. (2012). Chromothripsis: Chromosomes in Crisis. Developmental Cell *23*, 908-917.

Kadura, S., He, X., Vanoosthuyse, V., Hardwick, K. G., and Sazer, S. (2005). The A78V mutation in the Mad3-like domain of Schizosaccharomyces pombe Bub1p perturbs nuclear accumulation and kinetochore targeting of Bub1p, Bub3p, and Mad3p and spindle assembly checkpoint function. Molecular biology of the cell *16*, 385-395.

Kanoe, H., Nakayama, T., Hosaka, T., Murakami, H., Yamamoto, H., Nakashima, Y., Tsuboyama, T., Nakamura, T., Ron, D., and Sasaki, M. S. (1999). Characteristics of genomic breakpoints in TLS-CHOP translocations in liposarcomas suggest the involvement of Translin and topoisomerase II in the process of translocation. Oncogene *18*, 721.

Kanoh, J., and Ishikawa, F. (2001). spRap1 and spRif1, recruited to telomeres by Taz1, are essential for telomere function in fission yeast. Current Biology *11*, 1624-1630.

Kanoh, J., Sadaie, M., Urano, T., and Ishikawa, F. (2005). Telomere binding protein Taz1 establishes Swi6 heterochromatin independently of RNAi at telomeres. Current Biology *15*, 1808-1819.

Kasai, M., Aoki, K., Matsuo, Y., Minowada, J., Maziarz, R. T., and Strominger, J. L. (1994). Recombination hotspot associated factors specifically recognize novel target sequences at the site of interchromosomal rearrangements in T-ALL patients with t (8; 14)(q24; q11) and t (1; 14)(p32; q11). International immunology *6*, 1017-1025.

Kasai, M., Matsuzaki, T., Katayanagi, K., Omori, A., Maziarz, R., Strominger, J., Aoki, K., and Suzuki, K. (1997). The translin ring specifically recognizes DNA ends at recombination hot spots in the human genome. Journal of Biological Chemistry *272*, 11402.

Kasparek, T. R., and Humphrey, T. C. (2011). DNA double-strand break repair pathways, chromosomal rearrangements and cancer. Paper presented at: Seminars in cell & developmental biology (Elsevier).

Katto, J., and Mahlknecht, U. (2011). Epigenetic regulation of cellular adhesion in cancer. Carcinogenesis *32*, 1414-1418.

Kawashima, S., Nakabayashi, Y., Matsubara, K., Sano, N., Enomoto, T., Tanaka, K., Seki, M., and Horikoshi, M. (2011). Global analysis of core histones reveals nucleosomal surfaces required for chromosome bi-orientation. The EMBO journal *30*, 3353-3367.

Kendall, A., Hull, M. W., Bertrand, E., Good, P. D., Singer, R. H., and Engelke, D. R. (2000). A CBF5 mutation that disrupts nucleolar localization of early tRNA biosynthesis in yeast also suppresses tRNA gene-mediated transcriptional silencing. Proceedings of the National Academy of Sciences *97*, 13108-13113.

Kinsey, P. T., and Sandmeyer, S. B. (1991). Adjacent pol II and pol III promoters: transcription of the yeast retrotransposon Ty3 and a target tRNA gene. Nucleic acids research *19*, 1317-1324.

Klar, A. J. S. (2007). Lessons Learned from Studies of Fission Yeast Mating-Type Switching and Silencing. Annu Rev Genet *41*.

Kobayashi, S., Takashima, A., and Anzai, K. (1998). The dendritic translocation of translin protein in the form of BC1 RNA protein particles in developing rat hippocampal neurons in primary culture. Biochemical and biophysical research communications *253*, 448-453.

Kobayashi, T. (2011). Regulation of ribosomal RNA gene copy number and its role in modulating genome integrity and evolutionary adaptability in yeast. Cellular and Molecular Life Sciences *68*, 1395-1403.

Kobayashi, T., Vu, L., Horiuchi, T., Nomura, M., and Tongaonkar, P. (2004). SIR2 Regulates Recombination between Different rDNA Repeats, but Not Recombination within Individual rRNA Genes in Yeast. Cell *117*, 441-453.

Krejci, L., Altmannova, V., Spirek, M., and Zhao, X. (2012). Homologous recombination and its regulation. Nucleic acids research *40*, 5795-5818.

Krishnan, V., Han, M. H., Graham, D. L., Berton, O., Renthal, W., Russo, S. J., LaPlant, Q., Graham, A., Lutter, M., and Lagace, D. C. (2007). Molecular adaptations underlying susceptibility and resistance to social defeat in brain reward regions. Cell *131*, 391-404.

Krogh, B. O., and Symington, L. S. (2004). Recombination proteins in yeast. Annu Rev Genet *38*, 233-271.

Kumar-Sinha, C., Tomlins, S. A., and Chinnaiyan, A. M. (2008). Recurrent gene fusions in prostate cancer. Nature Reviews Cancer *8*, 497-511.

Küppers, R. (2005). Mechanisms of B-cell lymphoma pathogenesis. Nature Reviews Cancer *5*, 251-262.

Kwon, Y. K., and Hecht, N. B. (1991). Cytoplasmic protein binding to highly conserved sequences in the 3'untranslated region of mouse protamine 2 mRNA, a translationally regulated transcript of male germ cells. Proceedings of the National Academy of Sciences *88*, 3584-3588.

Lai, D., Visser-Grieve, S., and Yang, X. (2012). Tumour suppressor genes in chemotherapeutic drug response. Bioscience Reports *32*, 361.

Laufman, O., Yosef, R., Adir, N., and Manor, H. (2005). Cloning and characterization of the Schizosaccharomyces pombe homologs of the human protein Translin and the Translin-associated protein TRAX. Nucleic acids research *33*, 4128.

Li, L., Gu, W., Liang, C., Liu, Q., Mello, C. C., and Liu, Y. (2012). The translin–TRAX complex (C3PO) is a ribonuclease in tRNA processing. Nature Structural & Molecular Biology *19*, 824-830.

Li, X., and Heyer, W. D. (2008). Homologous recombination in DNA repair and DNA damage tolerance. Cell Research *18*, 99-113.

Li, Z., Wu, Y., and Baraban, J. M. (2008). The Translin/Trax RNA binding complex: clues to function in the nervous system. Biochimica et Biophysica Acta (BBA)-Gene Regulatory Mechanisms *1779*, 479-485.

Lieber, M. R., Gu, J., Lu, H., Shimazaki, N., and Tsai, A. G. (2010). Nonhomologous DNA end joining (NHEJ) and chromosomal translocations in humans. Genome Stability and Human Diseases, 279-296.

Liu, J., Carmell, M. A., Rivas, F. V., Marsden, C. G., Thomson, J. M., Song, J.-J., Hammond, S. M., Joshua-Tor, L., and Hannon, G. J. (2004). Argonaute2 is the catalytic engine of mammalian RNAi. Science Signalling *305*, 1437.

Liu, Y., Ye, X., Jiang, F., Liang, C., Chen, D., Peng, J., Kinch, L., Grishin, N., and Liu, Q. (2009). C3PO, an endoribonuclease that promotes RNAi by facilitating RISC activation. Science *325*, 750.

Lluis, M., Hoe, W., Schleit, J., and Robertus, J. (2010). Analysis of nucleic acid binding by a recombinant translin–trax complex. Biochemical and biophysical research communications *396*, 709-713.

Ma, Y., Pannicke, U., Schwarz, K., and Lieber, M. (2002). Hairpin opening and overhang processing by an Artemis/DNA-dependent protein kinase complex in nonhomologous end joining and V (D) J recombination. Cell *108*, 781-794.

Macho, B., Brancorsini, S., Fimia, G. M., Setou, M., Hirokawa, N., and Sassone-Corsi, P. (2002). CREM-dependent transcription in male germ cells controlled by a kinesin. Science Signalling *298*, 2388.

Mandell, J. G., Bahler, J., Volpe, T. A., Martienssen, R. A., and Cech, T. R. (2004). Global expression changes resulting from loss of telomeric DNA in fission yeast. Genome Biol *6*, R1.

Mandell, J. G., Goodrich, K. J., Bähler, J., and Cech, T. R. (2005). Expression of a RecQ helicase homolog affects progression through crisis in fission yeast lacking telomerase. Journal of Biological Chemistry *280*, 5249-5257.

Manning, A. L., Longworth, M. S., and Dyson, N. J. (2010). Loss of pRB causes centromere dysfunction and chromosomal instability. Genes & Development *24*, 1364-1376.

Manolis, K., Nimmo, E., Hartsuiker, E., Carr, A., Jeggo, P., and Allshire, R. (2001). Novel functional requirements for non-homologous DNA end joining in Schizosaccharomyces pombe. The EMBO journal *20*, 210-221.

Martienssen, R. A., Zaratiegui, M., and Goto, D. B. (2005). RNA interference and heterochromatin in the fission yeast Schizosaccharomyces pombe. Trends in Genetics *21*, 450-456.

Martin, C., and Zhang, Y. (2005). The diverse functions of histone lysine methylation. Nature Reviews Molecular Cell Biology *6*, 838-849.

Martinelli, G., Terragna, C., Amabile, M., Montefusco, V., Testoni, N., Ottaviani, E., De Vivo, A., Mianulli, A., Saglio, G., and Tura, S. (2000). Alu and translisin recognition site sequences flanking translocation sites in a novel type of chimeric bcr-abl transcript suggest a possible general mechanism for bcr-abl breakpoints. Haematologica *85*, 40.

Mazin, A. V., Mazina, O. M., Bugreev, D. V., and Rossi, M. J. (2010). Rad54, the motor of homologous recombination. DNA repair *9*, 286-302.

McCarthy, N. (2012). Metastasis: Leaky effect. Nature Reviews Cancer *12*, 157-157.

McFarlane, R. J., Al-Zeer, K., and Dalgaard, J. Z. (2011). Eukaryote DNA replication and recombination: an intimate association. DNA replication: current advances Intech, Croatia, 347-388.

McFarlane, R. J., and Whitehall, S. K. (2009). tRNA genes in eukaryotic genome organization and reorganization. Cell Cycle *8*, 3102-3106.

McStay, B., and Grummt, I. (2008). The epigenetics of rRNA genes: from molecular to chromosome biology. Annual review of cell and developmental biology *24*, 131-157.

Meister, G., Landthaler, M., Patkaniowska, A., Dorsett, Y., Teng, G., and Tuschl, T. (2004). Human Argonaute2 mediates RNA cleavage targeted by miRNAs and siRNAs. Molecular cell *15*, 185-197.

Meng, G., Aoki, K., Tokura, K., Nakahara, K., Inazawa, J., and Kasai, M. (2000). Genomic structure and chromosomal localization of the gene encoding TRAX, a Translin-associated factor X. Journal of Human Genetics *45*, 305-308.

Miller, K. M., Ferreira, M. G., and Cooper, J. P. (2005). Taz1, Rap1 and Rif1 act both interdependently and independently to maintain telomeres. The EMBO journal *24*, 3128-3135.

Misteli, T., and Soutoglou, E. (2009). The emerging role of nuclear architecture in DNA repair and genome maintenance. Nature Reviews Molecular Cell Biology *10*, 243-254.

Mitelman, F., Johansson, B., and Mertens, F. (2007). The impact of translocations and gene fusions on cancer causation. Nature Reviews Cancer *7*, 233-245.

Miyoshi, T., Sadaie, M., Kanoh, J., and Ishikawa, F. (2003). Telomeric DNA ends are essential for the localization of Ku at telomeres in fission yeast. Journal of Biological Chemistry *278*, 1924.

Moazed, D. (2009). Small RNAs in transcriptional gene silencing and genome defence. Nature *457*, 413-420.

Morales, C., Lefrancois, S., Chennathukuzhi, V., El-Alfy, M., Wu, X., Yang, J., Gerton, G., and Hecht, N. (2002). A TB-RBP and Ter ATPase complex accompanies specific mRNAs from nuclei through the nuclear pores and into intercellular bridges in mouse male germ cells. Developmental Biology *246*, 480-494.

Morales, C., Wu, X., and Hecht, N. (1998). The DNA/RNA-binding protein, TB-RBP, moves from the nucleus to the cytoplasm and through intercellular bridges in male germ cells. Developmental Biology *201*, 113-123.

Morgan, D. O. (2007). The cell cycle: principles of control: Sinauer Associates Incorporated).

Morris, C. A., and Moazed, D. (2007). Centromere assembly and propagation. Cell *128*, 647-650.

Moshous, D., Callebaut, I., de Chasseval, R., Corneo, B., Cavazzana-Calvo, M., Le Deist, F., Tezcan, I., Sanal, O., Bertrand, Y., and Philippe, N. (2001). Artemis, a novel DNA double-strand break repair/V (D) J recombination protein, is mutated in human severe combined immune deficiency. Cell *105*, 177-186.

Moshous, D., Li, L., de Chasseval, R., Philippe, N., Jabado, N., Cowan, M. J., Fischer, A., and de Villartay, J. P. (2000). A new gene involved in DNA double-strand break repair and V (D) J recombination is located on human chromosome 10p. Human molecular genetics *9*, 583-588.

Motamedi, M. R., Hong, E. J. E., Li, X., Gerber, S., Denison, C., Gygi, S., and Moazed, D. (2008). HP1 proteins form distinct complexes and mediate heterochromatic gene silencing by nonoverlapping mechanisms. Molecular cell *32*, 778-790.

Motamedi, M. R., Verdel, A., Colmenares, S. U., Gerber, S. A., Gygi, S. P., and Moazed, D. (2004). Two RNAi complexes, RITS and RDRC, physically interact and localize to noncoding centromeric RNAs. Cell *119*, 789-802.

Murakami, H., Goto, D. B., Toda, T., Chen, E. S., Grewal, S. I., Martienssen, R. A., and Yanagida, M. (2007). Ribonuclease activity of Dis3 is required for mitotic progression and provides a possible link between heterochromatin and kinetochore function. PloS one *2*, e317.

Nakamura, M., Kanda, S., Kawamura, M., Igawa, T., Kanetake, H., and Saito, Y. (1993). Effects of low concentration of vinblastine on the anchorage-independent growth and in vitro invasion of human renal carcinoma cell lines. Cancer letters *69*, 85-91.

Nambiar, M., Kari, V., and Raghavan, S. C. (2008). Chromosomal translocations in cancer. Biochimica et Biophysica Acta (BBA)-Reviews on Cancer *1786*, 139-152.

Nambiar, M., and Raghavan, S. C. (2012). Chromosomal translocations among the healthy human population: implications in oncogenesis. Cellular and Molecular Life Sciences, 1-12.

Negrini, S., Gorgoulis, V. G., and Halazonetis, T. D. (2010). Genomic instability—an evolving hallmark of cancer. Nature Reviews Molecular Cell Biology *11*, 220-228.

Niwa, O., Matsumoto, T., and Yanagida, M. (1986). Construction of a mini-chromosome by deletion and its mitotic and meiotic behaviour in fission yeast. Molecular and General Genetics MGG *203*, 397-405.

Nowell, P. (2007). Discovery of the Philadelphia chromosome: a personal perspective. Journal of Clinical Investigation *117*, 2033-2035.

Nussenzweig, A., and Nussenzweig, M. C. (2010). Origin of chromosomal translocations in lymphoid cancer. Cell *141*, 27-38.

Obbard, D. J., Gordon, K. H. J., Buck, A. H., and Jiggins, F. M. (2009). The evolution of RNAi as a defence against viruses and transposable elements. Philosophical Transactions of the Royal Society B: Biological Sciences *364*, 99-115.

Ohashi, S., Kobayashi, S., Omori, A., Ohara, S., Omae, A., Muramatsu, T., Li, Y., and Anzai, K. (2000). The single-stranded DNA-and RNA-binding proteins pur alpha and pur beta link BC1 RNA to microtubules through binding to the dendrite-targeting RNA motifs. Journal of neurochemistry *75*, 1781-1790.

Ohnishi, Y., Totoki, Y., Toyoda, A., Watanabe, T., Yamamoto, Y., Tokunaga, K., Sakaki, Y., Sasaki, H., and Hohjoh, H. (2010). Small RNA class transition from siRNA/piRNA to miRNA during pre-implantation mouse development. Nucleic acids research *38*, 5141-5151.

Okamura, K., Ishizuka, A., Siomi, H., and Siomi, M. C. (2004). Distinct roles for Argonaute proteins in small RNA-directed RNA cleavage pathways. Genes & Development *18*, 1655-1666.

Oki, M., and Kamakaka, R. T. (2005). Barrier Function at *HMR*. Molecular cell *19*, 707-716.

Okuda, A., Kishi, T., Okochi, T., Ikeda, M., Kitajima, T., Tsunoka, T., Okumukura, T., Fukuo, Y., Kinoshita, Y., and Kawashima, K. (2010). Translin-associated factor X gene (TSNAX) may be associated with female major depressive disorder in the Japanese population. Neuromolecular medicine *12*, 78-85.

Olsson, I., and Bjerling, P. (2011). Advancing our understanding of functional genome organisation through studies in the fission yeast. Current genetics *57*, 1-12.

Ono, Y., Tomita, K., Matsuura, A., Nakagawa, T., Masukata, H., Uritani, M., Ushimaru, T., and Ueno, M. (2003). A novel allele of fission yeast rad11 that causes defects in DNA repair and telomere length regulation. Nucleic acids research *31*, 7141-7149.

Palo, O. M., Antila, M., Silander, K., Hennah, W., Kilpinen, H., Soronen, P., Tuulio-Henriksson, A., Kieseppä, T., Partonen, T., and Lönnqvist, J. (2007). Association of distinct allelic haplotypes of DISC1 with psychotic and bipolar spectrum disorders and with underlying cognitive impairments. Human molecular genetics *16*, 2517-2528.

Park, M., and Lee, S. (2003). Cell cycle and cancer. Journal of biochemistry and molecular biology *36*, 60-65.

Parker, A. E., Clyne, R. K., Carr, A. M., and Kelly, T. J. (1997). The Schizosaccharomyces pombe rad11+ gene encodes the large subunit of replication protein A. Molecular and cellular biology *17*, 2381-2390.

Pedram, M., Sprung, C. N., Gao, Q., Lo, A. W. I., Reynolds, G. E., and Murnane, J. P. (2006). Telomere position effect and silencing of transgenes near telomeres in the mouse. Molecular and cellular biology *26*, 1865-1878.

Pezawas, L., Verchinski, B. A., Mattay, V. S., Callicott, J. H., Kolachana, B. S., Straub, R. E., Egan, M. F., Meyer-Lindenberg, A., and Weinberger, D. R. (2004). The brain-derived neurotrophic factor val66met polymorphism and variation in human cortical morphology. The Journal of neuroscience *24*, 10099-10102.

Phizicky, E. M., and Hopper, A. K. (2010). tRNA biology charges to the front. Genes & Development *24*, 1832-1860.

Pidoux, A. L., and Allshire, R. C. (2004). Kinetochore and heterochromatin domains of the fission yeast centromere. Chromosome Research *12*, 521-534.

Poon, B. P., and Mekhail, K. (2012). Effects of perinuclear chromosome tethers in the telomeric URA3/5FOA system reflect changes to gene silencing and not nucleotide metabolism. Frontiers in Genetics *3*.

Raghavan, S., and Lieber, M. (2006). DNA structures at chromosomal translocation sites. Bioessays *28*, 480-494.

Reddy, B. D., Wang, Y., Niu, L., Higuchi, E. C., Marguerat, S. B., Bähler, J., Smith, G. R., and Jia, S. (2011). Elimination of a specific histone H3K14 acetyltransferase complex bypasses the RNAi pathway to regulate pericentric heterochromatin functions. Genes & Development *25*, 214-219.

Ruiz, C., Tolnay, M., and Bubendorf, L. (2012). Application of personalised medicine to solid tumours: opportunities and challenges. Swiss medical weekly *142*, 0.

Saitoh, S., Takahashi, K., and Yanagida, M. (1997). Mis6, a fission yeast inner centromere protein, acts during G1/S and forms specialized chromatin required for equal segregation. Cell *90*, 131.

Sato, M., and Toda, T. (2010). Space shuttling in the cell: Nucleocytoplasmic transport and microtubule organization during the cell cycle. Nucleus *1*, 231-236.

Schatz, D. G., and Swanson, P. C. (2011). V (D) J recombination: mechanisms of initiation. Annual review of genetics *45*, 167-202.

Schoeftner, S., and Blasco, M. A. (2009). A 'higher order'of telomere regulation: telomere heterochromatin and telomeric RNAs. The EMBO journal *28*, 2323-2336.

Schosser, A., Gaysina, D., Cohen-Woods, S., Chow, P., Martucci, L., Craddock, N., Farmer, A., Korszun, A., Gunasinghe, C., and Gray, J. (2009). Association of DISC1 and TSNAX genes and affective disorders in the depression case–control (DeCC) and bipolar affective case–control (BACCS) studies. Molecular psychiatry *15*, 844-849.

Scott, K. C., White, C. V., and Willard, H. F. (2007). An RNA polymerase III-dependent heterochromatin barrier at fission yeast centromere 1. PloS one *2*, e1099.

Scott, S. P., and Pandita, T. K. (2006). The cellular control of DNA double-strand breaks. Journal of cellular biochemistry *99*, 1463-1475.

Shahbazian, M. D., and Grunstein, M. (2007). Functions of site-specific histone acetylation and deacetylation. Annu Rev Biochem *76*, 75-100.

Shankaranarayana, G. D., Motamedi, M. R., Moazed, D., and Grewal, S. I. (2003). Sir2 regulates histone H3 lysine 9 methylation and heterochromatin assembly in fission yeast. Current Biology *13*, 1240-1246.

Stein, J. M., Bergman, W., Fang, Y., Davison, L. K., Brensinger, C., Robinson, M. B., Hecht, N. B., and Abel, T. (2006). Behavioral and neurochemical alterations in mice lacking the RNA-binding protein translin. The Journal of neuroscience *26*, 2184-2196.

Stouffer, S. (1949). The American Soldier, Studies in Social Psychology in World War II. In, (Princeton, New Jersey: Princeton University Press).

Sugiura, I., Sasaki, C., Hasegawa, T., Kohno, T., Sugio, S., Moriyama, H., Kasai, M., and Matsuzaki, T. (2004). Structure of human translin at 2.2 A resolution. Acta Crystallographica Section D: Biological Crystallography *60*, 674-679.

Sugiyama, T., Cam, H. P., Sugiyama, R., Noma, K., Zofall, M., Kobayashi, R., and Grewal, S. I. S. (2007). SHREC, an effector complex for heterochromatic transcriptional silencing. Cell *128*, 491-504.

Sun, F. L., and Elgin, S. C. R. (1999). Putting Boundaries on Silence Minireview. Cell *99*, 459-462.

Suwaki, N., Klare, K., and Tarsounas, M. (2011). RAD51 paralogs: Roles in DNA damage signalling, recombinational repair and tumorigenesis. Paper presented at: Seminars in cell & developmental biology (Elsevier).

Suzuki, T., and Miyata, N. (2005). Non-hydroxamate histone deacetylase inhibitors. Current medicinal chemistry *12*, 2867-2880.

Symington, L. S., and Gautier, J. (2011). Double-strand break end resection and repair pathway choice. Annual review of genetics *45*, 247-271.

Szankasi, P., and Smith, G. R. (1995). A role for exonuclease I from S. pombe in mutation avoidance and mismatch correction. Science (New York, NY) *267*, 1166.

Takahashi, K., Imano, R., Kibe, T., Seimiya, H., Muramatsu, Y., Kawabata, N., Tanaka, G., Matsumoto, Y., Hiromoto, T., and Koizumi, Y. (2011). Fission yeast Pot1 and RecQ helicase are required for efficient chromosome segregation. Molecular and cellular biology *31*, 495-506.

Talbert, P. B., and Henikoff, S. (2006). Spreading of silent chromatin: inaction at a distance. Nature Reviews Genetics *7*, 793-803.

Thompson, K. S., and Towle, H. (1991). Localization of the carbohydrate response element of the rat L-type pyruvate kinase gene. Journal of Biological Chemistry *266*, 8679-8682.

Thomson, P., Wray, N., Millar, J., Evans, K., Le Hellard, S., Condie, A., Muir, W., Blackwood, D., and Porteous, D. (2005). Association between the TRAX/DISC locus and both bipolar disorder and schizophrenia in the Scottish population. Molecular psychiatry *10*, 657-668.

Thon, G., and Verhein-Hansen, J. (2000). Four chromo-domain proteins of Schizosaccharomyces pombe differentially repress transcription at various chromosomal locations. Genetics *155*, 551-568.

Thon, G. v., and Klar, A. (1992). The clr1 locus regulates the expression of the cryptic mating-type loci of fission yeast. Genetics *131*, 287-296.

Tian, Y., Simanshu, D. K., Ascano, M., Diaz-Avalos, R., Park, A. Y., Juranek, S. A., Rice, W. J., Yin, Q., Robinson, C. V., and Tuschl, T. (2011). Multimeric assembly and biochemical characterization of the Trax–translin endonuclease complex. Nature Structural & Molecular Biology *18*, 658-664.

Tomari, Y., and Zamore, P. D. (2005). Perspective: machines for RNAi. Genes & Development *19*, 517-529.

Trewick, S. C., Minc, E., Antonelli, R., Urano, T., and Allshire, R. C. (2007). The JmjC domain protein Epe1 prevents unregulated assembly and disassembly of heterochromatin. The EMBO journal *26*, 4670-4682.

Ueno, M., Nakazaki, T., Akamatsu, Y., Watanabe, K., Tomita, K., Lindsay, H. D., Shinagawa, H., and Iwasaki, H. (2003). Molecular characterization of the Schizosaccharomyces pombe nbs1+ gene involved in DNA repair and telomere maintenance. Molecular and cellular biology *23*, 6553-6563.

Valencia-Sanchez, M. A., Liu, J., Hannon, G. J., and Parker, R. (2006). Control of translation and mRNA degradation by miRNAs and siRNAs. Genes & Development *20*, 515-524.

VanLoock, M., Yu, X., Kasai, M., and Egelman, E. (2001). Electron microscopic studies of the translin octameric ring. Journal of Structural Biology *135*, 58-66.

Verdel, A., Jia, S., Gerber, S., Sugiyama, T., Gygi, S., Grewal, S. I. S., and Moazed, D. (2004). RNAi-mediated targeting of heterochromatin by the RITS complex. Science *303*, 672-676.

Verdel, A., and Moazed, D. (2005). RNAi-directed assembly of heterochromatin in fission yeast. FEBS letters *579*, 5872-5878.

Volpe, T., and Martienssen, R. A. (2011). RNA interference and heterochromatin assembly. Cold Spring Harbor perspectives in biology *3*.

Volpe, T., Schramke, V., Hamilton, G. L., White, S. A., Teng, G., Martienssen, R. A., and Allshire, R. C. (2003). RNA interference is required for normal centromere function infission yeast. Chromosome Research *11*, 137-146.

Volpe, T. A., Kidner, C., Hall, I. M., Teng, G., Grewal, S. I. S., and Martienssen, R. A. (2002). Regulation of heterochromatic silencing and histone H3 lysine-9 methylation by RNAi. Science *297*, 1833-1837.

Walker, S. C., and Engelke, D. R. (2006). Ribonuclease P: the evolution of an ancient RNA enzyme. Critical reviews in biochemistry and molecular biology *41*, 77-102.

Wang, J., Boja, E. S., Oubrahim, H., and Chock, P. B. (2004). Testis brain ribonucleic acid-binding protein/translin possesses both single-stranded and double-stranded ribonuclease activities. Biochemistry *43*, 13424-13431.

Watson, A. T., Garcia, V., Bone, N., Carr, A. M., and Armstrong, J. (2008). Gene tagging and gene replacement using recombinase-mediated cassette exchange in Schizosaccharomyces pombe. Gene *407*, 63-74.

Wei, Y., Sun, M., Nilsson, G., Dwight, T., Xie, Y., Wang, J., Hou, Y., Larsson, O., Larsson, C., and Zhu, X. (2003). Characteristic sequence motifs located at the genomic breakpoints of the translocation t (X; 18) in synovial sarcomas. Oncogene *22*, 2215-2222.

Weinbauer, G., Behr, R., Bergmann, M., and Nieschlag, E. (1998). Testicular cAMP responsive element modulator (CREM) protein is expressed in round spermatids but is absent or reduced in men with round spermatid maturation arrest. Molecular human reproduction *4*, 9-15.

West, A. G., Huang, S., Gaszner, M., Litt, M. D., and Felsenfeld, G. (2004). Recruitment of histone modifications by USF proteins at a vertebrate barrier element. Molecular cell *16*, 453-463.

Weterings, E., and van Gent, D. C. (2004). The mechanism of non-homologous end-joining: a synopsis of synapsis. DNA repair *3*, 1425-1435.

Weuts, A., Voet, T., Verbeeck, J., Lambrechts, N., Wirix, E., Schoonjans, L., Danloy, S., Marynen, P., and Froyen, G. (2012). Telomere length homeostasis and telomere position effect on a linear human artificial chromosome are dictated by the genetic background. Nucleic acids research *40*, 11477-11489.

White, R. J. (2011). Transcription by RNA polymerase III: more complex than we thought. Nature Reviews Genetics *12*, 459-463.

White, S. A., and Allshire, R. C. (2008). RNAi-mediated chromatin silencing in fission yeast. RNA Interference, 157-183.

Win, T. Z., Mankouri, H. W., Hickson, I. D., and Wang, S.-W. (2005). A role for the fission yeast Rqh1 helicase in chromosome segregation. Journal of cell science *118*, 5777-5784.

Wong, L. H. (2010). Epigenetic regulation of telomere chromatin integrity in pluripotent embryonic stem cells. Epigenomics *2*, 639-655.

Wood, V., Gwilliam, R., Rajandream, M., Lyne, M., Lyne, R., Stewart, A., Sgouros, J., Peat, N., Hayles, J., and Baker, S. (2002). The genome sequence of Schizosaccharomyces pombe. Nature *415*, 871-880.

Wu, R., Osatomi, K., Terada, L., and Uyeda, K. (2003). Identification of Translin/Trax complex as a glucose response element binding protein in liver. Biochimica et Biophysica Acta (BBA)-General Subjects *1624*, 29-35.

Wu, X., Gu, W., Meng, X., and Hecht, N. (1997). The RNA-binding protein, TB-RBP, is the mouse homologue of translin, a recombination protein associated with chromosomal translocations. Proceedings of the National Academy of Sciences of the United States of America *94*, 5640.

Wu, X. Q., and Hecht, N. B. (2000). Mouse testis brain ribonucleic acid-binding protein/translin colocalizes with microtubules and is immunoprecipitated with messenger ribonucleic acids encoding myelin basic protein, α calmodulin kinase II, and protamines 1 and 2. Biology of reproduction *62*, 720-725.

Wu, X. Q., Lefrancois, S., Morales, C. R., and Hecht, N. B. (1999). Protein-protein interactions between the testis brain RNA-binding protein and the transitional endoplasmic reticulum ATPase, a cytoskeletal γ actin and Trax in male germ cells and the brain. Biochemistry *38*, 11261-11270.

Yamada, T., Fischle, W., Sugiyama, T., Allis, C. D., and Grewal, S. I. S. (2005). The nucleation and maintenance of heterochromatin by a histone deacetylase in fission yeast. Molecular cell *20*, 173-185.

Yamamoto, M., Imai, Y., and Watanabe, Y. (1997). 12 Mating and Sporulation in Schizosaccharomyces pombe. Cold Spring Harbor Monograph Archive *21*, 1037-1106.

Yang, S., Cho, Y. S., Chennathukuzhi, V. M., Underkoffler, L. A., Loomes, K., and Hecht, N. B. (2004). Translin-associated factor X is post-transcriptionally regulated by its partner protein TB-RBP, and both are essential for normal cell proliferation. Journal of Biological Chemistry *279*, 12605-12614.

Yang, S., and Hecht, N. (2004). Translin associated protein X is essential for cellular proliferation. FEBS letters *576*, 221-225.

Yankulov, K. (2011). Dare to challenge the silence? Telomeric gene silencing revisited. Nucleus *2*, 513-516.

Yavuzer, U., Smith, G., Bliss, T., Werner, D., and Jackson, S. (1998). DNA end-independent activation of DNA-PK mediated via association with the DNA-binding protein C1D. Genes & Development *12*, 2188.

Ye, X., Huang, N., Liu, Y., Paroo, Z., Huerta, C., Li, P., Chen, S., Liu, Q., and Zhang, H. (2011). Structure of C3PO and mechanism of human RISC activation. Nature Structural & Molecular Biology *18*, 650-657.

Yuan, J., and Chen, J. (2010). MRE11-RAD50-NBS1 complex dictates DNA repair independent of H2AX. Journal of Biological Chemistry *285*, 1097-1104.

Zhang, K., Mosch, K., Fischle, W., and Grewal, S. I. S. (2008). Roles of the Clr4 methyltransferase complex in nucleation, spreading and maintenance of heterochromatin. Nature Structural & Molecular Biology *15*, 381-388.

Zou, Y., Millette, C. F., and Sperry, A. O. (2002). KRP3A and KRP3B: candidate motors in spermatid maturation in the seminiferous epithelium. Biology of reproduction *66*, 843-855.